



QUEENSLAND UNIVERSITY OF TECHNOLOGY

# In-Cylinder Pressure and Inter-Cycle Variability Analysis for a Compression Ignition Engine: Bayesian Approaches

**Timothy Alexis Bodisco**

BMaths, GradCertInfTech, MAppSc

A thesis by publication submitted in partial fulfillment of the requirements for the degree of  
Doctor of Philosophy (PhD)

School of Chemistry, Physics and Mechanical Engineering

Science and Engineering Faculty

Queensland University of Technology

August 2013

He who controls the spice controls the universe.

—Frank Herbert

# Statement of original authorship

The work contained in this thesis has not been previously submitted for a degree or diploma at any other education institution. To the best of my knowledge and belief, this thesis contains no material previously published or written by another person except where due reference is made.

**QUT Verified Signature**

[This page is intentionally left blank]

# Abstract

Global dependence on efficient energy and transportation is growing. Moreover, there is increasing pressure from the regulating authorities for a more sustainable approach to energy than the use of fossil fuels. However, there is currently a lack of knowledge on the effect that the use of alternative fuels have on combustion, especially in modern compression ignition engines.

Primarily this dissertation will investigate techniques to analyse in-cylinder pressure signals from a modern, multi-cylinder, heavy-duty, common-rail, direct-injection diesel engine, with a focus on combustion resonance. Combustion resonance is caused by the abrupt change in in-cylinder pressure associated with auto-ignition—it is a phenomena that is not well represented in the current literature. Because the speed of sound is related to the temperature of the medium that it is passing through, accurate isolation of the frequency information from combustion resonance can yield insights into the in-cylinder temperature and the rate of change of in-cylinder temperature.

Isolating the frequency information in combustion resonance is problematic. During combustion the in-cylinder temperature is non-stationary; therefore, the resonant frequency is also non-stationary. Many traditional spectral analysis techniques are unable to handle non-stationary frequencies and those that do typically do not have adequate resolution for in-depth analysis. Moreover, traditional techniques are normally very sensitive to noise, a problem often dealt with by cycle-averaging data, which effectively eliminates the potential for inter-cycle variability studies and can also produce potentially misleading results. This dissertation introduces the use of Bayesian statistical modelling to over-come these issues associated with the isolation of the resonant frequency.

Bayesian modelling is ideally suited to the problem of isolating non-stationary frequency information. If the frequency can be modelled empirically, then each model parameter can be accurately resolved using the Metropolis-Hastings algorithm—a special form of Markov-chain Monte Carlo. Unlike other techniques, the Bayesian technique requires that all analysis assumptions be explicitly stated. Whilst this may add an element of complexity to the analysis, it ensures that the analyst is completely aware of the problem being solved.

Bayesian models for isolating the resonant frequency information are shown in this dissertation. The utility of isolating the resonant frequency information is also demonstrated by determining: the start of pre-mixed combustion, the start of diffusion combustion, the in-cylinder temperature (as a function of crank angle) and the trapped mass. These parameters have traditionally been difficult to investigate, owing to the challenging nature of isolating

the resonant frequency.

Experimental campaigns were conducted to develop the in-cylinder pressure analysis techniques and a campaign involving ethanol fumigation (in-take manifold injection of ethanol), where ethanol displaced up to 40% of the diesel fuel by energy, was also done to show the utility of the in-cylinder techniques introduced in this dissertation. In the ethanol fumigation campaign the engine was operated at 2000 rpm on half, three quarters and full load. The effect of fumigating ethanol on combustion was assessed by investigating the inter-cycle variability of key in-cylinder parameters: peak pressure, peak pressure timing, maximum rate of pressure rise, ignition delay and indicated mean effective pressure. A monotonic relationship between the absolute air to fuel ratio (on a mole basis) and inter-cycle variability was shown.

The inter-cycle variability was assessed by viewing the results from four thousand consecutive cycles as kernel density estimates. Visualising the data in this manner has the advantage over using single statistical values (such as the mean, standard deviation and the coefficient of variation) that multi-modal behaviour can be identified. Moreover, the manner in which the data is distributed can also be determined.

Increasing the amount of diesel fuel displaced with fumigated ethanol significantly increased the inter-cycle variability of the engine. However, it was shown that whilst the absolute air to fuel ratio (on a mole basis) was maintained above 110, the increase in inter-cycle variability associated with the fumigated ethanol was minimal. Moreover, introducing ethanol also resulted in a systematic increase in the peak pressure and the maximum rate of pressure rise.

Investigating the start of combustion, by analysing the combustion resonance with the Bayesian method, found that in a heavy-duty, modern diesel engine with injection timing close to top dead centre (TDC), ethanol fumigation could result in a decrease in ignition delay. This result runs counter to the current literature. The current literature explains that the ignition delay is decreased with ethanol fumigation because of the so-called “cooling effect”—in this study the expected decrease in ignition delay is shown at low loads and ethanol substitutions. However, at sufficiently high load and ethanol substitutions there is potential for the ethanol to auto-ignite. This reaction prior to the introduction of the diesel fuel causes the charge air/ethanol mixture to ignite with either a shorter ignition delay or prior to the introduction of the diesel fuel. From a practical perspective, this result shows the importance of assessing the effect that alternative fuels have on representative engines. Combustion in a comparatively low pressure mechanically injected engine with injection timing well before TDC will be fundamentally different to a modern engine with advanced high-pressure injection timing and higher in-cylinder pressure.

# Keywords

Internal combustion engine; diesel engine; in-cylinder pressure; inter-cycle variability; combustion resonance; resonant frequency; spectral analysis; fast Fourier transforms; evolving frequencies; ignition delay; start of combustion; heat release; statistical modelling; Bayesian analysis; in-cylinder temperature; trapped mass; Markov-chain Monte Carlo (MCMC); differentiation, kernel density estimate; probability density function; alternative fuel; ethanol fumigation; common-rail injection; combustion; in-cylinder parameters (peak pressure, peak pressure timing, maximum rate of pressure rise, indicated mean effective pressure).

# Table of Abbreviations

BDC	bottom dead centre
BERF	Biofuel Engine Research Facility
BMEP	brake mean effective pressure
CO	carbon monoxide
CO <sub>2</sub>	carbon dioxide
COV	coefficient of variation
DI	direct injection
DIC	deviance information criterion
EGR	exhaust gas recirculation
EMS	engine management system
FFT	fast Fourier transform
HCCI	homogeneous charge compression ignition
IMEP	indicated mean effective pressure
KDE	kernel density estimate
LPG	liquefied petroleum gas
MCMC	Markov-chain Monte Carlo
NMR	nuclear magnetic resonance
NO <sub>x</sub>	nitrogen oxides (typically NO and NO <sub>2</sub> )
NRHR	net rate of heat release
<i>p-V</i>	pressure versus volume
<i>p-θ</i>	pressure versus crank angle
pdf	probability density function
QUT	Queensland University of Technology
RPM	revolutions per minute
RTD	resistance temperature detector
TDC	top dead centre
WVD	Wigner-Ville distribution



---

[This page is intentionally left blank]

# Publications During Candidature

## Journal Articles

Pham P., Bodisco T., Ristovski Z., Brown R.J. and Masri A.R., “The influence of fatty acid methyl ester profiles on inter-cycle combustion variations and emissions on a heavy duty compression ignition engine”, *Fuel*, 116, pp 140–150 (2014)

Bodisco T., Low Choy S. and Brown R.J., “A Bayesian approach to the determination of ignition delay”, *Applied Thermal Engineering*, 60(1-2), pp 79–87 (2013)

Surawski N., Miljevic B., Bodisco T., Brown R.J., Ristovski Z. and Ayoko G., “Application of multi-criteria decision making methods to compression ignition engine efficiency and gaseous, particulate and greenhouse gas emissions”, *Environmental Science and Technology*, 47(4), pp 1904–1912 (2013)

Pham P., Bodisco T., Stevanovic S., Rahman M., Hao W., Ristovski Z., Brown R.J. and Masri A., “Engine performance characteristics for biodiesels of different unsaturation degrees and carbon chain lengths”, *SAE International Journal of Fuels and Lubricants*, 6(1), pp 188–198 (2013)

Bodisco T. and Brown R.J., “Inter-cycle variability of in-cylinder pressure parameters in an ethanol fumigated common rail diesel engine”, *Energy*, 52(1), pp 55–65 (2013)

Bodisco T., Reeves R., Situ R., and Brown R.J., “Bayesian models for the determination of resonant frequencies in a DI diesel engine”, *Mechanical Systems and Signal Processing*, 26, pp 305-314 (2012)

Surawski N., Miljevic B., Bodisco T., Situ R., Brown R.J. and Ristovski Z., “Gaseous and particle emissions from a liquefied petroleum gas (LGP) fumigation compression ignition engine”, *Fuel*, under review

Banks J., Kelson N., Macintosh H., Dagg M., Hayward R., Bodisco T. and Brown R.J., “Calculation of engine parameters using reconfigurable hardware”, *International Journal of Computational Methods*, under-review

Bodisco T., Low Choy S., Masri A.R. and Brown R.J., “A Statistical Model for Combustion Resonance from a DI Diesel Engine: with Applications”, *Mechanical Systems and Signal Processing*, under-review

Bodisco T. and Brown R.J., “Inter-cycle variability of ignition delay in an ethanol fumigated common rail diesel engine”, *Energy*, in preparation for submission

## Conference Articles

Pham P., Bodisco T., Stevanovic S., Rahman M., Hao W., Ristovski Z., Brown R.J. and Masri A., “Engine performance characteristics for biodiesels of different unsaturation degrees and carbon chain lengths”, *SAE 2013 World Congress & Exhibition*, 16–18 April 2013, Detroit, Michigan, USA. (SAE Paper 2013-01-1680)

Banks J., Kelson N., Macintosh H., Dagg M., Hayward R., Bodisco T. and Brown R.J., “Calculation of volume from crank angle using reconfigurable hardware”, *4th International Conference on Computational Methods*, 25–28 November 2012, Queensland University of Technology, Gold Coast, Australia.

Bodisco T. and Brown R.J., “Ignition Delay in an Ethanol Fumigated Common Rail Diesel Engine”, *2011 Australian Combustion Symposium*, 29 November–2 December 2011, University of Newcastle, Newcastle, Australia.

Bodisco T. and Brown R.J., “Statistical modeling to determine resonant frequency information present in combustion chamber pressure signals”, *17th Australasian Fluid Mechanics Conference*, 5-9 December 2010, University of Auckland, Auckland, New Zealand.

## Conference Items

Pham P., Bodisco T., Rahman M.D., Ristovski Z.D., Brown R.J. and Masri A.R., “Biodiesels: The influences of fatty acid methyl ester profiles on inter-cycle combustion variability in a compression ignition engine”, *8th Australia and New Zealand Aerosol Workshop*, 26–27 November 2012, CSIRO, Canberra, Australia.

Surawski N., Miljevic B., Roberts B., Bodisco T., Situ R. and Brown R.J., “Particulate emissions from a dual-fuel compression ignition engine utilising ethanol fumigation”, *13th ETH Conference on Combustion Generated Nanoparticles*, 22–24 June 2009, ETH Zurich, Switzerland.

[This page is intentionally left blank]

# Table of Contents

Abstract . . . . .	v
Keywords . . . . .	vii
Table of Abbreviations . . . . .	viii
Publications During Candidature . . . . .	x
Table of Figures . . . . .	xix
Table of Tables . . . . .	xx
Acknowledgements . . . . .	1
<b>1 Current state of knowledge</b>	<b>5</b>
1.1 Context . . . . .	5
1.1.1 Alternative Fuel . . . . .	5
1.1.2 Modern Diesel Engines . . . . .	8
1.2 In-cylinder Pressure Analysis . . . . .	9
1.3 Combustion Resonance . . . . .	14
1.3.1 Traditional Techniques . . . . .	15
1.3.2 Bayesian Spectral Analysis . . . . .	17
1.4 Inter-cycle Variability . . . . .	19
1.5 References . . . . .	21
<b>2 Contribution</b>	<b>33</b>
<b>3 In Situ Calibration of a Piezoelectric Transducer in an Internal Combustion Engine</b>	<b>35</b>
3.1 Introduction . . . . .	35
3.2 Experimental Configuration . . . . .	36
3.3 Data Collection . . . . .	37
3.4 Data Analysis . . . . .	38
3.5 Results . . . . .	39
3.6 Conclusion . . . . .	39
3.7 Acknowledgements . . . . .	40
<b>4 Bayesian Models for the Determination of Resonant Frequencies in a DI Diesel Engine</b>	<b>41</b>
4.1 Introduction . . . . .	43
4.2 Experimental Configuration . . . . .	44
4.3 Model Development . . . . .	45
4.4 Cycle-by-cycle Analysis . . . . .	53
4.5 Trapped Mass . . . . .	54
4.6 Limitations . . . . .	56

4.7	Further Work . . . . .	57
4.8	Conclusion . . . . .	57
4.9	Acknowledgements . . . . .	58
4.10	References . . . . .	58
<b>5</b>	<b>Inter-cycle variability of in-cylinder pressure parameters in an ethanol fumigated common rail diesel engine</b>	<b>61</b>
5.1	Introduction . . . . .	63
5.2	Terminology and Abbreviations . . . . .	66
5.3	Experimental Configuration and Data Acquisition . . . . .	66
5.4	Determination of the Start of Combustion . . . . .	70
5.4.1	Combustion Resonance . . . . .	70
5.4.2	Net Rate of Heat Release . . . . .	71
5.5	Results . . . . .	72
5.5.1	Full Load Results . . . . .	73
5.5.2	Three Quarter Load Results . . . . .	77
5.5.3	Half Load Results . . . . .	80
5.5.4	Inter-cycle Variability . . . . .	84
5.5.5	Auto-ignition of Ethanol . . . . .	87
5.6	Conclusion . . . . .	89
5.7	Acknowledgements . . . . .	90
5.8	References . . . . .	90
<b>6</b>	<b>A Bayesian approach to the determination of ignition delay</b>	<b>95</b>
6.1	Introduction . . . . .	97
6.2	Experimental Configuration . . . . .	99
6.3	Experimental Data . . . . .	99
6.4	Determination of Ignition Delay . . . . .	102
6.4.1	Start of Diesel Injection – Estimating Injection Latency . . . . .	102
6.4.2	Net Rate of Heat Release . . . . .	103
6.4.3	Combustion Resonance . . . . .	105
6.4.4	Statistical Model . . . . .	106
6.4.5	Priors . . . . .	107
6.4.6	Metropolis-Hastings Computational Algorithm . . . . .	108
6.4.7	Simulation Results . . . . .	110
6.5	Inter-cycle Variability . . . . .	112
6.6	Comparison to Net Rate of Heat Release . . . . .	116
6.7	Conclusion . . . . .	116
6.8	Acknowledgements . . . . .	117
6.9	References . . . . .	117
<b>7</b>	<b>Inter-cycle variability of ignition delay in an ethanol fumigated common rail diesel engine</b>	<b>121</b>

Table of Contents	xv
7.1 Introduction . . . . .	124
7.2 Experimental Configuration . . . . .	127
7.3 Terminology and Abbreviations . . . . .	127
7.4 Ignition Delay . . . . .	127
7.5 Results . . . . .	129
7.5.1 Full Load Results . . . . .	129
7.5.2 Three Quarter Load Results . . . . .	132
7.5.3 Half Load Results . . . . .	134
7.6 Air to Fuel Ratio . . . . .	136
7.7 Numerical Modelling . . . . .	139
7.8 Conclusion . . . . .	143
7.9 Acknowledgements . . . . .	144
7.10 References . . . . .	144
<b>8 A Statistical Model for Combustion Resonance from a DI Diesel Engine: with Applications</b>	<b>149</b>
8.1 Introduction . . . . .	151
8.2 Experimental Configuration . . . . .	153
8.3 Experimental Data . . . . .	154
8.4 Conceptual Model . . . . .	157
8.5 Priors . . . . .	159
8.6 Model Implementation . . . . .	161
8.7 Simulation Results . . . . .	162
8.8 Application . . . . .	169
8.9 Conclusion . . . . .	173
8.10 Acknowledgements . . . . .	173
8.11 References . . . . .	173
<b>9 Conclusions</b>	<b>177</b>
9.1 In-cylinder pressure techniques . . . . .	177
9.2 Inter-cycle variability . . . . .	178
9.3 Ethanol fumigation . . . . .	179
9.4 Recommendations for the future . . . . .	180
<b>Reference List</b>	<b>182</b>
<b>Appendix</b>	<b>197</b>
A.1 Comment on Error . . . . .	a
A.1.1 Experimental Error . . . . .	a
A.1.2 Modelling Error . . . . .	b
A.1.3 References . . . . .	b
A.2 Fuel Certificates . . . . .	c

# Table of Figures

1.1	Pressure vs volume indicator diagram . . . . .	9
1.2	Typical DI engine heat release rate diagram identifying different diesel combustion phases . . . . .	12
1.3	Comparison of conventional analysis (middle panel) and Bayesian analysis (lower panel) of a simulated time series (upper panel) . . . . .	18
1.4	Comparison of conventional analysis (middle panel) and Bayesian analysis (lower panel) of the two channel NMR time series (upper two panels) . . . . .	18
3.1	Calibration system adapter (left) and it in place in the engine (right) . . . . .	36
3.2	Schematic of the piezoelectric transducer calibration system . . . . .	36
3.3	Voltage drop for a 384 kPa change in pressure . . . . .	38
3.4	Graphical comparison between the supplied pressure the measured pressure . . . . .	39
4.1	Pressure signal with the motoring frequency information removed . . . . .	45
4.2	Pressure signal from Figure 4.1 and Model 1 from Equation 4.1 . . . . .	46
4.3	Pressure signal from Figure 4.1 and Model 2 from Equation 4.2 . . . . .	47
4.4	Pressure signal from Figure 4.1 and Model 3 from Equation 4.3 . . . . .	48
4.5	Pressure signal from Figure 4.1 and Model 4 from Equation 4.4 . . . . .	49
4.6	Pressure signal from Figure 4.1 and Model 5 from Equation 4.5 . . . . .	50
4.7	Posterior density of the initial resonant frequency obtained from Model 5 (Equation 4.5) . . . . .	51
4.8	Fast Fourier transform of Figure 4.1 . . . . .	51
4.9	Comparison between the posterior density of the initial resonant frequency (Figure 4.7) and a fast Fourier transform of Figure 4.1 . . . . .	52
4.10	Drop in resonant frequency as a function of crank-angle. Taken from the final model (Model 5) . . . . .	53
4.11	Probability density functions of the initial resonant frequency across a range of cycles . . . . .	54
4.12	Estimated trapped mass calculated from combustion resonance and the ideal gas law . . . . .	55
4.13	Probability density functions for the initial resonant frequency from Models 1 to 5 . . . . .	56



5.1	Schematic of the ethanol injector and pressure/crank angle data acquisition systems . . . . .	68
5.2	Pressure vs crank angle plot at full load on neat diesel fuel . . . . .	69
5.3	Band-pass filtered voltage in-cylinder pressure signal at full load on neat diesel fuel . . . . .	70
5.4	Net rate of heat release, full load, neat diesel with the modal start of combustion marked . . . . .	72
5.5	Maximum rate of pressure rise, full load, 0%–40% ethanol substitutions . . . . .	73
5.6	Peak pressure, full load, 0%–40% ethanol substitutions . . . . .	74
5.7	Peak pressure timing, full load, 0%–40% ethanol substitutions . . . . .	75
5.8	Ignition delay, full load, 0%–40% ethanol substitutions . . . . .	76
5.9	Diesel injection timing, full load, 0%–40% ethanol substitutions . . . . .	76
5.10	Maximum rate of pressure rise, three quarter load, 0%–40% ethanol substitutions . . . . .	77
5.11	Peak pressure, three quarter load, 0%–40% ethanol substitutions . . . . .	78
5.12	Peak pressure timing, three quarter load, 0%–40% ethanol substitutions . . . . .	78
5.13	Ignition delay, three quarter load, 0%–40% ethanol substitutions . . . . .	79
5.14	Diesel injection timing, three quarter load, 0%–40% ethanol substitutions . . . . .	80
5.15	Maximum rate of pressure rise, half load, 0%–40% ethanol substitutions . . . . .	81
5.16	Peak pressure, half load, 0%–40% ethanol substitutions . . . . .	82
5.17	Peak pressure timing, half load, 0%–40% ethanol substitutions . . . . .	82
5.18	Ignition delay, half load, 0%–40% ethanol substitutions . . . . .	83
5.19	Diesel injection timing, half load, 0%–40% ethanol substitutions . . . . .	84
5.20	COV of IMEP Vs the Air to Fuel Ratio . . . . .	85
5.21	Standard Deviation of IMEP Vs the Air to Fuel Ratio . . . . .	86
5.22	Standard Deviation of the Maximum Rate of Pressure Rise Vs the Air to Fuel Ratio . . . . .	86
5.23	Standard Deviation of the Peak Pressure Vs the Air to Fuel Ratio . . . . .	87
5.24	In-cylinder pressure trace, full load, 50% ethanol substitution, established combustion and with diesel switched-off . . . . .	88
5.25	Normalised indicated work, full load, 50% ethanol substitution, established combustion and with diesel switched-off . . . . .	89
6.1	Pressure vs crank angle plot at 2000 rpm, full load on neat diesel fuel . . . . .	101
6.2	Band-pass filtered pressure signal at 2000 rpm, full load on neat diesel fuel . . . . .	101
6.3	Net rate of heat release: full load with neat diesel and misfired compared to the diesel injection signal . . . . .	103
6.4	Net rate of heat release curves with the location of TDC displaced $\pm 5$ crank angle degrees . . . . .	104

6.5	Net rate of heat release curves with the location of TDC displaced $\pm 5$ crank angle degrees . . . . .	105
6.6	Fast Fourier transform of the band-pass filtered in-cylinder pressure signal in Figure 6.2 . . . . .	108
6.7	Posterior density of the start of combustion, $\delta$ , of the band-pass filtered in-cylinder pressure signal in Figure 6.2 . . . . .	110
6.8	Posterior density of the combustion resonance, $\omega$ , of the band-pass filtered in-cylinder pressure signal in Figure 6.2 . . . . .	111
6.9	Model of the band-pass filtered in-cylinder pressure signal in Figure 6.2 . . .	112
6.10	Diesel injection timing at 2000 rpm . . . . .	114
6.11	Start of combustion as determined from the combustion resonance, parameter $\delta$ , at 2000 rpm . . . . .	115
6.12	Ignition delay as determined from the combustion resonance at 2000 rpm . .	115
6.13	Net rate of heat release and start of combustion as determined from the combustion resonance, parameter $\delta$ , at full load . . . . .	116
7.1	Band-pass filtered pressure signal at 2000 rpm, full load on neat diesel fuel .	128
7.2	Diesel injection timing, full load . . . . .	131
7.3	Start of combustion, full load . . . . .	131
7.4	Ignition delay, full load . . . . .	132
7.5	Diesel injection timing, three quarter load . . . . .	133
7.6	Start of combustion, three quarter load . . . . .	133
7.7	Ignition delay, three quarter load . . . . .	134
7.8	Diesel injection timing, half load . . . . .	135
7.9	Start of combustion, half load . . . . .	135
7.10	Ignition delay, half load . . . . .	136
7.11	Standard Deviation of the Ignition Delay Vs the Air to Fuel Ratio . . . . .	137
7.12	Coefficient of Variation of the Ignition Delay Vs the Air to Fuel Ratio . . . .	138
7.13	Ignition Delay Vs the Air to Fuel Ratio . . . . .	138
7.14	Numerical simulation results for increasing inlet air temperatures, simulating the experimental engine condition for full load, 2000 rpm. . . . .	140
7.15	Ignition delay times with varying initial temperatures showing the negative temperature coefficient region. . . . .	141
7.16	Sensitivity analyses of the different fuel compositions at a defined time step before auto-ignition with respect to temperature. . . . .	142
7.17	Ethanol and OH radical concentration at TDC. . . . .	143
8.1	Location of in-cylinder pressure transducer . . . . .	154
8.2	Band-pass (4-12 kHz) filtered pressure signal, full load, 2000 rpm . . . . .	156

8.3	Pressure vs crank angle plot, full load, 2000 rpm . . . . .	156
8.4	Apparent net rate of heat release, full load, 2000 rpm . . . . .	160
8.5	Model fit to signal shown in Figure 8.2 . . . . .	162
8.6	Residual plot showing that subtraction of the fitted model from the signal shown in Figures 8.2 and 8.5 . . . . .	163
8.7	Example resonant frequency with respect to crank angle from model fit shown in Figure 8.5 . . . . .	164
8.8	Resonant frequency of the signal shown in Figure 8.2 isolated using a contin- uous wavelet transform . . . . .	165
8.9	Distribution of the initial resonant frequency over 500 consecutive cycles . .	165
8.10	Distribution of the start of pre-mixed combustion over 500 consecutive cycles	166
8.11	Distribution of the ignition delay over 500 consecutive cycles . . . . .	167
8.12	Distribution of the start of diffusion combustion over 500 consecutive cycles .	167
8.13	Distribution of the initial multiplicative parameter, $\beta_1$ , over 500 consecutive cycles . . . . .	168
8.14	Distribution of the diffusion combustion multiplicative parameter, $\beta_2$ , over 500 consecutive cycles . . . . .	168
8.15	Distribution of the reduction in combustion intensity parameter, $\beta_3$ , over 500 consecutive cycles . . . . .	169
8.16	Distribution of the cycle resolved nominal trapped mass over 500 consecutive cycles . . . . .	171
8.17	In-cylinder bulk temperature as a function of crank angle . . . . .	172
8.18	Distribution of the initial in-cylinder bulk temperature across 500 consecutive cycles . . . . .	172

# Table of Tables

3.1	Results of the supplied pressure values and those measured from the piezo-electric transducer . . . . .	38
5.1	Ethanol substitutions at each test setting . . . . .	68
6.1	Engine and data acquisition specifications . . . . .	100
6.2	Model priors and parameter estimates of the band-pass filtered in-cylinder pressure signal shown in Figures 6.2 and 6.9 based on the model described by Equation 6.3 . . . . .	112
7.1	Ethanol energy substitutions at each test setting . . . . .	129
8.1	Engine and data acquisition specifications . . . . .	155
8.2	Model parameter prior and posterior distributions . . . . .	163

# Acknowledgements

It is rather fitting that the acknowledgements section of a PhD dissertation finds its way to the front. Whilst this dissertation has a single author, the work involved a great many people without whom I would not have made it this far. In this section I will endeavour to name as many of the people who have contributed to this work as possible; unfortunately, this list will not be exhaustive and some important people whose contribution was outside of the academic world will not be officially named in this document. To the numerous people who have given me emotional support throughout not only the PhD years but those that came before it, I give my deepest thanks. The small amount of sanity that I still cling to is owed to your friendship and support, this has been a long road and I am glad that I had good friends to help me along it.

## *Associate Professor Richard Brown*

Most of this list will not necessarily be in order of importance. However in this case, Associate Professor Richard Brown is not only the first to be acknowledged, but also the most important contributor to this work. Associate Professor Richard Brown was my principal supervisor, in fact for the vast majority of my PhD he was my only supervisor. Over the years we have learned a great deal and have enjoyed research and teaching together.

Student learning is very important to Associate Professor Richard Brown, this is evident not only in the manner in which he supervises but also in the effort and care he puts into teaching his undergraduate students. He works tirelessly to ensure that all of his students are well looked after and are achieving their set outcomes. Associate Professor Richard Brown has a knack for knowing what students require, and he is very good at ensuring they get it. On numerous occasions Associate Professor Richard Brown has even used his own finances to purchase needed equipment for experiments and offered financial support when the need was there.

From a research perspective, Associate Professor Richard Brown kept me on track whilst allowing me the freedom to really explore ideas. This PhD delved into an area foreign to both of us, instead of pushing me away from going in the direction I had chosen Associate Professor Richard Brown worked to enhance it with his own knowledge. I strongly believe that the quality of this work is attributable to the collaborative nature in which we worked together. Even during periods where the work was slow and not bearing any fruit, Associate Professor Richard Brown kept his faith in my ability to push through and make something out of it. It is mostly for this that I give my thanks, having someone believe in you and

maintaining your morale is essential in an undertaking such as a PhD, at the end of it I know for certain that I had the right supervisor to see me through this process.

*Doctor Robert Reeves*

When I first had the idea to apply Bayesian statistics to the problem of analysing in-cylinder pressure data, luck had me knock on Doctor Robert Reeves door—conveniently, he was the closest Bayesian statistician to my office. Without having previously met me he happily took the time to listen to my thoughts and research proposal and thankfully agreed that a Bayesian approach would indeed be sensible. Doctor Robert Reeves then took on the difficult task of teaching me statistics. At the time, I had only done the core first year statistics courses and those I did a good few years earlier. I signed on to take his honours mathematics unit in Bayesian statistics and each week Doctor Robert Reeves took hours out of his time to teach me all of the statistics that was missing from my education to catch me up as I went along through his unit.

Unfortunately, Doctor Robert Reeves part in my PhD journey was short. He retired to his true passion, music, and now teaches guitar instead of statistics. However, without his patience and insurance that the Bayesian approach would work for my problem, I likely would have gone a different path.

*Doctor Samantha Low Choy*

Doctor Samantha Low Choy came late into this process, but has undoubtedly saved me countless months of work; I found myself with many questions about applying Bayesian statistics and she came to the rescue. Over the last year she has invested a substantial amount of time correcting my assumptions and helping me develop more sophisticated models for determining resonant frequency information from combustion signals (a primary topic of this thesis). In addition to this, Doctor Samantha Low Choy has had a tremendous effect on the quality of this work and the rate at which it was produced.

*Peak 3 P/L and CEO Colin Chandler*

Peak 3 were the industry partner that funded this project, through an ARC Linkage grant. In many ways this is the most important acknowledgement, without funding this project would never have existed. Peak 3 were very supportive of my work and I expect that good relations with them will continue into the rest of my career.

*Doctor Nicholas Surawski*

Engine experiments were: long, challenging and oft times painful. Having started his PhD journey six months before me, Doctor Nicholas Surawski's work centred on the emission output of the diesel engine. We spent long hours together in the laboratory performing

experiments, trouble shooting technical issues and fixing problems. Prior to us the BERF did not exist, together we worked hard to setup the two sides of experimental engine research; I like to think that we have paved a legacy for engine research at QUT together.

#### *Professor Zoran Ristovski*

Along with Associate Professor Richard Brown, Professor Zoran Ristovski is the other chief investigator on this project. Professor Zoran Ristovski is involved mainly with the emission side of engine research; however, his contribution in terms of experimental design, acquisition of fuel and his general knowledge and leadership are instrumental to the success of the BERF laboratory.

#### *Professor Ted Steinberg*

Throughout the last 2 years of my candidature, Professor Ted Steinberg has acted as a mentor and has provided me with sage advice and his valuable time and help when I have required it. Certainly, without his support there are numerous things that I would not have achieved during my candidature and I would have struggled to support my family without his assistance in finding me adequate teaching work. I am very thankful for all of the assistance and effort that Professor Ted Steinberg has put into helping me survive this journey.

#### *The Technical Staff*

Engine research is very dependent on having competent technical staff. The very able gentlemen who looked after our lab were: Jon James, Glenn Geary, Noel Hartnett and Scott Abbett. Technologists: Anthony Morris, Ken McIvor and Mark Hayne were also valued contributors to this work. Without the time, effort and diligence of these staff members this project never would have left the ground.

#### *The Other PhD Candidates Working in the BERF*

I would like to acknowledge the work of all the other PhD candidates who have been working in BERF during my candidature. In particular I will name: David Lowe, Svetlana Stevanovic and Md Mostafizur Rahman, who have been involved in numerous campaigns with me. You have made being in the laboratory that much more interesting.

#### *The Undergraduates*

Each semester we received undergraduates completing their engineering degrees. There have been too many to thank; however, I will name a few who have gone above and beyond: Adrian Schmidt, Peter Clarke, Steven Herdy, Matthew Anderson and Jackson Kelley.

*My Family*

Last, and definitely not least, is my wonderful family. My wife, Katharina, and our beautiful son, Aurelius (who was born during my candidature). These two people have changed and enriched my life in ways unimaginable. When the work has been hard and stressful, they have provided me with comfort, love and the reason to persevere. I am glad that we've made this important journey together.

Also, to my father, Doctor Alex Bodisco, who has provided me with financial aid and support when times have been difficult, not only during my candidature but also before it.



# Chapter 1

## Current state of knowledge

The perspective of the work in this dissertation is largely in the area of mechanical engineering; however, the techniques employed are more firmly in the mathematics and physics domains. One of the goals of this dissertation, through the published works, is to introduce the use of Bayesian statistics to the engine research community. For this community, Bayesian statistics represent a means to obtain difficult to isolate information, which is directly related to tangible engine outputs: emission and power. However, given that this dissertation is in essence a work in mechanical engineering, this chapter will not focus on Bayesian statistics, but rather on the engineering aspects of this work. Those who are reading this dissertation with the intention of applying Bayesian statistics to their research problems are encouraged to read Chapters 4, 6 and 8 and to consult the text, *Bayesian Data Analysis* by Gelman et al. (2003).

### 1.1 Context

The context of this dissertation is at a time in Australia, and in a research environment (at QUT), where alternative fuels are under investigation. Ethanol fumigation has been selected as the alternative fuelling strategy employed in this work because of its immediate potential to be a sound mid-term solution to reduce the dependence on fossil diesel fuel. Niven (2005) in a review on ethanol in gasoline, states that a lack of vigour in studies involving ethanol in gasoline (easily extendable to any alternative fuel and engine type) is a major problem and that studies which omit details, or are not done in a professional manner, misinform the public and the decision makers. Ideally, the techniques introduced in this dissertation will be used to evaluate all manners of alternative fuels and fuelling strategies. Thus, providing a better understanding of the implications of the use of different alternative fuels. This work is primarily focused on in-cylinder pressure analysis and its role in modern engine research.

#### 1.1.1 Alternative Fuel

Primary fossil fuels include a large variety of products; a primary fossil fuel is a fuel that is non-renewable—for example: oil, coal and uranium. These fuels are often used to generate

power, not only for transport but also for electricity, construction, industrial activities and agriculture (Lloyd and Cackette, 2001). Unfortunately, the use of fossil fuels have negative impacts on our planet and the health of those who occupy it (Lloyd and Cackette, 2001). Further to the problem of harmful emissions and radiation from the use of fossil fuels, they are also in finite supply and that supply is dwindling (Lloyd and Cackette, 2001; US Department of Transportation, 1998; McArdle et al., 2007; Cohn et al., 2005; Kim and Dale, 2004; ICF International, 2008; Ragauskas et al., 2006). Moreover, this supply is also only found in some areas, creating foreign exchange problems for countries that do not have their own reserves or still need to source fuels from foreign suppliers (Ragauskas et al., 2006; Rakopoulos et al., 2007).

Ultimately, it would be advantageous to limit the use of fossil fuels—this work will focus on the research effort to offset diesel fuel. Biofuels are one such alternative that are a viable substitute to diesel fuel; some biofuels have, or can be made to have, similar characteristics to diesel and thus their implementation can be easily made (Yusuf et al., 2011). Biodiesel can be created out of virtually any vegetable oil, animal fat or microalgae (Yusuf et al., 2011; Huang et al., 2010). Alternatively, whilst not renewable, fuel can be synthesised from other more abundant fossil fuels, such as coal, via Fischer-Tropsch synthesis (Song et al., 2012; Dalai et al., 1997; Rajee et al., 1997).

Research has shown that biodiesel fuelled engines produce less carbon monoxide, unburned hydrocarbons, and particulate emissions compared to diesel fuel; however, this is not the case with  $\text{NO}_x$  emissions owing to the typically higher combustion temperature (Ramadhas et al., 2005; Frassoldati et al., 2006; Demirbas, 2007). Another drawback of biodiesel is that it is more prone to oxidation than petroleum-based diesel fuel (Monyem and Van Gerpen, 2001). An additional issue is that different materials and processes used to create biodiesel produce vastly different results in terms of contaminants, calorific value, viscosity and cetane number, therefore the performance, level of engine wear and potentially harmful emissions are not consistent between the various bio-derived fuels (Van Gerpen et al., 1997). In order to avoid consumer rejection it would very important to ensure that any bio-originated fuel is controlled with strict standards, but also understood well enough to set those standards at an economically achievable level.

With strict future goals to have bio-origin fuels offsetting fossil fuels in the transport sector, research into biofuels is being conducted worldwide, even by major oil companies (Skelton, 2007). A currently implemented strategy to do this is with ethanol in terms of gasoline/ethanol blends in the form of E10 and E85—10% ethanol and 85% ethanol substitution respectively (Niven, 2005). However, ethanol also has the potential to offset not only gasoline but also diesel fuel.

Offsetting diesel fuel by blending it with ethanol has a few critical issues. Firstly, ethanol is not directly soluble in diesel and requires an emulsifying agent to make it so (Hansen et al.,

2005; Karthikeyana and Mahalakshmi, 2007)—diesel/ethanol blends are not stable under all conditions mostly due to their low tolerance to water (Karthikeyana and Mahalakshmi, 2007; Havemann et al., 1954). Further, ethanol also has a lower cetane number and flash point, this makes its use in a blend with diesel without slight modification of the engine not optimally efficient (Hansen et al., 2005). From an engine stand point, the addition of ethanol changes the viscosity of the diesel fuel and can create wear problems with fuel pumps—although blends up to 15% (by volume) can be considered relatively safe from an engine durability viewpoint (Hansen et al., 2005; Demirbas and Balat, 2006; Rakopoulos et al., 2007). A solution to avoid blending is to introduce the ethanol separately with the intake air by a process known as fumigation.

Fumigation is the introduction of atomised fuel to the intake manifold so that it can be mixed with air before entering the cylinder (Alperstein et al., 1958). Manifold introduction of fuels into a compression ignition engine was experimented with at The Pennsylvania State University in the early 1940's (Van Overbeke, 1942; Alperstein et al., 1958); important early recognised work was done by Alperstein et al. (1958). The idea behind the introduction of this concept was to alleviate two of the major disadvantages of diesel engines: incomplete mixing of air and fuel and late combustion caused by ignition delay (Alperstein et al., 1958). As a further advantage, using alcohols in this manner also resolves the problem of separation when water comes into contact with a diesel/alcohol blend (Havemann et al., 1954).

In diesel engines fumigation can be achieved with virtually any gaseous fuel. Although lower alcohols, such as methanol and ethanol, are not gaseous there is still a large amount of interest in using them as a secondary fuel in diesel engines through this method. Up to 50% of the diesel fuel demand can be displaced using ethanol fumigation (Broukhiyan and Lestz, 1981; Hayes et al., 1988; Abu-Qudais et al., 2000). This method involves introducing the alcohol either by carburetting, vaporising or injecting it at high pressure into the intake air stream, or at the turbocharger (Alperstein et al., 1958; Hayes et al., 1988; Abu-Qudais et al., 2000).

It is widely accepted that the introduction of fumigated fuels increase ignition delay, peak pressure, and maximum rate of pressure rise (Alperstein et al., 1958; Chen et al., 1981; Shropshire and Goering, 1982; Hayes et al., 1988; Henham and Makkar, 1998; Prakash et al., 1999; Ajav et al., 2000). Some authors report that at lower loads there is a reduction in peak pressure and the rate of pressure rise, although in these studies the ignition delay still increased up to 35% (Chen et al., 1981; Hayes et al., 1988; Ajav et al., 2000). Suggested reasons for the increase in ignition delay include, the typically lower cetane value of the fumigated fuel and the so-called cooling effect from the increase in energy required to heat the charge air/fuel mixture during the compression stroke (Saeed and Henein, 1989; Tsang et al., 2010).

While this method is not completely ideal, it does have the potential to be a sound mid-

term solution to the world fuel crisis (Rosillo-Calle and Walter, 2006; Sorda et al., 2010). This is true not only in general transport but also in agriculture, particularly those industries that can produce their own ethanol, and for the use in electricity generators (RIRDC, 2007).

### 1.1.2 Modern Diesel Engines

Engines for general transport and power generation have undergone radical changes since their conception. At the beginning of the 19th century, there were four commercially available types of oil engines (Secor, 1913): the Brayton engine; the Hornsby-Akroyd engine; the Diesel engine; and, the Secor engine. The Brayton engine was a constant flame engine and is regarded as the predecessor of the Otto (gasoline) engine. In these early days, there was much speculation as to what was the most appropriate fuel, and hence style of engine, which should become the norm. Early strong fuel candidates were ethanol, gasoline and kerosene (Secor, 1913; Lucke, 1916). Ethanol was largely dismissed because at the time it was financially prohibitive—although, even at this early stage Secor (1913) already argued that if gasoline prices rose, ethanol would be a suitable alternative. However, oil was deemed near limitless at the time and greatly superior in quality, comparatively, as an automotive fuel (Secor, 1913). Diesel’s high thermal efficiency eventually made it the primary engine for heavy-duty transport (a diesel engine uses only  $\sim 70\%$  of the fuel that a comparable gasoline engine consumes for the same power output (Lloyd and Cackette, 2001)).

The diesel engine was originally patented in 1892 by Rudolf Diesel (Diesel, 1892). Originally, the brake thermal efficiency was low; but, in 1897 a form of fuel fumigation improved this to greater than 26% (Merrion, 1994). However, this was further improved in standard operation to 35% by as early as the 1910s (Secor, 1913). One hundred years later and although there have been great improvements to diesel engines, the brake thermal efficiency of a standard automotive diesel engine has not substantially risen from 35%—typical brake thermal efficiencies range between 35 and 40%.

Improvements with diesel engines have often focused on meeting emission standards and reducing noise. Typically, these improvements are in engine technology or fuel technology. The driving force behind these advancements are the stringent demands on emission levels set out by governing authorities (Velders et al., 2011; Shindell et al., 2011; EC, 2009; Needham et al., 1990).

In terms of the engine technology, recent important advances include: exhaust gas recirculation (EGR), combustion chamber geometry, high-pressure fuel delivery with common-rail injection and pilot and multi-stage injection (Uchida et al., 1998; Badami et al., 1999; Zamboni and Capobianco, 2012). High-pressure fuel delivery causes more rapid mixing of the fuel/air mixture, compared to the traditional in-line pump system, which results in shorter ignition delay and ignition that originates at the front of the spray (Xu-Guang et al., 2012). Injection timing close to top dead centre (TDC) with high pressure injection has been shown

to reduce emission levels without compromising fuel efficiency (Kanda et al., 2006).

Although the current literature has explored the effects of numerous alternative fuels and fuelling strategies, the significant difference that the injection pressure and timing has on combustion requires that these ideas be re-evaluated. For any alternative fuel, or new engine technology, to be successful it will need to be proven on a modern engine with that utilises technology that allows for advanced high pressure injection. Moreover, the effects of alternative fuels should also be evaluated on engines that resemble those used in practice, i.e. multi-cylinder engines with high indicated mean effective pressures.

## 1.2 In-cylinder Pressure Analysis

In-cylinder pressure is the means by which chemical energy is transformed during combustion into useful work (Amann, 1986). Hence, examination of the in-cylinder pressure can give insight into the engines ability to produce useful work; the area enclosed in a pressure vs volume ( $p$ - $V$ ) indicator diagram, example in Figure 1.1, is the work done by the cylinder (Amann, 1986; Heywood, 1988):

$$W = \oint p dV$$

However, as the greatest rate of change of pressure occurs during combustion near top dead centre (TDC), of the piston's motion, where the velocity of the piston is low, it is necessary to examine the pressure vs crank angle ( $p$ - $\theta$ ), or a pressure vs time, indicator diagram to obtain the detailed characteristics of combustion (Amann, 1986).

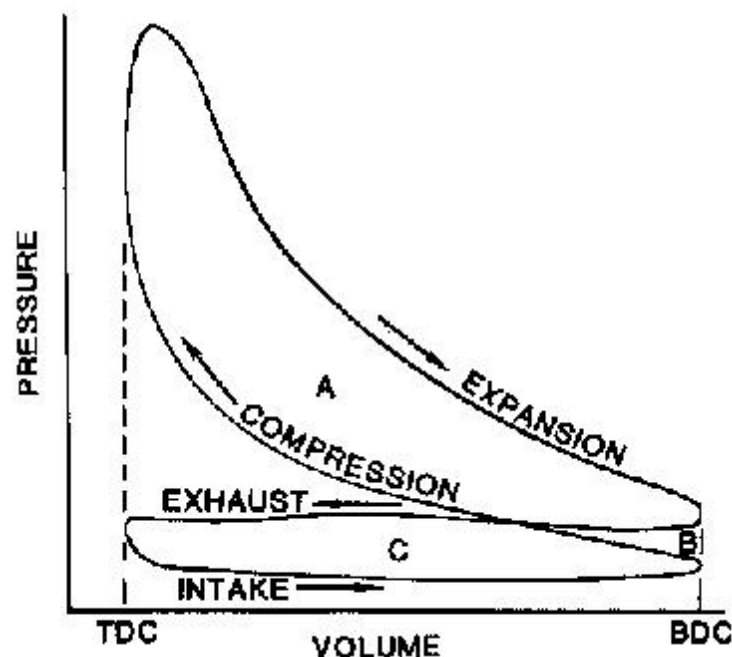


Figure 1.1: Pressure vs Volume indicator diagram (Amann, 1986)

Detonation is also something that can be determined from the in-cylinder pressure. In early work different systems were used for the detection of detonation from those used to create  $p$ - $V$  indicator diagrams. This area was pioneered by Midgely and Boyd (1922) and had significant early advances from Draper (1938).

Early indicator instruments produced  $p$ - $V$  indicator diagrams via an oscillating drum carrying a sheet of paper to record the piston stroke. Simultaneously, a small piston in direct connection to the engine cylinder would produce a pressure trace amplified by a system of links and levers (Greene and Lucas, 1969). Other popular early choices for obtaining pressure information was with the use of stroboscopic, or point-by-point, instruments (Taylor and Taylor, 1966). Kistler invented one of the first common place piezoelectric transducers to measure in-cylinder pressure (Kistler, 1950; Sion and Atkinson, 2002), since then they have become the standard in engine research (Lee et al., 2008).

A piezoelectric transducer does not measure absolute pressure. Rather, the measured voltage has a linear dependency with the in-cylinder pressure (Randolph, 1990; Lee et al., 2008):

$$P_{abs}(t) = kV(t) + P_{ref}$$

where,  $k$  is a constant (typically supplied by the manufacturer),  $V(t)$  is the measured voltage and  $P_{ref}$  is the sensor offset. Even though this type of transducer does not measure absolute pressure and requires the determination of an offset value, which can be inaccurate, it is ideal because of their fast response, small size and low sensitivity to environmental conditions (Lee et al., 2008; Brunt and Pond, 1997). This style of pressure transducer is the most commonly used in engine research.

The importance of accurate knowledge of in-cylinder pressure has lead to many advances in the technology to acquire it, Kistler is still a major player in the development of more sophisticated sensors. From a  $p$ - $V$  indicator diagram, the area between the compression and expansion lines is the indicated work done by the piston. Therefore, in-cylinder pressure is typically used to investigate quantities related to work, such as: the indicated power and the indicated mean effective pressure. In-cylinder pressure data is also commonly used to investigate: peak pressure, maximum rate of change of pressure, heat release, and thermal efficiency (Heisey and Letsz, 1981; Amann, 1986; Heywood, 1988; Randolph, 1990; Hasegawa et al., 2006). This information is determined by observing various aspects of pressure, volume and crank angle data.

Lapuerta et al. (1999) states that, ‘*the key to internal combustion engine optimisation lies in understanding the process taking place in the engine combustion chamber*’. Many important combustion related parameters can be determined from the in-cylinder pressure—many of these parameters are determined from heat release analysis involving the first law

of thermodynamics, Equation 1.1 (Heywood, 1988; Payri et al., 2010). As examples, in-cylinder pressure can be useful for: air mass flow estimation (Desantes et al., 2010), on-line combustion failure detection (Shimasaki et al., 2004), in-cylinder trapped mass estimation (Worm, 2005; Lapuerta et al., 1999), in-cylinder temperature estimation (Hickling et al., 1983), exhaust gas recirculation control (Sellnau et al., 2000; Hasegawa et al., 2006), torque estimation (Shimasaki et al., 2004), emission control (Beasley et al., 2006) and noise control (Payri et al., 2005).

$$\frac{dQ_n}{dt} = \frac{\gamma}{\gamma - 1} p \frac{dV}{dt} + \frac{1}{\gamma - 1} V \frac{dp}{dt}, \quad (1.1)$$

where,  $\frac{dQ_n}{dt}$  is the net rate of heat release,  $\gamma$  is the ratio of specific heats,  $p$  is the in-cylinder pressure,  $V$  is the in-cylinder volume and  $t$  is time. More complicated versions of Equation 1.1 exist that take into account heat loss to the walls, effects of crevice regions and other possible sources for heat loss.

A common operating parameter which can be obtained from the in-cylinder pressure signal is the start of combustion—coupled with knowledge of the start of injection can yield the ignition delay. In a recent study by Rothamer and Murphy (2012), six methods of determining the start of combustion were compared. The six methods were:

1. location of 50% of pressure rise due to premixed burn combustion;
2. extrapolation of the peak slope of pressure rise due to combustion to the zero crossing point;
3. location of the first peak of the second derivative of the pressure trace;
4. location of the first peak of the third derivative of the pressure trace;
5. location of 10% of the maximum heat release rate in the premixed burn; and,
6. a repeat of (5) using a low-pass (threshold 2000 Hz) filtered in-cylinder pressure trace.

Their study focused on jet fuels and diesel fuel in a heavy-duty direct-injection single-cylinder diesel and the data analysis was performed using 250 cycles of averaged data. A conclusion from their study found that the methods which required second or third derivatives were not optimal owing to the presence of noise and that the ignition delay determined by the heat release method using the low-pass filtered in-cylinder pressure signal gave a result 200-330  $\mu$ s shorter than the other methods.

A common theme among in-cylinder pressure methods for determining the start of combustion is differentiating (Heywood, 1988; Stone, 1999; Lata and Misra, 2011; Rothamer and Murphy, 2012). The most typical methods are: locating the time when the heat release slope begins increasing (Kouremenos et al., 1992; Rakopoulos et al., 2007; Shehata, 2010; Tautzia et al., 2010), locating the time when the heat release becomes positive (Lata and

Misra, 2011) and locating the time when the rate of pressure rise begins increasing rapidly (from either a first, second or third derivative of the in-cylinder pressure signal) (Stone, 1999; Rothamer and Murphy, 2012). However, there are issues with the use of heat release curves for the determination of the start of combustion. A few of these issues include (Heywood, 1988; Brunt and Platts, 1999; Tauzia et al., 2010):

- the difficulty in accounting for mixture nonuniformities in the air/fuel ratio and in the burned and unburned gas nonuniformities;
- the effect of crevice regions in the combustion chamber; and,
- assuming the wrong rate of heat transfer between the cylinder charge and combustion chamber walls (especially with the addition of a ‘cooling’ additive such as water, or a fumigated fuel in a dual-fuel engine).

Moreover, the calculation of the heat release relies on knowledge of the in-cylinder volume, which is sensitive to the exact knowledge of top dead centre (TDC).

Heat release diagrams are also useful for studies which involve looking at the effects of the intensity and duration of combustion. These types of studies are often seen with comprehensive emission work (Rakopoulos, 2012; Valentino et al., 2012). Sections of the heat release curve are typically split into the following phases: ignition delay period, premixed combustion phase, mixing-controlled combustion phase and the late combustion phase (Heywood, 1988). Figure 1.2 shows an example heat release rate diagram from Heywood (1988) of a DI engine. It should be noted, however, that in a modern engine the transition from the pre-mixed to the diffusion stage is not as clear and forms a partial motivator for the work shown later in Chapter 8.

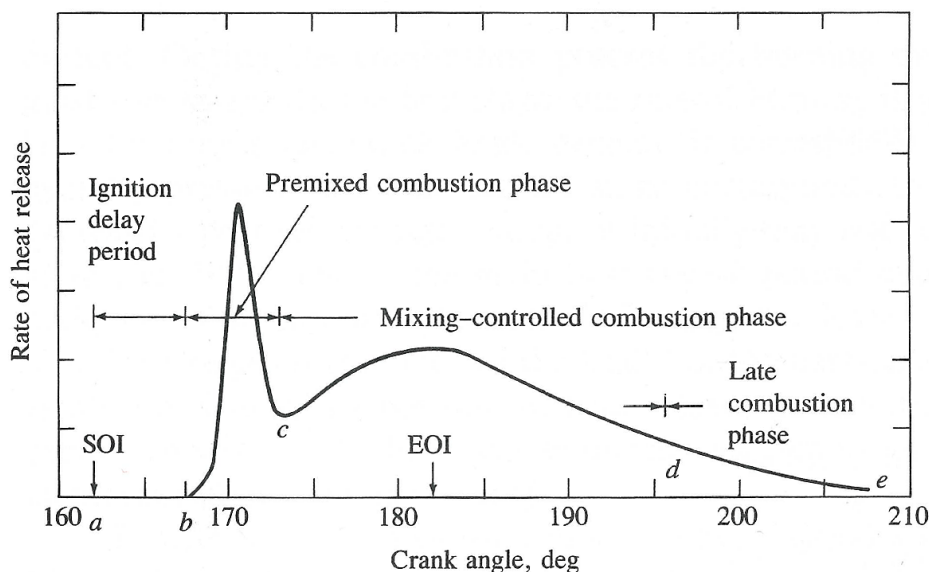


Figure 1.2: Typical DI engine heat release rate diagram identifying different diesel combustion phases (Heywood, 1988)



One valuable method for detecting the start of combustion is to examine a block vibration signal—the band-pass filtered in-cylinder pressure signal is similar to the vibration signal (Carlucci et al., 2006). Links between in-cylinder pressure and structure-borne sound make it an interesting area of investigation. Antoni et al. (2002b) have shown that a  $p$ - $V$  indicator diagram is even obtainable from analysis of the vibration measurements. This paper by Antoni et al. (2002b) also goes further into evaluating the combustion process phenomena, although they admit that techniques they employ are somewhat ad hoc. Stankovic and Bohme (1999) have also done an investigation linking in-cylinder pressure to structure-borne sound through both simulations and experimental data.

Structure-borne sound is widely used to monitor machines (Steel and Reuben, 2005). From an industry perspective phenomena such as wear, cavitation, plastic deformation, cracking and fracture can be detected through the use of structure-borne sound (Carpenter and Zhu, 1991; Miettinen and Siekkinen, 1995; Carolan et al., 1997; Neill et al., 1997; Rogers et al., 1998; Brown et al., 1999). However, from an engine research perspective it can be useful to detect mechanical events, processes such as: combustion, fuel efficiency, combustion conditions, lubrication and also fault detection (Fog, 1998; El Ghamry et al., 1998, 2003).

The highly transient nature of internal combustion engines makes their vibration very complex in nature (Antoni et al., 2002a). Therefore, the data collected from structure-borne sensors on engines are also non-stationary making traditional techniques of analysis non-suitable. Further, these types of sensors are sensitive to noise and that can introduce problems in the analysis (Steel and Reuben, 2005).

Antoni et al. (2002a) state that the main sources of excitation that are likely to be observable from the block vibration signal are associated with the following mechanisms:

- (i) rocking and twisting of the engine block on its supports, due to the action of inertial forces
- (ii) impacts due to clearances at links, those at the crankshaft bearings and the so-called piston slap being extremely noisy
- (iii) closures and openings of valves
- (iv) high-pressure injection of fuel in diesel engines; and
- (v) rapid rising of gas pressure in the cylinders during the combustion, especially in diesel engines where it has been compared with a hammer blow.

This dissertation has a significant focus on band-pass filtered in-cylinder pressure signals. Band-pass filtered in-cylinder pressure signals share many common features with block-vibration signals—including frequency content associated with combustion. Therefore, the analysis techniques described in this work can also be applied to block-vibration signals.

### 1.3 Combustion Resonance

Payri et al. (2005) decompose the in-cylinder pressure signal into three distinct parts: pseudo-motored, combustion and resonance excitation. The pseudo-motored frequencies are associated with the engine operating conditions: namely, engine load and speed (Payri et al., 2005). In the work by Payri et al. (2005), in-cylinder pressure information above the pseudo-motored frequencies are termed as ‘excess pressure’. This ‘excess pressure’ if analysed carefully can yield valuable information about the combustion processes (Hickling et al., 1983) and also provide useful condition monitoring information (i.e. knock detection) (Ren et al., 1999).

The in-cylinder resonance excitation has been attributed to the sudden pressure rise associated with pre-mixed combustion (Schaberg et al., 1990; Payri et al., 2005; Torregrosa et al., 2011). Typically, this resonance excitation, henceforth termed the combustion resonance, is seen in the frequencies above 6 kHz (Payri et al., 2005; Ren et al., 1999; Schmillen and Wolschendorf, 1989; Torregrosa et al., 2004). Of particular interest in this work is the resonant frequency that forms the combustion resonance. Isolation of the resonant frequency is important as it is related to the speed of sound and hence temperature (Hickling et al., 1983; Bohme and Konig, 1994; Ren et al., 1999; Torregrosa et al., 2004; Payri et al., 2005).

If the assumption of a homogeneous composition in the combustion chamber is assumed, then the in-cylinder temperature can be determined by the following relationships (Hickling et al., 1983):

$$\begin{aligned} c(t) &= \frac{r(t)B}{\alpha_{mn}} \\ c^2(t) &= \gamma RT(t) \\ \therefore T(t) &= (\gamma R)^{-1} \left( \frac{r(t)B}{\alpha_{mn}} \right)^2, \end{aligned}$$

where,  $\alpha_{mn}$  is a non-dimensional value determined by solving the equation:

$$J'_m(\pi\alpha_{mn}) = 0$$

and  $r(t)$  is the time-varying resonant frequency,  $B$  is the cylinder bore,  $\gamma$  is the ratio of specific heats of the bulk modulus in the combustion chamber,  $R$  is the characteristic gas constant and  $T(t)$  is the time-varying in-cylinder temperature.  $J'_m$  is the derivative of the Bessel function of the first kind and order  $m$  (Hickling et al., 1983; Morse and Ingard, 1968). The general Bessel function of the first kind and order  $m$  can be approximated by the infinite

series (Kaplan, 2003):

$$J_m(x) = \sum_{i=0}^{\infty} \frac{(-1)^i}{i! \Gamma(m+i+1)} \left(\frac{x}{2}\right)^{m+2i}$$

and the derivative of the Bessel function of the first kind can be shown to be:

$$J'_m(x) = \frac{1}{2}(J_{m-1}(x) - J_{m+1}(x)).$$

Hence,  $\alpha_{mn}$  can be solved for by:

$$J_{m-1}(\pi\alpha_{mn}) = J_{m+1}(\pi\alpha_{mn}).$$

The in-cylinder temperature can be an indicator of what is occurring during combustion and the thermodynamic processes in the cylinder of the engine (Hickling et al., 1983). Moreover, the in-cylinder temperature can be used in conjunction with the ideal gas law to estimate the trapped mass present in the combustion chamber (Hickling et al., 1983).

A key issue, of which this dissertation will address, is how to isolate the resonant frequency. A difficulty is that the combustion chamber is a complex environment, especially during combustion. Most notably, there are rapid changes in in-cylinder temperature during pre-mixed combustion, which greatly effect the speed of sound and hence the resonant frequency. Isolating a transient frequency from a signal has many issues and the following will briefly discuss some of the common techniques that are used for this type of signal processing. Namely, it will discuss: fast Fourier transforms, Burg spectral density estimates, Wigner-Ville spectral analysis and Bayesian inference. Other emerging techniques involving wavelet transforms and Hilbert transforms are not covered in this overview as they are not explored in this work.

### 1.3.1 Traditional Techniques

#### Fast Fourier Transforms

Since Cooley and Tukey (1965; 1969) introduced the fast Fourier transform (FFT) they have become the standard in basic spectral analysis. Applications of FFTs are vast and present in most fields of science and engineering—such as spectral analysis, signal processing, time series analysis, Fourier spectroscopy, image processing, and the solution of differential equations (Cooley et al., 1969). Typically, researchers interested in combustion resonance have used FFTs to find the desired frequency information (Li et al., 2001; Torregrosa et al., 2004; Payri et al., 2005). The increase in interest in digital signal processing in the 1970's has been attributed, by some, to the FFT (Duhamel and Vetterli, 1990; Oppenheim and Schaffer, 1975;

Rabiner and Rader, 1972).

Fast Fourier transforms are common practice in basic spectral analysis mostly because of their ease of use and computational efficiency (Cooley et al., 1969; Duhamel and Vetterli, 1990; Huang et al., 1998; Papandreou-Suppappola, 2003). However, a significant limitation is in the assumptions which underpin them—for example, the assumption of periodic stationary frequencies (Bretthorst, 1988a; Jaynes, 1987). Moreover, in order to produce any useful results multiple periods of data are required (Gregory and Loredo, 1992)—in some applications, such as isolating the resonant frequency, analysing multiple periods simultaneously is counter intuitive. Furthermore, the low resolution makes it impossible to resolve close together frequencies, giving the illusion of there only being a single frequency where there may be multiple—frequencies need to be separated by at least the Nyquist step ( $|\omega_1 - \omega_2| > \frac{2\pi}{N}$ ) for a difference to be distinguishable (Dou and Hodgson, 1995).

In most real world situations that data can be derived from, the frequency content are not stationary, free from noise or non-complex. Therefore, the FFT method may often produce, according to Jaynes (1987) and Bretthorst (1988a), potentially misleading results. Bretthorst (1988b) did, however, show that the FFT does give optimal frequency estimates to a signal, with noise, if each of the following conditions are met:

- (i) the number of data values  $N$  is large;
- (ii) there is no constant component in the data;
- (iii) there is no evidence of a low frequency;
- (iv) the data contain only one frequency;
- (v) that frequency is stationary; and,
- (vi) the noise is white.

Moreover, the interpretation of high frequencies as low frequencies (aliasing), which can occur when there are frequencies above half the sampling frequency, is also a potential issue if the data is not carefully digitised (Randall, 1987). Typically any misleading results obtained with FFTs are not incorrect because of the FFT, they are rather incorrect because the FFT is attempting to answer a different question (Dou and Hodgson, 1995). Hence, in many applications other methods of spectral analysis should be investigated to ensure that the results are accurate and therefore suitable for making decisions. In data analysis, emphasis should be given to scientific interest and less to convenience (Box and Tiao, 1992).

### **Burg Spectral Density Estimate**

Outside of FFTs another early method of spectral analysis is that from Burg (Burg, 1972). Burg's method of spectral analysis uses autoregressive models (Broersen, 2000). Similar to

the FFT, Burg's method relies on having large amounts of data and also has low resolution. However, the resolution is improved when compared to the FFT.

Burg's method requires the analyst to choose the auto-regression order, of which there is no theoretical means of selection (Bretthorst, 1988a). The issue of choosing the auto-regressive order can sometimes shift the location of the predicted frequency (Bretthorst, 1988a). Moreover, this method is also sensitive to noise and limited data.

## Wigner-Ville Spectral Analysis

In practice signals are seldom built from stationary frequencies, particularly in applications involving machinery (Randall, 1987). Therefore, analysis of real world signals do not necessarily lend themselves to basic sinusoidal decomposition. A result of this is the rise of the concept of the instantaneous frequency (Martin and Flandrin, 1985; Boashash, 1992).

Ville showed (Ville, 1948; Boashash, 1992) that the first moment of the Wigner-Ville distribution (WVD) with respect to frequency yields the instantaneous frequency. The WVD can be numerically evaluated using FFT algorithms (Martin and Flandrin, 1985; Boashash, 1988, 1992). This original work was before Cooley and Tukey (1965) created the FFT, and therefore it was a while after this concept that the use of the WVD became a fixture in spectral analysis.

Use of the Wigner-Ville method of spectral analysis is not uncommon in engine research (Bohme and Konig, 1994; Stankovic, 1994a,b; Samimy and Rizzoni, 1996; Ren et al., 1999). However, it suffers from many problems, with the most noted being issues with cross talk. Further problems associated with the use of the WVD for spectral analysis arise with sensitivity to noise and the need for large amounts of data. Indeed with the numerical application of the WVD being from the use of FFTs it is an easy conclusion to draw that it will have many of the same limitations.

### 1.3.2 Bayesian Spectral Analysis

E. T. Jaynes in his 1987 paper derived the discrete Fourier transform using Bayesian probability theory. Spectral analysis of this type is directly dependent on the signal-to-noise ratio and the resolution can be many orders of magnitude better than more conventional Fourier analysis (Jaynes, 1987; Gregory, 2001). Jaynes' (1987) work was the beginning of the Bayesian revolution in spectral analysis, with much of the earlier work done by Bretthorst (1988a; 1989).

Gregory (2001) uses examples from physics and astronomy to review the use of Bayesian inference in spectral analysis (Gregory, 2001). He mostly focuses on phenomena with periodic patterns, hence the strong focus on astronomy where this is especially relevant. The examples in Figures 1.3 and 1.4 are from Gregory (2001) and Bretthorst (1988b), respectively.

Figure 1.3 shows the superior resolution, and the resistance to noise, of the Bayesian

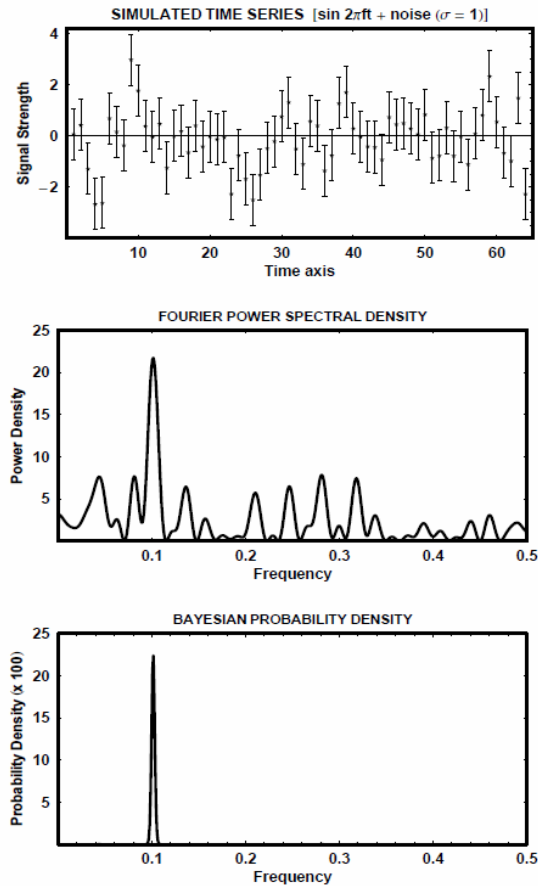


Figure 1.3: Comparison of conventional analysis (middle panel) and Bayesian analysis (lower panel) of a simulated time series (upper panel) (Gregory, 2001)

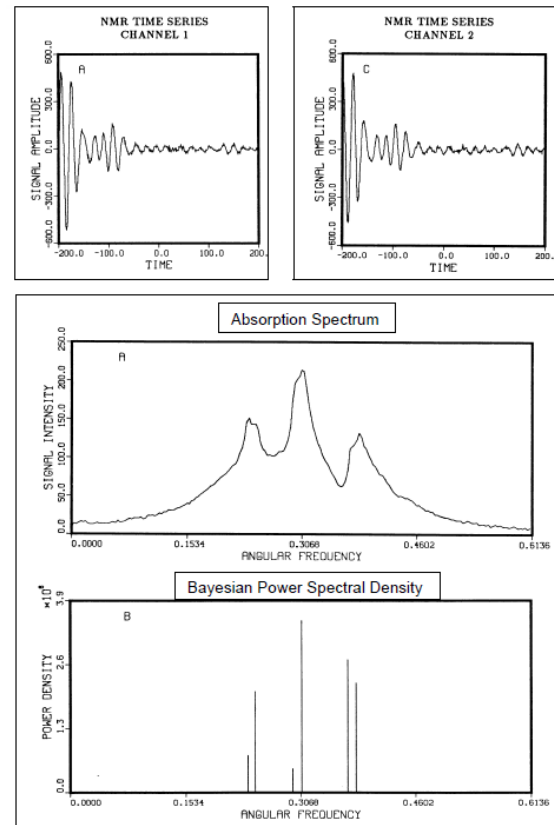


Figure 1.4: Comparison of conventional analysis (middle panel) and Bayesian analysis (lower panel) of the two channel NMR time series (upper two panels) (Bretthorst, 1988b; Gregory, 2001)

method compared to the Fourier one. Likewise, Figure 1.4 shows this along with demonstrating how the Fourier method can give misleading results. In Figure 1.4 the analysis with the Fourier method shows three clear distinct peaks, whereas the Bayesian analysis clearly shows that there are six frequencies present in the data. Further, it also gives evidence that the Fourier method can produce unclear and skewed results when there are close together frequencies.

Although Bayesian inference is not a new idea it has only been in the last decade that it has become a mainstream method in statistics and signal processing. Fitzgerald (2001) delivers a review style tutorial on numerical Bayesian methods of inference with a focus on signal processing applications. He also goes further to describe applications of Markov-chain Monte Carlo (MCMC) in audio and image restoration using this as an example of how Bayesian statistics can be exploited in applied engineering problems.

The power of Bayesian analysis, in any context, is the ability to introduce prior knowledge into the analysis (Bretthorst, 1988b; Jaynes, 2007). Even when there is no prior knowledge,

analysis can still be performed from a state of ignorance—this is often the case with scientific data (Box and Tiao, 1992). Gelman et al. (2003) gave a detailed discussion on prior distributions in their book *Bayesian Data Analysis*. Bayesian analysis also allows the analyst to keep track of all the assumptions and prior knowledge that is introduced. A distinct advantage of this is that if unacceptable inferences are made then it may be a result of inappropriate assumptions as opposed to inadequacies of the inferential system (Box and Tiao, 1992).

This dissertation will introduce, through the published works, the use of Bayesian statistics to analyse in-cylinder pressure data, with a particular interest in resolving the start of combustion and the frequency information during combustion. Moreover, it will be shown that using statistical modelling in a Bayesian framework eliminates the need for ad hoc methodologies, such as cycle averaging to obtain reliable results. The ability to analyse single consecutive cycles of engine operation allows further investigation into the inter-cycle variability. It should be noted that although a Bayesian approach has been taken for this work, there are other methods that show promise, such as using wavelet transforms (Kim and Min, 2008; Li et al., 2001).

## 1.4 Inter-cycle Variability

Kouremenos et al. (1992) investigated the cycle-by-cycle variation of key in-cylinder parameters: peak pressure, peak pressure timing, maximum rate of pressure rise and maximum rate of pressure rise timing. This study involved analysing 650 consecutive cycles of data from a single-cylinder Lister LV1, four-stroke, direct-injection diesel engine at a variety of injection timings and load conditions. By analysing the effect on the mean value, standard deviation, variance, coefficient of variation, probability density functions and power spectra across an increasing number of cycles, they concluded that for their engine setup a minimum of 400 cycles was required to ensure statistical stability. However, the required number of cycles to produce stable results will vary from one engine setup to another (Payri et al., 2010).

A follow-on study from the early work of Kouremenos et al. (1992) was done by Rakopoulos et al. (2008) investigating the effect on combustion cyclic variability of a diesel engine using ethanol/diesel blends—over 480 consecutive cycles. This work investigated the in-cylinder parameters: peak pressure, peak pressure timing, indicated mean effective pressure, injection timing and ignition delay. Cycle-by-cycle analysis allowed them to conclude that ethanol/diesel blends of up to 15% percent had no influence on cyclic-variability and hence performance degradation.

Analysing the cyclic variation of combustion processes can improve combustion control, resulting in improved: fuel economy, performance and emission (Johansson, 1996; Morey and Seers, 2010). Increased cyclic variability can be used as an indicator of degraded performance and emission management (Rakopoulos et al., 2008). Therefore, investigation into inter-cycle

variability should form the norm for all in-cylinder pressure analysis.

Research into inter-cycle variability in the past, however, has mostly only focused on spark-ignition engines, with some more recent work conducted on compression-ignition engines (Sen et al., 2008). It has been well observed that with spark-ignition engines that an increase in inter-cycle variability causes performance and noise issues and increases harmful emissions (Heywood, 1988; Johansson, 1996). The absence of early work with compression-ignition engines on this topic can be noted by it not being covered in John Heywood's (1988) comprehensive book, *Internal Combustion Engine Fundamentals*.

A major issue with in-cylinder pressure signals is noise (Payri et al., 2010). For many of the standard analyses (indicated mean effective pressure, indicated power and peak pressure) this noise does not overtly effect the results and therefore does not impact on the analysts ability to performance inter-cycle variability studies. However, for more sensitive analysis involving the first law of thermodynamics, the in-cylinder pressure signal needs to be differentiated (Brunt et al., 1998). Differentiating a noisy signal amplifies the noise and hence causes issues with the determination of combustion parameters, such as the start of combustion (Payri et al., 2010).

Payri et al. (2010) describe a methodology for over-coming the issue of noise with in-cylinder pressure signals. They outline a four step methodology which consists of: level correction, angle referencing, cycle averaging and filtering. Cycle averaging is a standard technique used to overcome noise in in-cylinder pressure data (Payri et al., 2010; Lujan et al., 2010; Rothamer and Murphy, 2012; Carlucci et al., 2008). It is not uncommon for authors to average only a relatively small number of cycles: Lujan et al. (2010) and Payri et al. (2010) used 25 cycles and Rakopoulos et al. (2008) used only 10 cycles. However if the engine data are cycle-averaged, then the ability to examine the data for cyclic variations or instabilities will be either removed or greatly diminished.

This dissertation aims to introduce new techniques based on Bayesian methods, which allow for cycle-by-cycle analysis of the data with high accuracy. If applied carefully, these methods can resolve parameters such as: start of combustion (ignition delay), in-cylinder resonant frequency, in-cylinder temperature and piston blow-by—parameters that are difficult to isolate on single cycles. Effectively, eliminating the need for cycle averaging to produce in-depth information about combustion. It will also comment on the inter-cycle variability of a dual-fuel ethanol diesel engine and provide new information regarding the relationship between inter-cycle variability and the use of fumigated fuels. This dissertation should be viewed as a step toward using more advanced analysis techniques in engine research, with the long term goal of eliminating the need for ad hoc methods such as cycle averaging in modern engine research.



## 1.5 References

- Abu-Qudais, M., Haddad, O., and Qudaisat, M. The effect of alcohol fumigation on diesel engine performance and emissions. *Energy Conversion and Management*, 41(4):389–399, 2000.
- Ajav, E. A., Singh, B., and Bhattacharya, T. K. Thermal balance of a single cylinder diesel engine operating on alternative fuels. *Energy Conversion and Management*, 41(14): 1533–1541, 2000.
- Alperstein, M., Swin, W. B., and Schweitzer, P. H. Fumigation kills smoke, improves diesel performance. *Society of Automotive Engineers*, (SAE Paper 580058), 1958.
- Amann, C. A. Cylinder-pressure measurement and its use in engine research. *Society of Automotive Engineers*, (SAE Paper 852067), 1986.
- Antoni, J., Daniere, J., and Guillet, F. Effective vibration analysis of IC engines using cyclostationarity. Part I-A methodology for condition monitoring. *Journal of Sound and Vibration*, 257(5):815–837, 2002a.
- Antoni, J., Daniere, J., Guillet, F., and Randall, R. B. Effective vibration analysis of IC engines using cyclostationarity. Part II–new results on the reconstruction of the cylinder pressures. *Journal of Sound and Vibration*, 257(5):839–856, 2002b.
- Badami, M., Nuccio, P., and Trucco, G. Influence of injection pressure on the performance of a DI diesel engine with a common rail fuel injection system. *Society of Automotive Engineers*, (SAE Paper 1999-01-0193), 1999.
- Beasley, M., Cornwell, R., Fussey, P., King, R., Noble, A., Salamon, T., and Truscott, A. Reducing diesel emissions dispersion by coordinated combustion feedback control. *Society of Automotive Engineers*, (SAE Paper 2006-01-0186), 2006.
- Boashash, B. Note on the use of the Wigner distribution for time-frequency signal analysis. *IEEE Transactions on Acoustics, Speech and Signal Processing*, 36:1518–1521, 1988.
- Boashash, B. Estimating and interpreting the instantaneous frequency of a signal – Part 1: Fundamentals. In *IEEE, Proceedings.*, volume 80, pages 520–538, 1992.
- Bohme, J. F. and Konig, D. Statistical processing of car engine signals for combustion diagnosis. In *IEEE Seventh SP Workshop on Statistical Signal and Array Processing*, pages 369–374, 1994.
- Box, George and Tiao, George. *Bayesian Inference in Statistical Analysis*. John Wiley and Sons, 1992.

- Bretthorst, G. L. Excerpts from Bayesian spectrum analysis and parameter estimation. *Maximum Entropy and Bayesian Methods in Science and Engineering*, 1:75–145, 1988a.
- Bretthorst, G. L. Bayesian spectrum analysis and parameter estimation. *Lecture Notes in Statistics*, 48, 1988b.
- Bretthorst, G. L. and Smith, C. R. Bayesian analysis of signals from closely-spaced objects. In *Infrared Systems and Components III, Proc. SPIE 1050*, 1989.
- Broersen, P. M. T. Facts and fiction in spectral analysis. *Instrumentation and Measurement, IEEE Transactions on*, 49(4):766–772, 2000.
- Broukhiyan, E. M. H. and Lestz, S. S. Ethanol fumigation of a light duty automotive diesel engine. *Society of Automotive Engineers*, (SAE Paper 811209), 1981.
- Brown, E. R., Reuben, R. L., Neill, G. D., and Stell, J. A. Acoustic emission source discrimination using a piezopolymer based sensor. *Materials evaluation*, 57(5):515–520, 1999.
- Brunt, M. and Platts, K. Calculation of heat release in direct injection diesel engines. *Society of Automotive Engineers*, (SAE Paper 1999-01-0187), 1999.
- Brunt, M. and Pond, C. Evaluation of techniques for absolute cylinder pressure correction. *Society of Automotive Engineers*, (SAE Paper 9700369), 1997.
- Brunt, M., Rai, H., and Emtage, A. The calculation of heat release energy from engine cylinder pressure data. *Society of Automotive Engineers*, (SAE Paper 981052), 1998.
- Burg, J. The relationship between maximum entropy spectra and maximum likelihood spectra. *Geophysics*, 37(2):375–376, 1972.
- Carlucci, A. P., Chiara, F. F., and Laforgia, D. Block vibration as a way of monitoring the combustion evolution in a direct injection diesel engine. *Society of Automotive Engineers*, (SAE Paper 2006-01-1532), 2006.
- Carlucci, A. P., de Risi, A., Laforgia, D., and Naccarato, F. Experimental investigation and combustion analysis of a direct injection dual-fuel diesel–natural gas engine. *Energy*, 33(2):256–263, 2008.
- Carolan, T. A., Kidd, S. R., Hand, D. P., Wilcox, S. J., Wilkinson, P., Barton, J. S., Jones, J. D. C., and Reuben, R. L. Acoustic emission monitoring of tool wear during the face milling of steels and aluminium alloys using a fibre optic sensor Part 2: frequency analysis. *Proceedings of the Institution of Mechanical Engineers, Part B: Journal of Engineering Manufacture*, 211(4):311–319, 1997.

- Carpenter, S. H. and Zhu, Z. Correlation of the acoustic emission and the fracture toughness of ductile nodular cast iron. *Journal of Materials Science*, 26(8):2057–2062, 1991.
- Chen, J., Gussert, D., Gao, X., Gupta, C., and Foster, D. Ethanol fumigation of a turbocharged diesel engine. *Society of Automotive Engineers*, (SAE Paper 810680), 1981.
- Cohn, D. R., Bromberg, L., and Heywood, J. B. Direct injection ethanol boosted gasoline engines: Biofuel leveraging for cost effective reduction of oil dependence and CO<sub>2</sub> emissions. *Massachusetts Institute of Technology*, 2005.
- Cooley, J. W. and Tukey, J. W. An algorithm for the machine calculation of complex Fourier series. *Mathematics of Computation*, 19(90):297–301, 1965.
- Cooley, J. W., Lewis, P. A. W., and Welch, P. D. The Fast Fourier transform and its applications. *Education, IEEE Transactions on*, 12(1):27–34, 1969.
- Dalai, A. K., Bakhshi, N. N., and Esmail, M. N. Conversion of syngas to hydrocarbons in a tube-wall reactor using Co—Fe plasma-sprayed catalyst: experimental and modeling studies. *Fuel Processing Technology*, 51(3):219–238, 1997.
- Demirbas, A. Progress and recent trends in biofuels. *Progress in Energy and Combustion Science*, 33(1):1–18, 2007.
- Demirbas, M. F. and Balat, M. Recent advances on the production and utilization trends of bio-fuels: A global perspective. *Energy Conversion and Management*, 47(15-16):2371–2381, 2006.
- Desantes, J. M., Galindo, J., Guardiola, C., and Dolz, V. Air mass flow estimation in turbocharged diesel engines from in-cylinder pressure measurement. *Experimental Thermal and Fluid Science*, 34:37–47, 2010.
- Diesel, R. German Patent 67207, 1892.
- Dou, L. and Hodgson, R. Bayesian inference and Gibbs sampling in spectral analysis and parameter estimation: I. *Inverse Problems*, 11(5):1069–1085, 1995.
- Draper, C. S. Pressure waves accompanying detonation in the internal combustion engine. *Journal of Aeronautical Sciences*, 5(6):219–226, 1938.
- Duhamel, P. and Vetterli, M. Fast Fourier transforms: a tutorial review and a state of the art. *Signal Processing*, 19(4):259–299, 1990.
- EC, . EC, 2009. Regulation (EC) No 595/2009 of the European Parliament and the Council of 18 June 2009 on type-approval of motor vehicles and engines with respect to emissions from heavy duty vehicles (Euro VI), European Commission, Brussels, Belgium., 2009.

- El Ghamry, M., Reuben, R. L., and Steel, J. A. The development of automated pattern recognition and statistical feature isolation techniques for the diagnosis of reciprocating machinery faults using acoustic emission. *Mechanical Systems and Signal Processing*, 17: 805–823, 2003.
- El Ghamry, M. H., Brown, E. R., Ferguson, I., Gill, J. D., Reuben, R. L., Steel, J. A., Scaife, M., and Middleton, S. Gaseous airfuel quality identification for a spark ignition gas engine using acoustic emission analysis. In *Proceedings of the 11th International Conference on Condition Monitoring and Diagnostic Engineering Management (COMADEM 98)*, Launceston, Tasmania, Australia, pages 235–244, 1998.
- Fitzgerald, W. J. Markov chain Monte Carlo methods with applications to signal processing. *Signal Processing*, 81(1):3–18, 2001.
- Fog, T. L. *Condition monitoring and fault diagnosis in marine diesel engines*. PhD thesis, Technical University of Denmark, 1998.
- Frassoldati, A., Faravelli, T., and Ranzi, E. A wide range modeling study of  $no_x$  formation and nitrogen chemistry in hydrogen combustion. *International Journal of Hydrogen Energy*, 31(15):2310–2328, 2006.
- Gelman, A., Carlin, J. B., Stern, H. S., and Rubin, D. B. *Bayesian Data Analysis: Second Edition*. Chapman & Hall/CRC, 2003.
- Greene, A. B. and Lucas, G. G. *The Testing of Internal Combustion Engines*. The English Universities Press Limited, 1969.
- Gregory, P. C. A Bayesian revolution in spectral analysis. In *AIP Conf. Proc.*, volume 568, pages 557–568, Gif-sur-Yvette (France), 2001. AIP.
- Gregory, P. C. and Lored, T. J. A new method for the detection of a periodic signal of unknown shape and period. *Astrophysical Journal*, 398(1):146–168, 1992.
- Hansen, A. C., Zhang, Q., and Lyne, P. W. L. Ethanol-diesel fuel blends – a review. *Bioresource Technology*, 96(3):277–285, 2005.
- Hasegawa, M., Shimasaki, Y., Yamaguchi, S., Kobayashi, M., Sakamoto, H., Kitayama, N., and Kanda, T. Study on ignition timing control for diesel engines using in-cylinder pressure sensor. *Society of Automotive Engineers*, (SAE Paper 2006-01-0180), 2006.
- Havemann, H. A., Rao, M. R. K., and Narasimhan, T. L. Alcohol in diesel engines. *Automotive Engineer*, pages 256–262, 1954.

- Hayes, T. K., Savage, L. D., and White, R. A. The effect of fumigation of different ethanol proofs on a turbocharge diesel engine. *Society of Automotive Engineers*, (SAE Paper 880497), 1988.
- Heisey, J. B. and Letsz, S. S. Aqueous alcohol fumigation of a single-cylinder direct injection diesel engine. *Society of Automotive Engineers*, (SAE Paper 811208), 1981.
- Henham, A. and Makkar, M. K. Combustion of simulated biogas in a dual-fuel diesel engine. *Energy Conversion and Management*, 39(16-18):2001–2009, 1998.
- Heywood, J. B. *Internal Combustion Engine Fundamentals*. McGraw-Hill, Inc., 1988.
- Hickling, R., Feldmaier, D. A., Chen, F. H. K., and Morel, J. S. Cavity resonances in engine combustion chambers and some applications. *Acoustical Society of America Journal*, 73: 1170–1178, 1983.
- Huang, G. H., Chen, F., Wei, D., Zhang, X., and Chen, G. Biodiesel production by microalgal biotechnology. *Applied Energy*, 87:38–46, 2010.
- Huang, N. E., Shen, Z., Long, S. R., Wu, M. C., Shih, H. H., Zheng, Q., Yen, N., Tung, C. C., and Liu, H. H. The empirical mode decomposition and the Hilbert spectrum for nonlinear and non-stationary time series analysis. *Proceedings: Mathematical, Physical and Engineering Sciences*, 454:903–995, 1998.
- ICF International, . Integrating climate change into the transportation planning process. Technical report, Federal Highway Administration, 2008.
- Jaynes, E. T. Bayesian spectrum and chirp analysis. *Maximum-Entropy and Bayesian Spectral Analysis and Estimation Problems*, 1987.
- Jaynes, E. T. *Probability Theory: The Logic of Science*. Cambridge University Press, 2007.
- Johansson, B. Cycle to cycle variations in S.I. engines – the effects of fluid flow and gas composition in the vicinity of the spark plug on early combustion. *Society of Automotive Engineers*, (SAE Paper 962084), 1996.
- Kanda, T., Hakozaki, T., Uchimoto, T., Hatano, J., Kitayama, N., and Sono, H. PCCI operation with fuel injection timing set close to TDC. *Society of Automotive Engineers*, (SAE Paper 2006-01-0920), 2006.
- Kaplan, W. *Advanced Calculus*. Pearson Education, Inc., 5th edition, 2003.
- Karthikeyana, R. and Mahalakshmi, N. V. Performance and emission characteristics of a turpentine–diesel dual fuel engine. *Energy*, 32(7):1202–1209, 2007.

- Kim, S. and Dale, B. E. Global potential bioethanol production from wasted crops and crop residues. *Biomass and Bioenergy*, 26(4):361–375, 2004.
- Kim, S. and Min, K. Detection of combustion start in the controlled auto ignition engine by wavelet transform of the engine block vibration signal. *Measurement Science and Technology*, 19(8), 2008.
- Kistler, W. P. Swiss Patent 267431. 1950.
- Kouremenos, D. A., Rakopoulos, C. D., and Kotsos, K. G. A stochastic-experimental investigation of the cyclic pressure variation in a DI single-cylinder diesel engine. *International Journal of Energy Research*, 16(9):865–877, 1992.
- Lapuerta, M., Armas, O., and Hernandez, J. J. Diagnosis of DI Diesel combustion from in-cylinder pressure signal by estimation of mean thermodynamic properties of gas. *Applied Thermal Engineering*, 19:513–529, 1999.
- Lata, D. B. and Misra, A. Analysis of ignition delay period of a dual fuel diesel engine with hydrogen and LPG as secondary fuels. *International Journal of Hydrogen Energy*, 36(5): 3746–3756, 2011.
- Lee, K., Yoon, M., and Sunwoo, M. A study on pegging methods for noisy cylinder pressure signal. *Control Engineering Practice*, 16:922–929, 2008.
- Li, W., Gu, F., Ball, A. D., Leung, A. Y. T., and Phipps, C. E. A study of the noise from diesel engines using the independent component analysis. *Mechanical Systems and Signal Processing*, 15(6):1165–1184, 2001.
- Lloyd, A. C. and Cackette, T. A. Diesel engines : Environmental impact and control. *Journal of the Air & Waste Management Association*, 51(6):809–847, 2001.
- Lucke, C. Kerosene versus gasoline in automobile engines. *Society of Automotive Engineers*, (SAE Paper 160022), 1916.
- Lujan, J. M., Bermudez, V., Guardiola, C., and Abbad, A. A methodology for combustion detection in diesel engines through in-cylinder pressure derivative signal. *Mechanical Systems and Signal Processing*, 24:2261–2275, 2010.
- Martin, W. and Flandrin, P. Wigner-Ville spectral analysis of nonstationary processes. *IEEE Transactions on Acoustics, Speech, and Signal Processing*, ASSP-33(6):1461–1470, 1985.
- McArdle, P., Lindstrom, P., and Calopedis, S. Emissions of greenhouse gases report. Technical Report DOE/EIA-0573(2006), Energy Information Administration, Office of Integrated Analysis and Forecasting, U.S. Department of Energy, Washington, DC, 2007. URL <http://www.eia.doe.gov/oiaf/1605/ggrpt/>.

- Merrion, D. F. Diesel engine design for the 1990s. *Society of Automotive Engineers*, (SAE Paper 940130), 1994.
- Midgley, T. and Boyd, T. A. Methods of measuring detonation in engines. *Society of Automotive Engineers*, (SAE Paper 220004), 1922.
- Miettinen, J. and Siekkinen, V. Acoustic emission in monitoring sliding contact behaviour. *Wear*, 181-183(Part 2):897–900, 1995.
- Morey, F. and Seers, P. Comparison of cycle-by-cycle variation of measured exhaust-gas temperature and in-cylinder pressure measurements. *Applied Thermal Engineering*, 30: 487–491, 2010.
- Morse, P. M. and Ingard, K. U. *Theoretical Acoustics*. McGraw-Hill Book Company, 1968.
- Needham, J. R., May, M. P., Doyle, D. M., Faulkner, S. A., and Ishiwata, H. Injection timing and rate control – a solution for low emissions. *Society of Automotive Engineers*, (SAE Paper 900854), 1990.
- Neill, G. D., Reuben, R. L., Sandford, P. M., Brown, E. R., and Steel, J. A. Detection of incipient cavitation in pumps using acoustic emission. *Proceedings of the Institution of Mechanical Engineers, Part E: Journal of Process Mechanical Engineering*, 311(4):267–277, 1997.
- Niven, R. K. Ethanol in gasoline: environmental impacts and sustainability review article. *Renewable and Sustainable Energy Reviews*, 9(6):535–555, 2005.
- Oppenheim, A. V. and Schaffer, R. W. *Digital Signal Processing*. Prentice-Hall, Inc., 1975.
- Papandreou-Suppappola, A., editor. *Applications in Time-Frequency Signal Processing*. CRC Press, 2003.
- Payri, F., Broatch, A., Tormos, B., and Marant, V. New methodology for in-cylinder pressure analysis in direct injection diesel engines: application to combustion noise. *Measurement Science and Technology*, 16(2):540–547, 2005.
- Payri, F., Lujan, J.M., Martin, J., and Abbad, A. Digital signal processing of in-cylinder pressure for combustion diagnosis of internal combustion engines. *Mechanical Systems and Signal Processing*, 24(6):1767–1784, 2010.
- Prakash, G., Shaik, A. B., and Ramesh, A. An approach for estimation of ignition delay in a dual fuel engine. *Society of Automotive Engineers*, (SAE Paper 1999-01-0232), 1999.
- Rabiner, L. R. and Rader, C. M., editors. *Digital Signal Processing*. IEEE Press, New York, 1972.

- Ragauskas, A. J., Williams, C. K., Davison, B. H., Britovsek, G., Cairney, J., Eckert, C. A., Frederick, W. J., Hallett, J. P., Leak, D. J., Liotta, C. L., Mielenz, J. R., Murphy, R., Templer, R., and Tschaplinski, T. The path forward for biofuels and biomaterials. *Science*, 311(5760):484–489, 2006.
- Raje, A., Inga, J. R., and Davis, B. H. Fischer-Tropsch synthesis: Process considerations based on performance of iron-based catalysts. *Fuel*, 76(3):273–280, 1997.
- Rakopoulos, C. D., Antonopoulos, K. A., and Rakopoulos, D. C. Experimental heat release analysis and emissions of a HSDI diesel engine fueled with ethanol-diesel fuel blends. *Energy*, 32(10):1791–1808, 2007.
- Rakopoulos, D. C. Combustion and emissions of cottonseed oil and its bio-diesel in blends with either *n*-butanol or diethyl ether in HSDI diesel engine. *Fuel*, 2012.
- Rakopoulos, D. C., Rakopoulos, C. D., Giakoumis, E. G., Papagiannakis, R. G., and Kyritsis, D. C. Experimental-stochastic investigation of the combustion cyclic variability in HSDI diesel engine using ethanol-diesel fuel blends. *Fuel*, 87(8-9):1478–1491, 2008.
- Ramadhas, A. S., Muraleedharan, C., and Jayaraj, S. Performance and emission evaluation of a diesel engine fuelled with methyl esters of rubber seed oil. *Renewable Energy*, 30(12):1789–1800, 2005.
- Randall, R. B. *Frequency Analysis*. Bruel & Kjaer, 1987.
- Randolph, A. L. Methods of processing cylinder-pressure transducer signals to maximize data accuracy. *Society of Automotive Engineers*, (SAE Paper 900170), 1990.
- Ren, Y., Randall, R. B., and Milton, B. E. Influence of the resonant frequency on the control of knock in diesel engines. *Proceedings of the Institution of Mechanical Engineers: Part D: Journal of Automobile Engineering*. London, 213(2):127–133, 1999.
- RIRDC, . Biofuels in Australia—issues and prospects. *Australian Government: Rural Industries Research and Development Corporation Publication Number 07/071*, 2007.
- Rogers, L. M., Cullen, J., Phillips, P., and Carlton, J. S. Use of acoustic emission methods for crack growth detection in offshore and other structures. discussion. *Transactions - Institute of Marine Engineers*, 110(3):171–180, 1998.
- Rosillo-Calle, F. and Walter, A. Global market for bioethanol: historical trends and future prospects. *Energy for Sustainable Development*, 10(1):20–32, 2006.
- Rothamer, D. and Murphy, L. Systematic study of ignition delay for jet fuels and diesel fuel in a heavy-duty diesel engine. *Proceedings of the Combustion Institute*, 2012.



- Saeed, M. N. and Henein, N. A. Combustion phenomena of alcohols in C.I. engines. *Journal of Engineering for Gas Turbines and Power*, 111(3):439–444, 1989.
- Samimy, B. and Rizzoni, G. Mechanical signature analysis using time-frequency signal processing: application to internal combustion engine knock detection. *Proceedings of the IEEE*, 84(9):1330–1343, 1996.
- Schaberg, P. W., Priede, T., and Dutkiewicz, R. K. Effects of a rapid pressure rise on engine vibration and noise. *Society of Automotive Engineers*, (SAE Paper 900013), 1990.
- Schmillen, K. and Wolschendorf, J. Cycle-to-cycle variations of combustion noise in diesel engines. *Society of Automotive Engineers*, (SAE Paper 890129), 1989.
- Secor, J. A. Kerosene engines. *Society of Automotive Engineers*, (SAE Paper 130019), 1913.
- Sellnau, M. C., Matekunas, F. A., Battiston, P. A., Chang, C., and Lancaster, D. Cylinder-pressure-based engine control using pressure-ratio management and low-coast non-intrusive cylinder pressure sensors. *Society of Automotive Engineers*, (SAE Paper 2000-01-0932), 2000.
- Sen, A. K., Longwic, R., Litak, G., and Gorski, Z. Analysis of cycle-to-cycle pressure oscillations in a diesel engine. *Mechanical Systems and Signal Processing*, 22:362–373, 2008.
- Shehata, M. S. Cylinder pressure, performance parameters, heat release, specific heats ratio and duration of combustion for spark ignition engine. *Energy*, 35(12):4710–4725, 2010.
- Shimasaki, Y., Kobayashi, M., Sakomoto, H., Ueno, M., Hasegawa, M., Yamaguchi, S., and Suzuki, T. Study on engine management system using chamber pressure sensor integrated with spark plug. *Society of Automotive Engineers*, (SAE Paper 2004-01-0519), 2004.
- Shindell, D., Faluvegi, G., Walsh, M., Anenberg, S. C., van Dingenen, R., Muller, N. Z., Austin, J., Koch, D., and Milly, G. Climate, health, agricultural and economic impacts of tighter vehicle-emission standards. *Nature Climate Change*, 1:59–66, 2011.
- Shropshire, G. J. and Goering, C. E. Ethanol injection into a diesel engine. *Transactions of the ASAE*, 25(3):570–575, 1982.
- Sion, R. and Atkinson, J. A novel low-cost sensor for measuring cylinder pressure and improving performance of an internal combustion engine. *Sensor Review*, 22(2):139–148, 2002.
- Skelton, B. Special issue: Bio-fuels. *Process Safety and Environmental Protection*, 85(5): 347–347, 2007.

- Song, C., Gong, G., Song, J., Lv, G., Cao, X., Liu, L., and Pei, Y. Potential for reduction of exhaust emissions in a common-rail direct-injection diesel engine by fueling with FischerTropsch diesel fuel synthesized from coal. *Energy Fuels*, 26(1):530–535, 2012.
- Sorda, G., Banse, M., and Kemfert, C. An overview of biofuel policies across the world. *Energy Policy*, 38(11):6977–6988, 2010.
- Stankovic, L. A multitime definition of the Wigner higher order distribution: L-Wigner distribution. *Signal Processing Letters, IEEE*, 1(7):106–109, 1994a.
- Stankovic, L. A method for time-frequency analysis. *Signal Processing, IEEE Transactions on*, 42(1):225–229, 1994b.
- Stankovic, L. and Bohme, J. F. Time-frequency analysis of multiple resonances in combustion engine signals. *Signal Processing*, 79(1):15–28, 1999.
- Steel, J. A. and Reuben, R. L. Recent developments in monitoring of engines using acoustic emission. *The Journal of Strain Analysis for Engineering Design*, 40(1):45–57, 2005.
- Stone, R. *Introduction to Internal Combustion Engines*. Macmillan Press Ltd, London, 1999.
- Tauzia, X., Maiboom, A., and Shah, S. R. Experimental study of inlet manifold water injection on combustion and emissions of an automotive direct injection diesel engine. *Energy*, 35(9):3628–3639, 2010.
- Taylor, C. F. and Taylor, E. D. *The Internal-Combustion Engine*. International Textbook Company, 1966.
- Torregrosa, A. J., Broatch, A., and Margot, X. Combustion chamber resonances in direct injection automotive diesel engines: a numerical approach. *International Journal of Engine Research*, 5(1):83–91, 2004.
- Torregrosa, A. J., Broatch, A., Novella, R., and Monico, L. F. Suitability analysis of advanced diesel combustion concepts for emissions and noise control. *Energy*, 36(2):825–838, 2011.
- Tsang, K. S., Zhang, Z. H., Cheung, C. S., and Chan, T. L. Reducing emissions of a diesel engine using fumigation ethanol and a diesel oxidation catalyst. *Energy & Fuels*, 24: 6156–6165, 2010.
- Uchida, N., Shimokawa, K., Kudo, Y., and Shimoda, M. Combustion optimization by means of common rail injection system for heavy-duty diesel engines. *Society of Automotive Engineers*, (SAE Paper 982679), 1998.

- US Department of Transportation, . Transportation and global climate change: a review and analysis of the literature. Technical Report DOT-T-97-03, Federal Highway Administration, Office of Environment and Planning, Washington, DC, 1998. URL <http://www.fhwa.dot.gov/environment/lit.htm>.
- Valentino, G., Corcione, F., Iannuzzi, E., and Serra, S. Experimental study on performance and emissions of a high speed diesel engine fuelled with n-butanol diesel blends under premixed low temperature combustion. *Fuel*, 92:295–307, 2012.
- Van Gerpen, J. H., Hammond, E. G., Johnson, L. A., Marley, S. J., Yu, L., Lee, I., and Monyem, A. Determining the influence of contaminants on biodiesel properties. *Society of Automotive Engineers*, (SAE Paper 971685), 1997.
- Van Overbeke, C. W. Manifold introduction of hydrocarbons as an aid for starting. Master’s thesis, The Pennsylvania State University, 1942.
- Velders, G., Geilenkirchen, G., and de Lange, R. Higher than expected  $NO_x$  emission from trucks may affect attainability of  $NO_2$  limit values in the netherlands. *Atmospheric Environment*, 45(16):3025–3033, 2011.
- Worm, J. An evaluation of several methods for calculating transient trapped mass with emphasis on the Delta P approach. *Society of Automotive Engineers*, (SAE Paper 2005-01-0990), 2005.
- Xu-Guang, T., Hai-Lang, S., Tao, Q., Zhi-Qiang, F., and Wen-Hui, Y. The impact of common rail systems control parameters on the performance of high-power diesel. *Energy Procedia*, 16:2067–2072, 2012.
- Yusuf, N. N. A. N., Kamarudin, S. K., and Yaakub, Z. Overview on the current trends in biodiesel production. *Energy Conversion and Management*, 52(7):2741–2751, 2011.
- Zamboni, G. and Capobianco, M. Experimental study on the effects of HP and LP EGR in an automotive turbocharged diesel engine. *Applied Energy*, 94:117–128, 2012.

---

[This page is intentionally left blank]

# Chapter 2

## Contribution

The principle aim of this dissertation is to introduce new techniques for the analysis of in-cylinder pressure. To achieve this aim, several engine testing campaigns have been undertaken—most of which involved ethanol fumigation. These engine campaigns were performed on a modern Euro III turbo-charged, common-rail, in-line six-cylinder diesel engine—a detailed description of the experimental setup, including a schematic, can be found in Chapter 5. Some early work was performed on an older, direct (mechanical) injection, four-cylinder diesel engine—Chapter 4.

Initially, a study was conducted to assess the feasibility of using Bayesian techniques on in-cylinder pressure signals. This work was inspired by a study from Hickling et al. (1983) that analysed combustion resonance evident in in-cylinder pressure signals, they isolated the in-cylinder resonant frequency to infer the in-cylinder temperature and trapped mass as a function of crank angle. The current work hypothesised that the in-cylinder pressure signal could be statistically modelled, in the Bayesian paradigm, with the goal of isolating the in-cylinder resonant frequency. Preliminary work to establish the feasibility of this approach was published in *Mechanical Systems and Signal Processing* and is shown in Chapter 4.

A key outcome from this initial study was not only demonstrating the feasibility of using Bayesian inference in engine research, but also highlighting the inter-cycle variability in combustion in diesel engines. Previous research that has investigated resonance in diesel engines have relied on cycle-averaging to increase the signal-to-noise ratio. However, this work has shown that the inter-cycle variation between cycles is large and that more advanced techniques capable of cycle-by-cycle analysis need to be employed in order to produce meaningful results.

Part of the motivation for this work was to investigate the effects of ethanol fumigation in a modern engine. Therefore, Chapter 5 (published in *Energy*) investigated key in-cylinder parameters: maximum rate of pressure rise, peak pressure, peak pressure timing and ignition delay. This chapter focused on the inter-cycle variability of these parameters and found a relationship between the absolute air to fuel ratio (on a mole basis) and the inter-cycle variability. Also, introduced in this chapter is a new methodology for determining the start of combustion using a band-pass filtered in-cylinder pressure signal. This preliminary study

showed that the ignition delay at high loads and high ethanol substitutions can be reduced.

The method for determining the start of combustion from combustion resonance shown in Chapter 5 had the limitation that it required the analyst to perform the data analysis manually; hence, restricting the scope of any true inter-cycle variability studies. To overcome this issue, a Bayesian modelling approach was taken. Published in *Applied Thermal Engineering*, Chapter 6 introduces a statistical model for determining the start of combustion in a diesel engine and demonstrates its utility on a modern diesel engine operating at rated engine speed on full, three quarters and half loads.

Chapter 7 applies the Bayesian model for determining the start of combustion from Chapter 6 to the data set from Chapter 5. This work was done to better understand the inter-cycle variability of the ignition delay of a modern common-rail diesel engine operated with fumigated ethanol. The same relationship between the air to fuel ratio and the in-cylinder parameters shown in Chapter 5 was confirmed with ignition delay.

Extending the early work shown in Chapter 4, Chapter 8 introduces a Bayesian model to investigate the time-evolving in-cylinder resonant frequency in a modern diesel engine. This model investigates the same parameters as Chapter 4: resonant frequency, in-cylinder temperature and trapped mass. In addition to this, the model given in Chapter 8 also resolves the timing of the start of diffusion combustion. Previously, this has been a difficult parameter to isolate and therefore the Bayesian modelling techniques explored in this dissertation represent a significant advancement in-cylinder pressure analysis. Importantly, this method of investigation allows for inter-cycle variability studies. The results of this study are shown for rated speed (2000 rpm) at full load for 500 consecutive cycles.

This dissertation fills a key gap in modern engine research by introducing new techniques for analysing in-cylinder pressure signals—the Bayesian modelling techniques described in this dissertation are also applicable to engine vibration signals and hence could form a future role in condition monitoring. Moreover, the application of these techniques, shown in this dissertation, have shown a need for more in-depth analysis tools in modern engine research.

The method for resolving evolving frequencies, shown in this dissertation, has applications beyond engine research and alternative fuel evaluation. With only minor adjustments, to make the assumptions applicable to the specific problem, the Bayesian techniques developed in this dissertation can be used to resolve frequency information from any signal type. Potential applications of this can include: condition monitoring of vibrating machinery, evaluating vibration in buildings and investigating turbulence and geometric effects in fluid flow.

## Chapter 3

# In Situ Calibration of a Piezoelectric Transducer in an Internal Combustion Engine

### 3.1 Introduction

Prolonged use of an internal combustion engine can cause a build-up of material on sensors and transducers. Further, it is also possible that extreme environmental conditions (such as those experienced in a combustion chamber) can have long term effects on the calibration of equipment. These factors make regular calibration of equipment used in internal combustion engines critical if reliable data is to be obtained.

Throughout an experimental campaign an unusually large discrepancy between the brake and the indicated power motivated the calibration of the in-cylinder piezoelectric pressure transducer. Piezoelectric transducers are often calibrated in specialist equipment, which is external from their place of use. Removing the transducer has a few key issues, namely: it is time-consuming, replacing the transducer after calibration could potentially offset the calibration and previously collected data will become void. Therefore, an in situ solution was investigated.

In situ calibration was important to account for any residue build-up on the face of the transducer. This residue will potentially attenuate the pressure change and thus effect the recorded pressure. As typical of piezoelectric transducers, this transducer does not measure absolute pressure, but rather a change in pressure. Therefore, a change in pressure has a corresponding change in frequency, which through a signal conditioning unit is converted to a corresponding voltage, which is read by an analogue-to-digital converter. Transducers of this type return to a ground position, of approximately zero volts, in the presence of a static pressure.

## 3.2 Experimental Configuration

Experiments were conducted on a naturally-aspirated, four-cylinder Ford direct injection diesel engine (2701C). The engine has a capacity of 4.152  $\ell$ , a bore of 108.2 mm, a stroke length of 115 mm, a compression ratio of 15.5 and maximum power of 48 kW at 2500 RPM. The engine was coupled to a water-brake Froude D.P.X Type dynamometer. In-cylinder pressure was measured with a PCB 112B11 piezoelectric transducer with a Data Translation (DT9832) simultaneous analogue-to-digital converter connected to a desktop computer running National Instruments LabView.

The calibration of the piezoelectric transducer was completed by replacing the diesel injector with an adapter, shown in Figure 3.1, allowing a gas system to be connected to the engine. This permitted the sensor calibration with only a minimal need to dismantle components of the engine. A high pressure Argon cylinder was used to provide the in-cylinder pressure and two valves were used to control the flow into the cylinder and to release the gas, from the cylinder, to the atmosphere, as shown in Figure 3.2.

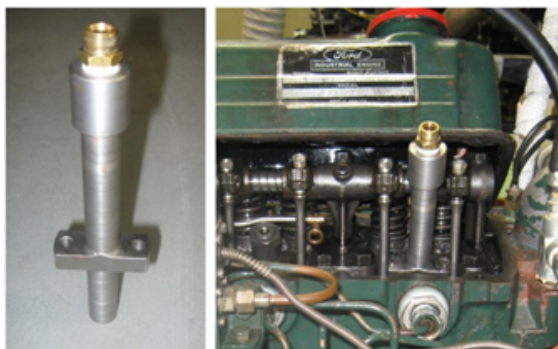


Figure 3.1: Calibration system adapter (left) and it in place in the engine (right)

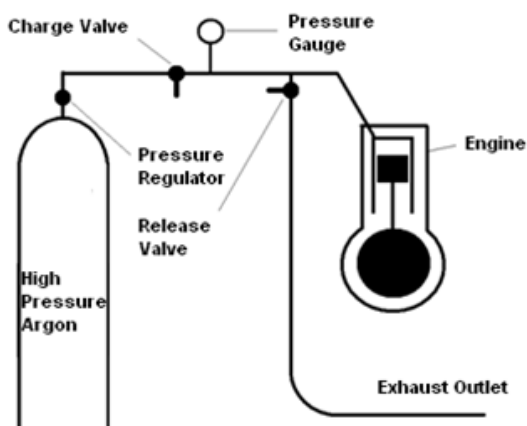


Figure 3.2: Schematic of the piezoelectric transducer calibration system



### 3.3 Data Collection

The piezoelectric transducer used in this engine is designed to measure the change of pressure in the combustion chamber during the engines operation. This transducer uses a quartz piezoelectric crystal, which responds to a change in force applied to the sensor, generating a voltage corresponding to the change in pressure. Hence if there is no change in pressure, the transducer will read zero volts—transducers of this type need to be utilised in a highly dynamic environment and are, therefore, well suited to internal combustion engines.

Calibration data can be collected in one of two ways. Firstly, the combustion chamber could be at atmospheric pressure and then increased quickly to a known pressure or secondly, the combustion chamber could be pressurised then depressurised back to atmospheric quickly. For this experiment the latter was chosen as it is easier to rapidly depressurise the combustion chamber than it is to pressurise it.

For this experiment the engine was locked into a fixed position. Top dead centre (TDC) was chosen because it requires the least amount of gas to pressurise, and hence reduces the time to depressurise—it also has the smallest rotational force applied to the engine crank, improving safety and allowing for a higher range of test points and at TDC the inlet and exhaust valves will be closed. Pressures from 500 kPa (5 bar) up to 3000 kPa (30 bar) were used for this experiment. Ideally, pressures up to the 80,000 kPa (80 bar) would have been tested; however, the safety risk did not outweigh the potential results.

The experimental calibration procedure was undertaken as follows:

1. The crankshaft was rotated until the cylinder was at TDC.
2. Once the crankshaft was in position, the engine was locked in place to ensure the piston would not move once filled with the compressed gas.
3. The apparatus was assembled, as shown in Figure 3.2, using components designed to withstand the pressures being measured—in this experiment the maximum pressure was 30 bar.
4. Argon gas was introduced into the combustion chamber by opening an inlet valve, shown in Figure 3.2, slowly until the required pressure was reached.
5. It was confirmed that the piezoelectric transducer voltage had stabilised back to zero.
6. Once data was recording, the pressure was released from the combustion chamber by simultaneously and quickly closing the inlet and opening the pressure valves, shown in Figure 3.2.
7. This procedure was repeated as necessary.

### 3.4 Data Analysis

Ideally the calibration data would show a sudden drop, with the corresponding voltage being directly proportional to the change in pressure. However, in reality the gas cannot escape the cylinder instantaneously due to a choked flow effect and drag—an example of the actual pressure signal is shown in Figure 3.3. A method, therefore, needed to be developed to determine what the equivalent change in voltage would have been if it were possible to have released the gas in an instant, and hence had an instantaneous change in pressure.

It was noted, by observing the resulting pressure signals (such as is shown in Figure 3.3) that the lag to return back to the zero state was roughly linear, as was the initial pressure drop. Using this assumption it was possible to predict what the actual pressure change was. Using Matlab, an algorithm that found these two linear equations was developed. The point that these equations intercepted was taken to be the equivalent instantaneous change in pressure, as shown in Figure 3.3. The results of this analysis are shown in Table 3.1.

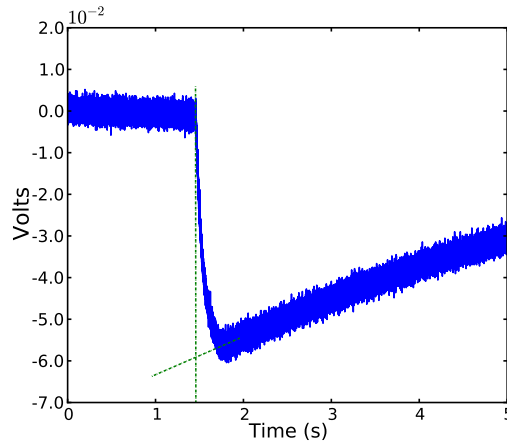


Figure 3.3: Voltage drop for a 384 kPa change in pressure

Supplied Pressure (kPa)	Measured Pressure (kPa)
384	381
855	845
1345	1346
1871	1845
2392	2374
2903	2923

Table 3.1: Results of the supplied pressure values and those measured from the piezoelectric transducer

## 3.5 Results

Figure 3.4 shows the data in Table 3.1 imposed over a perfectly linear line. The Pearson's linear correlation,  $r^2$ , as determined by a least squares method, between the supplied values and the measured values is 0.999, indicating a highly linear dependence between the supplied and measured values. Moreover, the measured gradient is 1.004, clearly indicating that the piezoelectric transducer was indeed still calibrated correctly. The small deviations have been assumed to come from the accuracy in the measurement in the supplied pressure rather than the pressure measured by the transducer.

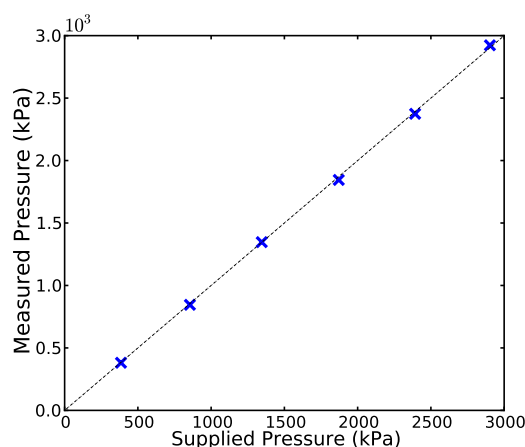


Figure 3.4: Graphical comparison between the supplied pressure the measured pressure

The largest deviation between the supplied value and the measured value was 26 kPa—occurring when the supplied pressure was 1871 kPa, the measured pressured deviated from the supplied pressure by 1.4%. The standard deviation, from the absolute difference, across all of the data was 0.4% with a mean absolute deviation of 0.8%. Therefore, the pressure transducer can be assumed to give accurate results within 1%.

## 3.6 Conclusion

This chapter has introduced a method for performing an in situ calibration of a piezoelectric transducer located in an internal combustion engine. Further, this methodology allows accurate calibration of piezoelectric transducers without the need to remove them from their environment—which can be vital if data has already been collected or if removing the transducer is too costly or time-consuming to be practical.

## **3.7 Acknowledgements**

This work was completed in collaboration with Mr. Anthony Morris, Mr. Steven Herdy and Assoc. Prof. Richard Brown. Mr. Anthony Morris and Mr. Steven Herdy were primarily involved in the data collection experiment—Mr. Anthony Morris contributed his knowledge and practical assistance and Mr. Steven Herdy designed the adapter shown in Figure 3.1, calibrated the pressure gauges used in this experiment and assisted in the data collection. Assoc. Prof. Richard Brown supervised the project.

## Chapter 4

# Bayesian Models for the Determination of Resonant Frequencies in a DI Diesel Engine

Timothy Bodisco<sup>a</sup>, Robert Reeves<sup>b</sup>, Rong Situ<sup>c</sup>, Richard J. Brown<sup>a</sup>

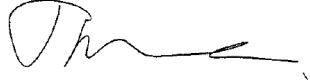
<sup>a</sup>School of Chemistry, Physics and Mechanical Engineering, Queensland University of Technology, Brisbane QLD, 4001, Australia

<sup>b</sup>School of Mathematical Science, Queensland University of Technology, Brisbane QLD, 4001, Australia

<sup>c</sup>School of Engineering and Physical Sciences, James Cook University, Townsville QLD, 4811, Australia


Publication: Mechanical Systems and Signal Processing (2012) 26, 305–314.

### Author Contribution

Contributor	Statement of Contribution
Timothy Bodisco	Conducted the experiment, proposed the concept, developed the models, wrote the algorithm and drafted the manuscript
Signature 	
Robert Reeves	Assisted with the statistics, supervised the model development process and edited the manuscript
Rong Situ	Aided with the experimental design
Richard Brown	Supervised the project, aided with the development of the paper and extensively revised the manuscript

### Principal Supervisor Confirmation

I have sighted email or other correspondence from all co-authors confirming their certifying authorship.

Name	Signature	Date
Associate Professor Richard Brown		

### Abstract

A time series method for the determination of combustion chamber resonant frequencies is outlined. This technique employs the use of Markov-chain Monte Carlo (MCMC) to infer parameters in a chosen model of the data. The development of the model is included and the resonant frequency is characterised as a function of time. Potential applications for cycle-by-cycle analysis are discussed and the bulk temperature of the gas and the trapped mass in the combustion chamber are evaluated as a function of time from resonant frequency information.

## 4.1 Introduction

Nomenclature	
Posterior	A probability distribution that summarises information about a random variable, or parameter, after information from empirical data is obtained (Everitt, 2006).
Prior	Information known about a parameter before empirical information is obtained.
Uninformative Prior	A prior that assumes no information was known about a particular parameter before obtaining empirical information.
Markov-chain Monte Carlo	or MCMC is a set of computational methods for sampling from probability distributions.
Gibbs Sampler	A particular MCMC method to generate predictive distributions.
DIC	The deviance information criterion, a relative goodness of fit measure from the posterior expectation of the deviance and the effective number of parameters as a measure of complexity (Berg et al., 2002).
Posterior Predictive Mean	The mean value of each modelled observations posterior distribution.
Precision	A term applied to the likely spread of estimates of a parameter in a statistical model.
Top Dead Centre	When the piston is at the highest possible location in the cylinder. Often denoted by a crank-angle of 0 or 360.

Calculating the resonant frequency accurately in an engine combustion chamber enables the characterisation of resonant frequencies that are associated with the speed of sound, and hence temperature (Hickling et al., 1983; Bohme and Konig, 1994; Ren et al., 1999; Payri et al., 2005; Torregrosa et al., 2004). Therefore, accurate isolation of resonant frequencies and their decay, as a function of time, or crank-angle, will allow the bulk temperature of the gas in the combustion chamber to be determined at any point within the region of interest. Further, an investigation into these frequencies will allow for cycle-by-cycle analysis to be conducted to investigate inter-cycle variability. The isolation of resonant frequencies also

has important implications in the detection of knock (Ren et al., 1999; Samimy and Rizzoni, 1996). Moreover, instantaneous resonant frequency information is of more practical use in the elimination of knock than more easily measured factors, such as the rate of pressure rise (Ren et al., 1999).

Conventional spectral analyses, such as those carried out a by Fourier transform, fail to accurately interpret the resonant frequencies precisely if the resonance is non-stationary (Ren et al., 1999). A common approach to get around non-stationary frequencies is the use of the Wigner-Ville Spectrum (Bohme and Konig, 1994; Ren et al., 1999; Samimy and Rizzoni, 1996; Stankovic, 1994a,b; Wang et al., 2008; Antoni, 2009). We propose, however, the use of Bayesian statistical inference which allows us to configure precisely a model for the observable information of interest. Markov-chain Monte Carlo (MCMC) using Gibbs Sampling is a statistical inference technique that can be used for parameter estimation in Bayesian statistical models and is the method employed in this paper (Tierney, 1994). Using this methodology has the advantage that it requires the user to state explicitly any assumptions being made in the calculation (Bretthorst and Smith, 1989). Hence, the user always knows exactly what problem is being solved. Our models are defined and fitted using the WinBUGS software package (Spiegelhalter et al., 1999).

Our technique for isolating resonant frequencies specifies an analytic form for the signal, then uses MCMC to estimate each model parameter. In our example of engine data, from in-cylinder pressure readings, we seek to obtain frequency as a function of time, and hence observe it in terms of crank-angle.

A further advantage of Bayesian statistical inference is that unlike other techniques (Jaynes, 1987) such as FFTs (Cooley and Tukey, 1965) or maximum entropy spectral analysis (Burg, 1967, 1975), which require a battery of data, it works effectively on a single cycle. This eliminates the need for ad hoc methods such as cycle averaging or spectrum averaging to extract useful information – not to speak of excessive laboratory time collecting data. Variations from cycle-to-cycle can also be explored by performing analysis on each cycle completely independently of the others.

## 4.2 Experimental Configuration

Experiments were conducted on a naturally aspirated 4-cylinder Ford direct injection diesel engine (2701C). The engine has a capacity of 4.152  $\ell$ , a bore of 108.2 mm, a stroke length of 115 mm, a compression ratio of 15.5 and maximum power of 48 kW at 2500 RPM. The engine was coupled to a Froude DPX type Hydraulic Dynamometer with load applied by increasing the flow rate of water inside the dynamometer housing. In-cylinder pressure was measured with a PCB 112B11 piezoelectric transducer with a Data Translation (DT9832) simultaneous analogue to digital converter connected to a desktop computer running National



Instruments LabView. Data was collected at a sample rate of 200,000 samples per second. During testing the engine was run on diesel fuel at 2000 RPM on full load. For a more detailed overview of the experimental setup, including emissions results, refer to the corresponding paper by Surawski et al. (Surawski et al., 2010).

### 4.3 Model Development

In this section we illustrate the process of model building for this problem by introducing more complex model specifications in an orderly sequence. At each step we compare an index of model fit, the deviance information criterion (DIC) (Spiegelhalter et al., 2002), to ensure that over-fitting has not occurred, and that an increase in complexity results in a better predictive model. The DIC is a relative measure of model fit; a decrease in DIC indicates an improvement in fit from the previous model. We also compare observed data to the posterior predictive mean to assess whether the model is capable of tracking important changes in the observed data. Figure 4.1 shows the signal that is the subject of this investigation.

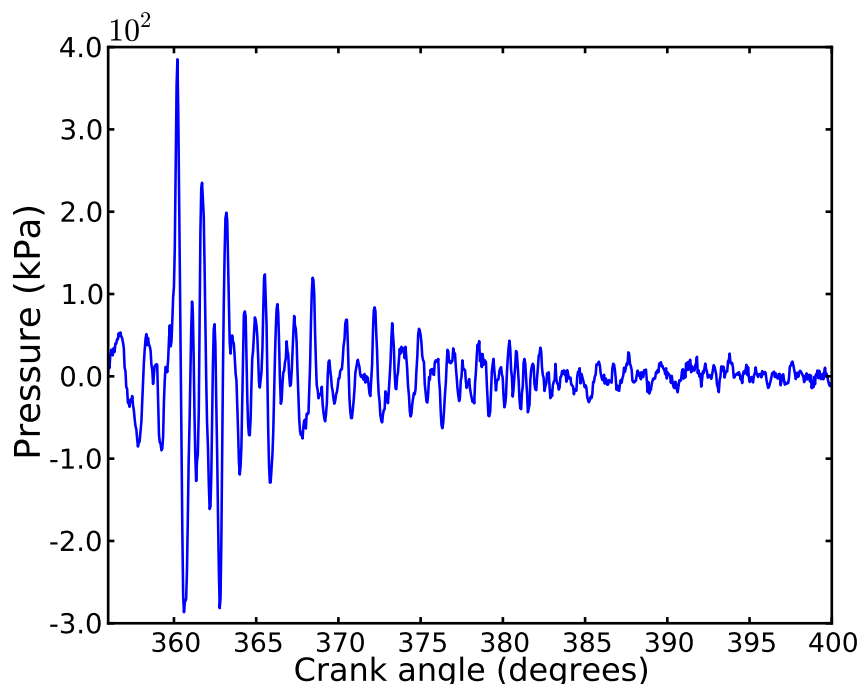


Figure 4.1: Pressure signal with the motoring frequency information removed

Although it is not necessary to separate the analysis into the following steps it is more convenient, and less time consuming, to fit simpler models. Starting with a very simple

model to observe what results can be obtained, a basic three parameter model is tested:

$$\begin{aligned} p(t) &\sim N(\mu(t), \tau_1) \\ \tau_1 &\sim \text{Gamma}(0.01, 0.01) \\ \mu(t) &= A \sin(\omega t + \phi). \end{aligned} \quad (4.1)$$

The signal,  $p(t)$ , is modelled around a normally distributed time varying mean,  $\mu$ , with a sinusoidal characteristic. Here, and subsequently, we parameterise the Normal density with a precision parameter,  $\tau$  where precision =  $\frac{1}{\text{variance}}$ , and give it an uninformative Gamma prior. This model attempts to fit a static amplitude and frequency to the signal.  $\phi$  is given a uniform prior between  $-\pi$  and  $\pi$ ,  $A$  is given an uninformative Normal prior and  $\omega$  is given a uniform prior between 5000 and 7500 Hz. The output from this model gives a DIC of 9505, and a posterior expectation of  $\omega$  as 5960 Hz. Visual inspection of the posterior predictive mean compared with the signal (Figure 4.2) tells us that this model does not adequately explain the observed changes.

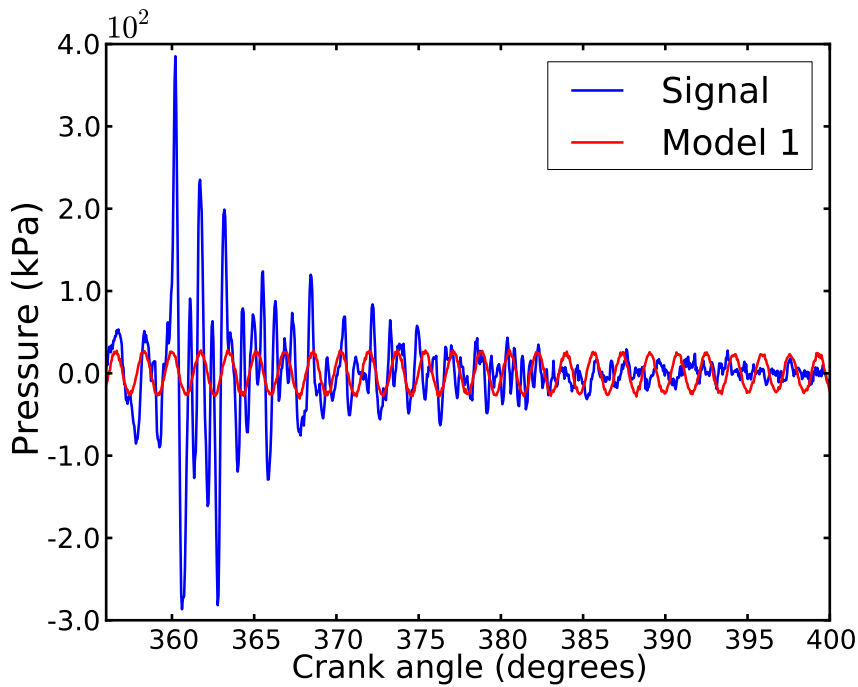


Figure 4.2: Pressure signal from Figure 4.1 and Model 1 from Equation 4.1

Including a term to model the decay in the amplitude seems to be a logical extension. Thus, we modify the model:

$$\mu(t) = Ae^{-\lambda t} \sin(\omega t + \phi), \quad (4.2)$$

giving  $\lambda$  an uninformative Normal prior. As expected there is a significant improvement in the model fit with a DIC now of 9362. Using this model the posterior expectation for  $\omega$  is now 5994 Hz. This is nearing our estimate, from a classical approach using FFTs (as shown later in Figures 4.8 and 4.9) of 6000 Hz. Figure 4.3 shows the model fit.

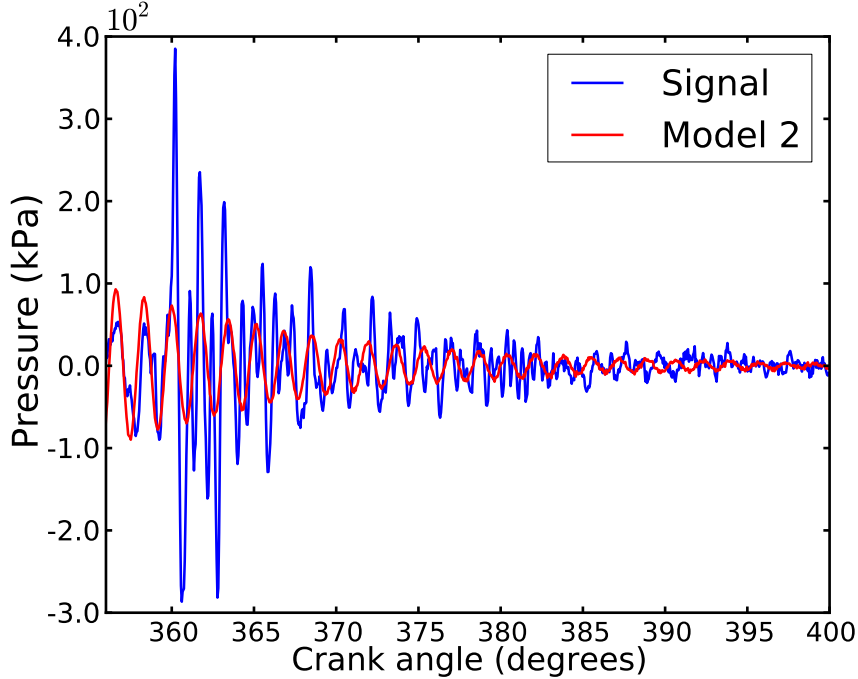


Figure 4.3: Pressure signal from Figure 4.1 and Model 2 from Equation 4.2

This model fails to capture significant observed behaviour. However, given that it is known that resonant frequencies decay over time (Ren et al., 1999; Samimy and Rizzoni, 1996; Stankovic and Bohme, 1999) it seems intuitive to include a parameter that models the frequency decay. Hence, we extend the model by defining:

$$\mu(t) = Ae^{-\lambda t} \sin(\omega_0 e^{-at} t + \phi), \quad (4.3)$$

setting  $a$  to have an uninformative Normal prior. In this model, and thereafter,  $\omega_0$  represents the initial first circumferential mode resonant frequency—from here out referred to as the resonant frequency. This model does not have a large effect on the deviance but, from a physics perspective, it is an important parameter—particularly from the aspect of what is desired from the model. It also stops the model from under-predicting the resonant frequency under the assumption that it is a stationary frequency. The minimal gain in the DIC, 9360, can be attributed to the very small decay in the resonant frequency, therefore providing evidence that there is minimal change in the resonant frequency as the crank-angle increases. Updated posterior expectations of our parameters are now 6107 Hz for  $\omega_0$  and

$2.1962 \times 10^{-10}$  for  $a$ , with our estimate for the resonant frequency now:

$$\omega(t) = 6107e^{-2.1962 \times 10^{-10}t}.$$

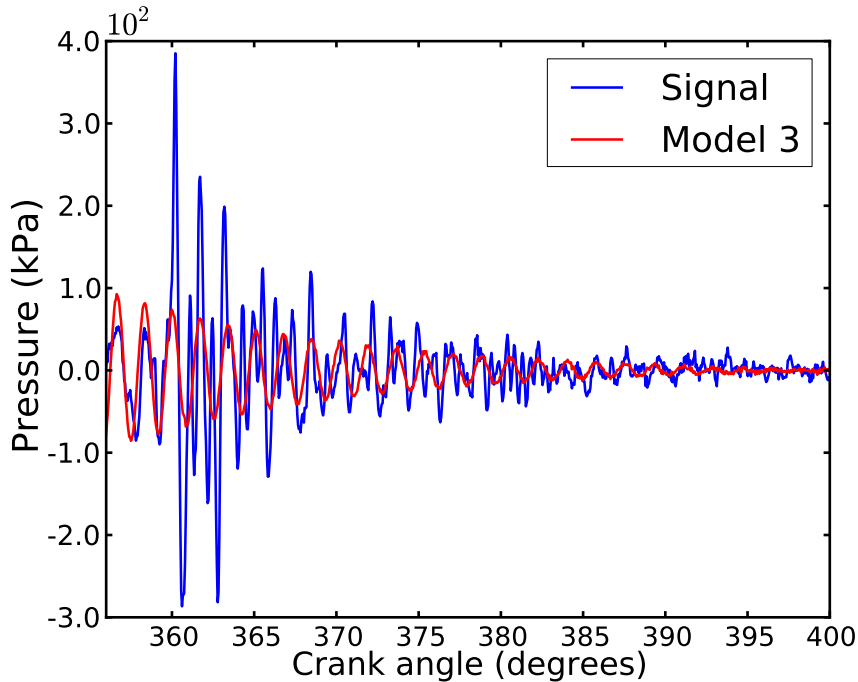


Figure 4.4: Pressure signal from Figure 4.1 and Model 3 from Equation 4.3

However, comparing the posterior predictive mean to the observed signal (Figure 4.4) indicates multiple frequencies exist. Additional terms can be added to this, making the next model:

$$\mu(t) = \sum_{i=1}^3 A_i e^{-\lambda_i t} \sin(W_i \omega_0 e^{-a_i t} t + \phi). \quad (4.4)$$

This will fit three different frequencies to the observed data. In this particular model,  $W_1$  is set at 1 and  $W_2$  and  $W_3$  are given uniform priors between 1.5 and 2.5, and 2.5 and 3.5 respectively. These priors were chosen to represent further higher frequency information that is present in the signal. The higher frequencies can be observed in an FFT (Figures 4.8 and 4.9). It is important that they do not overlap to avoid label switching and problems with convergence. Running this model yields a DIC of 9114, showing a significant improvement over the previous models.  $\omega_0$  is now estimated to be 6097 Hz with the exponential decay constant  $a$  estimated to be  $2.073 \times 10^{-10}$ . The resonant frequency is then estimated to be:

$$\omega(t) = 6097e^{-2.073 \times 10^{-10}t}.$$

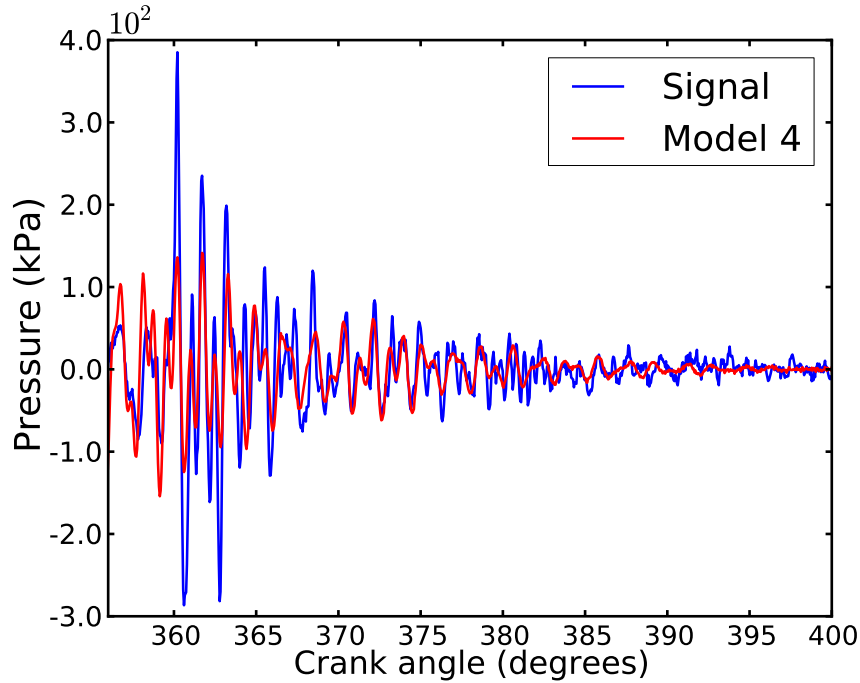


Figure 4.5: Pressure signal from Figure 4.1 and Model 4 from Equation 4.4

Figure 4.5 shows that the model does not account for the sharp rise in the signal around top dead centre. Examination of Figure 4.1 gives an indication that the higher frequencies tend to occur somewhere around the peak. The inclusion of a step function in the non-fundamental terms may be a possible solution. Therefore, the following model is suggested:

$$\begin{aligned}
 f_i(t) &= A_i e^{-\lambda_i t} \sin(W_i \omega_0 e^{-a_i t} t + \phi) \\
 \mu(t) &= f_1(t) + H(t - \delta) \sum_{i=2}^3 f_i(t),
 \end{aligned} \tag{4.5}$$

where  $H(t - \delta)$  is a step function where  $H(t - \delta) = 0$  for  $t < \delta$  and  $H(t - \delta) = 1$  for  $t \geq \delta$ .

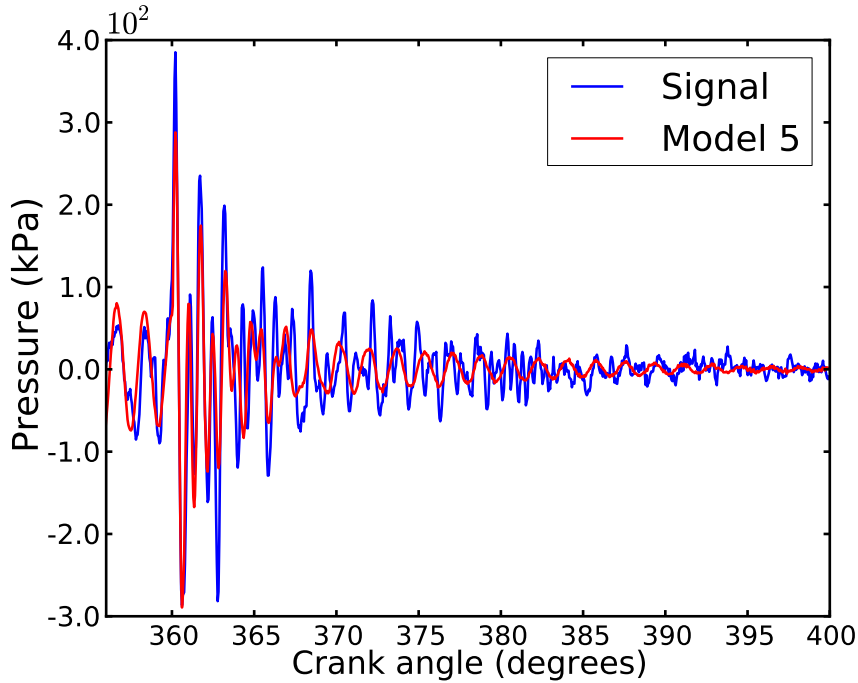


Figure 4.6: Pressure signal from Figure 4.1 and Model 5 from Equation 4.5

Figure 4.6 shows that this method of compensating for the start of the non-fundamental frequencies has returned a very significant improvement in model fit (indicated by the improvement of the DIC to 8658). Now,  $\omega_0$  is 6076 Hz with the exponential decay constant  $a$  being  $1.686 \times 10^{-10}$  estimating the resonant frequency as a function of time:

$$\omega(t) = 6076e^{-1.686 \times 10^{-10}t}. \quad (4.6)$$

Further parameters to fit this data are unnecessary and could be counter to the aim of the model; the DIC penalises the use of too many parameters as there is the risk of over fitting the data. Also, with the addition of more parameters there is an increased risk of non-convergence, potentially leading to very multi-modal probability density functions and hence a poor indicator of the desired result. Multi-modal pdf's can also occur as a result of label switching, especially with models where the parameters are heavily dependent on each other, such as in this case. Computationally, it is also wise to avoid over fitting the data with excessive parameters.

A posterior density plot of  $\omega_0$  (Figure 4.7) and a plot of a fast Fourier transform (FFT) (Figures 4.8 and 4.9) indicate the similarity. Note that the Bayesian method not only accurately describes the resonant frequency and its decay, but also it gives us the uncertainty in the parameter estimates, which is greatly improved when compared to the traditional

method. Further, the FFT method assumes stationary frequency components, whereas our approach allows for the inclusion of decaying frequency components, which physical knowledge of the situation suggests are present.

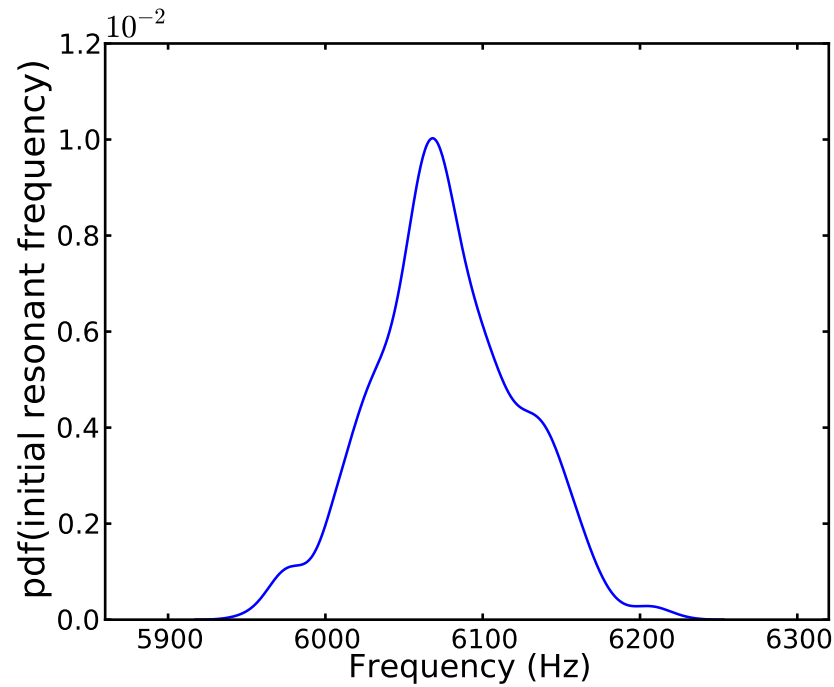


Figure 4.7: Posterior density of the initial resonant frequency obtained from Model 5 (Equation 4.5)

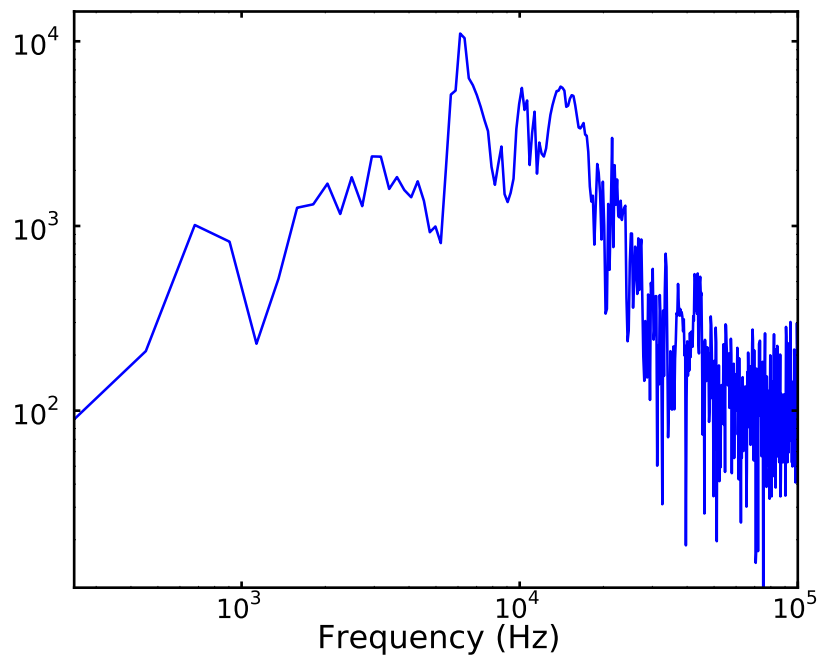


Figure 4.8: Fast Fourier transform of Figure 4.1

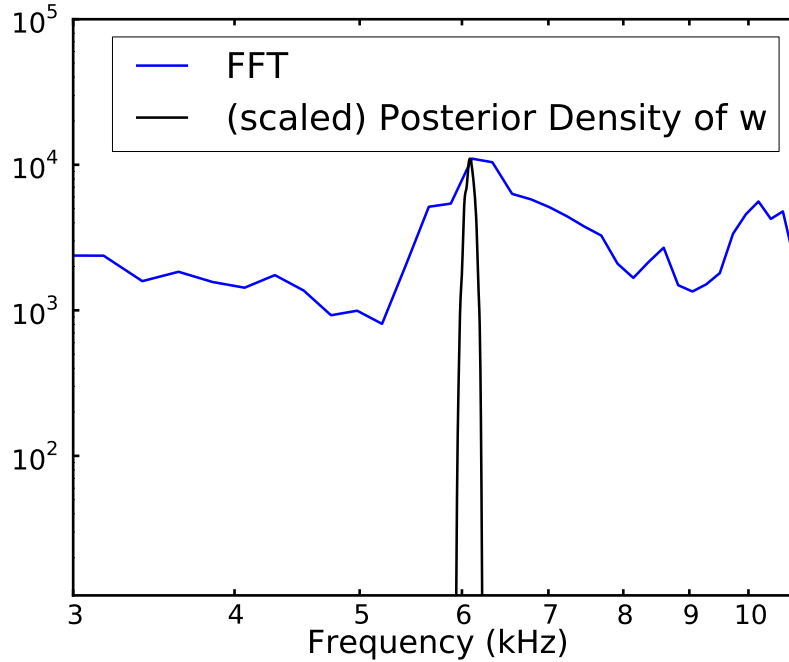


Figure 4.9: Comparison between the posterior density of the initial resonant frequency (Figure 4.7) and a fast Fourier transform of Figure 4.1

The original intention in developing this model was to determine the resonant frequency as a function of time, or crank-angle. This relationship is given in Equation 4.6 and shown in Figure 4.10 along with the third circumferential mode resonant frequency information that was also calculated. Our findings support the results obtained in (Stankovic and Bohme, 1999), which show, using time-frequency analysis, that the decay in the resonant frequencies are marginal. The similarity of the decay of both resonant frequencies is an indication that the model is working well, from a theoretical stand-point the decay rates should be equal. The difference is attributable to the start positions, the third circumferential term is prefixed by a step function, and because the decay for both modes are calculated independently.



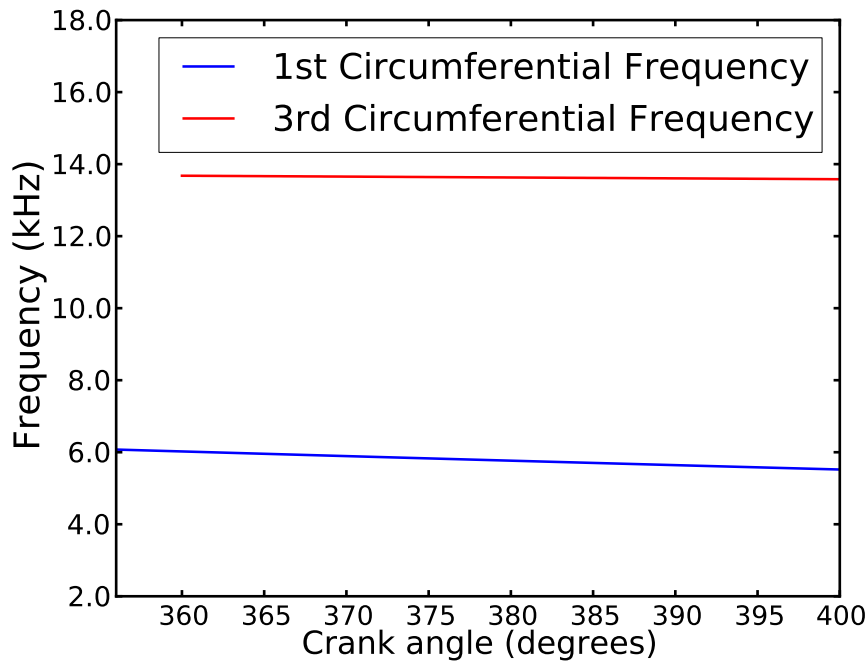


Figure 4.10: Drop in resonant frequency as a function of crank-angle. Taken from the final model (Model 5)

## 4.4 Cycle-by-cycle Analysis

Applying Model 5 across a range of cycles demonstrates the importance of using such a powerful inferential technique in this type of data analysis. Figure 4.11 shows the pdfs of many cycles taken from the same data set, showing the range of inter-cycle differences. Also visible are some cycles with lower resonant frequencies - these have been attributed to misfires and ignition delay.

The cycle-to-cycle variation that can be seen highlights the reason that ad hoc techniques such as cycle averaging or frequency spectrum averaging are inappropriate for conducting frequency analysis with internal combustion engines. The subtle information contained in these higher frequencies will be skewed, or removed, by cycle averaging; hence, eliminating the point and usefulness of spectral analysis when applied to resolving the resonant frequency from the in-cylinder pressure.

If the assumption of a homogeneous composition of the control volume is assumed, then the resonant frequency is related to the speed of sound and hence the temperature:

$$T = (\gamma R)^{-1} (fB/\alpha_{mn})^2, \quad (4.7)$$

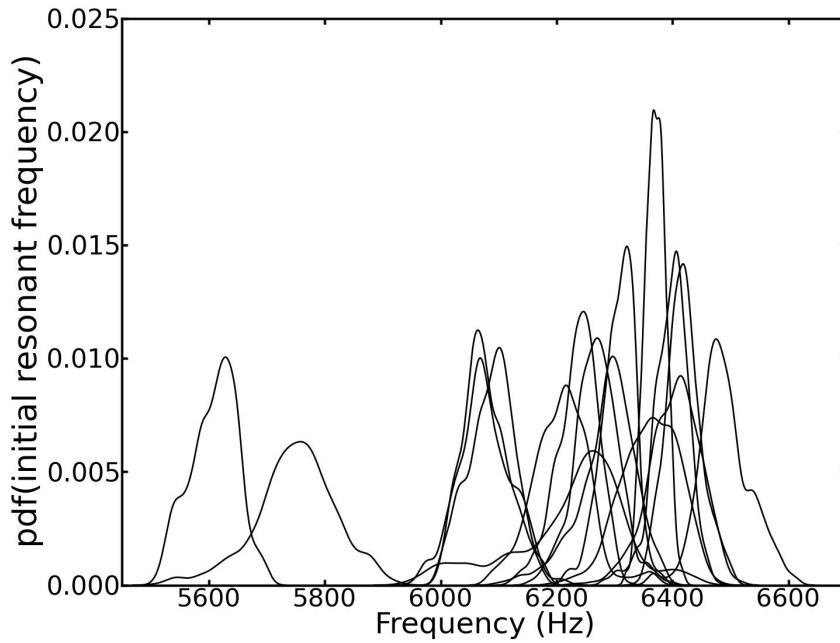


Figure 4.11: Probability density functions of the initial resonant frequency across a range of cycles

where  $T$  is temperature,  $\gamma$  is the ratio of the specific heat of the gas,  $R$  is the characteristic gas constant,  $f$  is the resonant frequency,  $B$  is the bore size and  $\alpha_{mn}$  is the non-dimensional number. This relationship between the resonant frequency and the temperature allows research into another facet of combustion phenomena.

Cycle-by-cycle analysis of the resonant frequency can yield interesting insights into the consistency of the combustion process. The relationship between frequency and temperature ( $T \propto f^2$ ) allows us to infer changes in combustion temperature and subsequently draw conclusions—such as attributing the lower frequency pdfs in Figure 4.11 to misfires and changes in ignition delay. Investigating the spread of the most likely estimate of these frequencies (the modal point) can be used both as a method to make judgments on the similarity of each combustion and as a vehicle for comparing operating conditions of an engine. Applications for this could be on-going condition monitoring or the evaluation of alternative fueling strategies.

## 4.5 Trapped Mass

Temperature of the gas in the combustion chamber, as a function of time, gives an indicator of what is occurring during combustion and the thermodynamic processes in the cylinder of the engine (Hickling et al., 1983). Equation 4.7 can be used to calculate the bulk temperature of the gas in the combustion chamber as a function of time, or crank-

angle, using the resonance information found from Model 5. Therefore, providing a method of determining this information from a standard engine testing laboratory. Values for  $\gamma$  and  $R$  are taken from AVL Boost simulations and the non-dimensional number  $\alpha_{mn}$  can be calculated by solving the equation:

$$J'_m(\pi\alpha_{mn}) = 0, \quad (4.8)$$

where  $J'_m$  is the derivative of the Bessel function of the first kind of order  $m$  (Hickling et al., 1983; Morse and Ingard, 1968).

$$\alpha_{1,0} = 0.5861$$

$$\alpha_{3,0} = 1.3373$$

Temperature, which is relatively constant at 3200 K, can be used to estimate the trapped mass in the cylinder using the ideal gas relationship  $PV = mRT$ , hence:

$$m(t) = \frac{P(t)V(t)}{RT(t)}, \quad (4.9)$$

where  $P(t)$  and  $V(t)$  are the experimentally measured pressure and volume time-series. Therefore, the trapped mass estimate as a function of crank-angle is shown in Figure 4.12.

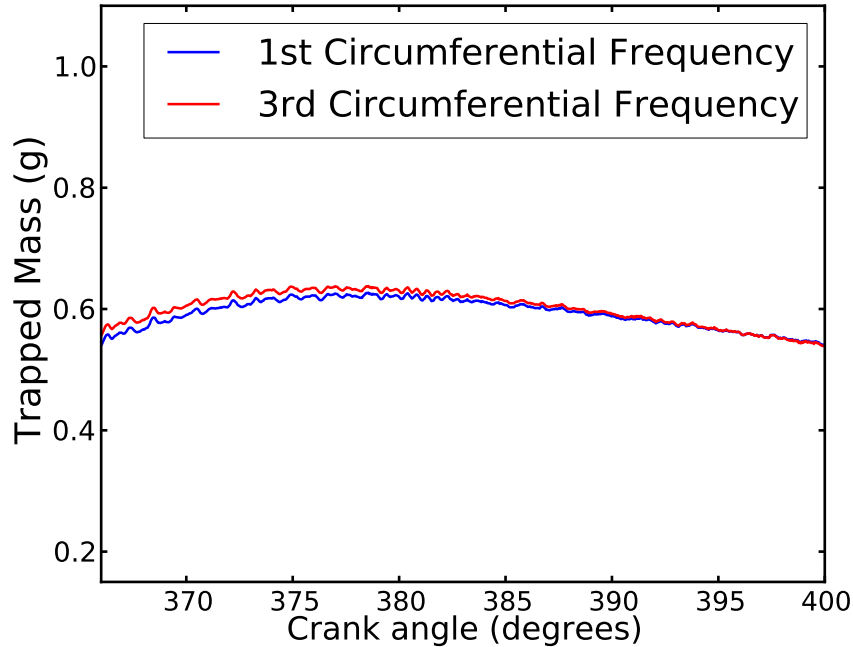


Figure 4.12: Estimated trapped mass calculated from combustion resonance and the ideal gas law

## 4.6 Limitations

The main limitation of this method is the problem of convergence. If the model used does not fit the data well then it is possible that results will not converge. This makes model selection very application dependent. In this instance, the desired application was to demonstrate the use of this method to obtain very specific frequency information from a cycle. Thus, the final model was very specific.

Having a very specific model also has a limitation in an application such as this in that should the data present itself in a manner that deviates from the expected, the model may no longer fit the data well and useful information may no longer be gained from it. Therefore, if the goal is to analyse every cycle across a period of time to investigate true cyclic variability it suggested that simpler models be used that still find the desired information. In this instance, the use of Model 3 would be a reasonable choice. The model is simple and hence more likely to converge with subtle changes in data, while still capturing the desired information well. Figure 4.13 shows the pdfs for the initial resonant frequency predicted by each model.

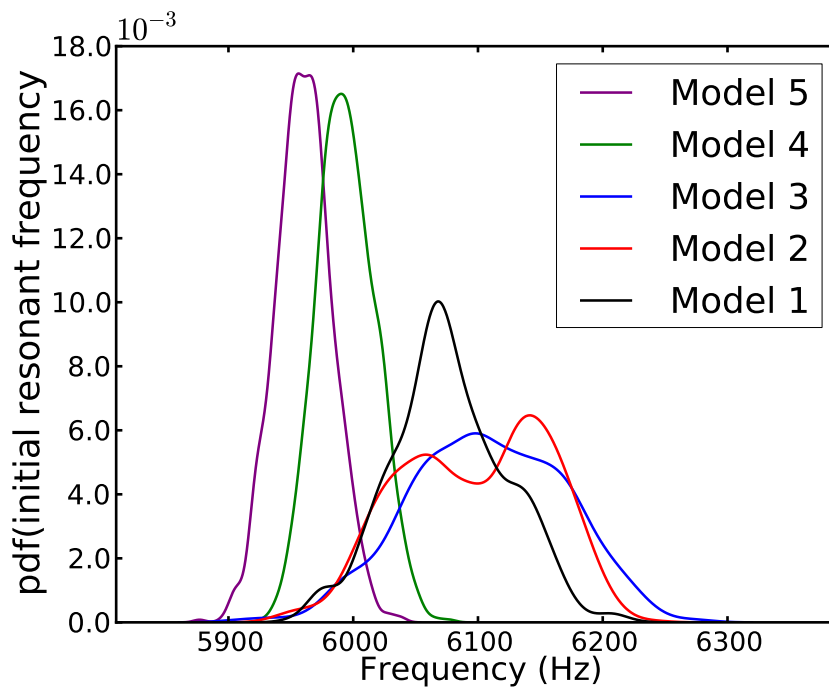


Figure 4.13: Probability density functions for the initial resonant frequency from Models 1 to 5

It can be seen that Models 1 and 2 give significantly different pdfs compared to the later models. This is to be expected as neither model allows the frequency to decay, and hence will return a result similar to that of the FFT which makes the same assumption. However, Models 3 and 5 return similar information, with the difference being that Model 5 has less uncertainty due to better model fit. This makes Model 3 an ideal choice for model selection

if many cycles in sequence are to be analysed and there are problems with cyclic changes that cause non-convergence.

A further issue is that the location of the pressure transducer, imperfections in the combustion chamber walls, design features of the combustion chamber and non-uniformities in the in-cylinder temperature will influence the determination of the in-cylinder temperature and the trapped mass calculation (Randall, 1987). This limitation can be overcome by estimating a correction factor and is discussed in Chapter 8. However, this does not remove the utility of this type of analysis if a correction factor cannot be resolved, especially for inter-cycle variability studies.

## 4.7 Further Work

The remainder of this dissertation will focus on a modern Cummins 5.9  $\ell$  turbo-charged diesel engine running on neat diesel fuel and also with fumigated ethanol. It is proposed that, under various fuelling strategies the engine will exhibit different cyclic behaviour, with respect to the resonant frequency, which will aid in the evaluation of alternative fuels and help us to further understand the phenomena of combustion of diesel engines in dual-fuel operation.

Applications of this method of analysis extend further than being able to identify resonant frequency information. With more sophisticated models that capture the initial rise in temperature at the onset of combustion investigations involving trapped mass could be done to experimentally determine blow-by on a cycle-by-cycle basis. This type of analysis is relevant to signals taken from accelerometers to quantify knock in a manner that would allow comparisons between operating conditions. A further application could be the extraction of resonant frequency information directly from an accelerometer signal. Careful filtering would be required in this case.

## 4.8 Conclusion

This paper has introduced a powerful inference technique for the determination of resonant frequencies in a DI diesel engine which explicitly model the time dependence of the resonant frequency. This leads to a superior characterisation of important frequency behavior over FFT methods, which assume frequency components are time invariant, without introducing the complexities of other time-frequency analyses. Compared to results obtained from FFTs our method provides superior resolution and information about the time dependence of the resonant frequency. Our results provide a solid reason for the use of Bayesian inference as a method of analysing in-cylinder pressure data.

## 4.9 Acknowledgements

The authors wish to thank the following undergraduate students for dynamometer operation during experimental campaigns: Mr. Adrian Schmidt, Mr. Peter Clarke, Mr. Yoaann Despiau and Mr. Steven Herdy. We also wish to thank Mr. Tony Morris for assisting with the design of experimental campaigns and Mr. Jon James and Mr. Glenn Geary for enabling an undergraduate teaching engine to be used for research purposes. Further thanks also to Technologist Mr. Ken McIvor for his assistance in setting up the data acquisition software. Also, thanks to Ph.D candidate Mr. Nicholas Surawski for his work in making the experiments a success. This work was undertaken under an Australian Research Council Linkage Grant (LP0775178) in association with Peak3 P/L.

## 4.10 References

- Antoni, J. Cyclostationarity by examples. *Mechanical Systems and Signal Processing*, 23(4): 987–1036, 2009.
- Berg, A., Meyer, R., and Yu, J. Deviance information criterion for comparing stochastic volatility models. *Journal of Business & Economic Statistics*, 22:107–120, 2002.
- Bohme, J. F. and Konig, D. Statistical processing of car engine signals for combustion diagnosis. In *IEEE Seventh SP Workshop on Statistical Signal and Array Processing*, pages 369–374, 1994.
- Bretthorst, G. L. and Smith, C. R. Bayesian analysis of signals from closely-spaced objects. In *Infrared Systems and Components III, Proc. SPIE 1050*, 1989.
- Burg, J. Maximum entropy spectral analysis. In Childers, D., editor, *Proceedings of the 37th Meeting of the Society of Exploration Geophysicists. Reprinted (1978) in Modern Spectrum Analysis*, 1967.
- Burg, J. *Maximum entropy spectral analysis*. PhD thesis, Stanford University, 1975.
- Cooley, J. W. and Tukey, J. W. An algorithm for the machine calculation of complex Fourier series. *Mathematics of Computation*, 19(90):297–301, 1965.
- Everitt, B. S. *The Cambridge Dictionary of Statistics, Third Edition*. Cambridge University Press, 2006.
- Hickling, R., Feldmaier, D. A., Chen, F. H. K., and Morel, J. S. Cavity resonances in engine combustion chambers and some applications. *Acoustical Society of America Journal*, 73: 1170–1178, 1983.

- Jaynes, E. T. Bayesian spectrum and chirp analysis. *Maximum-Entropy and Bayesian Spectral Analysis and Estimation Problems*, 1987.
- Payri, F., Broatch, A., Tormos, B., and Marant, V. New methodology for in-cylinder pressure analysis in direct injection diesel engines: application to combustion noise. *Measurement Science and Technology*, 16(2):540–547, 2005.
- Randall, R. B. *Frequency Analysis*. Bruel & Kjaer, 1987.
- Ren, Y., Randall, R. B., and Milton, B. E. Influence of the resonant frequency on the control of knock in diesel engines. *Proceedings of the Institution of Mechanical Engineers: Part D: Journal of Automobile Engineering. London*, 213(2):127–133, 1999.
- Samimy, B. and Rizzoni, G. Mechanical signature analysis using time-frequency signal processing: application to internal combustion engine knock detection. *Proceedings of the IEEE*, 84(9):1330–1343, 1996.
- Spiegelhalter, D. J., Thomas, A., and Best, N. G. *WinBUGS Version 1.2 User Manual*. MRC Biostatistics Unit, 1999.
- Spiegelhalter, David J., Best, Nicola G., Carlin, Bradley P., and Linde, Angelika van der. Bayesian measures of model complexity and fit. *Journal of the Royal Statistical Society. Series B (Statistical Methodology)*, 64(4):583–639, 2002.
- Stankovic, L. A multitime definition of the Wigner higher order distribution: L-Wigner distribution. *Signal Processing Letters, IEEE*, 1(7):106–109, 1994a.
- Stankovic, L. A method for time-frequency analysis. *Signal Processing, IEEE Transactions on*, 42(1):225–229, 1994b.
- Stankovic, L. and Bohme, J. F. Time-frequency analysis of multiple resonances in combustion engine signals. *Signal Processing*, 79(1):15–28, 1999.
- Surawski, N. C., Miljevic, B., Roberts, B. A., Modini, R. L., Situ, R., Brown, R. J., Bottle, S. E., and Ristovski, Z. D. Particle emissions, volatility, and toxicity from an ethanol fumigated compression ignition engine. *Environmental Science & Technology*, 44(1):229–235, 2010.
- Tierney, L. Markov chains for exploring posterior distributions. *The Annals of Statistics*, 22(4):1701–1728, 1994.
- Torregrosa, A. J., Broatch, A., and Margot, X. Combustion chamber resonances in direct injection automotive diesel engines: a numerical approach. *International Journal of Engine Research*, 5(1):83–91, 2004.

Wang, C., Zhang, Y., and Zhong, Z. Fault diagnosis for diesel valve trains based on time-frequency images. *Mechanical Systems and Signal Processing*, 22(8):1981–1993, 2008.



## Chapter 5

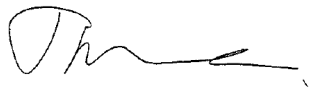
# Inter-cycle variability of in-cylinder pressure parameters in an ethanol fumigated common rail diesel engine

Timothy Bodisco, Richard J. Brown

Science and Engineering Faculty, Queensland University of Technology, Brisbane QLD, 4001, Australia

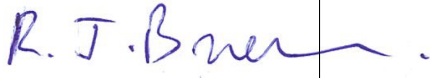
Publication: Energy (2013) 52(1), 55–65.

### Author Contribution

Contributor	Statement of Contribution
Timothy Bodisco	Conducted the experiments, performed the data analysis and drafted the manuscript
Signature 	
Richard Brown	Supervised the project, aided with the development of the paper and extensively revised the manuscript

### Principal Supervisor Confirmation

I have sighted email or other correspondence from all co-authors confirming their certifying authorship.

Name	Signature	Date
Associate Professor Richard Brown		

### Abstract

The effects of ethanol fumigation on the inter-cycle variability of key in-cylinder pressure parameters in a modern common rail diesel engine have been investigated. Specifically, maximum rate of pressure rise, peak pressure, peak pressure timing and ignition delay were investigated. A new methodology for investigating the start of combustion was also proposed and demonstrated—which is particularly useful with noisy in-cylinder pressure data as it can have a significant effect on the calculation of an accurate net rate of heat release indicator diagram. Inter-cycle variability has been traditionally investigated using the coefficient of variation. However, deeper insight into engine operation is given by presenting the results as kernel density estimates; hence, allowing investigation of otherwise unnoticed phenomena, including: multi-modal and skewed behaviour. This study has found that operation of a common rail diesel engine with high ethanol substitutions (>20% at full load, >30% at three quarter load) results in a significant reduction of ignition delay. Further, this study also concluded that if the engine is operated with absolute air to fuel ratios (mole basis) less than 80, the inter-cycle variability is substantially increased compared to normal operation.

## 5.1 Introduction

The need to move away from fossil fuels was outlined in a recent study by Shafiee and Topal (Shafiee and Topal, 2009) which showed that after 2042 it is probable the only fossil fuel still available will be coal. Further, in Australia greenhouse gas emissions, carbon dioxide equivalent emissions, from the transport sector make up approximately 15% of the total greenhouse gas emissions (Australian National Greenhouse Accounts, 2010)—this value in the United States is considerably higher at 28% (McArdle et al., 2007). Indicators such as these place pressure for viable, cleaner bio-origin fuels as alternatives to fossil fuels for transport to be developed and implemented (Skelton, 2007).

Fumigation, which is the introduction of supplementary fuels into the intake air, has been under investigation for diesel fuel substitution since the late 1920s and the first commercial dual-fuel vehicle was built in 1939 (Sahoo et al., 2009); however, it was first mentioned in Rudolf Diesel's original patent for internal combustion engines in 1892 (Diesel, 1892). Fumigation in diesel engines can be achieved with many liquid and gaseous fuels. Lower alcohols, such as methanol or ethanol are suitable as secondary fuels (injected either as a vapour or an atomised liquid) in diesel engines (Hayes et al., 1988; Abu-Qudais et al., 2000; Sahoo et al., 2009; Surawski et al., 2010, 2012). This paper will focus on the effects that ethanol fumigation has on in-cylinder pressure, and its relationship to combustion.

Ethanol fumigation represents a currently viable option for reducing diesel fuel consumption (Rosillo-Calle and Walter, 2006; Sorda et al., 2010). This is true not only in general transport but also in agriculture, particularly those industries that can produce their own ethanol, and for the use in electricity generators (RIRDC, 2007).

This current study represents a first step in evaluating the practicality of ethanol fumigation in a modern common rail diesel engine by investigating inter-cycle variability using neat diesel fuel and with ethanol fumigation up to 40% by energy. The current literature has only explored ethanol fumigation in older direct (mechanical) injection diesel engines which typically have diesel injection 15 to 35 degrees before top dead centre (TDC). Whereas, this paper investigates a modern common rail engine where injection occurs near TDC and at a much higher pressure; thereby, completely changing the performance and emissions characteristics. Moreover, most of the current work is performed on low power single-cylinder engines; given that in-cylinder temperature is a function of engine load it is reasonable to assume that different characteristics would be found in a higher capacity multi-cylinder engine operated with fumigated fuels.

Chauhan et al. (2011) recently did an experimental study on ethanol fumigation. This study was performed on a single-cylinder compression ignition engine with injection timing at 26 degrees before TDC and a rated power of 7.5 kW at 1500 rpm. Their work focused on the use of ethanol as a secondary fuel with ethanol substitutions as high as 48%. Results from their work showed that the emission output of the engine can be improved with the

introduction of ethanol as a fumigated fuel. However, the addition of ethanol did increase the hydrocarbon emission and past certain ethanol percentage thresholds all emissions showed increases. They concluded that the optimal ethanol substitution was 15%.

Lakshmanan and Nagarajan (2010) investigated dual fuel operation of a diesel engine with timed manifold injections of acetylene. The engine used in their study was a single-cylinder compression ignition engine with injection timing at 27 degrees before TDC and a rated power of 4.4 kW at 1500 rpm. In their study the acetylene was introduced into the engine intake manifold through an electronic gas injector. Acetylene was injected at 5, 10 and 15 degrees after TDC for various injection durations. They determined that the optimal injection time was 10 degrees after TDC for 9.9 ms. The use of acetylene slightly increased the smoke output of the engine; however, it had a positive effect on the emission output of hydrocarbons, NO<sub>x</sub>, CO and CO<sub>2</sub>.

Sahin et al. (2008) performed an experimental investigation into gasoline fumigation. As part of their work they have also reviewed the advantages of fumigating fuels in diesel engines and investigated the cost effects of using gasoline as a fumigated fuel. Their main study involved fumigating gasoline into a single-cylinder compression ignition engine with injection timing at 22 degrees before TDC at engines powers less than 6.4 kW. They concluded that: power increases were possible with gasoline substitutions (by volume) of 6-8%, specific fuel consumption decreases up to gasoline substitutions of 4-6% and the most favourable gasoline substitutions lied between 4-6% boasting both power increases (4-9%) and lower specific fuel consumption (1.5-4%).

Carlucci et al. (2008) studied the effects of natural gas (methane) in a dual fuel single-cylinder diesel engine. For their experiment they controlled the diesel injection timing to force the combustion peak to occur at 10 degrees after TDC. However, for their baseline (diesel only) testing pilot diesel injection occurred at 24 and 39 degrees before TDC for 1500 and 2000 rpm, respectively, with the main diesel injection occurring at 7.5 and 11 degrees before TDC, respectively. Results in this paper were reported on mean combustion cycles generated by averaging 50 consecutive cycles, which were then filtered with a low-pass numeric filter. Their research focused on investigating rate of heat release diagrams and emission. An important conclusion from this work was that with pilot injection the jet penetration is of the same importance as the quantity of the fuel used.

Karthikeyan and Mahalakshmi (2007) investigated the use of turpentine in a dual fuel diesel engine. Their experiments were performed on a single-cylinder compression ignition engine with a rated power of 4.4 kW at 1500 rpm and diesel injection timing at 26 degrees before TDC. The use of turpentine performed well at loads less than 75%; however, above 75% load substantial increases in emission and decreases in volumetric efficiency were evident.

Kouremenos et al. (1990) performed a comparative study comparing fumigated diesel fuel to fumigated gasoline as a supplementary fuel in a single cylinder compression ignition engine.

The experiments conducted by Kouremenos et al. (1990) were done on a research engine capable of being run in both Otto or four-stroke diesel mode. During their experiments the engine was run in diesel mode with a Comet MK.V turbulence-chamber head with diesel injection timing set at 38 degrees before TDC. Their work made use of a form of the equivalence ratio, defined by Kouremenos et al. (1990) as:

$$\alpha = \frac{\dot{m}_g}{\dot{m}_d + \dot{m}_g}$$

where,  $\dot{m}_g$  is the supplementary diesel or gasoline mass flow rate and  $\dot{m}_d$  is the primary diesel mass flow rate. For Kouremenos et al. (1990) this was convenient because of the similar density and gross calorific properties of diesel and gasoline fuels. Their results showed that knock occurred for gasoline fumigation at  $\alpha \approx 0.20$  and for diesel fumigation at  $\alpha \approx 0.30$ . In contrast, the present analysis does not use this approach because of the significant differences between ethanol and diesel fuels—the approach used in this paper is outlined in Section 5.3.

Selim (2005) showed that dual-fuel operation of a single-cylinder compression ignition engines gave rise to more inter-cycle variability. His work focused on examining combustion noise, sound frequency around 1.6-2 kHz, by investigating the maximum rate of pressure rise and follows on from cyclic variability work that began with Kouremenos et al. (1992) which focused on the inter-cycle variability of the following key parameters: peak pressure, peak pressure timing, maximum rate of pressure rise, indicated mean effective pressure and ignition delay in a single-cylinder diesel engine. In a later work Selim (2008) investigated the effects of changing the primary fuel from diesel to a bio-derived fuel, jojoba methyl ester, and concluded that the properties of this bio-fuel reduced the inter-cycle variability and the onset of knock, owing to a higher cetane number.

Fang et al. (2012) investigated the influence of pilot injection and exhaust gas recirculation on combustion and emissions in a HCCI-DI combustion engine. The engine used in their study was a heavy-duty four-cylinder engine with a common rail injection system. As part of their study Fang et al. (2012) explored the effect of exhaust gas recirculation and pilot injection quantity on inter-cycle variability. Inter-cycle variability was discussed in terms of the coefficient of variation (COV) of indicated mean effective pressure (IMEP) and of peak pressure. They show that increasing the pilot quantity decreases the inter-cycle variability to a threshold and then further increases in pilot quantity increase the inter-variability—in all instances exhaust gas recirculation decreased inter-cycle variability.

The current study will focus on the inter-cycle variability parameters investigated by Kouremenos et al. (1992); however, with a modern 6-cylinder common rail diesel engine with a rated power of 162 kW at 2000 rpm operated with neat diesel fuel and fumigated ethanol substitutions up to 40% by energy. The higher relative capacity of the engine in this investigation results in a mean effective pressure that is at least 30% higher than that of the

vast majority of engines used to investigate light fuel fumigation with compression ignition engines. This higher mean effective pressure will directly correlate to a higher in-cylinder temperature, and hence will impact directly on the combustion of the fumigated fuel.

## 5.2 Terminology and Abbreviations

DXXXEYYY	DXXXEYYY represents the nominal XXX% of diesel fuel by energy and the nominal YYY% substitution of ethanol by energy
EMS	Engine management system
IMEP	Indicated mean effective pressure
Kernel density estimate	An estimation of the probability density function
Neat diesel	Neat diesel refers to the case where the engine is run on diesel fuel only, no ethanol substitution
NRHR	Net rate of heat release
RTD	Resistance Temperature Detector
TDC	Top dead centre (0 and 360 crank-angle degrees)

## 5.3 Experimental Configuration and Data Acquisition

Experiments were conducted on a modern turbo-charged inline 6-cylinder Cummins diesel engine (ISBe220 31) with common rail injection at the QUT Biofuel Engine Research Facility (BERF) in June 2011. See Figure 5.1 for a detailed schematic of the engine setup featuring the ethanol fumigation system and the pressure and crank angle data acquisition system. The engine has a capacity of 5.9  $\ell$ , a bore of 102 mm, a stroke length of 120 mm, a compression ratio of 17.3:1 and maximum power of 162 kW at 2000 rpm and maximum torque of 820 Nm at 1500 rpm. Each cylinder has two inlet and two exhaust valves. Cylinders two to five share their inlet ports with their adjacent cylinders. Whilst, cylinders one and six each have one of their inlet valves supplied by a separate inlet port directly from the inlet manifold because they only have one adjacent cylinder each to share with.

The engine was coupled to an electronically controlled hydraulic dynamometer with load applied by increasing the flow rate of water inside the dynamometer housing. In-cylinder pressure was measured by a Kistler (6053CC60) piezoelectric transducer with a Data Translation (DT9832) simultaneous analogue-to-digital converter connected to a desktop computer running National Instruments LabView. Data was collected at a sample rate of 200 kHz for 4 minutes at each setting.

Specific data collected was in-cylinder pressure, band-pass filtered in-cylinder pressure (allowing 4-20 kHz, both pressure signals collected as a differential voltage signal), diesel injection timing and degrees of crank angle rotation information. The band-pass filter settings were set to capture the combustion resonance whilst minimising the effects of the knocking frequencies ( $<4$  kHz) and the noise from the injector signal ( $>28$  kHz). The diesel injection timing was controlled by the engine management system (EMS) and was unable to be actively controlled—in all test cases the diesel injection strategy was a sustained single injection where combustion commences prior to the diesel injection completing. An impact of this is the diesel injection retarding with increasing ethanol substitutions. The ethanol injection system is independent of the EMS; therefore, the energy input from the ethanol is unknown to the EMS and it will treat this energy as though it came from an operating condition such as descending a hill. The crank angle rotation information is acquired from a Kistler crank angle encoder set (type 2614) with a resolution of 0.5 crank angle degrees—crank angle values were interpolated between the known points. The limit of crank angle resolution, based on the sampling frequency, 0.06 degrees per sample at 2000 rpm, this results in a maximum uncertainty of 0.06 crank angle degrees.

The engine was run at 2000 rpm on neat automotive diesel and with ethanol fumigation substitutions of 10%, 20%, 30%, and 40% at full load (760 Nm) and at three quarters (570 Nm) and half (380 Nm) of full load. The substitutions were performed by stabilising the engine at the required load, then reducing the diesel energy (as inferred by the engine load) by the substitution percentage and introducing fumigated ethanol until the original engine load was achieved. Table 5.1 shows the exact diesel reductions and corresponding energy distributions for each test setting. All of the flow meters were calibrated to an absolute standard (using a known volume and stopwatch) and were found to be operating within a 2% uncertainty. Ethanol fumigation was achieved by directly introducing the ethanol as a vapour into the air in-take at the inlet manifold directly after the turbocharger and before the intercooler, Injector 2 in Figure 5.1, at an injection frequency of 50 Hz. The flow of the manifold arrangement may have an effect on combustion air supplied to the engine. Modelling experiments in AVL Boost indicate that the mass of the charge air can vary as great as 2% between the cylinders. In order to achieve repeatable fuel delivery at all engine loads, the difference in pressure between the ethanol fuel rail and the post turbo-charger manifold pressure was monitored and used as feedback to the ethanol pressure relief valve, in the case of Ethanol Injector 2 this is Pressure Relief Valve 2 in Figure 5.1. It is assumed, given the frequency of the ethanol injection and the feedback mechanism to regulate the pressure relief valve, that the supply of ethanol to the cylinders was steady.

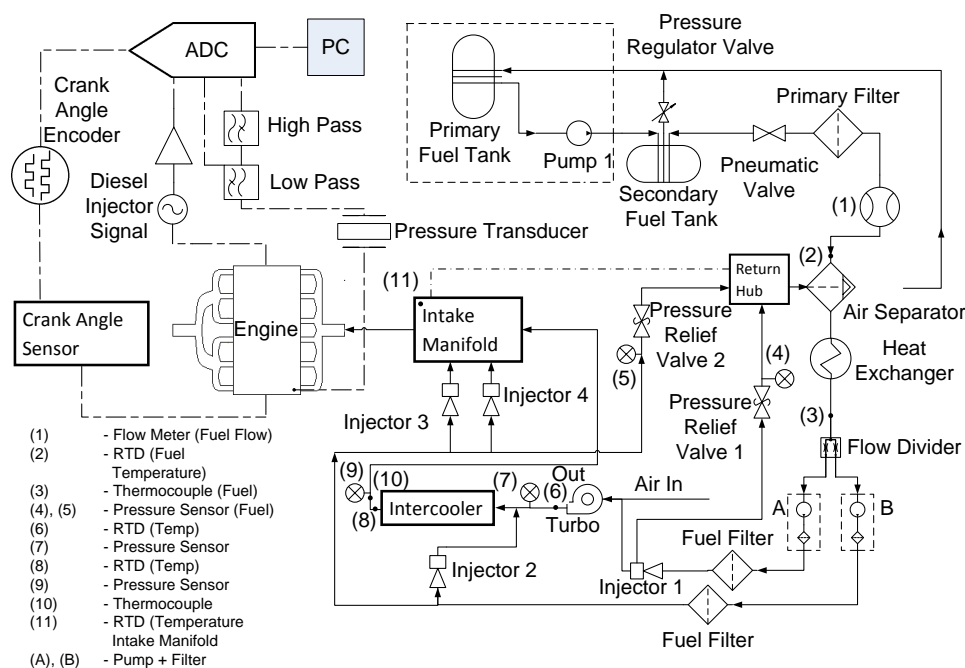


Figure 5.1: Schematic of the ethanol injector and pressure/crank angle data acquisition systems

Load	Nominal ethanol substitution	Diesel reduction	Diesel energy	Ethanol energy
Full	0%	0%	100%	0%
	10%	10.3%	92.1%	7.9%
	20%	21.1%	80.0%	20.0%
	30%	29.3%	71.3%	28.7%
	40%	38.1%	66.1%	33.9%
Three Quarters	0%	0%	100%	0%
	10%	9.2%	94.0%	6.0%
	20%	18.1%	81.7%	18.3%
	30%	26.8%	71.1%	28.9%
	40%	36.2%	65.9%	34.1%
Half	0%	0%	100%	0%
	10%	6.8%	93.9%	6.1%
	20%	15.9%	68.3%	31.7%
	30%	26.1%	66.8%	33.2%
	40%	32.8%	57.2%	42.8%

Table 5.1: Ethanol substitutions at each test setting

The acquisition of temporally resolved in-cylinder pressure data from an internal combustion engine provides many insights into the operation of an engine. For example, the analysis of pressure data with respect to crank angle, and by extension volume, is able to provide



insights into how efficiently an engine is operating; peak pressure, maximum rate of pressure rise, heat release, indicated work, indicated power, indicated mean effective pressure, and thermal efficiency are the most commonly investigated (Amann, 1986; Heywood, 1988; Randolph, 1990). Moreover, statistical analysis of the above mentioned engine parameters are able to provide indicators of the reliability of engine operation (Bodisco et al., 2012). Figure 5.2 shows an example of pressure versus crank angle data. As work is related to pressure, investigating in-cylinder pressure can yield many insights into combustion phenomena.

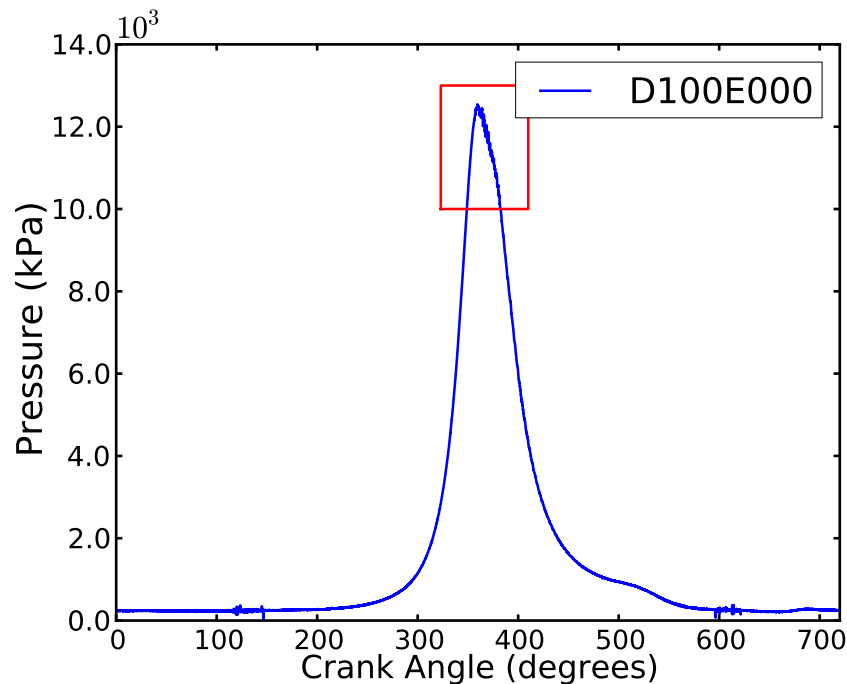


Figure 5.2: Pressure vs crank angle plot at full load on neat diesel fuel

The fluctuation located at the peak of Figure 5.2 is related to the combustion of the fuel—indicated by a box. This fluctuation can be isolated and analysed; the dominant frequency through this area is the first circumferential mode frequency, and hence forth will be referred to as combustion resonance. Figure 5.3 shows the combustion resonance from the in-cylinder pressure trace in Figure 5.2, 4-20 kHz band-pass filter in-cylinder pressure data—since the change in output voltage from the pressure transducer and the change in actual pressure differ only by a linear scale, conversion from the voltage signal to pressure is an unnecessary computational penalty. The box indicates the start of ignition, detailed in the next section.

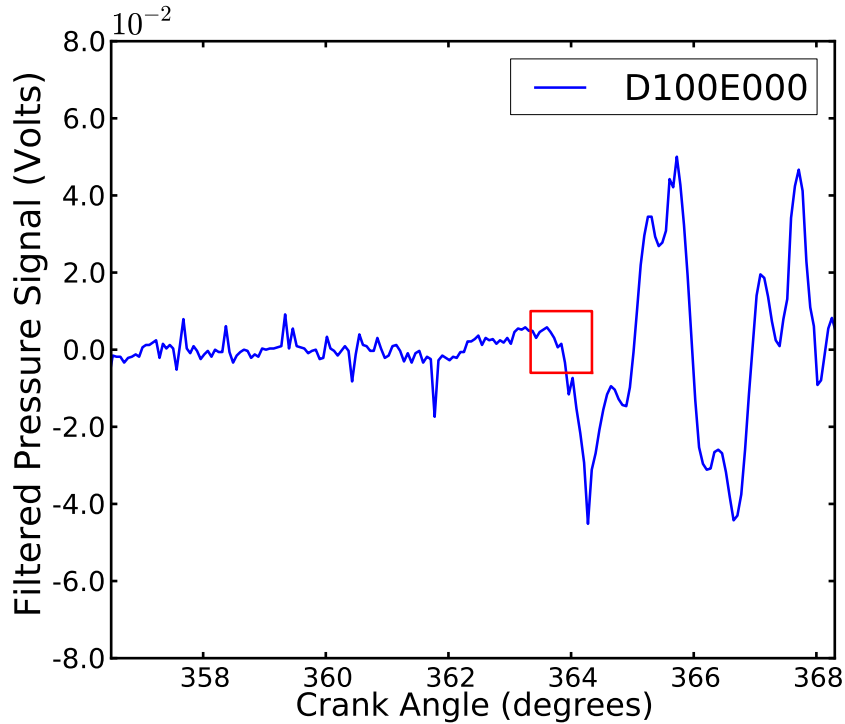


Figure 5.3: Band-pass filtered voltage in-cylinder pressure signal at full load on neat diesel fuel

## 5.4 Determination of the Start of Combustion

### 5.4.1 Combustion Resonance

An extensive analysis of combustion resonance by the authors has been undertaken in (Bodisco et al., 2012)—some important early work in the area of combustion resonance was done by Hickling et al. (1979; 1983). Interest in combustion resonance is owed to its relationship with the speed of sound, and hence in the case of a combustion chamber, temperature (Hickling et al., 1983; Bohme and Konig, 1994; Ren et al., 1999; Payri et al., 2005; Torregrosa et al., 2004). In Bodisco (2012) the resonant frequency was isolated in a direct (mechanical) injection diesel engine and used to estimate the in-cylinder temperature and the trapped mass in the combustion chamber during combustion as a function of time, or crank angle. This paper also demonstrated the large amount of cycle-to-cycle variability of combustion in diesel engines and established a strong argument against cycle averaging. Further, the isolation of combustion resonance also has important applications in the detection of knock (Ren et al., 1999; Samimy and Rizzoni, 1996).

In this study the injection timing was obtained by directly interrogating the electronic diesel injector driver signal. Unfortunately, the mechanical latency in the injector is un-

known. However, latency would be approximately uniform across all of the cycles, a repeatable charge time; hence, meaningful comparisons of ignition delay can be made. Modern injectors are designed for the dimensions of the internals to change in a highly accurate manner, allowing for fast, precise and repeatable needle motion (Lee et al., 2006). The signal shown in Figure 5.3 starts exactly where the electronic injection signal occurs and the observed fluctuations in in-cylinder pressure between 356 and 364 degrees crank angle are associated with interference from the electronic diesel injection signal—the increase in voltage seen at  $\sim 362$  is attributable to a change in the electronic injection signal frequency. Following this, the start of combustion can be seen to commence at approximately 364 degrees crank angle, after which a strong resonance can be seen—clearly visible on the right-hand side of Figure 5.3. For the purposes of this investigation the ignition delay was defined as the number of crank angle degrees from nominal injection, detected from the electronic diesel injector driver signal, to the start of combustion which was taken to be when the signal no longer only exhibited noise-like behaviour and the combustion resonance commenced—the commencement of the combustion resonance has been indicated with a red box in Figure 5.3. The combustion resonance is at approximately 6 kHz. Analysis was performed in all cases by at least 2 independent investigators, the maximum deviation in individual cycle results was never more than 2 data points, corresponding to approximately 0.12 crank angle degrees. Therefore, over the 200 cycles analysed at each test case, the natural variation in interpretation between investigators showed the same mode and variability within the experimentally determined uncertainty of 0.12 crank angle degrees. Ignition delay results are displayed relative to the modal ignition delay of the neat diesel case at each load.

### 5.4.2 Net Rate of Heat Release

Determination of the start of combustion by analysing the net rate of heat release (NRHR) is standard practice in engine research. Net rate of heat release models are typically based on the first law of thermodynamics and often provide very valuable insight into combustion processes, an example NRHR diagram can be seen in Figure 5.4. However, this approach to determining the start of combustion has a few short comings which are not easily overcome. Namely, it is very difficult to account for mixture non-uniformity in the air/fuel ratio and in the burned and unburned gas non-uniformity, the effect of crevice regions in the combustion chamber, and assuming the wrong rate of heat transfer between the cylinder charge and combustion chamber walls (especially with the addition of a ‘cooling’ additive such as water, or ethanol) (Heywood, 1988; Brunt and Platts, 1999; Tauzia et al., 2010). However, under standard operating conditions, such as running an engine with neat diesel fuel, this approach to determine the start of combustion works very successfully, as can be seen in Figure 5.4. In Figure 5.4 the vertical line represents the modal start of combustion as determined by the use of combustion resonance.

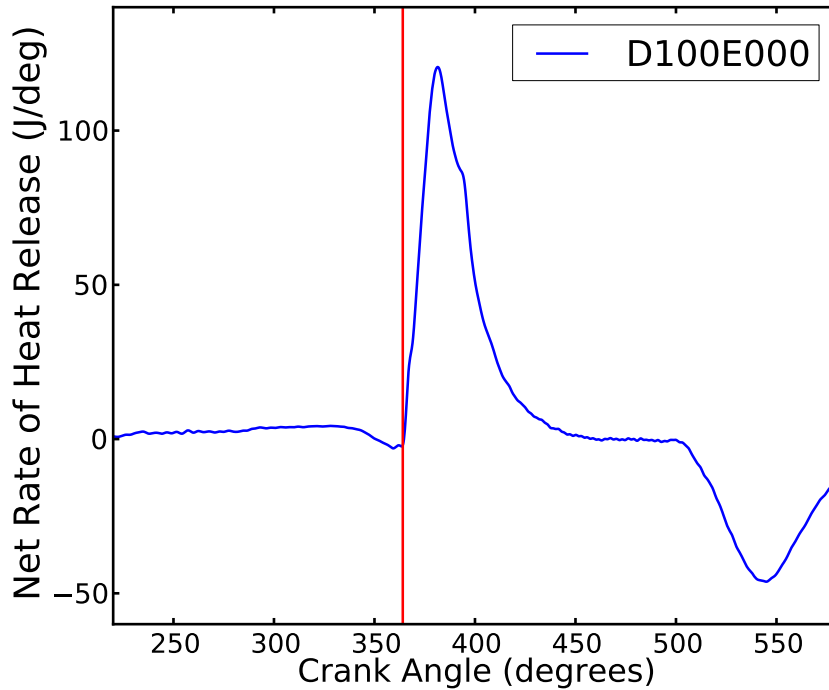


Figure 5.4: Net rate of heat release, full load, neat diesel with the modal start of combustion marked

Calculated in-cylinder pressure parameters, such as NRHR, are typically generated from cycle averaged data (Kouremenos et al., 1992; Rakopoulos et al., 2007; Shehata, 2010; Tazua et al., 2010). That is, to reduce noise and to have the ability to read off single values as representative of the experiment many cycles are combined before the NRHR is calculated—Figure 5.4 was generated from 4000 consecutive cycles. This approach can be quite problematic if the inter-cycle variability is high, such as is possible when the engine is run with different fuels, or under different operating strategies. Moreover, filtering is required to be able to interpret the NRHR because of the high frequency noise generated from differentiating already noisy data—particularly in the case of the data shown in this paper, where the diesel injector signal has interfered with the in-cylinder pressure signal. Essentially, cycle averaging or filtering can potentially skew the interpretation of the NRHR.

## 5.5 Results

In order to investigate the inter-cycle variability of the parameters of interest: peak pressure, peak pressure timing, maximum rate of pressure rise and ignition delay, kernel density estimates (probability density functions) are created (Rosenblatt, 1956; Parzen, 1962). Owing to the discrete nature of the electronic injector signal, histograms were created to investigate

the cycle-to-cycle variation. This was done to allow a visual representation of the inter-cycle variability and will also avoid ambiguous interpretations, such as quoting mean values of multi-modally distributed data—when single data values are given they are taken as the mode of the data, defined as the peak of a kernel density estimate. For each data set the engine was run for 4 minutes, resulting in approximately 4000 cycles at 2000 rpm. However, the ignition delay results are derived from 200 consecutive cycles only, owing to the time consuming nature of the analysis.

Results are presented by engine load, rather than by parameter because engine load has the greatest influence on the parameters under consideration. Such a presentation is also consistent with the method of ethanol substitution where  $x\%$  is the amount of ethanol required to offset  $x\%$  of the diesel energy input to the engine.

### 5.5.1 Full Load Results

Figures 5.5 to 5.9 show the results for full load (760 Nm) as probability density functions of the parameters of interest. Maximum rate of pressure rise results are shown in Figure 5.5, a small decrease in maximum rate of pressure rise can be seen with low ethanol substitutions and also a small increase in inter-cycle variability. At high ethanol substitutions (above 20%) increasing ethanol significantly increases the maximum rate of pressure rise and the inter-cycle variability. Moreover, at these high substitution settings the engine had audible knock.

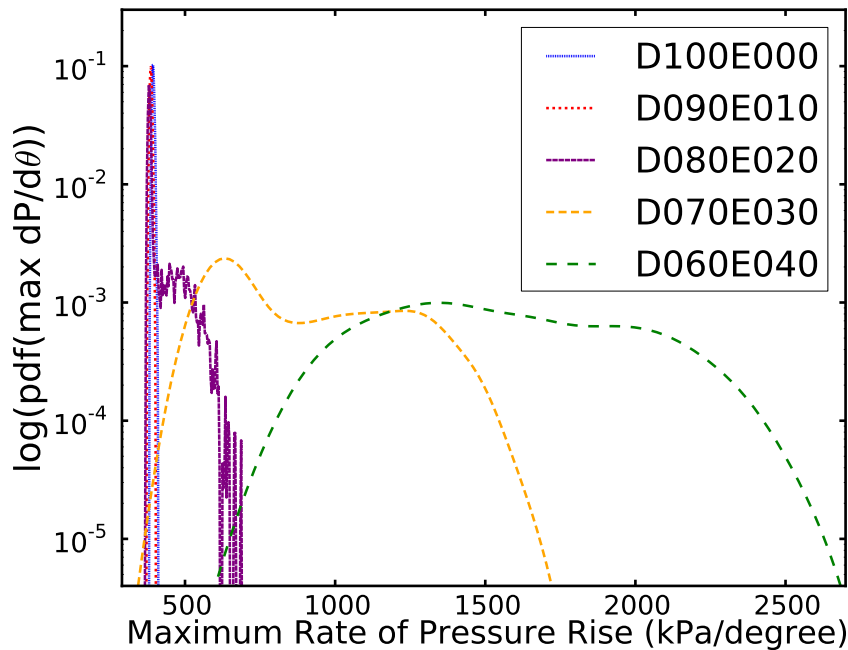


Figure 5.5: Maximum rate of pressure rise, full load, 0%–40% ethanol substitutions

There is a systematic increase in peak pressure and peak pressure inter-cycle variability with increasing ethanol substitutions, shown in Figure 5.6. However, the peak pressure timing, Figure 5.7, shows that the 10% ethanol substitution yielded the least inter-cycle variability. The neat diesel case and the 20% ethanol substitution case are bi-modal. In the neat diesel case, this is a result of the first peak in pressure, a motoring peak just before TDC, being similar to the combustion peak pressure, just after TDC. The similarity of these two pressure peaks is evident in Figure 5.6 which is showing very little inter-cycle variability in the peak pressure result for neat diesel. Also, discounting the neat diesel case there is an increase in the inter-cycle variability as the ethanol substitution increases.

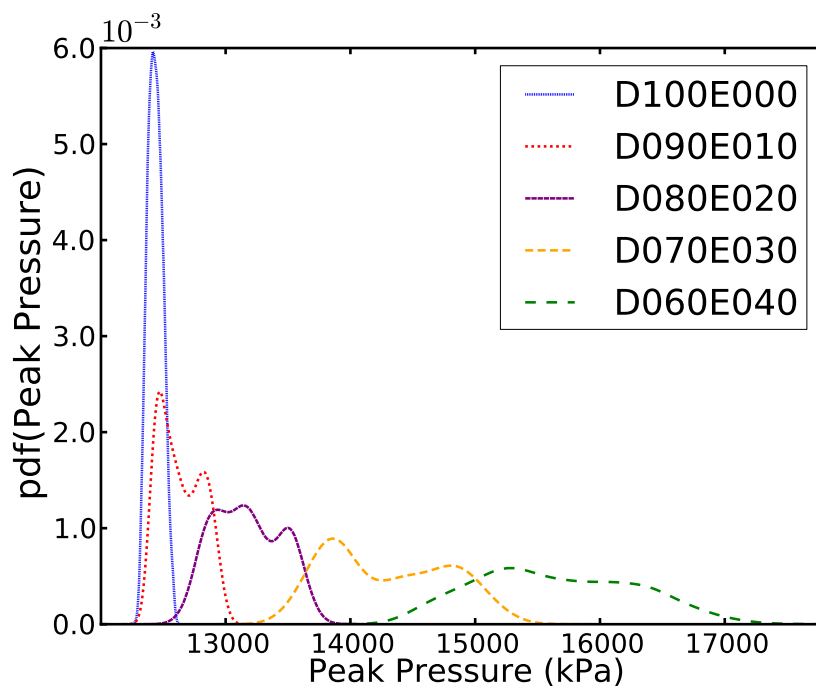


Figure 5.6: Peak pressure, full load, 0%–40% ethanol substitutions

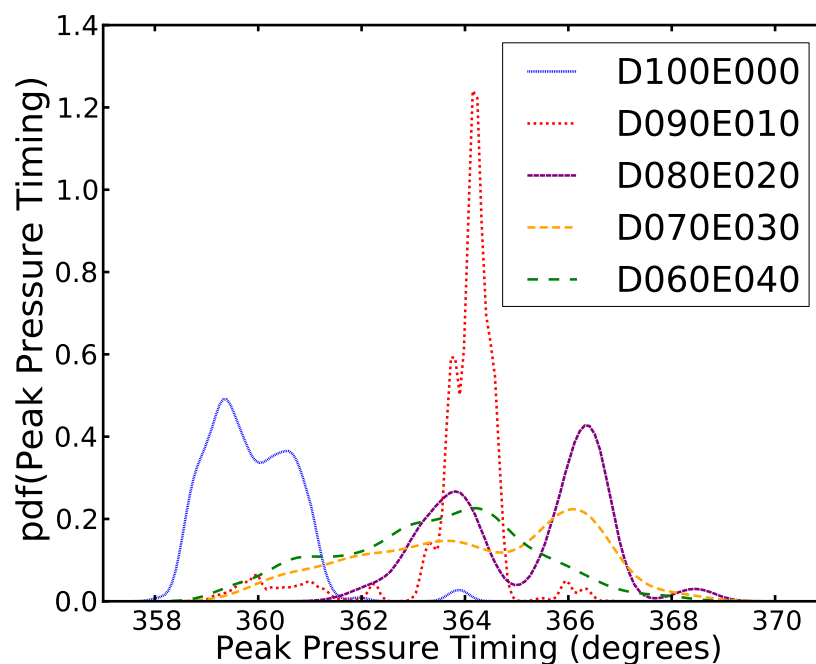


Figure 5.7: Peak pressure timing, full load, 0%–40% ethanol substitutions

With increasing ethanol substitutions, at full load the ignition delay decreases, as shown in Figure 5.8. The diesel injection timing is shown in Figure 5.9, the small difference observed in the injection timing is assumed to have had a minimal effect on ignition delay. However, the diesel injection for the 40% substitution case was approximately a degree more advanced than the lower substitutions and may have had an impact. The ignition delay for the 10% substitution case exhibited the least inter-cycle variability with the high substitutions exhibiting the most. At the high substitutions the very short ignition delay time and increased peak pressure timing indicate that the combustion process takes place over a longer period of time than that of neat diesel or lower ethanol substitutions. Figure 5.8 indicates that the ignition delay period for the 30% case is shorter than that of the 40% case—going against the trend. This is most likely an artifact of the low number of cycles analysed (200 for each case)—due to the time consuming nature of manual analysis. Had all 4000 cycles been analysed it is likely that a more systematic trend would have been presented. However, the value of this result is not lessened. A very obvious decrease in ignition delay and increase in inter-cycle variability past some threshold between 20% and 30% ethanol substitution is still shown in the results.

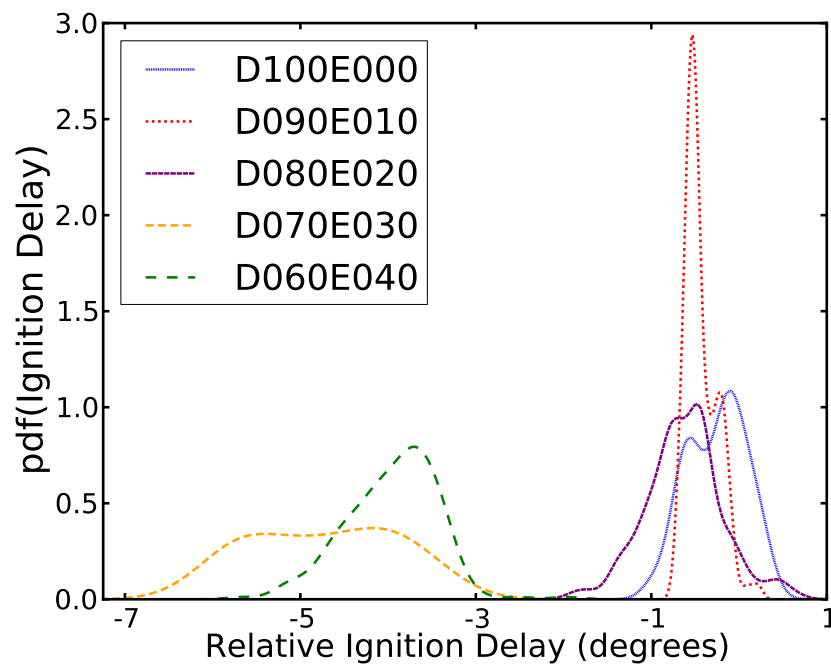


Figure 5.8: Ignition delay, full load, 0%–40% ethanol substitutions

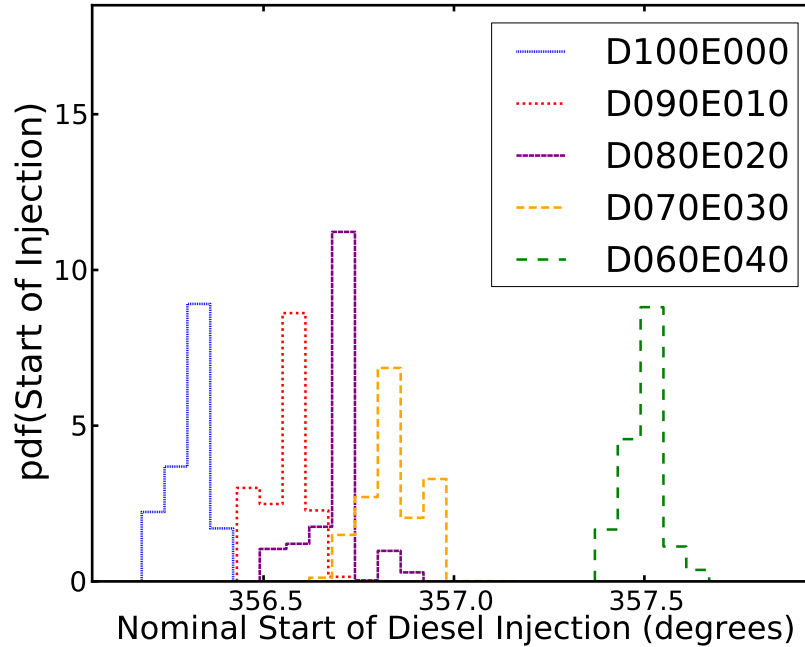


Figure 5.9: Diesel injection timing, full load, 0%–40% ethanol substitutions



### 5.5.2 Three Quarter Load Results

Figures 5.10 to 5.13 show the results for three quarter load. Results for the maximum rate of pressure rise can be seen in Figure 5.10. Initially, increasing the ethanol substitution decreases the maximum rate of pressure rise and only slightly reduces the inter-cycle variability. However, past some threshold substitution the maximum rate of pressure rise inter-cycle variability significantly increases, the modal value is similar to those of the lower substitutions; but, there is a second mode significantly higher and values lower than those of the lower substitutions were also observed.

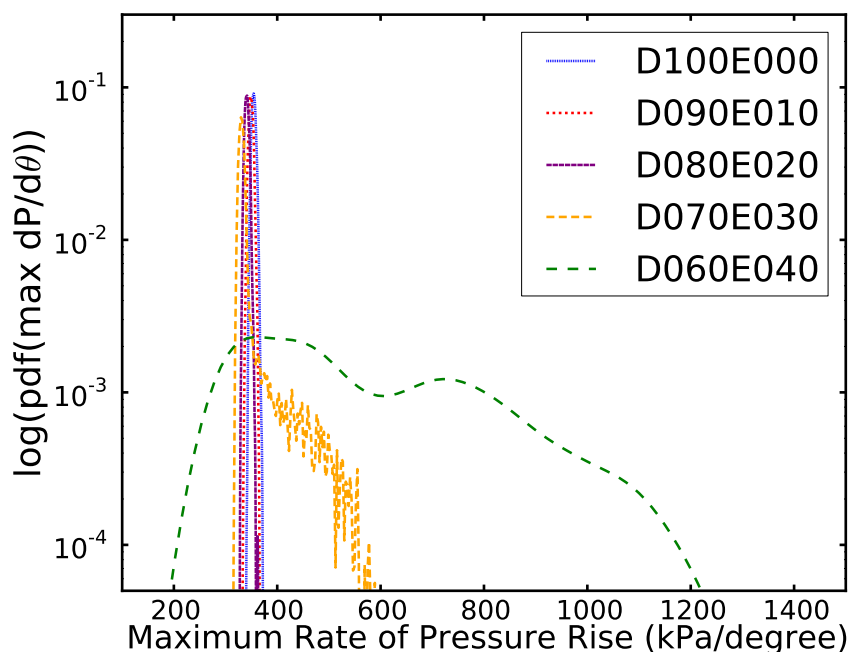


Figure 5.10: Maximum rate of pressure rise, three quarter load, 0%–40% ethanol substitutions

Similar to the maximum rate of pressure rise results, the peak pressure also decreases with increasing ethanol substitutions, until some threshold, as shown in Figure 5.11. The 20% substitution case yielded the least inter-cycle variability with only a small difference between the neat diesel case and the 10% substitution case. Both the 30% and the 40% ethanol substitutions yielded significantly greater inter-cycle variability than the lower substitutions and the neat diesel case. Also, in both of these higher substitutions the results spread from significantly lower to significantly higher than the those obtained with the lower substitutions, with the greatest extremes in the 40% ethanol substitution case.

The peak pressure timing, Figure 5.12, for neat diesel and 10% ethanol substitution were quite similar, and both exhibited a similar amount of inter-cycle variability. At the 20% substitution the predominate modal value is similar to the neat diesel and the 10%

substitution cases. However, there is also evidence of two further modes, that are more characteristic of the higher 30% and 40% substitutions, which occur later. The inter-cycle variability increases from the 10% substitution to the 20% substitution and then again from the 20% to the 30% substitution with a similar amount of inter-cycle variability present in the 30% and 40% substitutions.

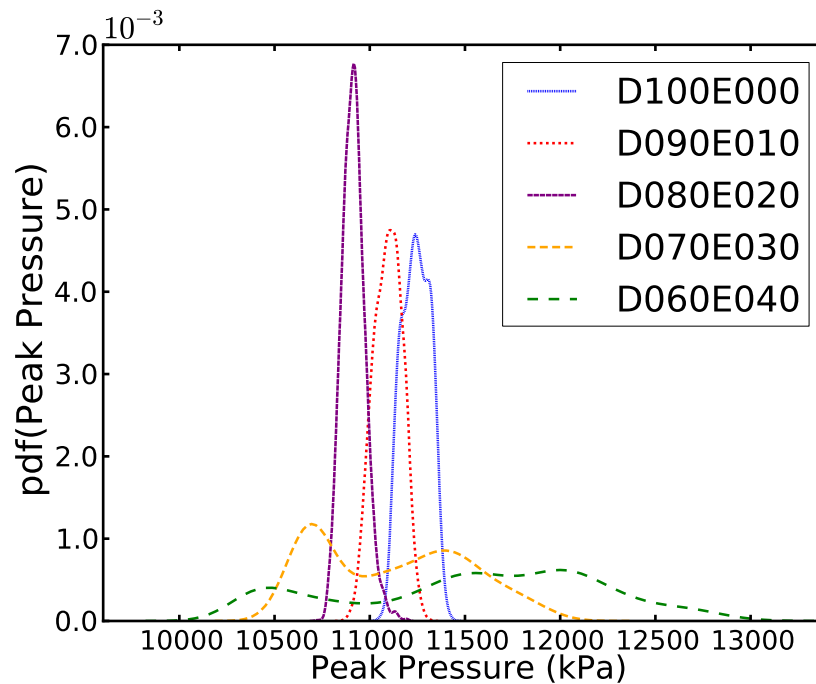


Figure 5.11: Peak pressure, three quarter load, 0%–40% ethanol substitutions

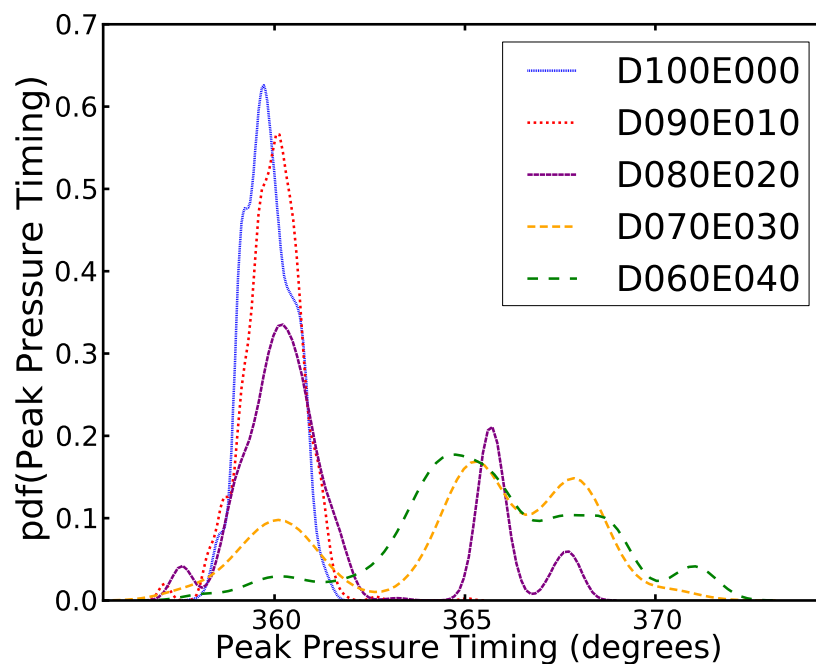


Figure 5.12: Peak pressure timing, three quarter load, 0%–40% ethanol substitutions

Initially, Figure 5.13 shows that the ignition delay increases as the ethanol substitution is increased. A slight decrease in ignition delay is observed in the 30% ethanol substitution case. This delay period is very similar for the neat diesel and 10% to 30% ethanol substitution cases with the most consistent result coming from the 20% substitution. Interestingly, the 30% substitution result shows evidence of less inter-cycle variability than the neat diesel case. Past some threshold substitution the ignition delay significantly decreases and the inter-cycle variability dramatically increases. This result mirrors that of the maximum rate of pressure rise results shown in Figure 5.10.

Figure 5.14 shows the diesel injection timing. The engine management system systematically retarded the diesel injection timing as the ethanol substitution increased. From the neat diesel case to the 40% ethanol substitution there was a difference of approximately 1.5 crank angle degrees, with most jumps between settings (10% ethanol substitution increments) resulted in the timing increasing by approximately half a degree. Much the same as the full load case, it is assumed that this change only had a small effect on the ignition delay as the change in pressure and volume this close to TDC would only be minimal.

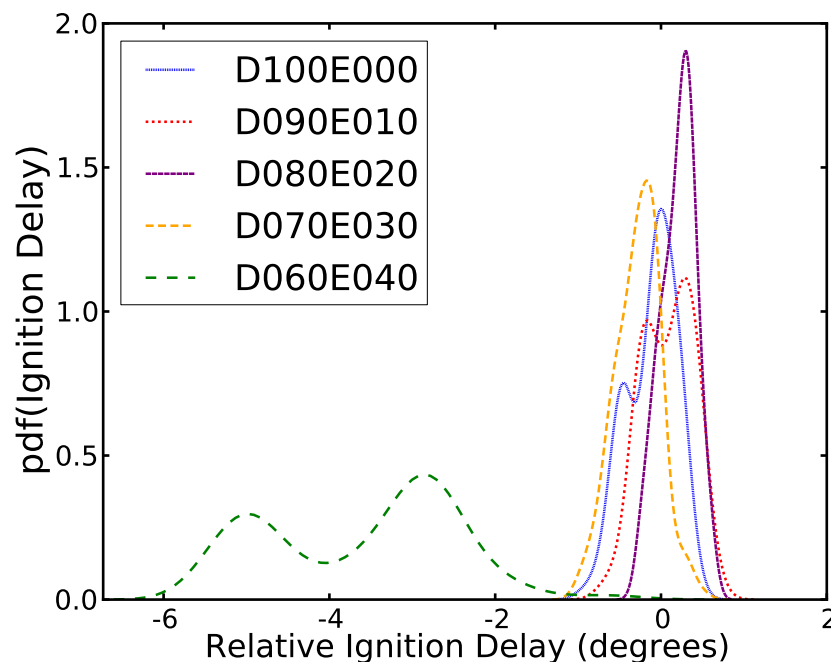


Figure 5.13: Ignition delay, three quarter load, 0%–40% ethanol substitutions

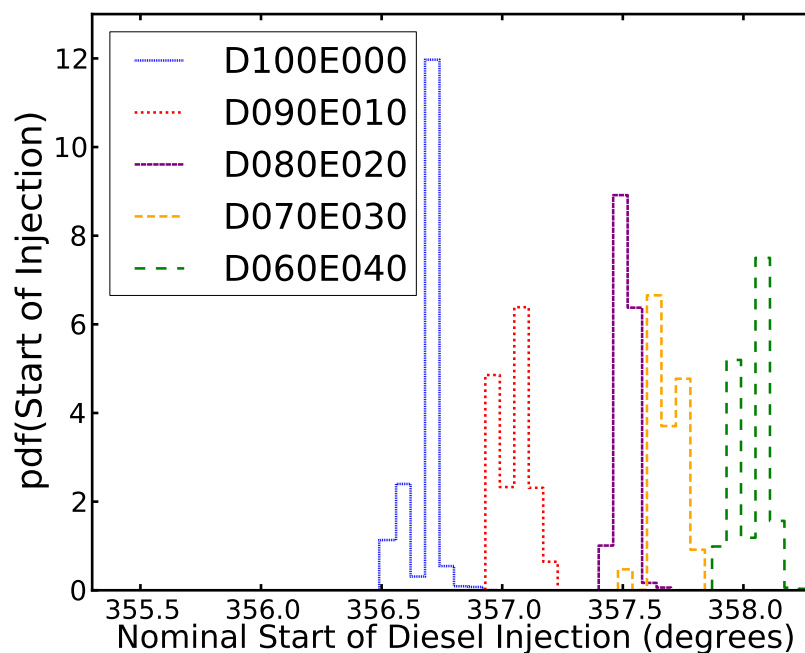


Figure 5.14: Diesel injection timing, three quarter load, 0%–40% ethanol substitutions

### 5.5.3 Half Load Results

The maximum rate of pressure rise results in Figure 5.15 indicate that there is little difference in the modal value or the inter-cycle variability in any of the test cases. However, there is evidence to show that the introduction of ethanol initially increases the maximum rate of pressure rise and that increasing the ethanol reduces the maximum rate of pressure rise—the 40% substitution case shows a result very similar to that of neat diesel. Also, although not a significant change in inter-cycle variability Figure 5.15 does show that the introduction of ethanol has increased the variability and that increasing the ethanol substitution increases the inter-cycle variability.

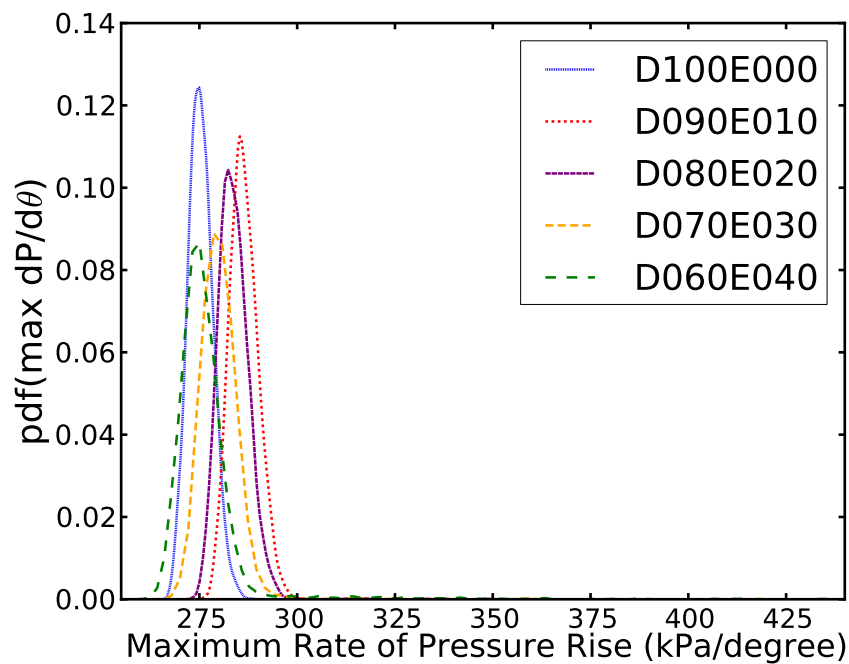


Figure 5.15: Maximum rate of pressure rise, half load, 0%–40% ethanol substitutions

Much the same as the trend shown in Figure 5.15 with the maximum rate of pressure rise, the peak pressure, shown in Figure 5.16, has an initial increase with the introduction of ethanol and then decreases as the substitution increases. Also, the 40% ethanol substitution case is similar to the neat diesel case, but with increased inter-cycle variability. However, the 20% substitution yielded the least inter-cycle variability. The peak pressure timing, Figure 5.17, shows very little difference between any of the test settings, they all exhibit multi-modal behaviour and have a similar amount of inter-cycle variability. The neat diesel case in this instance is showing the greatest amount of inter-cycle variability.

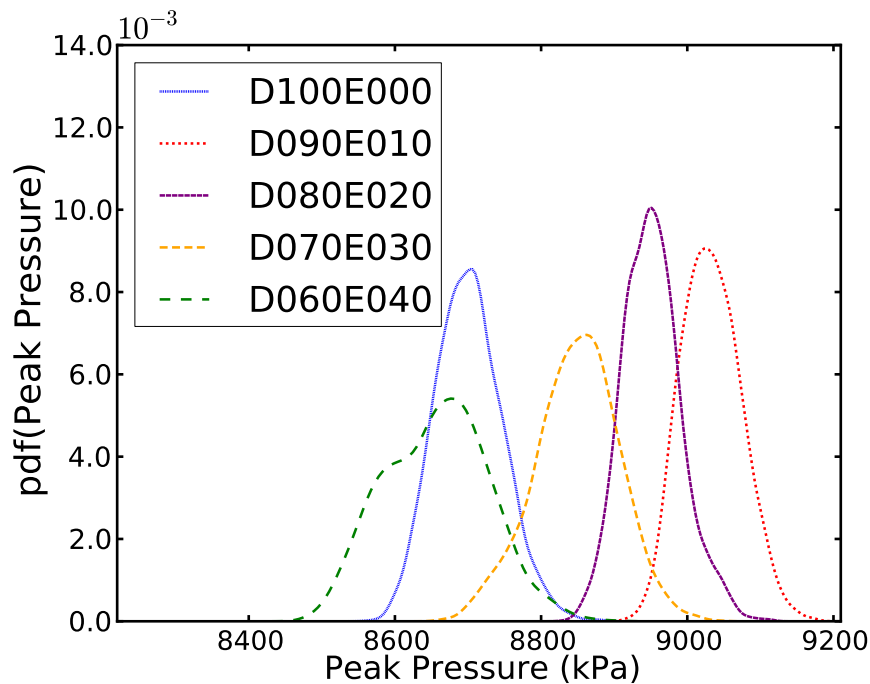


Figure 5.16: Peak pressure, half load, 0%–40% ethanol substitutions

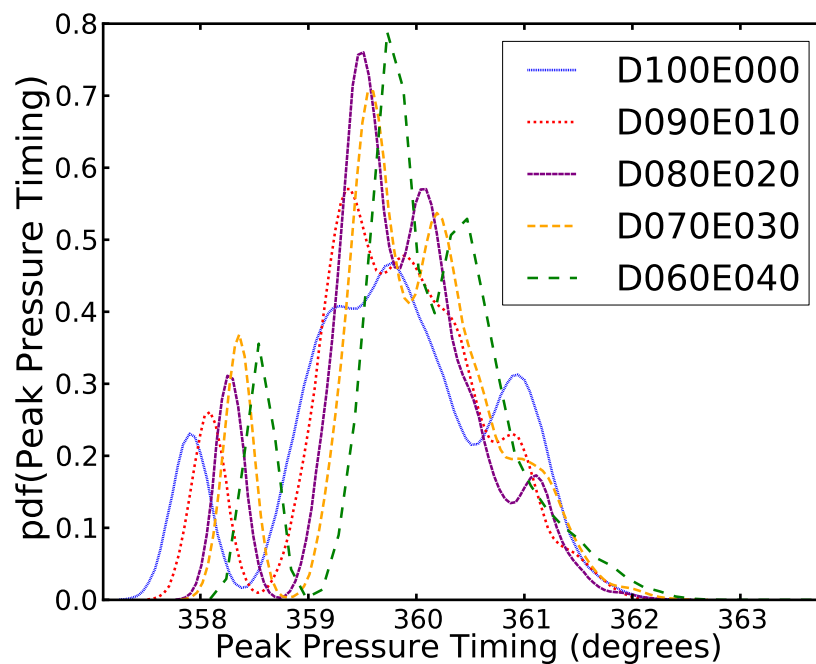


Figure 5.17: Peak pressure timing, half load, 0%–40% ethanol substitutions

In contrast to the results shown earlier in Figures 5.8 and 5.13 for ignition delay at full and three quarter loads, respectively, Figure 5.18 does not show any instance that the ignition delay period is less than that of neat diesel for any ethanol substitution. At half

load the ignition delay period increases as the ethanol substitution increases; however, at 40% ethanol substitution the ignition delay decreases from the 30% substitution—the delay period is still longer than that of neat diesel. This result reflects that of the current literature where it has been extensively documented that ethanol fumigation increases ignition delay owing to the so-called cooling effect that it has on the charge air (Saeed and Henein, 1989; Tsang et al., 2010).

The diesel injection timing at half load, much the same as the three quarter load case, was systematically retarded with increasing ethanol substitutions. However, this increase was much less substantial than in the three quarter load case and the neat diesel case and the 40% ethanol substitution case were only approximately 1 degree apart from each other.

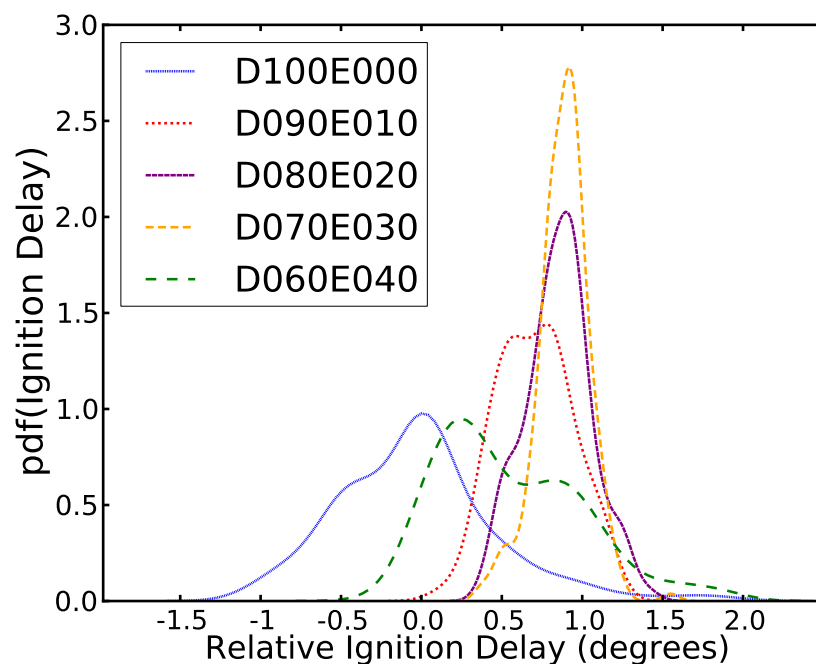


Figure 5.18: Ignition delay, half load, 0%–40% ethanol substitutions

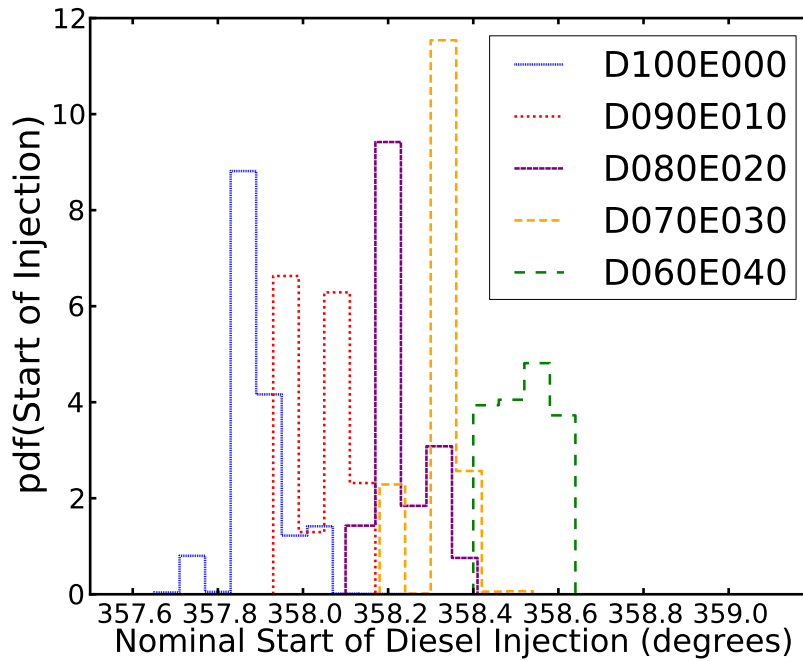


Figure 5.19: Diesel injection timing, half load, 0%–40% ethanol substitutions

#### 5.5.4 Inter-cycle Variability

The results, shown in Sections 5.5.1 to 5.5.3, indicate that a threshold ethanol substitution may exist that causes increased inter-cycle variability. Absolute air to fuel ratios (mole basis) were calculated for each test setting—absolute values, rather than relative values ( $\lambda$ ), are shown in this section because the data collapses better allowing limits for this test engine to be evident. A representative diesel fuel composition was determined from the known density of the diesel fuel, this corresponded to a representative composition of  $C_{12}H_{23}$  (Gupta and Demirbas, 2010). Moreover, the flow rates of both fuels, diesel and ethanol, and the in-take air were recorded directly from flow meter sensors at a rate of 1 Hz.

The COV of IMEP, shown in Figure 5.20, is a standard used by engine researchers for investigating inter-cycle variability. Figure 5.20 clearly indicates an increase in COV of IMEP as the air to fuel ratio decreases. However, normalising by the mean, in this case, is also showing a contradicting result that the general effect of ethanol is greater at lower loads. The standard deviation alone could be considered as a more meaningful view of the inter-cycle variability as it shows the extent of the spread only. Figure 5.21 shows the standard deviation of the IMEP with respect to the air to fuel ratio.

Further investigation was conducted into operating parameters that have an effect on the longevity of the engine, maximum rate of pressure rise and peak pressure. Figures 5.22 and 5.23, which are not normalised by their means, confirm the results shown earlier in the paper in Sections 5.5.1 to 5.5.3 indicating that with increasing load the effects of ethanol, especially



at high substitutions (low air to fuel ratios), also increase—intuitively, this makes sense as at higher loads the in-cylinder pressure is higher and hence the ethanol is compressed to a higher temperature prior to the diesel being injected. If the ethanol has undergone premixed combustion then the stability of the engine would be much lower. Figures 5.20 to 5.23 all show a monotonic trend, as the air to fuel ratio decreases the inter-cycle variability increases. These figures also indicate that at air to fuel ratios greater than 110 the inter-cycle variability is not significantly effected by the ethanol fumigation and that at air to fuel ratios less than 80 the effect is very significant.

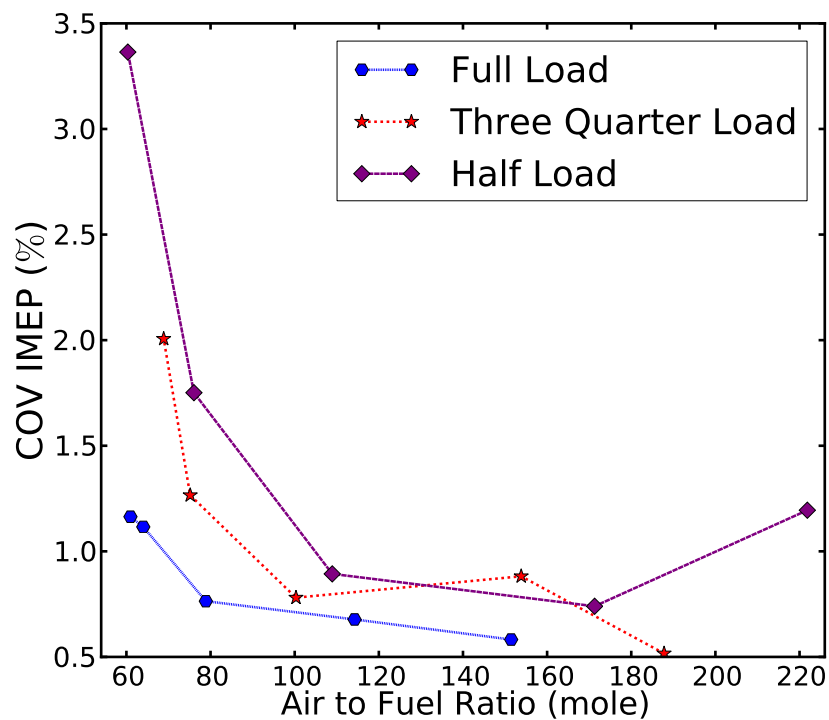


Figure 5.20: COV of IMEP Vs the Air to Fuel Ratio

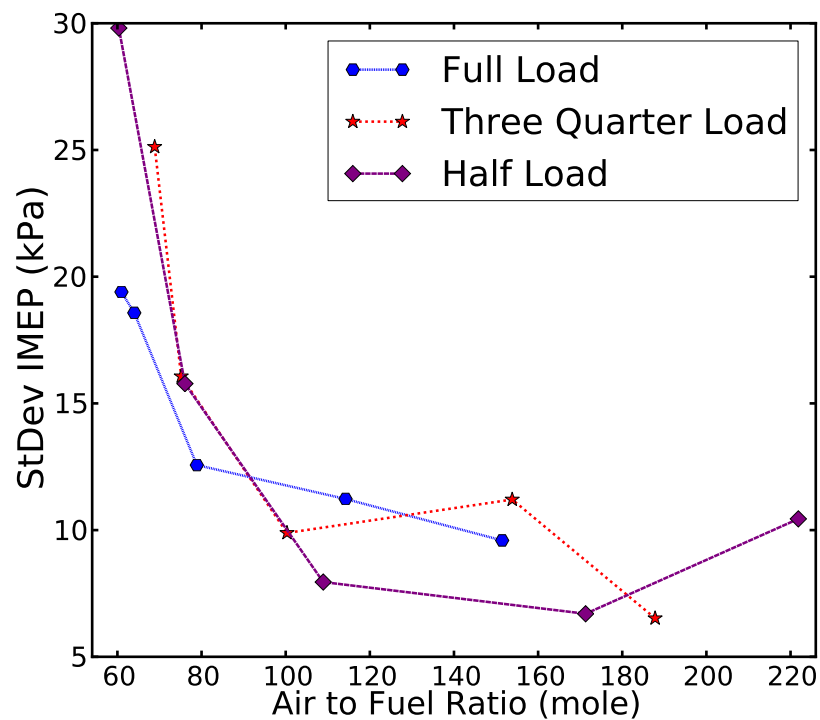


Figure 5.21: Standard Deviation of IMEP Vs the Air to Fuel Ratio

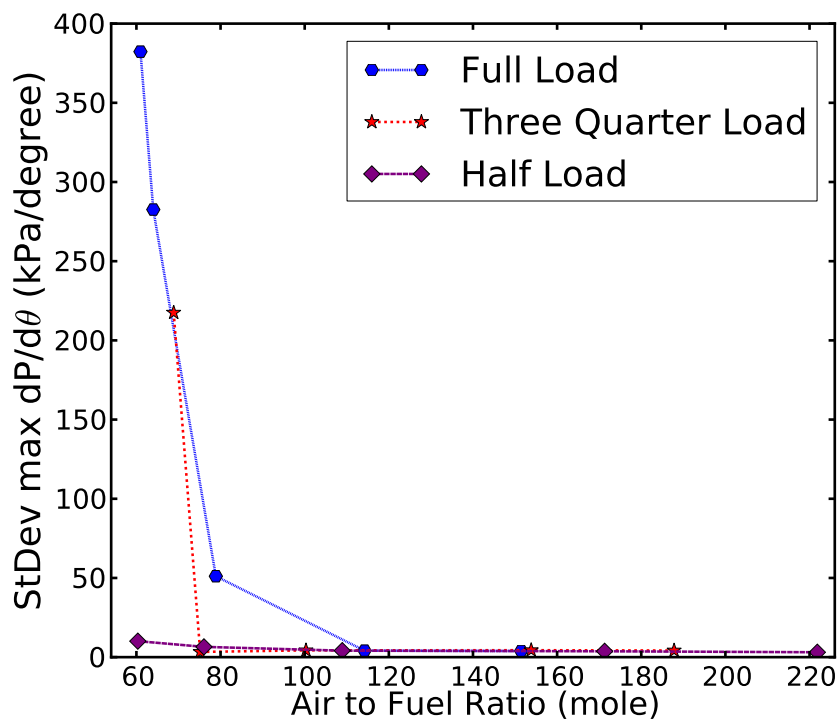


Figure 5.22: Standard Deviation of the Maximum Rate of Pressure Rise Vs the Air to Fuel Ratio

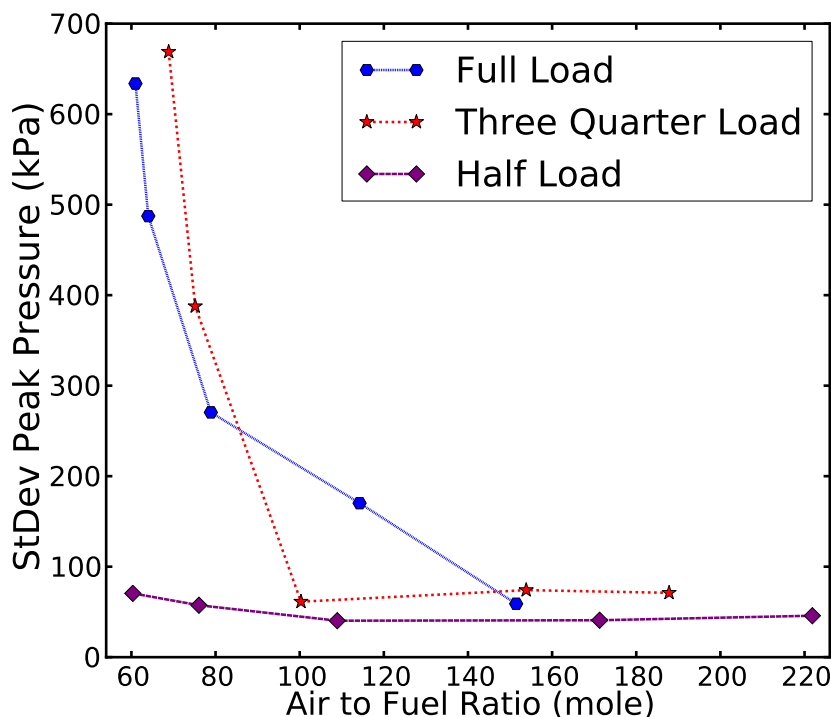


Figure 5.23: Standard Deviation of the Peak Pressure Vs the Air to Fuel Ratio

### 5.5.5 Auto-ignition of Ethanol

Given that the current literature suggests that ethanol fumigation increases ignition delay, an experiment was designed to test if combustion was possible with ethanol fumigation prior to diesel injection. In order to investigate this the engine was setup at an extreme case, full load with a 50% ethanol substitution. Once engine operation was established the diesel fuel was shut off to number one cylinder, where the in-cylinder pressure transducer is located. Figure 5.24 shows the collected data.

The top in-cylinder pressure traces, in Figure 5.24, are those of the established combustion prior to the diesel being switched off—50% of the energy by ethanol. Combustion without diesel can be seen in the traces after the diesel was shut off—test case denoted as D000E050. Data from Figure 5.24 was used to investigate the decrease in indicated work. Figure 5.25 shows a plot of normalised indicated work—the indicated work at full load was 1.7 kJ, averaged across the 15 cycles prior to shutting off the diesel, and the indicated work on the first cycle without diesel was 0.63 kJ (37%) (the normalisation was performed by dividing each indicated work value by 1.7 kJ). Subsequent cycles show a gradual decrease in pressure (and therefore indicated work) throughout the relatively short experiment. It appears that this reduction in indicated work during ethanol-only combustion is caused by a progressive

decrease in in-cylinder temperature due to the lower total value of heat released. Importantly, Figures 5.24 and 5.25 establish that it is possible to run a diesel engine with ethanol alone by showing positive net work during the ethanol-only operation. Whilst this mode of operation may not be ideal for stability, it is important in-terms of understanding the practical effects that ethanol fumigation has in diesel engine combustion and hence the outputs of the engine: work and emissions.

In a modern heavy duty diesel engine, such as the one described in this paper, the diesel injection timing is typically near TDC. The advanced diesel injection allows the ethanol in the charge air more time to undergo pre-combustion heat addition. It would be, therefore, expected that if the ethanol in the charge air was either close to, or had already commenced combustion when diesel fuel was introduced that the effect on in-cylinder parameters would be significant. Moreover, because the diesel is injected from a high pressure rail it is expected that the diesel will be more finely atomised when compared with an older engine, with greater combustion chamber penetration. Possible effects from this would be changes to the flame front development, potential homogeneous charge compression ignition combustion and non-uniform combustion from the presence of hot-spots created from isolated ethanol-only combustion. These effects result in greatly increased inter-cycle variability in in-cylinder pressure parameters such as maximum rate of pressure rise, peak pressure and ignition delay with relatively minimal effects to the engine work output.

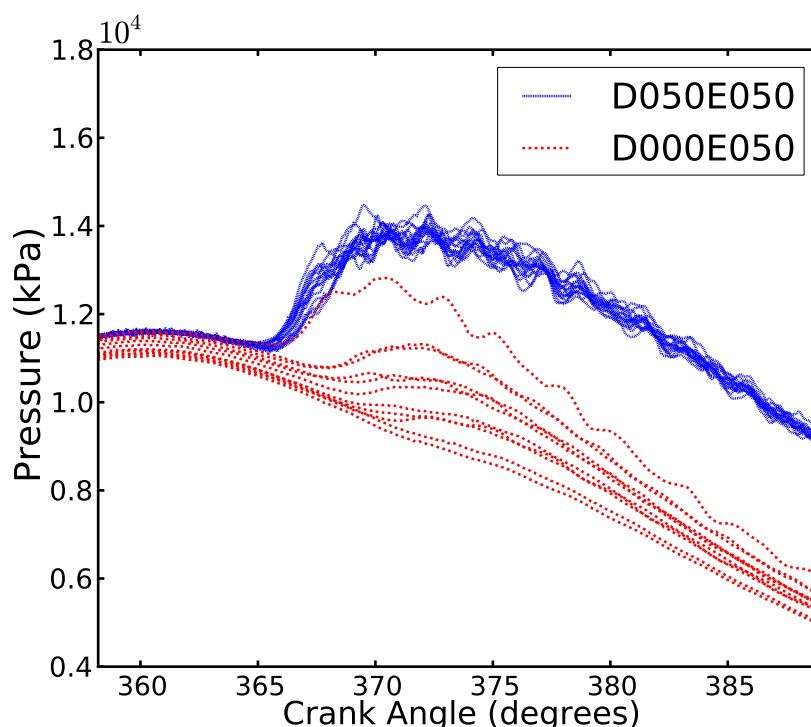


Figure 5.24: In-cylinder pressure trace, full load, 50% ethanol substitution, established combustion and with diesel switched-off

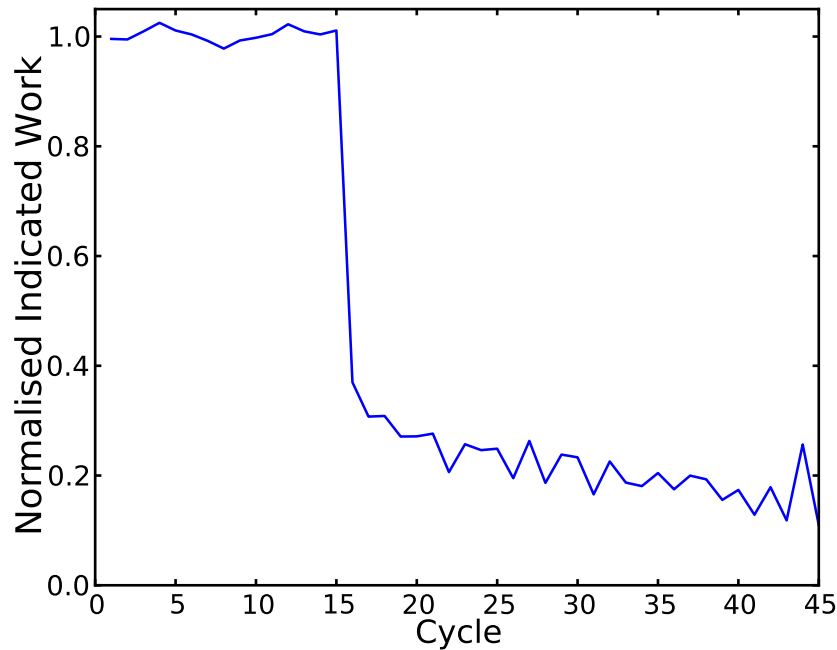


Figure 5.25: Normalised indicated work, full load, 50% ethanol substitution, established combustion and with diesel switched-off

## 5.6 Conclusion

This paper has shown comprehensive results from an experimental campaign on a common rail diesel engine operated with neat diesel fuel and with ethanol substitutions up to 40% at full, three quarters and half load. The effect of the ethanol on the maximum rate of pressure rise, peak pressure, peak pressure timing, ignition delay and inter-cycle variability was explored. At full load ethanol substitutions of up to 20% by energy have only a minimal effect on the values of these parameters and the inter-cycle variability. The full load result is similar to the three quarter load case, which indicate that substitutions near 30% are achievable without significant negative effects. At half load the inter-cycle variability is relatively constant; however, the ignition delay results indicate that at the 40% substitution the ignition delay stops increasing and begins to decrease, given this information substitutions above this may result in significantly increased inter-cycle variability. The correlation between inter-cycle variability and the absolute air to fuel ratio was explored and showed a monotonic trend with a critical ratio lying between 80 to 110. Ethanol-only combustion was also explored and established through an experiment that involved running one cylinder of the engine without diesel fuel. Early ignition of the fumigated ethanol was identified as a cause for the decrease in ignition delay and the increase in inter-cycle variability with high ethanol substitutions.

## 5.7 Acknowledgements

The authors wish to thank Mr. Anthony Morris and Mr. Noel Hartnett for assisting with the design of the experimental campaigns and their invaluable technical knowledge. Further thanks also to Technologist Mr. Ken McIvor for his assistance in setting up the data acquisition software and to Ms. Svetlana Stevanovic and Mr. Jackson Kelley for their aid during the experimental campaign and continued support after. The ethanol used during this campaign was kindly donated by Caltex. This work was undertaken under an Australian Research Council Linkage Grant (LP0775178) in association with Peak3 P/L.

## 5.8 References

- Abu-Qudais, M., Haddad, O., and Qudaisat, M. The effect of alcohol fumigation on diesel engine performance and emissions. *Energy Conversion and Management*, 41(4):389–399, 2000.
- Amann, C. A. Cylinder-pressure measurement and its use in engine research. *Society of Automotive Engineers*, (SAE Paper 852067), 1986.
- Australian National Greenhouse Accounts, . Quarterly Update of Australia's National Greenhouse Gas Inventory. *March Quarter 2010*, 2010. URL <http://www.climatechange.gov.au/>.
- Bodisco, T., Reeves, R., Situ, R., and Brown, R. J. Bayesian models for the determination of resonant frequencies in a DI diesel engine. *Mechanical Systems and Signal Processing*, 26:305–314, 2012.
- Bohme, J. F. and Konig, D. Statistical processing of car engine signals for combustion diagnosis. In *IEEE Seventh SP Workshop on Statistical Signal and Array Processing*, pages 369–374, 1994.
- Carlucci, A. P., de Risi, A., Laforgia, D., and Naccarato, F. Experimental investigation and combustion analysis of a direct injection dual-fuel diesel–natural gas engine. *Energy*, 33(2):256–263, 2008.
- Chauhan, B. S., Kumar, N., Pal, S. S., and Du Jun, Y. Experimental studies on fumigation of ethanol in a small capacity diesel engine. *Energy*, 36(2):1030–1038, 2011.
- Diesel, R. German Patent 67207, 1892.
- Fang, Q., Fang, J., Zhuang, J., and Huang, Z. Influences of pilotinjection and exhaustgasrecirculation (EGR) on combustion and emissions in a HCCI-DI combustion engine. *Applied Thermal Engineering*, 48:97–104, 2012.

- Gupta, R. B. and Demirbas, A. *Gasoline, Diesel, and Ethanol Biofuels from Grasses and Plants*. Cambridge University Press, 2010.
- Hayes, T. K., Savage, L. D., and White, R. A. The effect of fumigation of different ethanol proofs on a turbocharge diesel engine. *Society of Automotive Engineers*, (SAE Paper 880497), 1988.
- Heywood, J. B. *Internal Combustion Engine Fundamentals*. McGraw-Hill, Inc., 1988.
- Hickling, R., Feldmaier, D. A., and Sung, S. H. Knock-induced cavity resonances in open chamber diesel engines. *Acoustical Society of America Journal*, 65(6):1474–1479, 1979.
- Hickling, R., Feldmaier, D. A., Chen, F. H. K., and Morel, J. S. Cavity resonances in engine combustion chambers and some applications. *Acoustical Society of America Journal*, 73: 1170–1178, 1983.
- Karthikeyana, R. and Mahalakshmi, N. V. Performance and emission characteristics of a turpentine–diesel dual fuel engine. *Energy*, 32(7):1202–1209, 2007.
- Kouremenos, D. A., Rakopoulos, C. D., and Kotsopoulos, P. Comparative performance and emission studies for vaporized diesel fuel and gasoline as supplements in swirl-chamber diesel engines. *Energy*, 15(12):1153–1160, 1990.
- Kouremenos, D. A., Rakopoulos, C. D., and Kotsos, K. G. A stochastic-experimental investigation of the cyclic pressure variation in a DI single-cylinder diesel engine. *International Journal of Energy Research*, 16(9):865–877, 1992.
- Lakshmanan, T. and Nagarajan, G. Experimental investigation of timed manifold injection of acetylene in direct injection diesel engine in dual fuel mode. *Energy*, 35(8):3172–3178, 2010.
- Lee, J. W., Min, K. D., Kang, K. Y., Bae, C. S., Giannadakis, E., Gavaises, M., and Arcoumanis, C. Effect of piezo-driven and solenoid-driven needle opening of common-rail diesel injectors on internal nozzle flow and spray development. *International Journal of Engine Research*, 7:489–502, 2006.
- McArdle, P., Lindstrom, P., and Calopedis, S. Emissions of greenhouse gases report. Technical Report DOE/EIA-0573(2006), Energy Information Administration, Office of Integrated Analysis and Forecasting, U.S. Department of Energy, Washington, DC, 2007. URL <http://www.eia.doe.gov/oiaf/1605/ggrpt/>.
- Parzen, E. On estimation of a probability density function and mode. *The Annals of Mathematical Statistics*, 33(3):1065–1076, 1962.

- Payri, F., Broatch, A., Tormos, B., and Marant, V. New methodology for in-cylinder pressure analysis in direct injection diesel engines: application to combustion noise. *Measurement Science and Technology*, 16(2):540–547, 2005.
- Rakopoulos, C. D., Antonopoulos, K. A., and Rakopoulos, D. C. Experimental heat release analysis and emissions of a HSDI diesel engine fueled with ethanol-diesel fuel blends. *Energy*, 32(10):1791–1808, 2007.
- Randolph, A. L. Methods of processing cylinder-pressure transducer signals to maximize data accuracy. *Society of Automotive Engineers*, (SAE Paper 900170), 1990.
- Ren, Y., Randall, R. B., and Milton, B. E. Influence of the resonant frequency on the control of knock in diesel engines. *Proceedings of the Institution of Mechanical Engineers: Part D: Journal of Automobile Engineering*. London, 213(2):127–133, 1999.
- RIRDC, . Biofuels in Australia—issues and prospects. *Australian Government: Rural Industries Research and Development Corporation Publication Number 07/071*, 2007.
- Rosenblatt, M. Remarks on some nonparametric estimates of a density function. *The Annals of Mathematical Statistics*, 27(3):832–837, 1956.
- Rosillo-Calle, F. and Walter, A. Global market for bioethanol: historical trends and future prospects. *Energy for Sustainable Development*, 10(1):20–32, 2006.
- Saeed, M. N. and Henein, N. A. Combustion phenomena of alcohols in C.I. engines. *Journal of Engineering for Gas Turbines and Power*, 111(3):439–444, 1989.
- Sahin, Z., Durgun, O., and Bayram, C. Experimental investigation of gasoline fumigation in a single cylinder direct injection (DI) diesel engine. *Energy*, 33(8):1298–1310, 2008.
- Sahoo, B. B., Sahoo, N., and Saha, U. K. Effect of engine parameters and type of gaseous fuel on the performance of dual-fuel gas diesel engines—a critical review. *Renewable and Sustainable Energy Reviews*, 13(6-7):1151–1184, 2009.
- Samimy, B. and Rizzoni, G. Mechanical signature analysis using time-frequency signal processing: application to internal combustion engine knock detection. *Proceedings of the IEEE*, 84(9):1330–1343, 1996.
- Selim, M. Y.E. Effect of engine parameters and gaseous fuel type on the cyclic variability of dual fuel engines. *Fuel*, 84(7-8):961–971, 2005.
- Selim, M. Y.E., Radwan, M. S., and Saleh, H. E. Improving the performance of dual fuel engines running on natural gas/LPG by using pilot fuel derived from jojoba seeds. *Renewable Energy*, 33(6):1173–1185, 2008.



- Shafiee, S. and Topal, E. When will fossil fuel reserves be diminished. *Energy Policy*, 37: 181–189, 2009.
- Shehata, M. S. Cylinder pressure, performance parameters, heat release, specific heats ratio and duration of combustion for spark ignition engine. *Energy*, 35(12):4710–4725, 2010.
- Skelton, B. Special issue: Bio-fuels. *Process Safety and Environmental Protection*, 85(5): 347–347, 2007.
- Sorda, G., Banse, M., and Kemfert, C. An overview of biofuel policies across the world. *Energy Policy*, 38(11):6977–6988, 2010.
- Surawski, N. C., Miljevic, B., Roberts, B. A., Modini, R. L., Situ, R., Brown, R. J., Bottle, S. E., and Ristovski, Z. D. Particle emissions, volatility, and toxicity from an ethanol fumigated compression ignition engine. *Environmental Science & Technology*, 44(1):229–235, 2010.
- Surawski, N. C., Ristovski, Z. D., Brown, R. J., and Situ, R. Gaseous and particle emissions from an ethanol fumigated compression ignition engine. *Energy Conversion and Management*, 54(1):145–151, 2012.
- Tauzia, X., Maiboom, A., and Shah, S. R. Experimental study of inlet manifold water injection on combustion and emissions of an automotive direct injection diesel engine. *Energy*, 35(9):3628–3639, 2010.
- Torregrosa, A. J., Broatch, A., and Margot, X. Combustion chamber resonances in direct injection automotive diesel engines: a numerical approach. *International Journal of Engine Research*, 5(1):83–91, 2004.
- Tsang, K. S., Zhang, Z. H., Cheung, C. S., and Chan, T. L. Reducing emissions of a diesel engine using fumigation ethanol and a diesel oxidation catalyst. *Energy & Fuels*, 24: 6156–6165, 2010.

---

[This page is intentionally left blank]

## Chapter 6

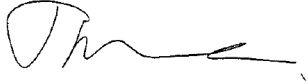
# A Bayesian approach to the determination of ignition delay

Timothy Bodisco, Samantha Low Choy, Richard J. Brown

Science and Engineering Faculty, Queensland University of Technology, Brisbane QLD, 4001, Australia


Publication: Applied Thermal Engineering (2013) 60(1–2), 79–87.

**Author Contribution**

<b>Contributor</b>	<b>Statement of Contribution</b>
Timothy Bodisco	Conducted the experiments, developed the Bayesian model, performed the data analysis and drafted the manuscript
Signature 	
Samantha Low Choy	Assisted with preparing the manuscript, in particular with the description of the statistical model
Richard Brown	Supervised the project, aided with the development of the paper and extensively revised the manuscript

**Principal Supervisor Confirmation**

I have sighted email or other correspondence from all co-authors confirming their certifying authorship.

<b>Name</b>	<b>Signature</b>	<b>Date</b>
Associate Professor Richard Brown		

**Abstract**

A novel in-cylinder pressure method for determining ignition delay has been proposed and demonstrated. This method proposes a new Bayesian statistical model to resolve the start of combustion, defined as being the point at which the band-pass in-cylinder pressure deviates from background noise and the combustion resonance begins. Further, it is demonstrated that this method is still accurate in situations where there is noise present. The start of combustion can be resolved for each cycle without the need for ad hoc methods such as cycle averaging. Therefore, this method allows for analysis of consecutive cycles and inter-cycle variability studies. Ignition delay obtained by this method and by the net rate of heat release have been shown to give good agreement. However, the use of combustion resonance to determine the start of combustion is preferable over the net rate of heat release method because it does not rely on knowledge of heat losses and will still function accurately in the presence of noise. Results for a six-cylinder turbo-charged common-rail diesel engine run with neat diesel fuel at full, three quarters and half load have been presented. Under these conditions the ignition delay was shown to increase as the load was decreased with a significant increase in ignition delay at half load, when compared with three quarter and full loads.

## 6.1 Introduction

Standard methods for determining the start of combustion have changed little in the last few decades. Most current studies (Papagiannakis and Hountalas, 2003; Ren et al., 2006; Ghojel et al., 2006; Sahoo and Das, 2009; Cinar et al., 2010; Lata and Misra, 2011; Donkerbroek et al., 2011) that examine the start of combustion, or ignition delay, use the net rate of heat release, with most citing the 1988 book *Internal Combustion Engine Fundamentals* written by John Heywood (1988). This method is commonly used because it is considered reliable and the net rate of heat release is simple to calculate. However, this paper will introduce the use of a statistical model in the Bayesian paradigm to accurately determine the start of combustion.

Calculation of the net rate of heat release comes from analysing the heat losses in an engine from a first law of thermodynamics perspective, in its most commonly used form (Heywood, 1988):

$$\frac{dQ_n}{dt} = \frac{\gamma}{\gamma - 1} p \frac{dV}{dt} + \frac{1}{\gamma - 1} V \frac{dp}{dt}, \quad (6.1)$$

where,  $\frac{dQ_n}{dt}$  is the net rate of heat release,  $\gamma$  is the ratio of specific heats,  $p$  is the in-cylinder pressure,  $V$  is the in-cylinder volume and  $t$  is time. More complicated versions of Equation 6.1 exist that take into account heat loss to the walls, effects of crevice regions and other possible sources for heat loss—which are mostly engine specific and not general. The start of combustion is defined as the point when the net rate of heat release begins increasing rapidly—some authors use the point that the net rate of heat release becomes positive (Lata and Misra, 2011).

From experimental in-cylinder pressure, another method for determining the start of combustion is from the rate of pressure rise (Stone, 1999). This method locates the point at which the rate of pressure rise begins to increase rapidly, and can be done by analysing either the first or second derivative of the in-cylinder pressure signal. It has parallels with the net rate of heat release, which also requires the differentiation of the in-cylinder pressure data.

In a recent study by Rothamer and Murphy (2012), six methods of determining the ignition delay were compared. The six methods used were:

1. location of 50% of pressure rise due to premixed burn combustion;
2. extrapolation of the peak slope of pressure rise due to combustion to the zero crossing point;
3. location of the first peak of the second derivative of the pressure trace;
4. location of the first peak of the third derivative of the pressure trace;
5. location of 10% of the maximum heat release rate in the premixed burn; and,

6. a repeat of (5) using a low-pass (threshold 2000 Hz) filtered in-cylinder pressure trace.

Their study focused on jet fuels and diesel fuel in a heavy-duty direct-injection single-cylinder diesel and the data analysis was performed using 250 cycles of averaged data. A conclusion from their study found that the methods which required second or third derivatives were not optimal owing to the presence of noise and that the ignition delay determined by the heat release method using the low-pass filtered in-cylinder pressure signal gave a result 200-330  $\mu\text{s}$  shorter than the other methods.

Flame luminosity is another method used by researchers for determining the start of combustion. Heywood (1988) argues that the use of flame luminosity detectors as a means to determine the start of combustion increases the potential for error. This is because the first appearance of the flame occurs after the increase in pressure. However, a recent study has argued that the first appearance of the flame coincides well with results from analysing the net rate of heat release (Payri et al., 2012). Perhaps, with improving technology this method is becoming more reliable. Flame luminosity sensors are, however, prohibitively expensive for wide-spread practical use.

An early method for estimating ignition delay was proposed by Hardenberg and Hase (1979). They developed an empirical relationship between the parameters which they determined had the most impact on ignition delay: mean piston speed (m/s),  $M_{PS}$ ; in-cylinder temperature at the time of injection (K),  $T$ ; the compression ratio,  $r_c$ ; the polytropic index of compression,  $n$ ; the cetane number,  $CN$ ; and, the absolute charge-air pressure at the time of injection (bar),  $P$ . Whilst this empirical relationship may not represent reality in a modern engine and does not have the capacity to tell the analyst about any inter-cycle variability, it does give insight into the effect of different engine parameters on the ignition delay. In crank-angle degrees the empirical relationship as determined by Hardenberg and Hase (1979) is:

$$ID = (0.36 + 0.22M_{PS}) e^{\frac{618840}{CN+25}(\frac{1}{RT} - \frac{1}{17190}) + (\frac{21.2}{P-12.4})^{0.063}}, \quad (6.2)$$

where,  $R$  is the universal gas constant (8.31434 J/mole). The polytropic index of compression,  $n$ , and the compression ratio,  $r_c$ , impact on the temperature and pressure of the charge-air. Estimates of  $T$  and  $P$  can be obtained from the inlet manifold conditions (Hardenberg and Hase, 1979; Heywood, 1988).

$$\begin{aligned} T &= T_i r_c^{n-1} \\ P &= P_i r_c^n \end{aligned}$$

Later work done by Prakash et al. (1999) extended this model to incorporate dual-fuel operation of diesel engines.

Since the work done by Hardenberg and Hase, other estimators of ignition delay based on engine parameters have been developed. Assanis et al. (2003) has extensively reviewed these

and proposed their own method for estimating ignition delay. However, for experimentally validating their ignition delay estimator, Assanis et al. (2003) compared their estimator to measured values by taking the peak of the second derivative to be the start of combustion.

All of these approaches have practical difficulties or offer little, or no, information regarding cycle-by-cycle changes and hence do not allow for inter-cycle variability studies. In this paper a methodology for determining the start of combustion is proposed that requires no knowledge of difficult to estimate parameters such as heat loss to the walls and is still accurate with noisy data. Using only the in-cylinder pressure signal a statistical modelling approach is used to determine the start of combustion. A Bayesian approach to statistical modelling is used because it estimates the plausible range of parameter values (which includes the start of combustion), given the data observed (Ellison, 2004). In contrast a classical statistical analysis would provide the logical reverse: being estimates of the plausibility of the data, under specific (null or alternative) hypothesis of the parameter values. The latter would be better suited to confirmatory analyses where experimentalists wished to confirm whether parameter values took on specific values in a new situation. In this paper a new Bayesian modelling framework which provides posterior estimates of the start of combustion is given and is implemented across 4000 consecutive cycles at various engine loads to demonstrate its utility.

## 6.2 Experimental Configuration

Experiments were conducted at the QUT Biofuel Engine Research Facility (BERF) in June 2011. Table 6.1 contains the technical specifications of the engine and data acquisition equipment. The engine was run at 2000 rpm on neat automotive diesel at full load (760 Nm) and at three quarters (570 Nm) and half (380 Nm) of full load.

## 6.3 Experimental Data

Band-pass filtering was applied directly to the in-cylinder pressure signal, Figure 6.1 is an example of the in-cylinder pressure signal, prior to digitising. This was achieved with a two channel analogue Krohn-Hite model 3202 filter, by first passing the in-cylinder pressure signal through a high-pass filter with a threshold of 4 kHz and then through a low-pass filter with a threshold of 20 kHz. The high-pass threshold was set this close to the frequency of interest, approximately 5-7 kHz, to minimise the potential impacts of knocking frequencies. Experiments with the filter settings confirmed that at this threshold the frequency range of interest was unaffected. The low-pass threshold was set to minimise the effects of the cross talk from the diesel injection signal, approximately 28 kHz, whilst maintaining as much of the integrity in the signal as possible.

<b>Engine Specifications</b>	
Make	Cummins ISBe220 31
Capacity	5.9 ℓ
Maximum power	162 kW at 2000 rpm
Maximum torque	820 Nm at 1500 rpm
Number of cylinders	6
Number of valves per cylinder	4
Compression ratio	17.3:1
Bore	102 mm
Stroke length	120 mm
Dynamometer	Electronically controlled water brake dynamometer
Injection system	Common-rail
<b>Data acquisition</b>	
Pressure transducer	Kistler piezoelectric transducer (6053CC60)
Analogue-to-digital converter	Data Translation (DT9832)
Software	National Instruments LabView
Sample rate	200 kHz
Sample time	4 minutes
Data collected	In-cylinder pressure Band-pass filtered in-cylinder pres- sure (allowing 4-20 kHz) Diesel injection timing Crank-angle rotation information

Table 6.1: Engine and data acquisition specifications

Figure 6.2 shows an example of the band-pass filtered signal—it is taken from the same cycle as the in-cylinder pressure trace shown in Figure 6.1. Because this band-pass filtering took place whilst the signal was still in its analogue form, the dependent scale in Figure 6.2 is in Volts. An advantage of using the technique described in this paper to determine the start of combustion is that it is unnecessary to calibrate the pressure signal. Hence, the processing to convert from the unscaled differential signal to pressure has not been done; from the perspective of the analysis, it would be an extraneous use of computation time.



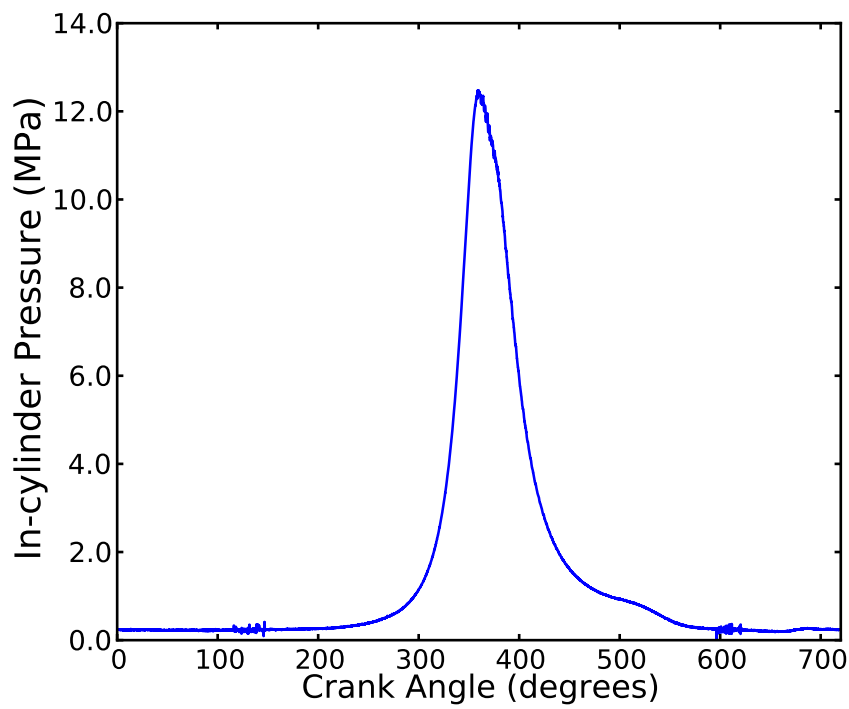


Figure 6.1: Pressure vs crank angle plot at 2000 rpm, full load on neat diesel fuel

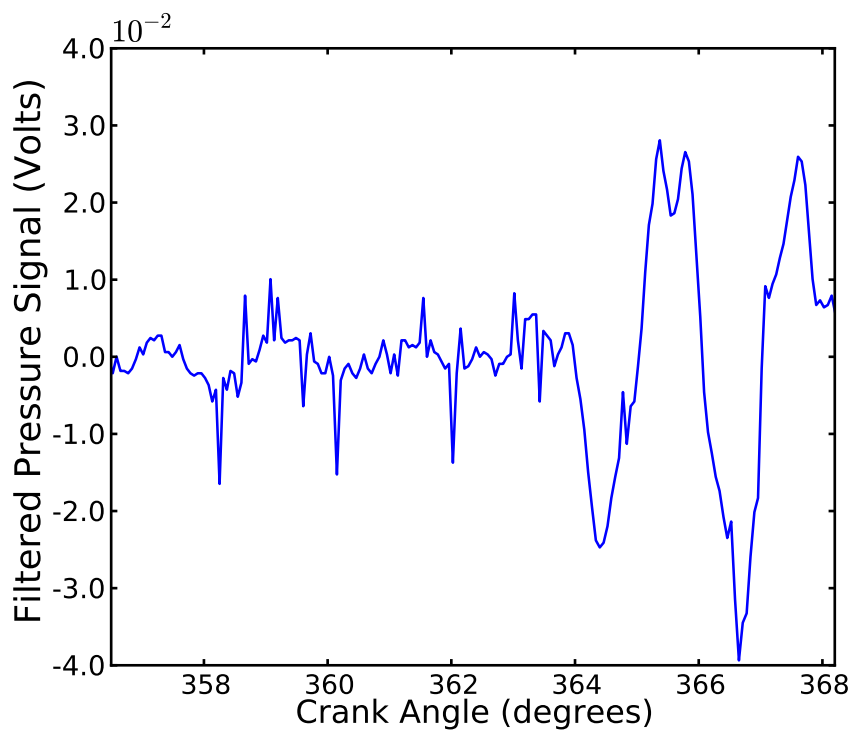


Figure 6.2: Band-pass filtered pressure signal at 2000 rpm, full load on neat diesel fuel

## 6.4 Determination of Ignition Delay

Ignition delay will be defined as being the time period between the start of diesel injection and the start of combustion (Bodisco and Brown, 2013a). Therefore, in order to determine the ignition delay it is important to obtain accurate knowledge of the diesel injection timing, detailed in Section 6.4.1, and the start of combustion, detailed from Section 6.4.3. In the engine setup under investigation in this paper nominal diesel injection timing was able to be determined by directly interrogating the signal sent from the engine management system. For this work, the start of combustion is determined using Bayesian modelling, described in detail from Section 6.4.3. The Bayesian method described in this paper allows for cycle-by-cycle results to be obtained without any need for cycle averaging.

### 6.4.1 Start of Diesel Injection – Estimating Injection Latency

Accurate knowledge of the start of fuel injection is important in a study involving ignition delay; however, a common problem is a lack of easily obtainable information regarding injector latency. In the engine setup used in this paper, nominal injection information is obtained by directly interrogating the diesel injection signal sent from the engine management system. Comparative ignition delay studies, such as in this paper, will generally be more interested in the differences between test settings rather than absolute knowledge of ignition delay. However, it is still advantageous to consider the injection latency to account for cycle-to-cycle changes in the engine speed.

Figure 6.3 shows the diesel injection signal super-imposed over net rate of heat release curves of the engine running with neat diesel fuel at full load and of the engine running with cylinder one, where the pressure transducer is located, being motored, both at 2000 rpm. The point at which the two net rate of heat release curves deviate from each other will be taken to be the point at which the actual diesel injection begins. Suh and Lee (2008) showed in the results of their 2008 study of common-rail diesel injectors that for the injector they investigated latencies as small as approximately 0.25 ms were normal. Similarly, in a recent study Donkerbroek et al. (2011) showed using high speed imaging and by examining a pressure trace of the rail pressure a 3.5 degree crank-angle latency between the injection timing signal and the actual start of injection for their engine setup. In the present engine setup an injection latency of 0.25 ms correlates exactly with the trough of the dip in the net rate of heat release shown in Figure 6.3 and the point at which the two net rate of heat release curves deviate. Therefore, it is assumed that the injector latency in this engine setup is 0.25 ms.

Results of the Bayesian analysis shown later in Section 6.5 will be discussed relative to each other; hence, precisely accurate determination of this value is not completely necessary. However, slight changes in rpm from cycle-to-cycle will have a small impact on the number

of crank angle degrees which occur in a given time period (i.e. the rate of change of engine speed across 2 consecutive samples may not be precisely the same at each engine cycle during a given test). Therefore, the more accurate the knowledge of the injector latency the better the results will be and hence estimating this latency should not be overlooked.

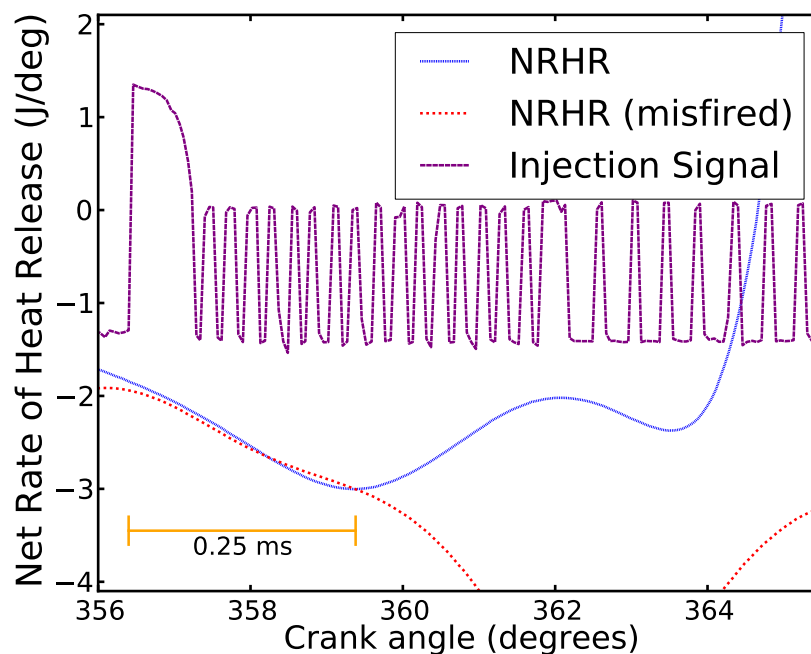


Figure 6.3: Net rate of heat release: full load with neat diesel and misfired compared to the diesel injection signal

#### 6.4.2 Net Rate of Heat Release

Many authors determine the start of combustion by the analysis of cycle-averaged net rate of heat release curves, such as in Figures 6.3–6.5 (Kouremenos et al., 1992; Rakopoulos et al., 2007; Shehata, 2010; Tauzia et al., 2010). Inspection of Figure 6.3 reveals that the start of combustion is at approximately 363.5 degrees crank angle—this result closely correlates to the start of combustion resonance shown in Figure 6.2. However, even though the traditional net rate of heat release method appears to work well, there are issues with the use of heat release curves for the determination of ignition delay. A few of these issues include (Heywood, 1988; Brunt and Platts, 1999; Tauzia et al., 2010):

- the difficulty in accounting for mixture non-uniformity in the air/fuel ratio and in the burned and unburned gas non-uniformity;
- the effect of crevice regions in the combustion chamber; and,

- assuming the wrong rate of heat transfer, or no heat transfer, between the cylinder charge and combustion chamber walls (especially with the addition of a ‘cooling’ additive such as water, or a fumigated fuel in a dual-fuel engine).

Moreover, the calculation of the net rate of heat release relies on accurate knowledge of the in-cylinder volume and in-cylinder pressure. In-cylinder volume is analytically determined from crank angle data, although crank angle is directly measured there can be inaccuracies in the calibration of top dead centre (TDC). Therefore, the determination of in-cylinder volume is sensitive to the accurate determination of TDC. Figures 6.4 and 6.5 show the extent of this sensitivity, Figure 6.5 is centred around the region of interest to give a clearer indicator of the extent of difference each degree of offset from TDC makes in the calculation of net rate of heat release.

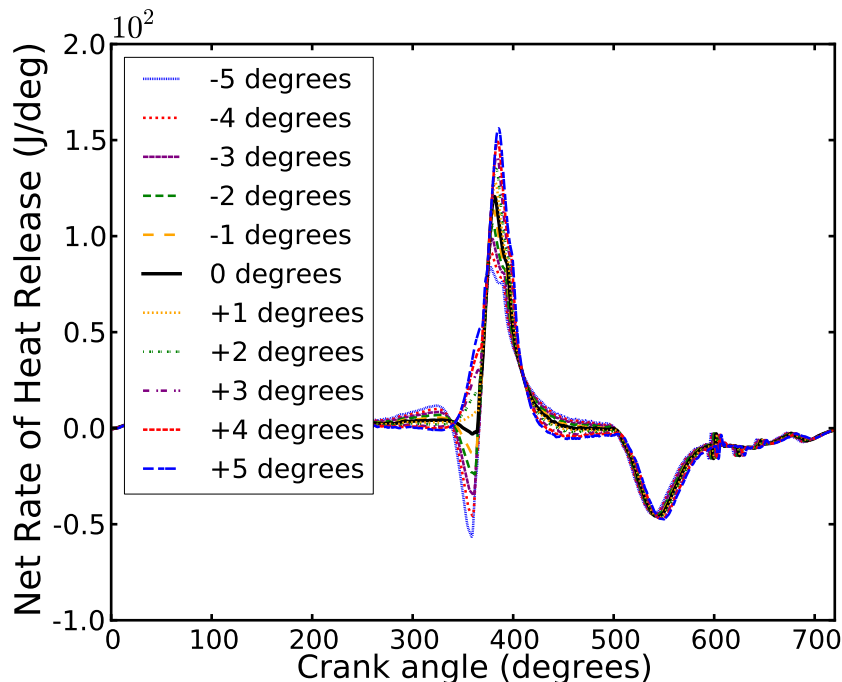


Figure 6.4: Net rate of heat release curves with the location of TDC displaced  $\pm 5$  crank angle degrees

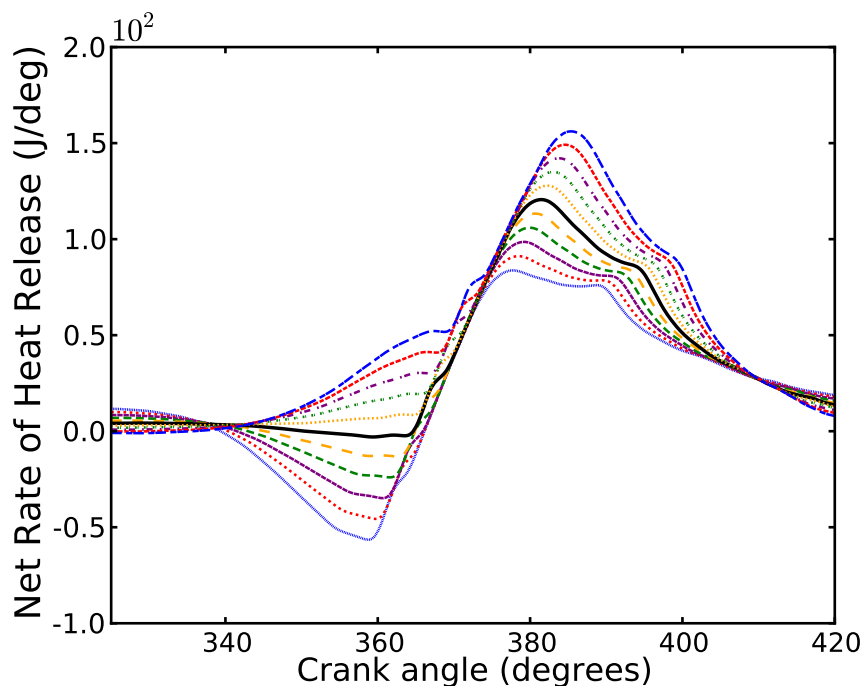


Figure 6.5: Net rate of heat release curves with the location of TDC displaced  $\pm 5$  crank angle degrees, for figure legend refer to Figure 6.4.

Lastly, the need to cycle average, to reduce noise, can potentially skew results if there is a reasonable amount of inter-cycle variability. In the above examples running under standard conditions this is not a large issue because of the engine's repeatability from cycle-to-cycle. However, if the engine is run under non-standard conditions, that result in even a moderate amount of inter-cycle variability, this approach has the potential to be problematic. Moreover, the need to cycle average also removes any possibility of exploring the inter-cycle variation that may be present. Therefore, alternative methods should be explored if the engine is run under non-standard conditions, or if the intention of the investigation is to explore inter-cycle variability.

### 6.4.3 Combustion Resonance

Using combustion resonance to determine the start of combustion overcomes the issues outlined in Section 6.4.2. As the band-pass filtered in-cylinder pressure is in essence a directly measured quantity, no assumptions or further calculations are required for its generation. This means that combustion resonance can be used for the determination of the start of combustion in any engine condition without concern about the aforementioned issues, particularly those related to post-processing of the in-cylinder pressure data. Work previously done by Bodisco et al. (2012) showed that combustion resonance can be modelled using Bayesian statistical modelling. However, their paper focused on the isolation of combustion

resonance for the determination of in-cylinder parameters such as temperature and trapped mass. This current work proposes to use a similar approach to determine the start of combustion and, hence, the ignition delay.

For the purposes of this investigation we will qualitatively define the start of combustion as being the point from which the band-pass filtered in-cylinder pressure signal ceases to exhibit only noise-like behaviour and a strong resonance begins (Carlucci et al., 2006; Bodisco and Brown, 2013a). Therefore, analysis to determine the start of combustion can easily be undertaken manually (Bodisco and Brown, 2013a); however, in order to obtain statistically stable results it would become very time consuming to analyse enough cycles, especially when comparisons between multiple settings are desired. It is proposed that this problem can be overcome with statistical modelling in a Bayesian framework; thus, automating the process of determining the start of combustion. A similar approach has been undertaken by Kim and Min (2008) which used wavelet transforms on the block vibration to determine the start of combustion.

A basic statistical model of the signal in Figure 6.2 can be used in the determination of the start of combustion. If the assumption that the combustion resonance is built from a stationary frequency—whilst this is not true, over such a small time interval it is sufficient for the purposes of this investigation, more complex models require more computation time and will not significantly improve the accuracy of the result (Hickling et al., 1983; Ren et al., 1999; Bodisco et al., 2012)—a very simple model can be used. The conceptual model developed for the determination of the start of combustion is:

$$\begin{aligned} y &= s(t) \sim N(\mu(t), \tau) \\ \mu(t) &= H(t - \delta)A \sin\left(\frac{2\pi}{\lambda}\omega t + \phi\right), \end{aligned} \quad (6.3)$$

where,  $s(t)$ , the band-pass in-cylinder pressure signal (such as the example in Figure 6.2), is assumed to be Normally distributed about some time varying mean,  $\mu(t)$ , with some standard deviation,  $\tau$ . The time varying mean,  $\mu(t)$ , is controlled by a step-function— $\mu$  is zero before the change point defined by the parameter  $\delta$  and when  $t > \delta$ ,  $\mu$  is periodic with a constant amplitude,  $A$ , sample rate,  $\lambda$  (200 kHz), and frequency,  $\omega$ . Hence using this model, the start of combustion can be determined by resolving the change point parameter,  $\delta$ .

#### 6.4.4 Statistical Model

A statistical approach can be used to estimate the parameters  $\delta$ ,  $A$ ,  $\omega$  and  $\phi$  from data tuples  $\{y_i = s(t_i), t_i \in \mathcal{T}\}$ . We estimate these parameters within the Bayesian paradigm to provide marginal posterior plausibility of parameter values based on the data observed e.g.  $p(\delta|y, t)$ . The joint posterior distribution of all parameters is proportional to the product of two terms: the likelihood of the data when parameters are known  $p(y|\delta, A, \omega, \phi)$ ; and the

priori distribution of all model parameters  $p(\delta, A, \omega, \phi)$  (Gelman et al., 2003):

$$p(\delta, A, \omega, \phi|y) \propto p(y|\delta, A, \omega, \phi)p(\delta, A, \omega, \phi)$$

### 6.4.5 Priors

A Bayesian approach requires specification of prior plausibility of parameter values, as defined in Section 6.4.4. If we assume that a priori, what is known about the plausible values of each model parameter, is independent of what is known about all other parameters, then we can factorise  $p(\delta, A, \omega, \phi) = p(\delta)p(A)p(\omega)p(\phi)$ . Moreover, prior distributions should encompass all plausible values a parameter can take (Gelman et al., 2003). In this investigation somewhat informative priors will be utilised.

Uniform prior distributions can be appropriate in circumstances where there is insufficient knowledge of the nature of the tendency of the model parameter—this is based on Laplace’s rationale which has been termed the so-called ‘principle of insufficient reason’ (Gelman et al., 2003). Applying the same logic a Uniform prior is assigned to  $\phi$ . All that is known for a certainty is that  $\phi$  could take on any value between 0 and  $\pi$ , there is no further knowledge about where in this distribution it potentially lies. Therefore,  $\phi \sim \text{Unif}(0, \pi)$ .

Likewise, examination of the fast Fourier transform of the signal in Figure 6.2, shown in Figure 6.6, indicates that the plausible region for the resonant frequency is between 4,500 Hz and 7000 Hz. Therefore,  $\omega \sim \text{Unif}(4500, 7000)$ . In this case, it could be argued that a Normal distribution would be a more appropriate choice. However, the Uniform distribution was used because of its limiting nature; it was important that the MCMC did not attempt to model a different frequency to the combustion resonance as this would likely result in an undesired posterior distribution for the change point parameter,  $\delta$  and hence an incorrect calculation of the start of combustion.

The signal window, such as in Figure 6.2, was shifted based on an assumed ignition delay so that the start of combustion would be approximately in the middle of the window. Therefore, the start of combustion can be considered unlikely to occur towards the edges of the time period. Here the time period extends for 200 samples ( $\sim 12$  crank angle degrees), so the furthest point from the edges occurs at the centre (at  $t = 100$  samples). Therefore, in choosing a prior for the change point parameter,  $\delta$ , a Normal distribution is used to reflect that our uncertainty, centred around the best estimate, behaves like a classical measurement error distribution. By presuming that there is a 95% chance that the combustion time occurs in the middle half of the time period (i.e.  $50 \leq t \leq 150$ ) a prior of  $\delta \sim N(100, 25)$  is obtained.

A common aspect of the band-pass filtered signals from this particular engine is that the amplitude is about 0.04 Volts. It is important that the prior for this is reasonably informative; it would not be appropriate if the model parameter,  $A$ , could be small enough to simply model noise. Much the same, if the amplitude is too large then changes in the

other model parameters are unlikely to make any significant difference to the model fit and hence they may not converge, and if they do it may not be to the true value. A Normal distribution has also been selected for  $A$  to keep it near to the 0.04 Volt estimate, but to not be as restrictive as the Uniform distribution for the scenarios where a signal may have a slightly higher or lower amplitude than is expected. The prior distribution does not need to be central around the true value of the parameter as the information about the parameter in the data is stronger (Gelman et al., 2003). Therefore, the prior is centred about a previous Volt estimate:  $A \sim N(0.04, 0.01)$ .

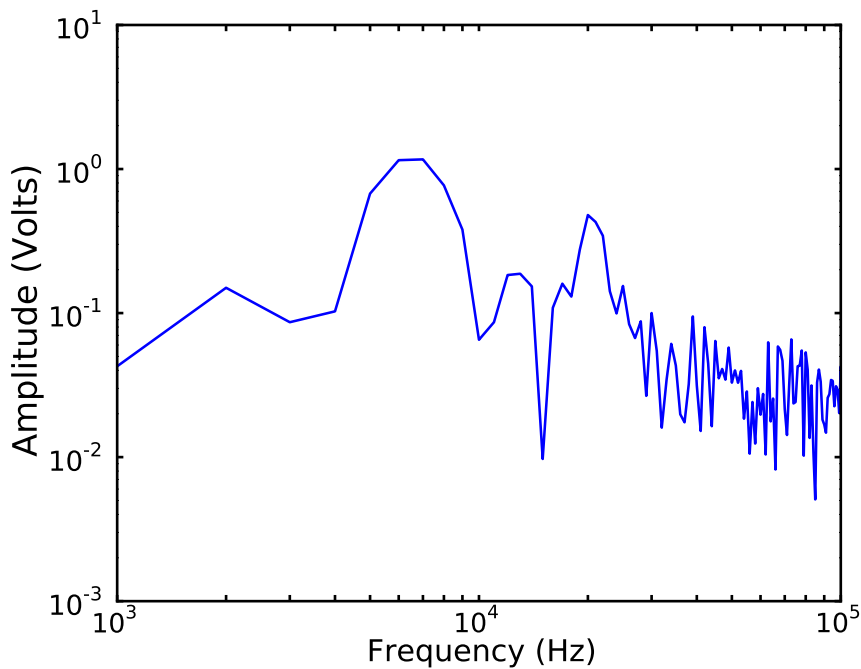


Figure 6.6: Fast Fourier transform of the band-pass filtered in-cylinder pressure signal in Figure 6.2

#### 6.4.6 Metropolis-Hastings Computational Algorithm

In order to estimate the posterior distribution of model parameters, we use a standard Bayesian computational approach based on simulation rather than analytic computations. The ergodic theorem ensures that Markov Chain Monte Carlo (MCMC) simulations will in the long run provide a dependent (rather than independent) set of simulations from the posterior distribution (Gelman et al., 2003). Implementing MCMC through the freely available software package WinBUGS (Spiegelhalter et al., 1999) was not found to be computationally fast enough to be feasible. The prepackage software approach was inappropriate mainly due to an emphasis on exploring inter-cycle variability across thousands of consecutive cycles; however, for this type of work it is an acceptable developmental platform.



In situations, such as this, where the posterior cannot be analytically derived, a flexible approach to computation is the Metropolis-Hastings algorithm—which is a special case of the MCMC algorithm (Gelman et al., 2003). The Metropolis-Hastings algorithm cycles through two steps.

1. Propose a candidate value of the parameter from an appropriate proposal distribution  $\theta^* \sim R(\theta)$ .
2. Accept this new proposed value with a probability that depends on its relative plausibility under the posterior distribution, compared to the previous parameter value.

A generic Metropolis-Hastings approach to sampling is selected, where a new value of a parameter is proposed from its full conditional distribution, based on a proposal distribution, and then accepted or rejected using a probability of acceptance that is the minimum of unity and the product of the ratio of proposal likelihoods and the ratio of posterior probabilities evaluated at the old and new proposed value.

$$\alpha = \min \left\{ 1, \frac{R(\theta^*)}{R(\theta^{m-1})} \frac{p(\theta^*|\cdot)}{p(\theta^{m-1}|\cdot)} \right\}$$

where,  $m = 1, \dots, M$  denotes the  $m^{\text{th}}$  MCMC simulation from the chain,  $\frac{R(\theta^*)}{R(\theta^{m-1})}$ , the proposal ratio, is selected to evaluate to unity and,

$$p(\theta|\cdot) = p(\theta)p(y|\theta;\cdot)$$

where,  $\cdot$  denotes the full set of parameters  $\{\mu_t; \delta, A, \omega, \phi\}$  omitting the parameter of interest, here generically denoted as  $\theta$ . Therefore,

$$\theta^m = \begin{cases} \theta^* & \text{with probability } \alpha \\ \theta^{m-1} & \text{otherwise.} \end{cases}$$

Each candidate parameter, denoted as  $\theta^*$ , is selected by a cyclic sampling strategy from its conditional posterior distribution with the existing value of the parameter,  $\theta^{m-1}$ , as the mean (Gelman et al., 2003).

$$\theta^* \sim N(\theta^{m-1}, \sigma_\theta)$$

Hence  $\sigma_\theta$  acts as a tuning parameter, which determines how far the algorithm seeks for candidate parameter values at each step. A large value of  $\sigma_\theta$  promotes large steps but could provide many wasted proposals. Conversely, a value of  $\sigma_\theta$  that is too small promotes small steps that may take longer to converge towards the true value, and may also induce high cross-correlation of parameter values. Selection of the candidate parameter for  $\delta$  is done

similarly; however, instead of sampling from a Normal distribution a Uniform distribution is used:

$$\delta^* \sim \text{Unif}(\delta^{m-1} - n, \delta^{m-1} + n)$$

where,  $n$  defines the maximum possible deviation the candidate parameter for  $\delta$  can have from the existing value of  $\delta$ —the candidate parameter is selected from the integers in  $\mathbb{Z}$  that fall within  $n$  units of  $\delta^{m-1}$ . The use of a Uniform proposal distribution for  $\delta$  is to ensure broad exploration.

### 6.4.7 Simulation Results

After a suitable burn-in time (in this case 2000 iterations) model parameters are saved in an array (in this case 200 values, every fifth value out of 1000 iterations) to create a posterior density for each model parameter. Examination of the kernel density estimate (probability density function) for each parameter, the posterior density, will not only yield the most plausible value (taken to be the posterior mode), but also give the analyst an indication of the uncertainty in the result (Rosenblatt, 1956; Parzen, 1962; Gelman et al., 2003). From the analysis of the signal shown in Figure 6.2, it can be seen in Figure 6.7 that the most plausible start of combustion timing is  $363.97^\circ$  with a 95% credible interval of  $[363.78, 364.14]$ . Similarly, the analysis also shows that the most plausible initial resonant frequency (Figure 6.8) is 6215 Hz with a 95% credible interval of  $[6202, 6233]$ .

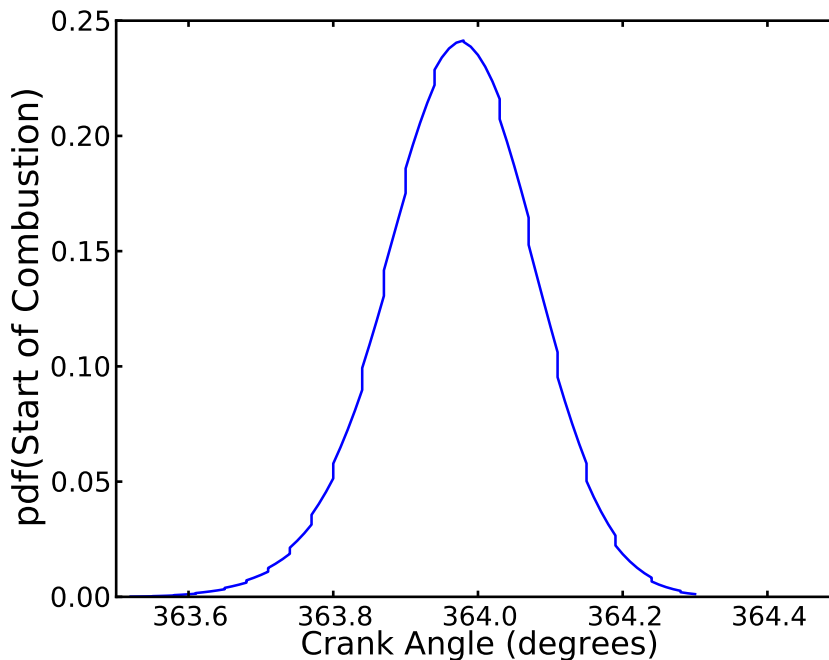


Figure 6.7: Posterior density of the start of combustion,  $\delta$ , of the band-pass filtered in-cylinder pressure signal in Figure 6.2

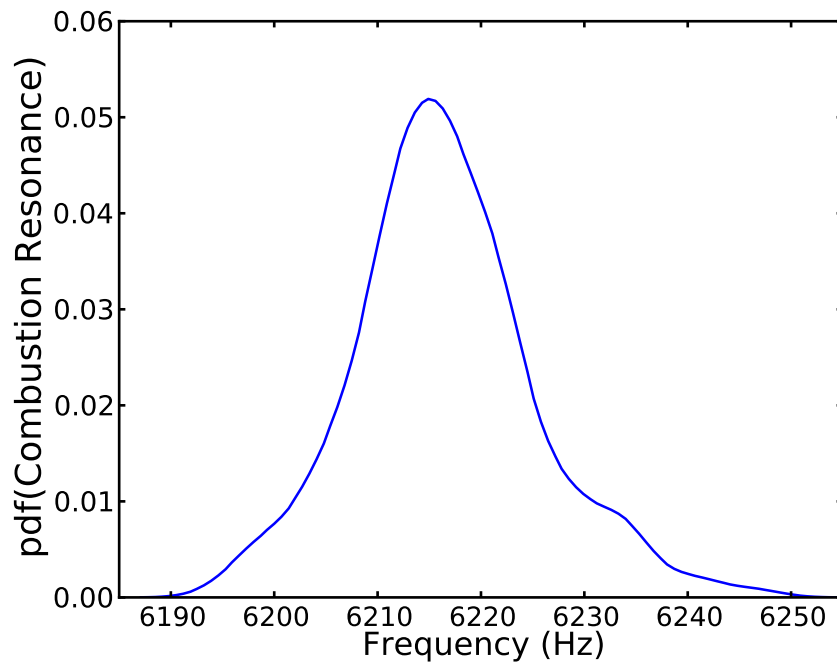


Figure 6.8: Posterior density of the combustion resonance,  $\omega$ , of the band-pass filtered in-cylinder pressure signal in Figure 6.2

Reconstructing the signal from the model allows the analyst to visually determine if the model outputs are feasible. Figure 6.9 shows the signal in Figure 6.2 with a visualisation of the model, as described in Equation 6.3. Parameter estimates for this cycle are shown in Table 6.2. It can be visually seen that the model and the signal agree well, especially in relation to the change point parameter. This is evident by how closely the model follows the signal it was fitted to: the resonant frequency,  $\omega$ , matches that of the signal and the periodic part of the model begins at the same time as the combustion resonance.

Another outcome of this simulation is an estimate of the initial resonant frequency,  $\omega$ —as it is only fitting across a small section of the data the assumption of a stationary frequency will not be significantly incorrect enough to produce a misleading result. In the case of Figure 6.9, two periods of the combustion resonance are present, if it were much more than this the assumption of a stationary frequency would fail and a misleading result may be obtained. Therefore, the model described in this paper can be used effectively as a means of determining the start of combustion and the initial resonant frequency.

Variable	Prior Mean	Prior StDev	Posterior Mode	Posterior StDev
$A$ (Volts)	0.04	0.01	0.024	0.001
$\delta$ ( $^\circ$ crank angle)	100 (362.34 $^\circ$ )	20 ( $\approx 1.52^\circ$ )	127 (363.97 $^\circ$ )	1 (0.05 $^\circ$ )
Uniform Prior	Low	High		
$\omega$ (Hz)	4500	7000	6215	9
$\phi$	0	$\pi$	2.92	0.03

Table 6.2: Model priors and parameter estimates of the band-pass filtered in-cylinder pressure signal shown in Figures 6.2 and 6.9 based on the model described by Equation 6.3

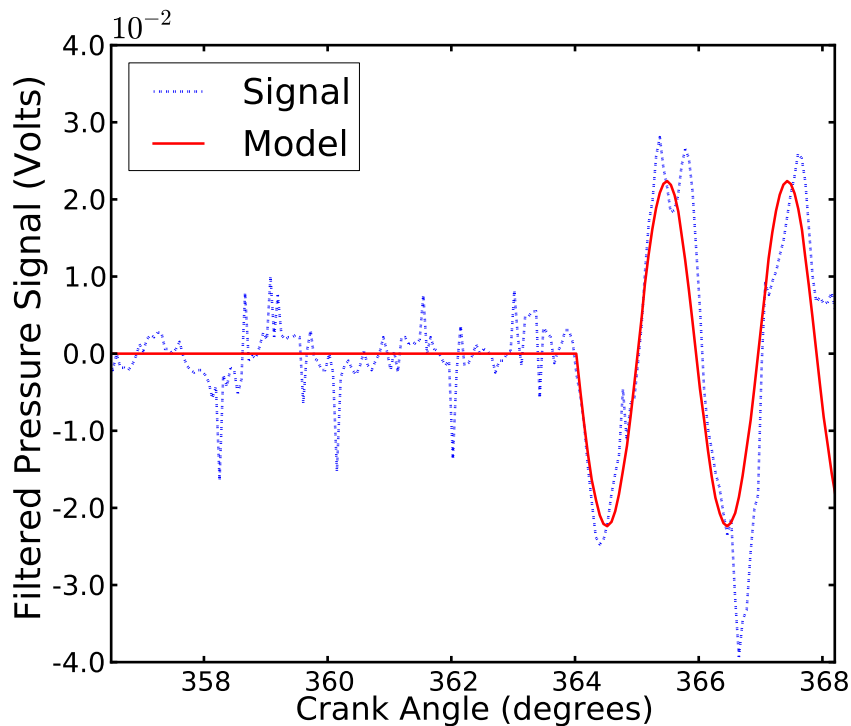


Figure 6.9: Model of the band-pass filtered in-cylinder pressure signal in Figure 6.2

## 6.5 Inter-cycle Variability

An important justification for using the analysis methodology described in the previous section was to allow for cycle-by-cycle analysis of the data. As the Bayesian method is reliable with noisy data the need to cycle average is removed and individual cycles can be examined independently. Hence, the data can be investigated across large numbers of consecutive cycles—the results shown in the section are from 4000 consecutive cycles (4 minutes of data). This investigation was performed on a standard desktop computer in

C++ and the analysis took approximately 15 seconds per cycle to perform.

Ignition delay is influenced by the injection timing because of changes in the charge air temperature and pressure (Heywood, 1988). The empirical relationship for estimating ignition delay given by Hardenberg and Hase (1979) in Equation 6.2 shows the temperature and pressure dependence at the time of injection. Therefore, no ignition delay study would be complete without first examining the injection timing. Figure 6.10 shows the injection timing—this data is presented in a histogram because of the discrete nature of the diesel injection timing. The injection timing is controlled by the engine management system, in all test cases the injection strategy was one a single sustained injection and combustion occurred before the diesel injection was completed.

Advanced injection timing, such as exhibited by the engine under investigation, is common among modern diesel engines to mitigate harmful emission (Choi et al., 2005; Genzale et al., 2009). Improved Emission control is achieved with advanced injection timing because of an increase in premixed combustion and subsequent changes to in-cylinder pressure and decreased in-cylinder temperature (Prabhakar and Boehman, 2012). Nitrogen oxides (NO<sub>x</sub>), along with particulate matter, are a key emission from diesel engines. Excessive NO<sub>x</sub> formation is normally related to high in-cylinder temperature and excess oxygen (Lavoie et al., 1970) and is therefore directly influenced by the injection timing, injection pressure and the amount of mixing prior to combustion, and hence the ignition delay.

Knowledge of the injection timing is determined from interrogating the diesel injector signal and is corrected for injector latency, as explained in Section 6.4.1. At half load the diesel injection timing is significantly later than at full and three quarter load. There is more than a crank-angle degree difference between the start of diesel injection for half load when compared with three quarter and full load. At half load injection typically occurs at approximately 360.9 degrees crank-angle, whereas at three quarter load injection typically occurs at approximately 359.7 crank-angle degrees and at full load injection typically occurs at approximately 359.3 degrees crank-angle.

Figure 6.11 shows the combustion timing,  $\delta$ . Similar to the injection timing shown in Figure 6.10, full and three quarter load commence combustion at a similar time, approximately 365 degrees crank-angle for three quarter load and approximately 364 degrees crank-angle for full load, whereas the start of combustion for half load is much later at approximately 368 degrees crank-angle. Also worthy of noting is that, as the load is decreased the inter-cycle variability of the diesel injection timing and the start of combustion is increased. This is most likely an artifact of the stability of the in-cylinder temperature. At half load the inter-cycle variability is considerably increased when compared to the higher loads, the inter-cycle variability at full and three quarter load is very similar with only a fractional increase as the load was decreased. This is also clearly seen in the ignition delay results, shown in Figure 6.12. The ignition delay at half load is approximately two degrees crank-angle longer than at

full and three quarter loads, and significantly less stable. Both Figures 6.11 and 6.12 show that on some cycles at half load combustion occurs much later than the rest of the cycles. This may be caused by a low frequency (period of approximately 50 s) fluctuation in the in-cylinder temperature as a result of instabilities in the dynamometer control system at this operating condition. Including these cycles which are exhibiting unusual behaviour does not significantly change the calculation of ignition delay—the modal, mean and median ignition delay at half load is 6.9 crank-angle degrees, at three quarter load the ignition delay is 5.2 crank-angle degrees and at full load the ignition delay is 4.8 crank-angle degrees.

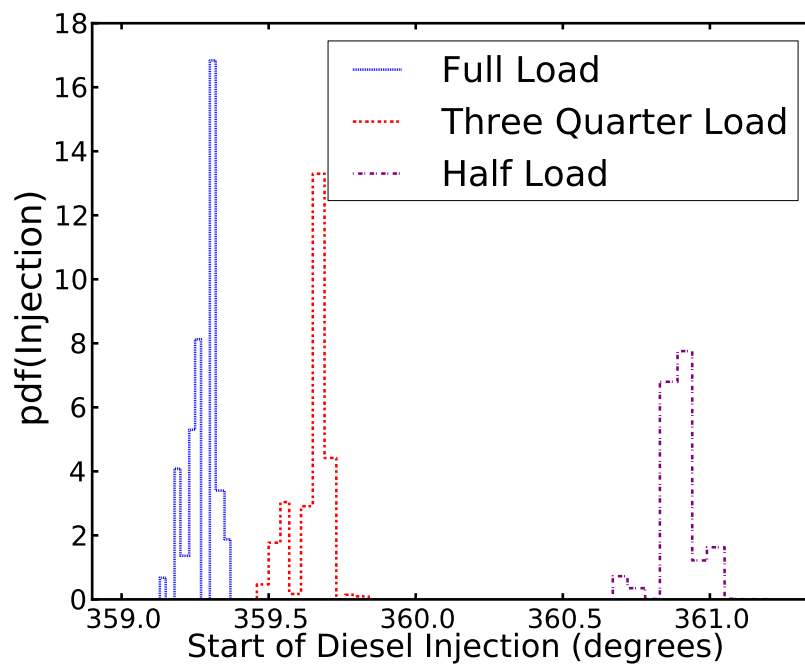


Figure 6.10: Diesel injection timing at 2000 rpm

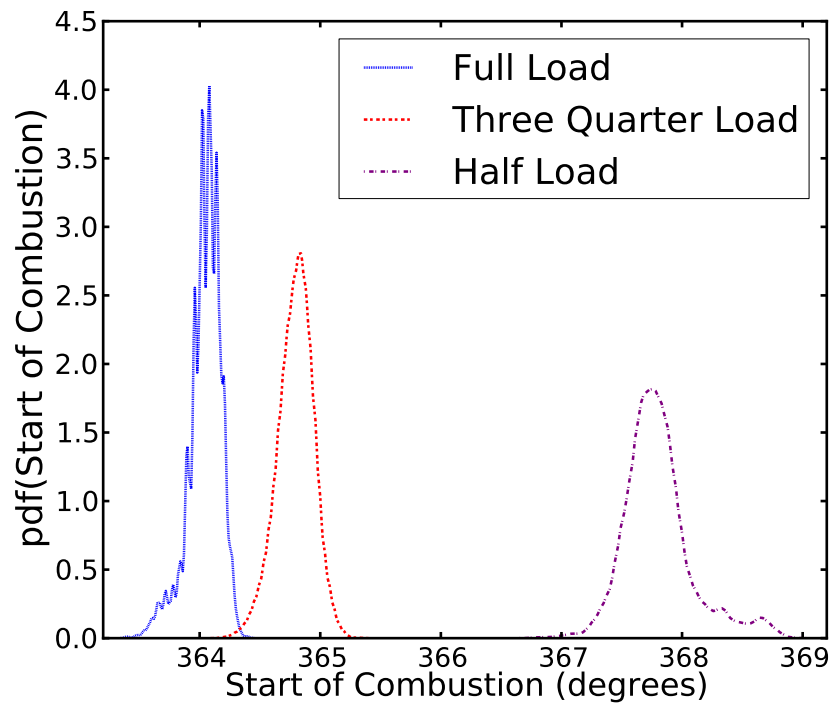


Figure 6.11: Start of combustion as determined from the combustion resonance, parameter  $\delta$ , at 2000 rpm

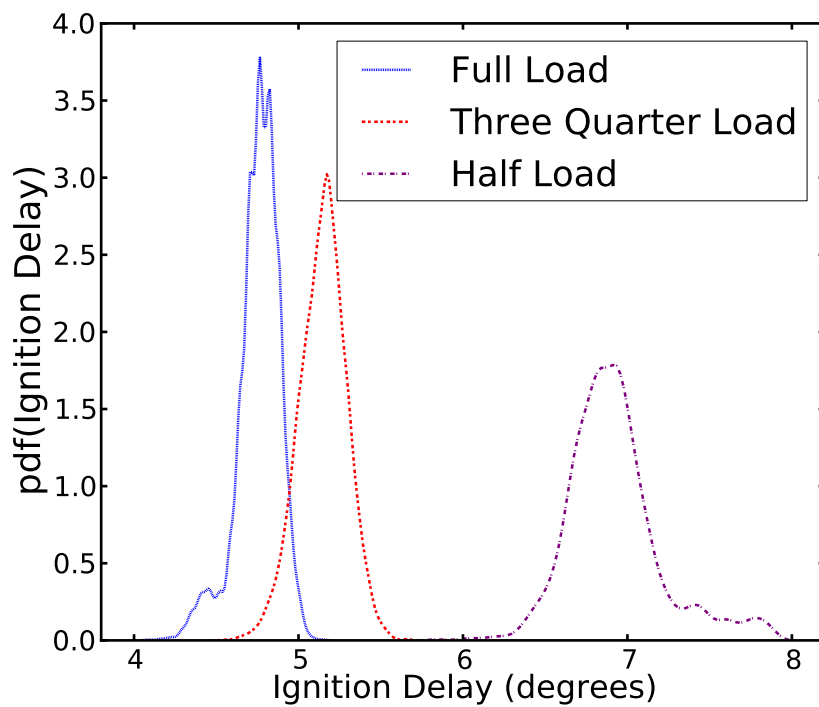


Figure 6.12: Ignition delay as determined from the combustion resonance at 2000 rpm

## 6.6 Comparison to Net Rate of Heat Release

Traditionally the start of combustion was determined by examining a net rate of heat release plot Heywood (1988)—the start of combustion is usually characterised to be the point at which the net rate of heat release becomes positive. Figure 6.13 shows a net rate of heat release plot generated from the average of 4000 engine cycles at 2000 rpm and full load using Equation 6.1. On the opposing axis of Figure 6.13 is the start of combustion distribution shown in Figure 6.11, generated from the same 4000 engine cycles as the net rate of heat release. Good agreement between the two methods can be seen; the start of combustion, as determined by the Bayesian analysis, lines up well with the start of the increase in net rate of heat release at approximately 364 degrees crank-angle. Also of note in Figure 6.13 is that the start of combustion distribution, from the Bayesian analysis described in this paper, lines up with the start of the increase in the net rate of heat release, rather than when the net rate of heat release becomes positive.

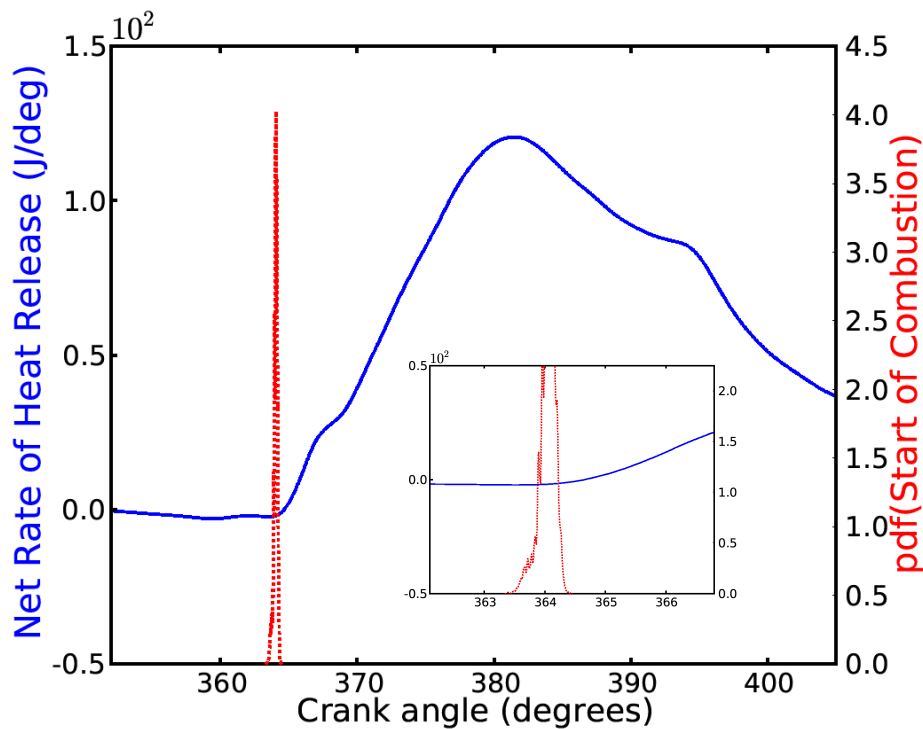


Figure 6.13: Net rate of heat release and start of combustion as determined from the combustion resonance, parameter  $\delta$ , at full load

## 6.7 Conclusion

This paper has introduced a powerful new method for determining ignition delay. In contrast to standard techniques this method uses combustion resonance, in the form of band-pass



filtered in-cylinder pressure, and Bayesian statistical modelling to accurately resolve the start of combustion. It was also demonstrated that this method allows for true inter-cycle variability studies and does not suffer from some of the issues surrounding the use of in-cylinder pressure directly to determine the start of combustion. The results shown in this paper demonstrate the utility of this technique by examining 4000 consecutive cycles at 3 different engine loads: full, three quarter and half loads. At half load the ignition delay was much longer than at the higher loads and the inter-cycle variability was greatly increased when compared to the higher loads.

The Bayesian modelling method shown in this paper for determining the start of combustion uses in-cylinder pressure. In-cylinder pressure methods are optimal because they are inexpensive, when compared to optical sensors; also, using a measured engine parameter that is directly related to the engine work for a study into ignition delay makes intuitive sense. Moreover, this is the only in-cylinder pressure technique currently available for determining ignition delay that does not involve differentiation. Differentiating noisy data decreases the signal-to-noise ratio and therefore complicates sensitive analysis such as this. Further, Bayesian modelling requires only a small number of data points to be effective and is not adversely effected by noise. Therefore, the methodology shown in this paper for determining the start of combustion can be used to accurately resolve the ignition delay for individual cycles, which is important if inter-cycle variability studies are required.

## 6.8 Acknowledgements

The authors wish to thank Mr. Anthony Morris for assisting with the design of the experimental campaigns and his invaluable technical knowledge and Mr. Noel Hartnett for his work in maintaining the engine for research. Further thanks also to Technologist Mr. Ken McIvor for his assistance in setting up the data acquisition software. This work was undertaken under an Australian Research Council Linkage Grant (LP0775178) in association with Peak3 P/L.

## 6.9 References

- Assanis, D. N., Filipi, Z. S., Fiveland, S. B., and Syrimis, M. A predictive ignition delay correlation under steady-state and transient operation of a direct injection diesel engine. *J. Eng. Gas Turbines Power*, 125(2):450–457, 2003.
- Bodisco, T. and Brown, R. J. Inter-cycle variability of in-cylinder pressure parameters in an ethanol fumigated common rail diesel engine. *Energy*, 52(1):55–65, 2013a.
- Bodisco, T., Reeves, R., Situ, R., and Brown, R. J. Bayesian models for the determination

- of resonant frequencies in a DI diesel engine. *Mechanical Systems and Signal Processing*, 26:305–314, 2012.
- Brunt, M. and Platts, K. Calculation of heat release in direct injection diesel engines. *Society of Automotive Engineers*, (SAE Paper 1999-01-0187), 1999.
- Carlucci, A. P., Chiara, F. F., and Laforgia, D. Block vibration as a way of monitoring the combustion evolution in a direct injection diesel engine. *Society of Automotive Engineers*, (SAE Paper 2006-01-1532), 2006.
- Choi, D., Miles, P., Yun, H., and Reitz, R. A parametric study of low-temperature late-injection combustion in a HSDI diesel engine. *JSME International Journal Series B*, 48(4):656–664, 2005.
- Cinar, C., Can, O., Sahin, F., and Yucesu, H. S. Effects of premixed diethyl ether (DEE) on combustion and exhaust emissions in a HCCI-DI diesel engine. *Applied Thermal Engineering*, 30(4):360–365, 2010.
- Donkerbroek, A. J., Boot, M. D., Luijten, C. C. M., Dam, N. J., and ter Meulen, J. J. Flame lift-off length and soot production of oxygenated fuels in relation with ignition delay in a DI heavy-duty diesel engine. *Combustion and Flame*, 158(3):525–538, 2011.
- Ellison, A. Bayesian inference in ecology. *Ecology Letters*, 7(6):509–520, 2004.
- Gelman, A., Carlin, J. B., Stern, H. S., and Rubin, D. B. *Bayesian Data Analysis: Second Edition*. Chapman & Hall/CRC, 2003.
- Genzale, C., Reitz, R., and Musculus, M. Effects of spray targeting on mixture development and emissions formation in late-injection low-temperature heavy-duty diesel combustion. *Proceedings of the Combustion Institute*, 32(2):2767–2774, 2009.
- Ghojel, J., Honnery, D., and Al-Khaleefi, K. Performance, emissions and heat release characteristics of direct injection diesel engine operating on diesel oil emulsion. *Applied Thermal Engineering*, 26(17-18):2132–2141, 2006.
- Hardenberg, H. O. and Hase, F. W. An empirical formula for computing the pressure rise delay of a fuel from its cetane number and from the relevant parameters of direct-injection diesel engines. *Society of Automotive Engineers*, (SAE Paper 790493), 1979.
- Heywood, J. B. *Internal Combustion Engine Fundamentals*. McGraw-Hill, Inc., 1988.
- Hickling, R., Feldmaier, D. A., Chen, F. H. K., and Morel, J. S. Cavity resonances in engine combustion chambers and some applications. *Acoustical Society of America Journal*, 73: 1170–1178, 1983.

- Kim, S. and Min, K. Detection of combustion start in the controlled auto ignition engine by wavelet transform of the engine block vibration signal. *Measurement Science and Technology*, 19(8), 2008.
- Kouremenos, D. A., Rakopoulos, C. D., and Kotsos, K. G. A stochastic-experimental investigation of the cyclic pressure variation in a DI single-cylinder diesel engine. *International Journal of Energy Research*, 16(9):865–877, 1992.
- Lata, D. B. and Misra, A. Analysis of ignition delay period of a dual fuel diesel engine with hydrogen and LPG as secondary fuels. *International Journal of Hydrogen Energy*, 36(5): 3746–3756, 2011.
- Lavoie, G., Heywood, J., and Keck, J. Experimental and theoretical study of nitric oxide formation in internal combustion engines. *Combustion Science and Technology*, 1:313–326, 1970.
- Papagiannakis, R.G and Hountalas, D.T. Experimental investigation concerning the effect of natural gas percentage on performance and emissions of a DI dual fuel diesel engine. *Applied Thermal Engineering*, 23(3):353–365, February 2003.
- Parzen, E. On estimation of a probability density function and mode. *The Annals of Mathematical Statistics*, 33(3):1065–1076, 1962.
- Payri, R., Garcia-Oliver, J. M., Bardi, M., and Manin, J. Fuel temperature influence on diesel sprays in inert and reacting conditions. *Applied Thermal Engineering*, 35:185–195, 2012.
- Prabhakar, B. and Boehman, A. Effect of common rail pressure on the relationship between efficiency and particulate matter emissions at NOx parity. *Society of Automotive Engineers*, (SAE Paper 2012-01-0430), 2012.
- Prakash, G., Shaik, A. B., and Ramesh, A. An approach for estimation of ignition delay in a dual fuel engine. *Society of Automotive Engineers*, (SAE Paper 1999-01-0232), 1999.
- Rakopoulos, C. D., Antonopoulos, K. A., and Rakopoulos, D. C. Experimental heat release analysis and emissions of a HSDI diesel engine fueled with ethanol-diesel fuel blends. *Energy*, 32(10):1791–1808, 2007.
- Ren, Y., Randall, R. B., and Milton, B. E. Influence of the resonant frequency on the control of knock in diesel engines. *Proceedings of the Institution of Mechanical Engineers: Part D: Journal of Automobile Engineering*. London, 213(2):127–133, 1999.
- Ren, Y., Huang, Z., Jiang, D., Liu, L., Zeng, K., Liu, B., and Wang, X. Combustion characteristics of a compression-ignition engine fuelled with diesel-dimethoxy methane

- blends under various fuel injection advance angles. *Applied Thermal Engineering*, 26(4): 327–337, 2006.
- Rosenblatt, M. Remarks on some nonparametric estimates of a density function. *The Annals of Mathematical Statistics*, 27(3):832–837, 1956.
- Rothamer, D. and Murphy, L. Systematic study of ignition delay for jet fuels and diesel fuel in a heavy-duty diesel engine. *Proceedings of the Combustion Institute*, 2012.
- Sahoo, P. K. and Das, L. M. Combustion analysis of Jatropa, Karanja and Polanga based biodiesel as fuel in a diesel engine. *Fuel*, 88(6):994–999, 2009.
- Shehata, M. S. Cylinder pressure, performance parameters, heat release, specific heats ratio and duration of combustion for spark ignition engine. *Energy*, 35(12):4710–4725, 2010.
- Spiegelhalter, D. J., Thomas, A., and Best, N. G. *WinBUGS Version 1.2 User Manual*. MRC Biostatistics Unit, 1999.
- Stone, R. *Introduction to Internal Combustion Engines*. Macmillan Press Ltd, London, 1999.
- Suh, H. K. and Lee, C. S. Experimental and analytical study on the spray characteristics of dimethyl ether (DME) and diesel fuels within a common-rail injection system in a diesel engine. *Fuel*, 87(6):925–932, 2008.
- Tauzia, X., Maiboom, A., and Shah, S. R. Experimental study of inlet manifold water injection on combustion and emissions of an automotive direct injection diesel engine. *Energy*, 35(9):3628–3639, 2010.

## Chapter 7

# Inter-cycle variability of ignition delay in an ethanol fumigated common rail diesel engine


Timothy Bodisco<sup>a</sup>, Philipp Tröndle<sup>b</sup>, Richard J. Brown<sup>a</sup>

<sup>a</sup>Science and Engineering Faculty, Queensland University of Technology, Brisbane QLD, 4001, Australia

<sup>b</sup>Lehrstuhl und Institut für Technische Thermodynamik, Karlsruher Institut für Technologie, Germany


Publication: Energy, in preparation.

### Author Contribution

Contributor	Statement of Contribution
Timothy Bodisco	Conducted the experiments, performed the data analysis and drafted the manuscript
Signature 	
Philipp Tröndle	Generated the results from the numerical analysis in Section 7.7
Richard Brown	Supervised the project, aided with the development of the paper and extensively revised the manuscript

### Principal Supervisor Confirmation

I have sighted email or other correspondence from all co-authors confirming their certifying authorship.

Name	Signature	Date
Associate Professor Richard Brown		

## Abstract

An experimental study has been performed to investigate the ignition delay of a modern heavy-duty common-rail diesel engine run with fumigated ethanol substitutions up to 40% on an energy basis. The ignition delay was determined through the use of statistical modelling in a Bayesian framework—this framework allows for the accurate determination of the start of combustion from single consecutive cycles and does not require any differentiation of the in-cylinder pressure signal. At full load the ignition delay has been shown to decrease with increasing ethanol substitutions and evidence of combustion with high ethanol substitutions prior to diesel injection have also been shown experimentally and by modelling. Whereas, at half load increasing ethanol substitutions have increased the ignition delay. A threshold absolute air to fuel ratio (mole basis) of above  $\sim 110$  for consistent operation has been determined from the inter-cycle variability of the ignition delay, a result that agrees well with previous research of other in-cylinder parameters and further highlights the correlation between the air to fuel ratio and inter-cycle variability.

Numerical modelling to investigate the sensitivity of ethanol combustion has also been performed. It has been shown that ethanol combustion is sensitive to the initial air temperature around the feasible operating conditions of the engine. Moreover, a negative temperature coefficient region of approximately 900–1050 K (the approximate temperature at fuel

injection) has been shown with for *n*-heptane and *n*-heptane/ethanol blends in the numerical modelling. A consequence of this is that the dominate effect influencing the ignition delay under increasing ethanol substitutions may rather be from an increase in chemical reactions and not from in-cylinder temperature. Further investigation revealed that the chemical reactions at low ethanol substitutions are different compared to the high (> 20%) ethanol substitutions.

## 7.1 Introduction

In the mid-term to mitigate fossil fuel usage in diesel engines, the dual-fuel approach, particularly with ethanol, has been of research interest for decades (Surawski et al., 2012; Boretta, 2012; Chauhan et al., 2011; Surawski et al., 2010; Cheng et al., 2008; Sahin and Durgun, 2007; Selim, 2005; Abu-Qudais et al., 2000; Alperstein et al., 1958). This research area exists because of the serious need to move toward more sustainable fuels (Shafiee and Topal, 2009; Sahoo et al., 2009; Skelton, 2007; Bo et al., 2006). However, in the current literature there is very little experimental published research on dual-fuel operation of heavy-duty common-rail diesel engines, such as would be found in common practical applications (Bodisco and Brown, 2013a).

Ignition delay is an important parameter in alternative fuel studies owing to its correlation to emission (Valentino et al., 2012; Abu-Qudais et al., 2000; Cheng et al., 2008). An increase in ignition delay is an indicator of a lower temperature throughout the cycle, causing a reduced CO oxidation reaction rate (Abu-Qudais et al., 2000). Moreover, a longer ignition delay can aid mixing prior to combustion, improving NO<sub>x</sub> and smoke emission (Valentino et al., 2012). Whilst some studies have highlighted the importance of investigating ignition delay, there has been limited investigation on the inter-cycle variability of ignition delay, with the notable exception of the engine research group at the National Technical University of Athens (Rakopoulos et al., 2008, 2010; Kouremenos et al., 1992), and limited investigation into new techniques to improve the accuracy of its calculation (Bodisco et al., 2013b).

The engine research group at the National Technical University of Athens have investigated numerous alternative fuels, including: methane, methanol and dodecane (Rakopoulos and Kyritsis, 2001), vegetable oil (Rakopoulos et al., 2006), ethanol (Rakopoulos et al., 2008) and bio-diesels (Rakopoulos et al., 2010; Rakopoulos, 2012). They have also investigated using supplementary diesel and gasoline as a fumigated fuel (Kouremenos et al., 1989, 1990). However, this work was all performed on a low power naturally aspirated single-cylinder engine (in their investigation high load corresponds to a brake mean effective pressure (BMEP) of 5.37 bar). It should be noted that alternative fuel research at the National Technical University of Athens has not been limited to the single-cylinder engine, but has also been performed on a heavy-duty, turbo-charged, direct injection six-cylinder engine (Rakopoulos et al., 2011).

Common-rail engines tend to have later injection when compared to their direct (mechanical) injection counter-parts. Subsequently, this later injection has an effect on the performance and emission output of the engine—in dual-fuel operation with ethanol this has a significant effect on the inter-cycle variability (Bodisco and Brown, 2013a). The current literature, which is focused on direct (mechanical) injection diesel engines, suggests that fumigated ethanol causes longer ignition delays owing to the higher specific heat capacity of ethanol, when compared to the charge-air without ethanol (Bodisco and Brown, 2013a).



This results in the charge-air having a lower temperature, the so-called ‘cooling effect’ of ethanol. Moreover, the significantly higher injection pressure, with common-rail engines, enhances the atomisation and fuel penetration (Bruneaux, 2001); hence, higher injection pressures cause more homogeneous combustion and reduced ignition delay times.

Rothamer and Murphy (2012) compared the six commonly used in-cylinder pressure methods of determining ignition delay in a recent study. The six methods compared were:

1. location of 50% of pressure rise due to premixed burn combustion;
2. extrapolation of the peak slope of pressure rise due to combustion to the zero crossing point;
3. location of the first peak of the second derivative of the pressure signal;
4. location of the first peak of the third derivative of the pressure signal;
5. location of 10% of the maximum heat release rate in the premixed burn; and,
6. a repeat of (5) using a low-pass (threshold 2000 Hz) filtered in-cylinder pressure signal.

They noted that out of these methods the most reliable were ones that required the least differentiation—differentiating data increases the noise. However, all of the in-cylinder methods tested by Rothamer and Murphy (2012) required some form of differentiation; whereas, the method employed in this work requires no differentiation (Bodisco et al., 2013b). Also of note, the ignition delay calculated with the low-pass filtered in-cylinder pressure signal was 200-330  $\mu\text{s}$  shorter than the other methods.

In a study by Rodriguez et al. (2011) to investigate a predictive correlation for the ignition delay period for biodiesels, specifically palm oil and rapeseed oil, found that the inter-cycle variation in ignition delay for their engine was as great as 2.2%—this value is similar to that reported by Assanis et al. (2003), who found an inter-cycle variation of 2%. However, the representative values reported in their work were based on the analysis of the average of 50 consecutive in-cylinder pressure cycles. They also argue that in-cylinder pressure analysis for the determination of ignition delay is preferable to other methods, particularly those utilising luminosity detectors, as in-cylinder pressure changes are often detectable prior to other indicators of combustion (Heywood, 1988; Rodriguez et al., 2011).

A promising method for determining the start of combustion is with the use of vibration or acoustic emission signals (Chiavola et al., 2010; Arnone et al., 2009; Carlucci et al., 2006). Even in constant volume bombs there is good agreement between the sudden increase in pressure and the mechanical vibration (Reyes et al., 2012). The technique for determining the start of combustion with a vibration signal is to simply identify the sharp onset of the mechanical vibration. In a practical application, the use of an accelerometer is a cheap alternative to the more expensive in-cylinder pressure transducer. However, as the engine

setup in this current work has been undertaken on has an in-cylinder pressure transducer, details in Section 7.2, the use of vibration signals has not been explored. Carlucci et al. (2006) has argued that the high-pass filtered in-cylinder pressure signal is analogous to the vibration signal—the start of combustion results shown in this work are determined through the use of high-pass filtered in-cylinder pressure signals and are therefore assumed to match those that could have been obtained with vibration signals.

Recent work by Bodisco et al. (2013a; 2013b) has shown the use of high-pass filtered in-cylinder pressure signals as a means for determining the start of combustion in a heavy-duty diesel engine. The current work will explore the statistical modelling technique employed in Bodisco et al. (2013b) to investigate the inter-cycle variability of the start of combustion, and hence ignition delay, in a heavy-duty Cummins common-rail multi-cylinder diesel engine operated with fumigated ethanol up to 40% by energy. In the earlier work (Bodisco and Brown, 2013a), it was shown that at high ethanol substitutions and high loads, hence higher in-cylinder temperatures, that the fumigated ethanol undergoes auto-ignition and can reduce ignition delay. However, that study was limited to 200 consecutive cycles owing to the analysis tool used.

The conclusion to the ignition delay portion of the study in Chapter 5 was left uncertain. The preliminary analysis showed a contradicting result with the full load data. It was shown that the nominal ignition delay for the 40% ethanol substitution was longer than that of the 30% substitution, going against the trend showing a systematic decrease in ignition delay with increasing ethanol substitutions. However, it was left uncertain if this result was true or an artifact of the low number of cycles analysed. The limited number of analysed cycles also prohibited an investigation into the relationship between the inter-cycle variability and the air to fuel ratio. Moreover, it was left unknown if auto-ignition occurred prior to diesel injection at the high ethanol substitutions because of limited knowledge related to the actual fuel injection timing.

This chapter will explore the same data set as Chapter 5 using the statistical techniques introduced in Chapter 6 to further investigate the ignition delay in an ethanol fumigated common-rail diesel engine to validate the results available in Chapter 5. In this study the diesel fuel injection timing will be determined by directly interrogating the electronic fuel injection signal and then correcting for injector lag (Bodisco et al., 2013b). Injector lag is the time period between the injector being excited and the actual fuel injection. Numerical modelling will also be employed to investigate the sensitivity of auto-ignition in ethanol-only combustion to the initial air temperature. As an extension, the sensitivity to auto-ignition of *n*-heptane and *n*-heptane/blends at various injection temperatures will also be investigated.

## 7.2 Experimental Configuration

Experiments were conducted on a modern turbo-charged, 5.9  $\ell$ , inline 6-cylinder Cummins diesel engine (ISBe220 31) with common rail injection at the QUT Biofuel Engine Research Facility (BERF). For detailed engine specifications, including relevant results, refer to corresponding Chapters 5 and 6. Moreover, the results shown in this paper are from the same data set described in Chapter 5.

As described in Chapter 5, the data collected was in-cylinder pressure, band-pass filtered in-cylinder pressure (allowing 4-20 kHz, both pressure signals collected as a differential voltage signal), diesel injection timing and degrees of crank-angle rotation information. The engine was run at 2000 rpm on neat automotive diesel and with ethanol fumigation substitutions of 10%, 20%, 30%, and 40% on an energy basis at full load (760 Nm) and at three quarters (570 Nm) and half (380 Nm) of full load. Ethanol fumigation was achieved by directly introducing the ethanol as a vapour into the air in-take at the inlet manifold after the turbocharger—a detailed schematic of the ethanol fumigation system, along with a schematic of the data acquisition system, is available in Chapter 5.

## 7.3 Terminology and Abbreviations

DXXXEYYY	DXXXEYYY represents the nominal XXX% of diesel fuel by energy and the nominal YYY% substitution of ethanol by energy
Neat diesel	Neat diesel refers to the case where the engine is run on diesel fuel only, no ethanol substitution
EMS	Engine management system
NRHR	Net rate of heat release
Kernel density estimate	An estimation of the probability density function
TDC	Top dead centre (0 and 360 crank-angle degrees)
COV	Coefficient of Variation – standard deviation normalised by the mean

## 7.4 Ignition Delay

For this work the ignition delay will be defined as the period from the start of diesel fuel injection until the time that combustion commences (Bodisco et al., 2013b)—the combustion

timing will be determined by resolving the time at which the combustion chamber resonance begins (Bodisco and Brown, 2013a; Bodisco et al., 2013b). In the methodology shown in Chapter 6 the band-pass filtered in-cylinder pressure signal, example shown in Figure 7.1, is modelled with a statistical model in a Bayesian framework. The conceptual model employed in Chapter 6 is:

$$\begin{aligned} y &= s(t) \sim \mathcal{N}(\mu(t), \sigma) \\ \mu(t) &= \mathbb{H}(t - \delta)A \sin\left(\frac{2\pi}{\lambda}\omega t + \phi\right), \end{aligned} \quad (7.1)$$

where, the band-pass filtered in-cylinder pressure signal,  $s(t)$ , is modelled as a Normal distribution with time varying mean,  $\mu(t)$ , and standard deviation,  $\sigma$ . The model parameter,  $\delta$ , acts as a change point, when  $t$  is less than  $\delta$ ,  $\mu$  is zero and when  $t$  is greater than  $\delta$ ,  $\mu$  is a basic periodic function with amplitude  $A$ , frequency  $\omega$  and phase shift  $\phi$ . Therefore, the change point parameter,  $\delta$ , defines the start of combustion and resolving this model parameter allows for the determination of ignition delay. The fraction  $\frac{2\pi}{\lambda}$  is a constant where  $\lambda$  is the sample-rate in Hz ( $\lambda = 200,000$  Hz); hence, the resolved distribution for  $\omega$  is also in Hz. For detailed information on the model parameter priors and model implementation refer to Chapter 6. Individual ignition delay results are assumed to be accurate within 0.2 crank angle degrees.

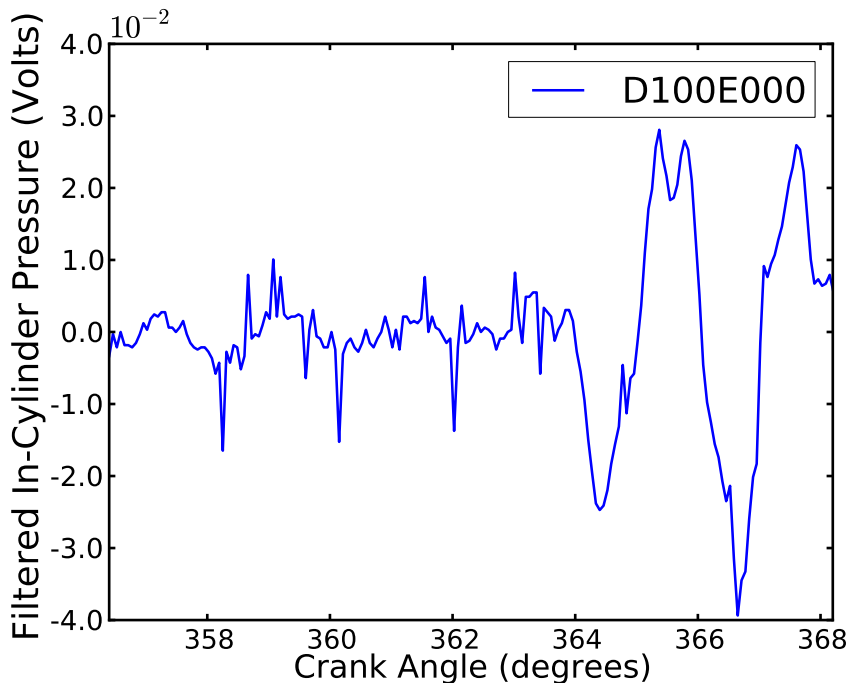


Figure 7.1: Band-pass filtered pressure signal at 2000 rpm, full load on neat diesel fuel

## 7.5 Results

For each of these experiments the data was collected for four minutes after a suitable period of time had elapsed to ensure data integrity—engine stability was determined by monitoring the carbon monoxide output. At 2000 rpm, four minutes of data corresponds to 4000 cycles. Further, in this study to gain a true perspective of the inter-cycle variability all 4000 cycles in each data set were analysed consecutively.

Following the convention set out in Chapter 5, the results here will be grouped by engine load and will be presented beginning with full load. In-cylinder temperature and pressure are dependent upon load; therefore, for an investigation focusing on ignition delay it is sensible to segregate the results by load. Further, ethanol substitutions are done on a percentage energy basis; for example, a 30% ethanol substitution at one load is not equivalent to a 30% ethanol substitution at another load—in this paper the named substitutions are nominal values only, see Table 7.1. The results are shown as kernel density estimates to allow for visual representation of the inter-cycle variability. A kernel density estimate is an estimation of the probability density function, therefore the area under the kernel density estimate is 1.

Load	Nominal ethanol substitution	Diesel reduction	Diesel energy	Ethanol energy	Air fuel ratio (diesel + ethanol)	Air fuel ratio (diesel + ethanol) stoichiometric	Air fuel ratio (ethanol only)*
Full	D100E000%	0%	100%	0%	151.45	84.49	-
	D90E010%	10.3%	92.1%	7.9%	114.24	61.26	345.27
	D080E020%	21.1%	80.0%	20.0%	78.88	43.08	133.74
	D070E030%	29.3%	71.3%	28.7%	64.01	35.43	91.61
	D060E040%	38.1%	66.1%	33.9%	60.96	32.05	81.62
	D050E050%**	51.4%	51.09%	48.91%	47.11	25.03	55.63
Three Quarters	D100E000%	0%	100%	0%	187.81	84.49	-
	D090E010%	9.2%	94.0%	6.0%	153.84	65.70	574.68
	D080E020%	18.1%	81.7%	18.3%	100.306	44.94	178.05
	D070E030%	26.8%	71.1%	28.9%	75.1611	35.26	107.20
	D060E040%	36.2%	65.9%	34.1%	68.86	31.90	91.92
Half	D100E000%	0%	100%	0%	221.85	84.49	-
	D090E010%	6.8%	93.9%	6.1%	171.29	65.42	630.52
	D080E020%	15.9%	68.3%	31.7%	108.92	43.36	185.96
	D070E030%	26.1%	66.8%	33.2%	76.05	32.41	102.53
	D060E040%	32.8%	57.2%	42.8%	60.34	27.51	74.34

\* Air fuel ratio for stoichiometric ethanol combustion = 14.28

\*\* Inferred result

Table 7.1: Ethanol energy substitutions at each test setting

### 7.5.1 Full Load Results

Figure 7.2 shows the diesel injection timing at full load—the diesel injection timing shown in this figure, and subsequent figures, has been corrected for injector lag and is therefore assumed to represent the most plausible actual diesel injection timing (Bodisco et al., 2013b).

Injector lag is the time period between the injector being excited and the actual fuel injection. Of note in this figure is the systematic increase in the diesel injection timing as the ethanol substitution increases, with a marked increase for the 40% substitution case.

Using the statistical model developed in Chapter 6, Equation 7.1, the start of combustion was determined, shown in Figure 7.3. The only truly unimodal distribution is for the neat diesel case, showing a start of combustion consistent at  $\sim 364$  crank-angle degrees. At a 10% ethanol substitution, the distribution is bimodal with modes directly either side of the neat diesel case, with the most predominate mode showing that combustion generally occurs slightly later than under the neat diesel case, the two modes are approximately 0.7 crank-angle degrees apart, less than half a degree each side of the neat diesel case. Following the trend, at the 20% ethanol substitution the most predominate combustion timing occurs later than in both the neat diesel case and the 10% ethanol substitution case. Furthermore, some cycles show a significant decrease in the combustion timing, this decrease is as great as 2 crank-angle degrees lower than the neat diesel case.

Most interestingly, however, are the results for the 30% and the 40% ethanol substitutions. At these high substitutions a significant increase in inter-cycle variability is observed, as is significantly earlier combustion timing. The 30% ethanol substitution case exhibits the greatest amount of inter-cycle variability and shows combustion timings both later and earlier than any other case. Confirming the result obtained in Chapter 5.

The ignition delay, shown in Figure 7.4, for the neat diesel case and the 10% and 20% ethanol substitutions all exhibit the same predominate mode,  $\sim 5$  crank-angle degrees. Evidence that these low substitutions, in general, have only a small effect on ignition delay. However, the bimodal features remain and indicate that combustion occurs earlier in some cycles.

In both the 30% and 40% ethanol substitutions there is evidence of combustion prior to diesel injection (denoted as negative ignition delay in Figure 7.4). The onset of combustion occurs as early as 3 crank-angle degrees before diesel injection in some cycles. However, in most cycles combustion occurs after diesel injection, in the 40% ethanol substitution case the most frequent combustion timing occurs within a crank-angle degree after diesel injection. The timing for the 30% substitution case is fairly uniform across -3 to 6 crank-angle degrees from diesel injection. Moreover, the inter-cycle variability in the 30% and 40% ethanol substitutions are very large when compared with neat diesel—standard deviations 17.7 and 10.8 times higher, respectively.

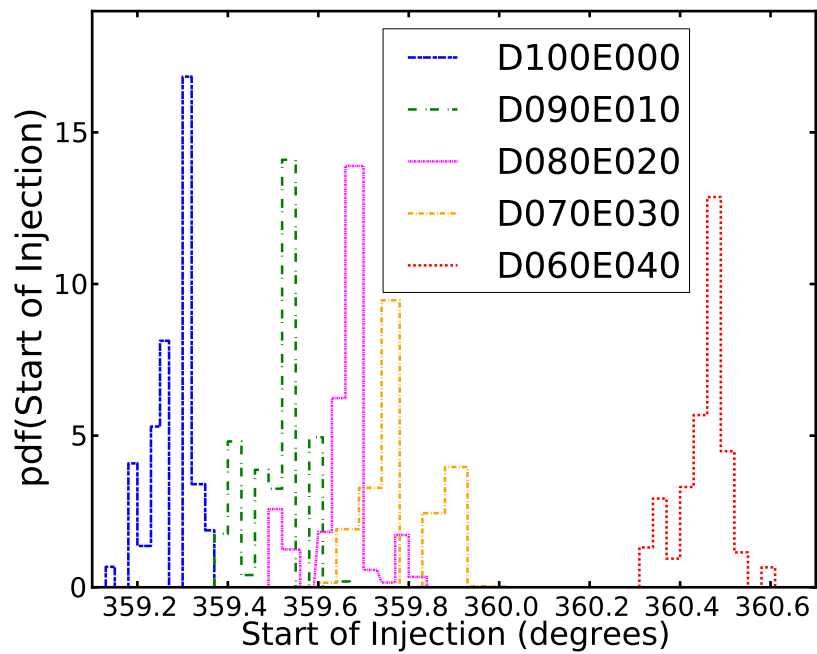


Figure 7.2: Diesel injection timing, full load

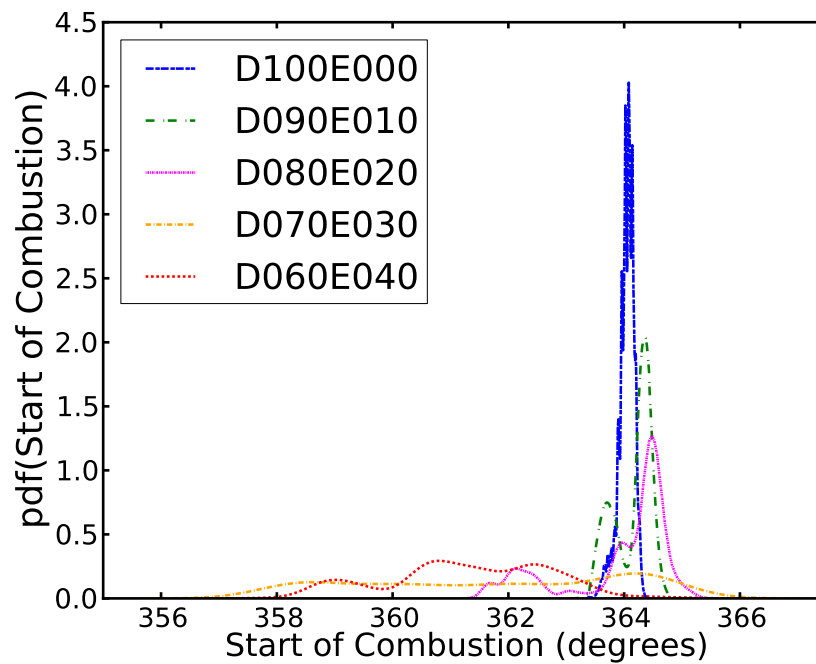


Figure 7.3: Start of combustion, full load

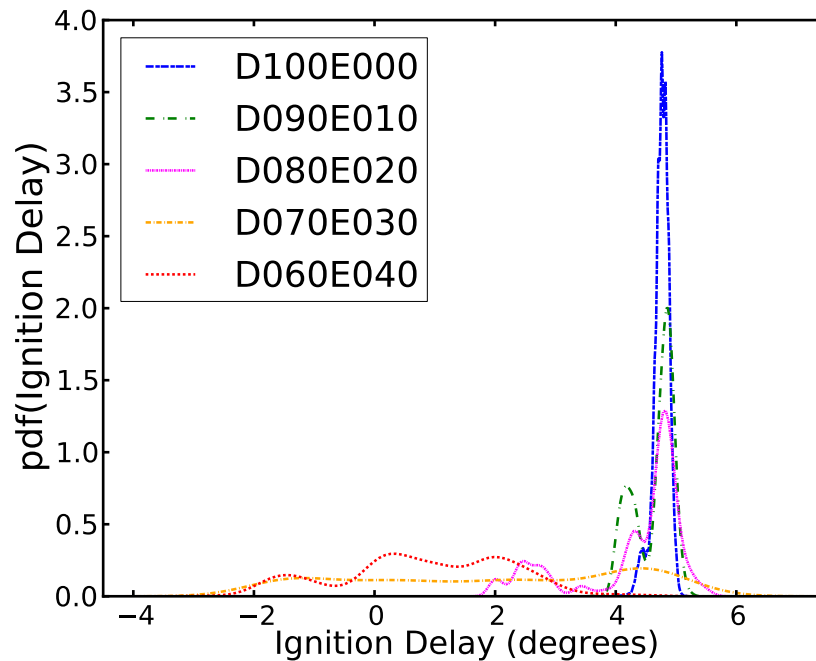


Figure 7.4: Ignition delay, full load

### 7.5.2 Three Quarter Load Results

Much the same as the full load diesel injection timing results, shown in Figure 7.2, the three quarter load diesel injection timing results, shown in Figure 7.5, show a systematic increase in diesel injection timing. However, in this case the difference between each setting is typically much larger, approximately a half a crank-angle degree increase in diesel injection timing per 10% ethanol substitution increase. The most extreme case, 40% ethanol substitution, has a 1.5 crank-angle degree increase in diesel injection timing.

Figure 7.6 shows the start of combustion for three quarter load. A systematic increase in the combustion timing is evident from neat diesel to the 30% ethanol substitution case. The neat diesel and the 10% and 20% ethanol substitution cases all have unimodal distributions and are not showing any significant amount of inter-cycle variability. Whilst the 30% ethanol substitution is predominately showing later combustion than the neat diesel case, there are some cycles where the combustion timing is earlier. Also, the combustion timing distribution for the 30% ethanol substitution is quite multimodal. Much like the 30% and 40% ethanol substitutions at full load, shown in Figure 7.3, the 40% ethanol substitution at three quarter load is exhibiting a large amount of inter-cycle variability with combustion timings ranging from 6 crank-angle degrees earlier to 3 crank-angle degrees later than the neat diesel case.

Most of the increase in combustion timing from the neat diesel case to the 30% ethanol substitution case is explained by the advancing diesel injection timing. This is evident by the



similar ignition delay, shown in Figure 7.7, the predominate mode for all the cases at three quarter load is approximately 5 crank-angle degrees. However, combustion is commencing in the 40% ethanol substitution from as early as 2 degrees before diesel injection and as late as 7 degrees after in a comparatively uniform distribution; however, it is slightly bi-modal.

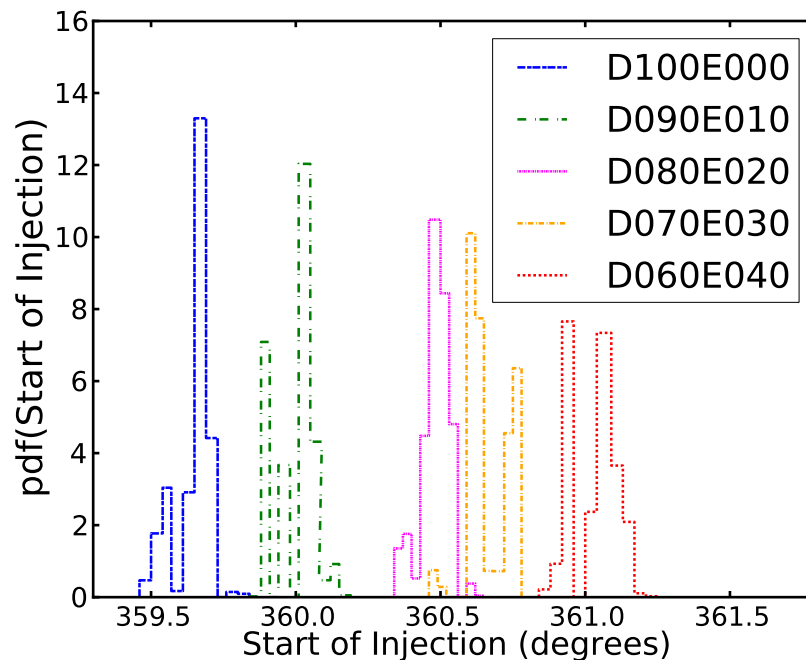


Figure 7.5: Diesel injection timing, three quarter load

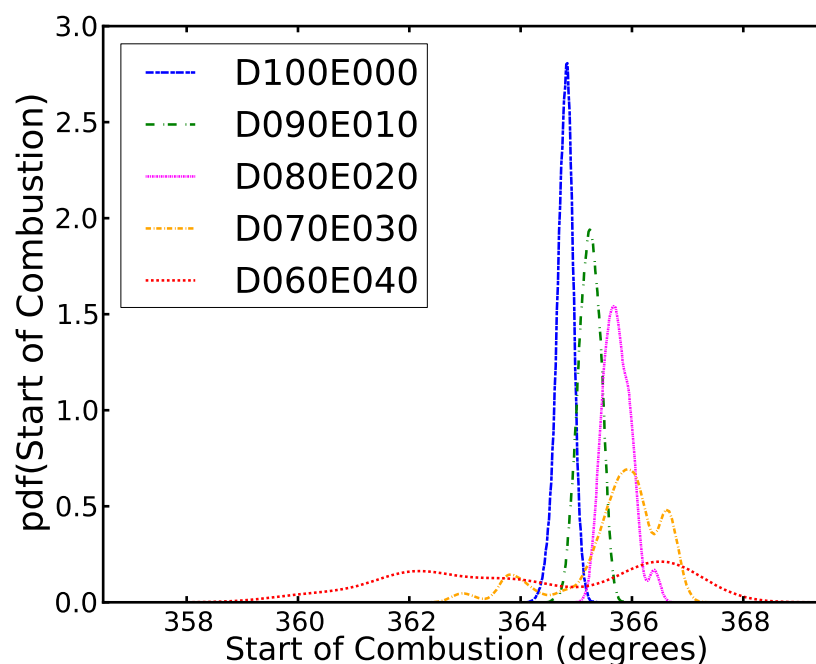


Figure 7.6: Start of combustion, three quarter load

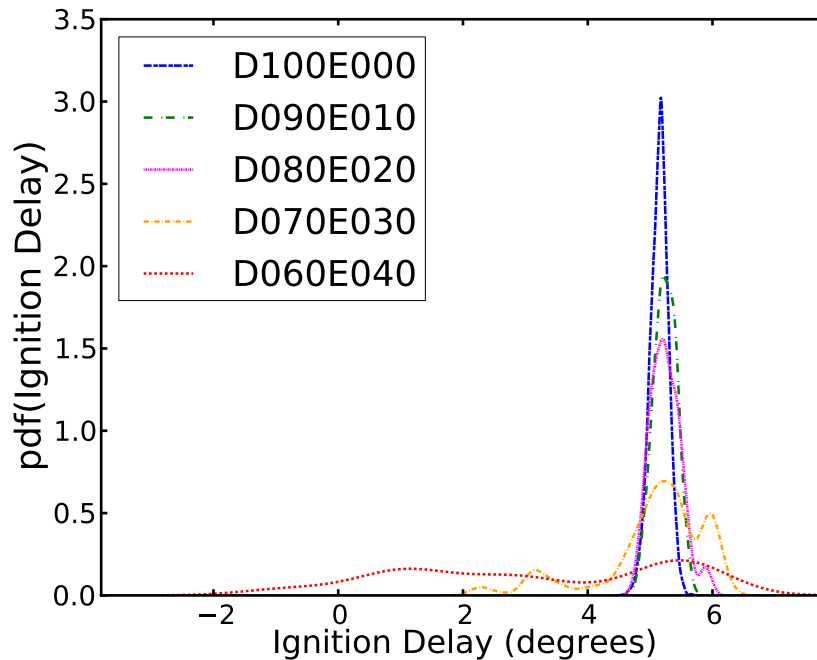


Figure 7.7: Ignition delay, three quarter load

### 7.5.3 Half Load Results

Similar to the full load results, the diesel injection timing at half load follows an approximate 0.2 crank-angle degree increase per 10% ethanol substitution increase, shown in Figure 7.8. Moreover, throughout all of the tested load settings the EMS increased the diesel injection timing as the ethanol substitutions were increased. Also, at each test setting, at all loads and ethanol substitutions, the diesel injection timing had a range of approximately 0.3 crank-angle degrees.

Figure 7.9 shows a systematic advancing of the start of combustion timing with increasing ethanol substitutions. With the exception of the 40% substitution case, the most extreme case, this advanced start of combustion can be explained by the advancing diesel injection timing. The 40% ethanol substitution case is bimodal with the larger peak occurring significantly later, approximately two crank angle degrees, than the lower substitutions. This trend is clearly visible in Figure 7.10. At half load the effect of the 40% ethanol substitution is that of the ‘cooling’ effect described in the literature in older engines (Bodisco and Brown, 2013a).

The difference in inter-cycle variability between the ethanol substitution settings at half load is minimal, except at the 40% substitution case, shown in Figures 7.9 and 7.10. However, at the lower substitutions the inter-cycle variability at half load is greater than that at higher

loads. This is most likely an artifact of the engines' dynamometer stability at this load rather than some underlying phenomena.

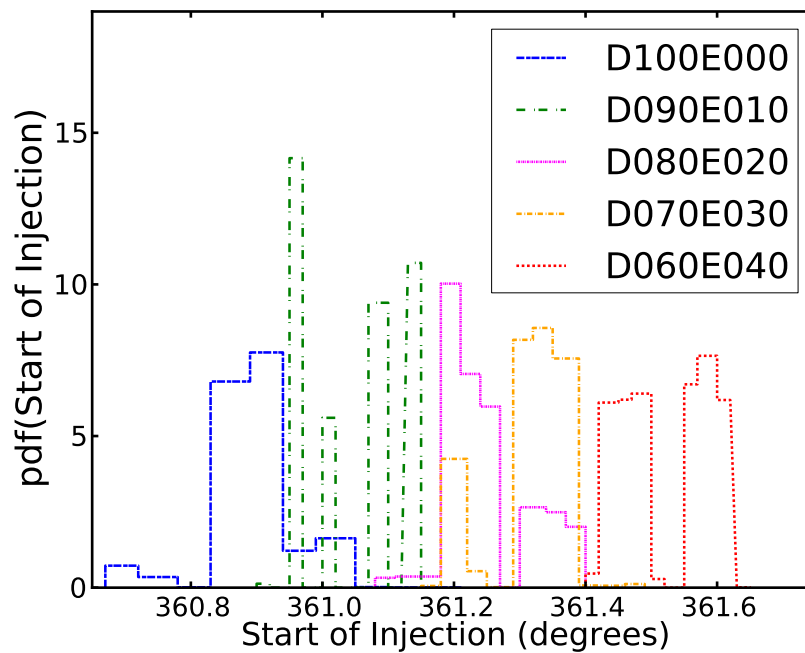


Figure 7.8: Diesel injection timing, half load

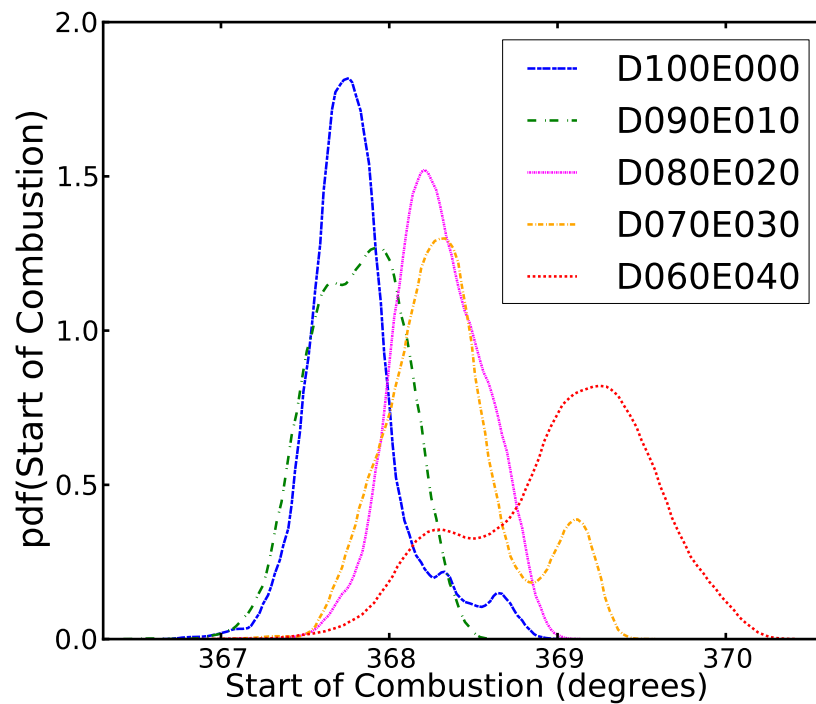


Figure 7.9: Start of combustion, half load

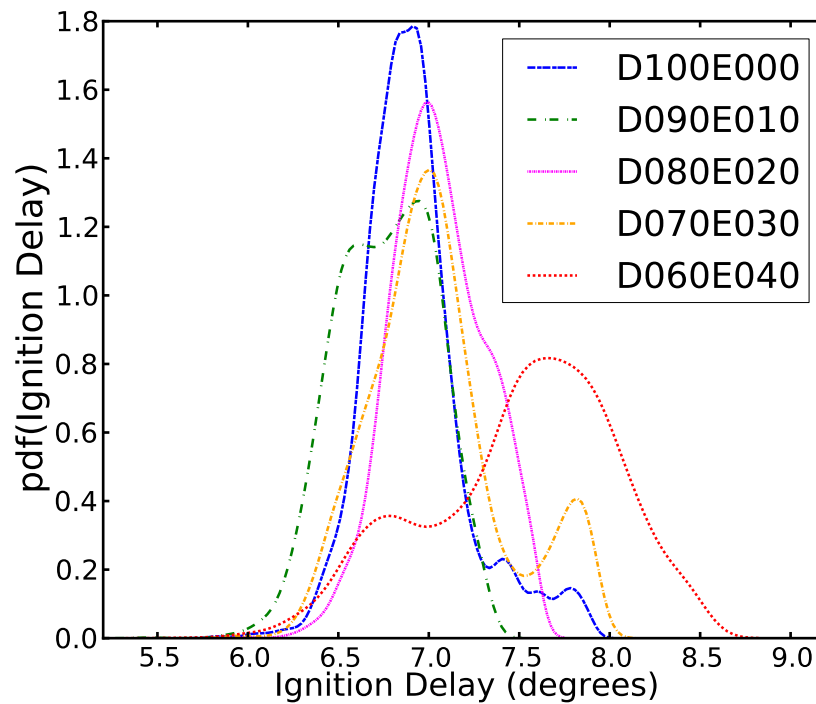


Figure 7.10: Ignition delay, half load

## 7.6 Air to Fuel Ratio

Chapter 5 highlighted the correlation between inter-cycle variability and the absolute air to fuel ratio on a mole basis. For the engine described it was shown that the inter-cycle variability increased with air to fuel ratio's less than 110 and significantly increased with air to fuel ratios less than 80. The parameters of interest in this study were: maximum rate of pressure rise, peak pressure and indicated mean effective pressure.

Figure 7.11 shows the standard deviation of the ignition delay with respect to the absolute air to fuel ratio. A similar trend to that shown in Chapter 5 with maximum rate of pressure rise, peak pressure and indicated mean effective pressure is evident. At air to fuel ratios less than 110 a significant increase in inter-cycle variability is present for the full load and three quarter load cases.

In contrast to the earlier results (Bodisco and Brown, 2013a) where the standard deviation was a better measure of inter-cycle variability, in the case of ignition delay the coefficient of variation (COV) is shown to give more meaningful results. A comparison between the results shown in Figures 7.11 and 7.12 shows that the data collapses better using the COV of ignition delay instead of the standard deviation of ignition delay. This is explained by the opposing trends in ignition delay at the different loads. At full load the ignition delay decreases with increasing ethanol substitutions (decreasing air to fuel ratios); whereas, at

half load the ignition delay increases with increasing ethanol substitutions, shown in Figure 7.13. Furthermore, using the COV corrects the decrease shown in Figure 7.11 at full loads lowest air to fuel ratio. Also at the full load and three quarter load cases, the COV values are very similar with respect to the air to fuel ratios, particularly at air to fuel ratios less than 110 where the engine's performance is impaired from the increase in ethanol substitution. It is also worth noting that at air to fuel ratios greater than 110 that all of the test settings present a similar value for the COV, indicating minimal inter-cycle variability with the introduction of ethanol before a threshold that is well described by the air to fuel ratio.

Figure 7.13 also shows that the ignition delay increases as the engine load decreases. This relationship is primarily a result of a decrease in residual in-cylinder temperature at the time of fuel injection—at lower loads each cycle has less heat release because of a decrease in fuel consumption. The engine under investigation also has variable rail pressure, at lower loads the rail pressure is not as high which will result in increased ignition delay times.

The neat diesel case at half load gives a contradicting result—this is true even with the other in-cylinder parameters explored in Chapter 5. An environment that is too lean can have a negative impact on combustion, causing increases in ignition delay (Saleh, 2011). Therefore, the increase in the inter-cycle variability at half load is most likely attributable to the combustion environment being too lean. Note that the stoichiometric air to fuel ratio (mole basis) for the diesel-only case was 84.49.

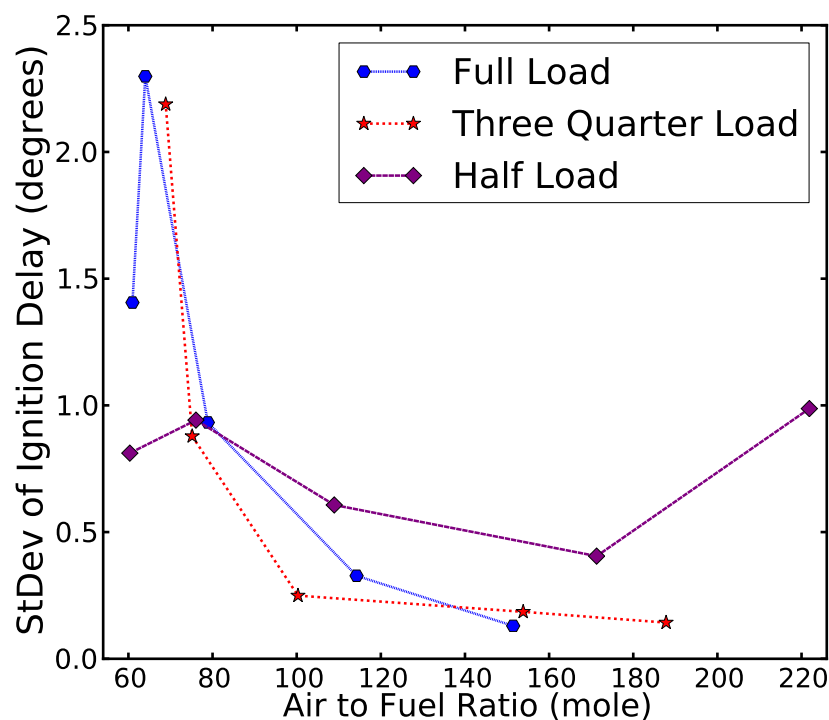


Figure 7.11: Standard Deviation of the Ignition Delay Vs the Air to Fuel Ratio

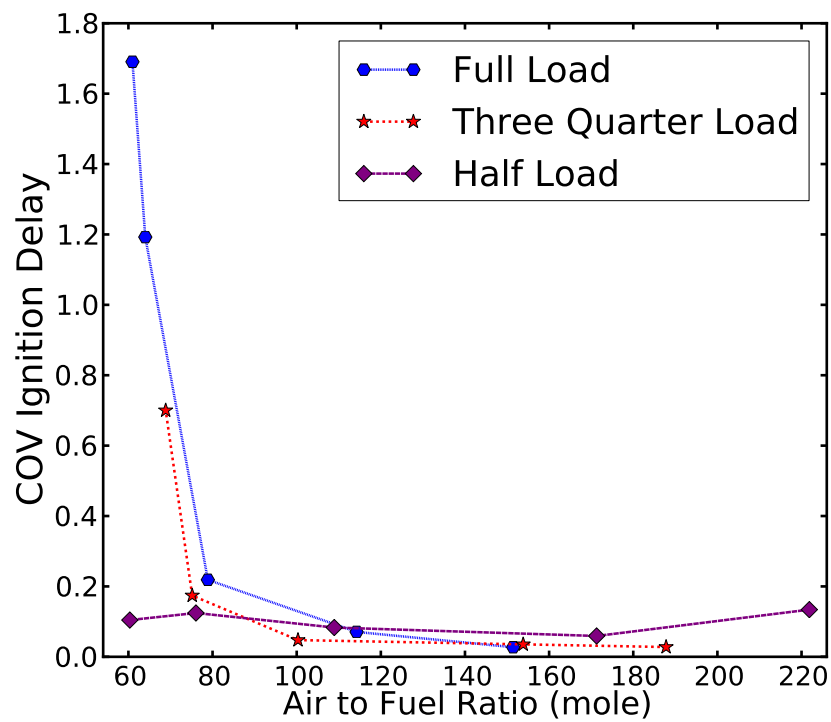


Figure 7.12: Coefficient of Variation of the Ignition Delay Vs the Air to Fuel Ratio

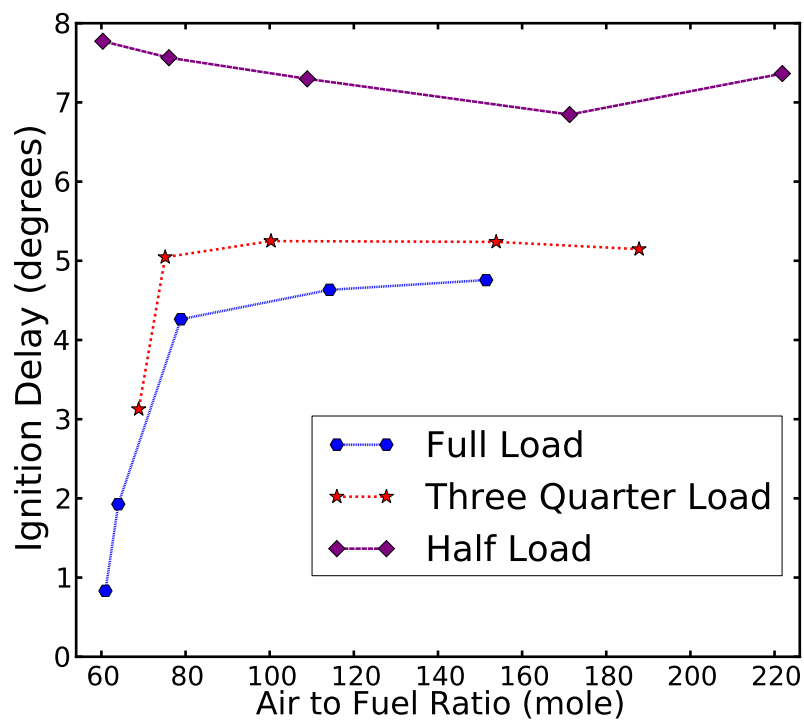


Figure 7.13: Ignition Delay Vs the Air to Fuel Ratio

## 7.7 Numerical Modelling

Presented here are the results of numerical modelling to investigate the sensitivity of ethanol combustion. The numerical simulations are performed with the in-house program HOMREA (HOMogeneous REActor) (Maas and Warnatz, 1988) which allows the simulation of systems such as: homogeneous charge compression ignition (HCCI) engines or rapid compression machines (RCM), taking into account detailed chemical kinetics. Setting initial conditions, stroke length, bore, compression ratio, inlet air temperature, pressure, volume and mixture composition, it is possible to calculate the temporal development of temperature, pressure and the reaction species occurring in the reaction mechanism (Schubert et al., 2005; Warnatz et al., 2001). All simulations are based on the primary reference fuel (PRF) mechanism from Curran et al. (2002)—the mechanism includes more than 1000 species and 10000 reactions. The chosen mechanism also includes next to the primary reference fuels (iso-octane and *n*-heptane), toluene and ethanol. In all simulations, an engine cycle with a homogeneous load is simulated in which:

- an engine volume curve is set as a temporal constraint;
- initial pressures are set to correspond to the absolute experimental boost pressure: 195 kPa (half load), 245 kPa (three quarter load) and 272 kPa (full load); and,
- the parameters of the engine used in the experimental study are set as initial conditions.

Owing to software limitations, phenomena such as heat loss to the walls and piston blow-by have not been taken into account with this simulation. A homogenous air-ethanol mixture can be safely assumed because of the long mixing time as a consequence of injecting the ethanol into the intake manifold directly after the turbocharger into the intake airflow.

In a preliminary investigation into ethanol-only combustion, using the HOMREA software, it was found that a stoichiometric mixture with an initial pressure of 272 kPa and initial temperature of 47°C (to match the experimental conditions at full load) yielded no ignition; however, the software did show evidence that the ethanol was starting to be consumed in chemical reactions. Owing to the relatively high octane and low cetane values of ethanol, ignition can be complicated, or avoided, especially at low inlet air temperatures.

It was shown in Chapter 5, from an experiment that performed ethanol-only combustion, that in a modern diesel engine ethanol was able to auto-ignite. This was achieved by establishing combustion with a 50% by energy ethanol substitution at full load, 2000 rpm and then shutting off the diesel supply to cylinder one and monitoring the in-cylinder pressure. However, the indicated work output from that cylinder (at a constant engine speed of 2000 rpm) progressively dropped off, indicating that there was potentially a sensitivity to the initial temperature in the combustion chamber—assuming that all other initial conditions must have remained the same. To investigate the sensitivity to the initial temperature, the

engine condition has been simulated using a stoichiometric air-ethanol mixture with increasing initial inlet air temperatures. Inlet air temperatures starting at 320 K were tested at 1 K intervals. Figure 7.14 shows the results from 391 K to 400 K. It can clearly be seen that there is great sensitivity to the initial inlet air temperature around the feasible experimental initial conditions. Hence, Figure 7.14 validates the claim made that the negative and significantly shorter ignition delay shown in Chapter 5 and Figures 7.4 and 7.7 was likely impart due to the auto-ignition of ethanol.

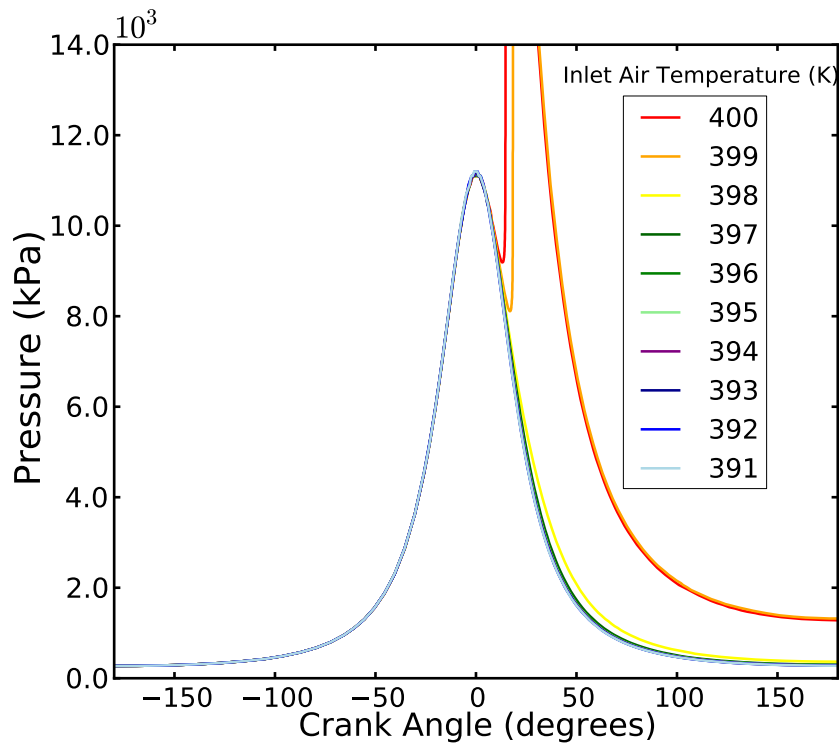


Figure 7.14: Numerical simulation results for increasing inlet air temperatures, simulating the experimental engine condition for full load, 2000 rpm.

A challenge to auto-ignition in a compression ignition engine is the short time period at high pressure and temperature. If ignition has not occurred before the in-cylinder volume, and hence the temperature and pressure, decrease the chemical reactions may freeze. Cancino et al. (2011) have shown that for stoichiometric air-ethanol mixtures and pressures up to 50,000 kPa that temperatures above 850 K are necessary for auto-ignition, especially if the ignition delay time is to be less than 3 ms (comparable to the time taken from  $-18^\circ$  to  $18^\circ$  crank angle at 2000 rpm).

Saisirirat et al. (2009) show a negative temperature coefficient (NTC) region between 630 K and 925 K for *n*-heptane/ethanol blends in a simulated HCCI engine. They concluded from this that the chemical reactions have a greater effect on the ignition delay than the temperature history in HCCI combustion. Similar results have been found in this work, showing



a NTC region of approximately 900–1050 K for *n*-heptane and *n*-heptane/ethanol blends using the HOMREA software, shown in Figure 7.15, using initial conditions representative of the engine under investigation. As a surrogate fuel, *n*-heptane is appropriate because it has a similar cetane number to automotive diesel fuel and hence ignition characteristics (Curran et al., 1998; Saisirirat et al., 2011).

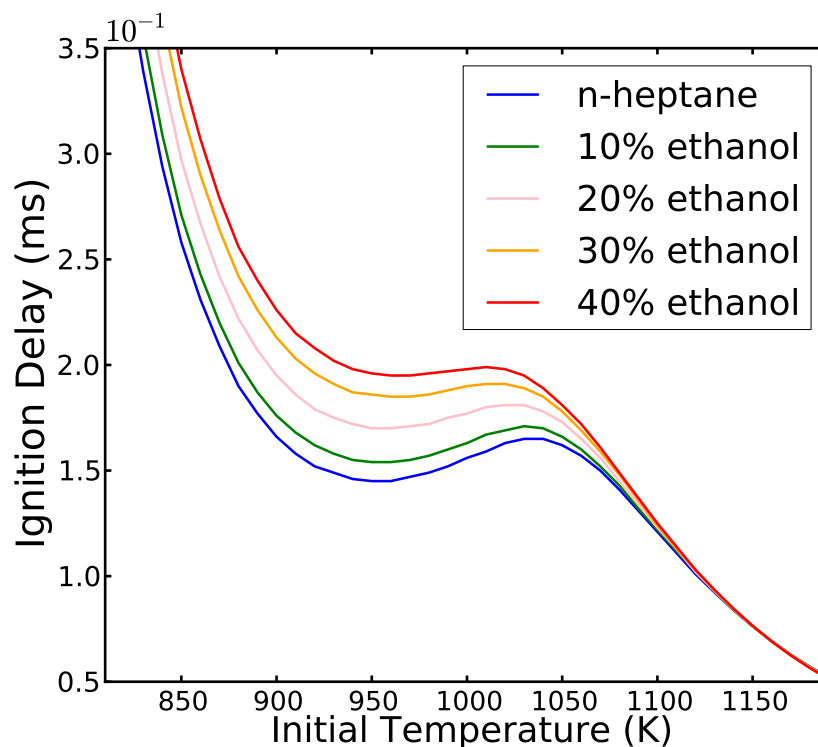


Figure 7.15: Ignition delay times with varying initial temperatures showing the negative temperature coefficient region.

In the experiments, the final in-cylinder temperature, after compression, lies in this NTC region shown with the *n*-heptane/ethanol blends simulations. Therefore at the higher loads, the dominate effect influencing the ignition delay may be that of the increased chemical reactions and not that of the increased in-cylinder temperature. In this case the shorter ignition delay times, with the high substitutions, could be explained by the increased chemical reactions with ethanol prior to the diesel injection.

Complete reaction mechanisms for hydrocarbons normally consist of thousands of elementary reactions. To determine which reactions have the greatest influence on combustion two different methods can be used: sensitivity analysis which identifies the rate limiting reaction steps and reaction flow analysis which determines the characteristic reaction paths (Warnatz et al., 2006).

A sensitivity analysis is conducted to investigate a range of diesel/ethanol ratios corresponding to that of the full load experimental investigation detailed earlier in the paper.

*n*-heptane is used as a representative of hydrocarbon diesel and the simulation is run with pure *n*-heptane and *n*-heptane mixed with different ethanol ratios (10%, 20%, 30% and 40% by energy) to identify the most sensitive reactions and their change with increasing ethanol ratios. The model proceeds with a homogeneous ethanol/air mixture which is compressed until TDC, then mixed with *n*-heptane and the ignition delay time is determined. In the next step, global sensitivity analyses of the *n*-heptane/ethanol mixture at a defined time step (10% before auto-ignition occurs) are made. The result of the sensitivity analyses with respect to the temperature are recorded (see Figure 7.16) for all reactions which do not appear have a negligible sensitivity. The maximum compression temperature decreases a significant amount with increasing ethanol substitutions, from 930 K (only air, D100E000) to 897 K (D060E040).

Figure 7.16 clearly shows that Reactions 8 and 9 are the most sensitive. For low ratios of ethanol, the internal H-abstraction of Hydroperoxy heptyl (Warnatz et al., 2006; Machrafik et al., 2008) in Reaction 8 is predominant. For high ethanol ratios (20% by energy and more) the OH abstraction of Reaction 9 is the most sensitive one. Negative sensitivities indicate that the main emphasis is on the reactant side and positive is that it is on the product side.

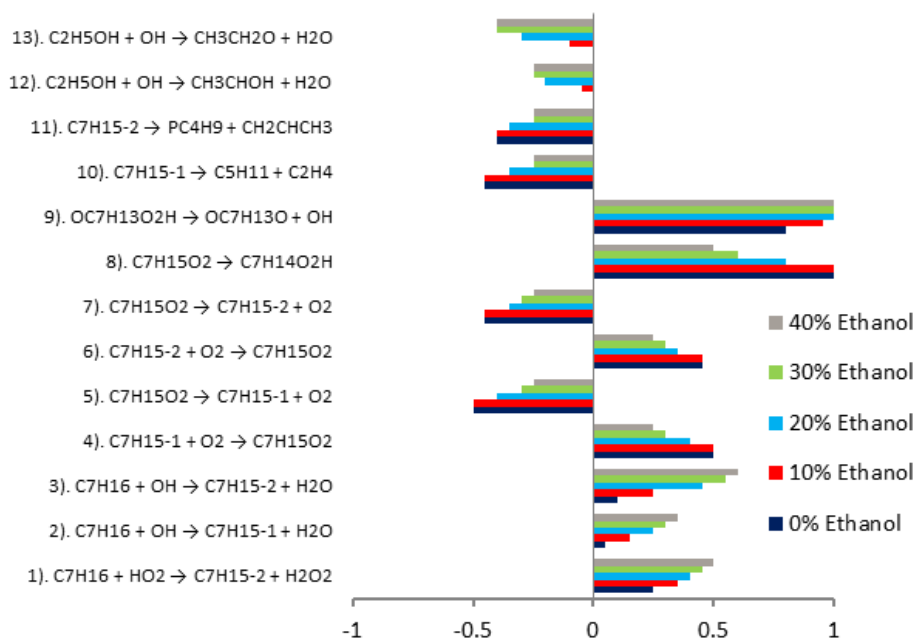


Figure 7.16: Sensitivity analyses of the different fuel compositions at a defined time step before auto-ignition with respect to temperature.

During the compression phase, ethanol starts to decompose and stable intermediates such as formaldehyde and acetaldehyde in addition to radicals such as OH or HO<sub>2</sub> are formed. In Figure 7.17 the ethanol concentration is shown on the left axis and the OH radical on the right axis. The concentration is plotted over the ethanol ratio and represents the value at TDC. It is apparent that the OH-concentration increases very strong until 20% ethanol

substitution by energy and then decreases again almost as quickly as it increased.

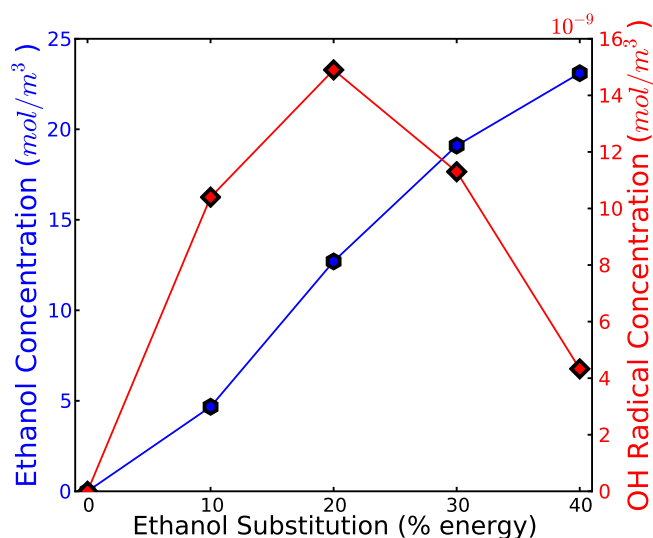


Figure 7.17: Ethanol and OH radical concentration at TDC.

## 7.8 Conclusion

Utilising a new in-cylinder pressure technique to explore ignition delay (Bodisco et al., 2013b), this chapter has explored the effect of ethanol fumigation on a modern heavy-duty common-rail diesel engine. The ignition delay was determined through the use of statistical modelling in a Bayesian framework—this framework allowed the accurate determination of the start of combustion from single consecutive cycles and did not require any differentiation of the in-cylinder pressure signal. This method resolves parameters given in an empirical statistical model using Markov-chain Monte Carlo. In the model employed in this work, a change point parameter, denoted as  $\delta$ , represents the start of combustion.

Experiments were run at 2000 rpm for four minutes (4000 cycles) with ethanol substitutions from 0-40% on an energy basis. To ensure meaningful results, all 4000 cycles were analysed at each engine setting (full, three quarters and half loads). In contrast to the current literature, at full load the ignition delay decreased with increasing ethanol substitutions and evidence of combustion with high ethanol substitutions prior to diesel injection was also shown. Whereas, at half load increasing ethanol substitutions increased the ignition delay. This has been explained by numerical simulation evidence that suggests the engine may be reaching a condition that allows HCCI operation with ethanol and that the ignition delay may have a greater dependence on the chemical reactions, than changes in in-cylinder temperature.

A threshold absolute air to fuel ratio (mole basis) of  $\sim 110$  for consistent operation has been determined from the inter-cycle variability of the ignition delay, a result that agrees

well with previous research (Bodisco and Brown, 2013a) of other in-cylinder parameters. Also shown is the significant increase in ignition delay that occurs at air to fuel ratios less than 80 and the increase in ignition delay when the combustion environment is too lean.

Numerical modelling was employed to explore the sensitivity of the auto-ignition of ethanol in a diesel engine. It was shown that auto-ignition was possible, but that it was sensitive to the inlet air temperature with auto-ignition not occurring prior to inlet air temperatures of 399 K. However, the modelling work did show that ethanol was being consumed in chemical reactions prior to ignition. As a further study, the modelling work explore *n*-heptane and *n*-heptane/ethanol blends across injection temperatures of 800–1200 K. A NTC region was shown to exist from 900–1050 K, indicating that around this region that chemical reactions may have a greater influence on ignition delay than changes in temperature.

An investigation into the sensitivity of the combustion chemistry using numerical modelling showed that under the full load experimental conditions that the chemical reactions at low ethanol substitutions were different to the high (> 20% by energy) ethanol substitutions. It was also shown that OH radical concentration at TDC was the highest at the 20% ethanol substitution.

## 7.9 Acknowledgements

The authors wish to thank Mr. Anthony Morris for assisting with the design of the experimental campaigns and his invaluable technical knowledge and Mr. Noel Hartnett for his work in maintaining the engine for research. Further thanks also to Technologist Mr. Ken McIvor for his assistance in setting up the data acquisition software. This work was undertaken under an Australian Research Council Linkage Grant (LP0775178) in association with Peak3 P/L.

## 7.10 References

- Abu-Qudais, M., Haddad, O., and Qudaisat, M. The effect of alcohol fumigation on diesel engine performance and emissions. *Energy Conversion and Management*, 41(4):389–399, 2000.
- Alperstein, M., Swin, W. B., and Schweitzer, P. H. Fumigation kills smoke, improves diesel performance. *Society of Automotive Engineers*, (SAE Paper 580058), 1958.
- Arnone, L., Manelli, S., Chiatti, G., and Chiavola, O. Engine block vibration measures for time detection of diesel combustion phases. *Society of Automotive Engineers*, (SAE Paper 2009-24-0035), 2009.

- Assanis, D. N., Filipi, Z. S., Fiveland, S. B., and Syrimis, M. A predictive ignition delay correlation under steady-state and transient operation of a direct injection diesel engine. *J. Eng. Gas Turbines Power*, 125(2):450–457, 2003.
- Bo, Z., Weibiao, F., and Jingsong, G. Study of fuel consumption when introducing DME or ethanol into diesel engine. *Fuel*, 85(5-6):778–782, 2006.
- Bodisco, T. and Brown, R. J. Inter-cycle variability of in-cylinder pressure parameters in an ethanol fumigated common rail diesel engine. *Energy*, 52(1):55–65, 2013a.
- Bodisco, T., Low Choy, S., and Brown, R. J. A Bayesian approach to the determination of ignition delay. *Applied Thermal Engineering*, 60(1–2):79–87, 2013b.
- Boretti, A. Advantages of converting diesel engines to run as dual fuel ethanol/diesel. *Applied Thermal Engineering*, 47:1–9, 2012.
- Bruneaux, G. Liquid and vapor spray structure in high-pressure common rail diesel injection. *Atomization and Sprays*, 11(5):533–556, 2001.
- Cancino, L., Fikri, M., Oliveira, A., and Schulz, S. Ignition delay times of ethanol containing multi-component gasoline surrogates: Shock-tube experiments and detailed modeling. *Fuel*, 90:1238–1244, 2011.
- Carlucci, A. P., Chiara, F. F., and Laforgia, D. Block vibration as a way of monitoring the combustion evolution in a direct injection diesel engine. *Society of Automotive Engineers*, (SAE Paper 2006-01-1532), 2006.
- Chauhan, B. S., Kumar, N., Pal, S. S., and Du Jun, Y. Experimental studies on fumigation of ethanol in a small capacity diesel engine. *Energy*, 36(2):1030–1038, 2011.
- Cheng, C. H., Cheung, C. S., Chan, T. L., Lee, S. C., Yao, C. D., and Tsang, K. S. Comparison of emissions of a direct injection diesel engine operating on biodiesel with emulsified and fumigated methanol. *Fuel*, 87(10-11):1870–1879, 2008.
- Chiavola, O., Chiatti, G., Arnone, L., and Manelli, S. Combustion characterization in diesel engines via block vibration analysis. *Society of Automotive Engineers*, (SAE Paper 2010-01-0168), 2010.
- Curran, H., Gaffuri, P., Pitz, W., and Westbrook, C. A comprehensive modeling study of *n*-heptane oxidation. *Combustion and Flame*, 114:149–177, 1998.
- Curran, H., Gaffuri, P., Pitz, W., and Westbrook, C. A comprehensive modeling study of iso-octane oxidation. *Combustion and Flame*, 129(3):253–280, 2002.
- Heywood, J. B. *Internal Combustion Engine Fundamentals*. McGraw-Hill, Inc., 1988.

- Kouremenos, D. A., Rakopoulos, C. D., and Kotsiopoulos, P. Performance and emission characteristics of a diesel engine using supplementary diesel fuel fumigated to the intake air. *Heat Recovery Systems and CHP*, 9(5):457–465, 1989.
- Kouremenos, D. A., Rakopoulos, C. D., and Kotsiopoulos, P. Comparative performance and emission studies for vaporized diesel fuel and gasoline as supplements in swirl-chamber diesel engines. *Energy*, 15(12):1153–1160, 1990.
- Kouremenos, D. A., Rakopoulos, C. D., and Kotsos, K. G. A stochastic-experimental investigation of the cyclic pressure variation in a DI single-cylinder diesel engine. *International Journal of Energy Research*, 16(9):865–877, 1992.
- Maas, U. and Warnatz, J. Ignition processes in hydrogen-oxygen mixtures. *Combustion and Flame*, 74:53–69, 1988.
- Machrafi, H., Cavadias, S., and Gilbert, P. An experimental and numerical analysis of the HCCI auto-ignition process of primary reference fuels, toluene reference fuels and diesel fuel in an engine, varying the engine parameters. *Fuel Processing Technology*, 89:1107–1016, 2008.
- Rakopoulos, C. D. and Kyritsis, D. C. Comparative second-law analysis of internal combustion engine operation for methane, methanol, and dodecane fuels. *Energy*, 26(7):705–722, 2001.
- Rakopoulos, C. D., Rakopoulos, D. C., Giakoumis, E. G., and Dimaratos, A. M. Investigation of the combustion of neat cottonseed oil or its neat bio-diesel in a hsdie diesel engine by experimental heat release and statistical analysis. *Fuel*, 89:3814–3826, 2010.
- Rakopoulos, C.D., Antonopoulos, K.A., and Rakopoulos, D.C. Multi-zone modeling of diesel engine fuel spray development with vegetable oil, bio-diesel or diesel fuels. *Energy Conversion and Management*, 47(11-12):1550–1573, 2006.
- Rakopoulos, D. C. Combustion and emissions of cottonseed oil and its bio-diesel in blends with either *n*-butanol or diethyl ether in HSDI diesel engine. *Fuel*, 2012.
- Rakopoulos, D. C., Rakopoulos, C. D., Giakoumis, E. G., Papagiannakis, R. G., and Kyritsis, D. C. Experimental-stochastic investigation of the combustion cyclic variability in HSDI diesel engine using ethanol-diesel fuel blends. *Fuel*, 87(8-9):1478–1491, 2008.
- Rakopoulos, D. C., Rakopoulos, C. D., Papagiannakis, R. G., and Kyritsis, D. C. Combustion heat release analysis of ethanol or *n*-butanol diesel fuel blends in heavy-duty DI diesel engine. *Fuel*, 90:1855–1867, 2011.

- Reyes, M., Tinaut, F. V., Andres, C., and Perez, A. A method to determine ignition delay times for Diesel surrogate fuels from combustion in a constant volume bomb: Inverse Livengood-Wu method. *Fuel*, 102:289–298, 2012.
- Rodriguez, R., Sierens, R., and Verhelst, S. Ignition delay in a palm oil and rapeseed oil biodiesel fuelled engine and predictive correlations for the ignition delay period. *Fuel*, 90:766–772, 2011.
- Rothamer, D. and Murphy, L. Systematic study of ignition delay for jet fuels and diesel fuel in a heavy-duty diesel engine. *Proceedings of the Combustion Institute*, 2012.
- Sahin, Z. and Durgun, O. High speed direct injection (DI) light-fuel (gasoline) fumigated vehicle diesel engine. *Fuel*, 86(3):388–399, 2007.
- Sahoo, B. B., Sahoo, N., and Saha, U. K. Effect of engine parameters and type of gaseous fuel on the performance of dual-fuel gas diesel engines—a critical review. *Renewable and Sustainable Energy Reviews*, 13(6-7):1151–1184, 2009.
- Saisirirat, P., Foucher, F., Chanchaona, S., and Mounaim-Rouselle, C. A study of *n*-heptane/ethanol HCCI combustion characteristics by experiment and detailed chemical kinetics simulation. *Proceedings of the European Combustion Meeting*, 2009.
- Saisirirat, P., Togbe, C., Chanchaona, S., Foucher, F., Mounaim-Rouselle, C., and Dagaut, P. Auto-ignition and combustion characteristics in HCCI and JSR using 1-butanol/*n*-heptane and ethanol/*n*-heptane blends. *Proceedings of the Combustion Institute*, 33:3007–3014, 2011.
- Saleh, H. E. The preparaton and shock tube investigation of comparative ignition delays using blends of diesel fuel with bio-diesel of cottonseed oil. *Fuel*, 90(1):421–429, 2011.
- Schubert, A., Maiwald, O., Koenig, K., Schiessl, R., and Maas, U. An approach to the efficient modeling of lean premixed HCCI-operation. *Proceedings of the European Combustion Meeting*, 2005.
- Selim, M. Y.E. Effect of engine parameters and gaseous fuel type on the cyclic variability of dual fuel engines. *Fuel*, 84(7-8):961–971, 2005.
- Shafiee, S. and Topal, E. When will fossil fuel reserves be diminished. *Energy Policy*, 37:181–189, 2009.
- Skelton, B. Special issue: Bio-fuels. *Process Safety and Environmental Protection*, 85(5):347–347, 2007.

- Surawski, N. C., Miljevic, B., Roberts, B. A., Modini, R. L., Situ, R., Brown, R. J., Bottle, S. E., and Ristovski, Z. D. Particle emissions, volatility, and toxicity from an ethanol fumigated compression ignition engine. *Environmental Science & Technology*, 44(1):229–235, 2010.
- Surawski, N. C., Ristovski, Z. D., Brown, R. J., and Situ, R. Gaseous and particle emissions from an ethanol fumigated compression ignition engine. *Energy Conversion and Management*, 54(1):145–151, 2012.
- Valentino, G., Corcione, F., Iannuzzi, E., and Serra, S. Experimental study on performance and emissions of a high speed diesel engine fuelled with n-butanol diesel blends under premixed low temperature combustion. *Fuel*, 92:295–307, 2012.
- Warnatz, J., Maas, U., and Dibble, R. *Combustion: Third Edition*. Springer Verlag, 2001.
- Warnatz, J., Dibble, R., and Maas, U. *Combustion – Physical and Chemical Fundamentals, Modeling and Simulation, Experiments, Pollutant Formation: Fourth Edition*. Springer Verlag, 2006.



## Chapter 8

# A Statistical Model for Combustion Resonance from a DI Diesel Engine: with Applications


Timothy Bodisco<sup>a</sup>, Samantha Low Choy<sup>a</sup>, Assaad Masri<sup>b</sup>, Richard J. Brown<sup>a</sup>

<sup>a</sup>Science and Engineering Faculty, Queensland University of Technology, Brisbane QLD, 4001, Australia

<sup>b</sup>Faculty of Engineering and Information Technologies, University of Sydney, Sydney NSW, 2006, Australia


Publication: Mechanical Systems and Signal Processing, under-review.

**Author Contribution**

<b>Contributor</b>	<b>Statement of Contribution</b>
Timothy Bodisco	Conducted the experiments, developed the Bayesian model, performed the data analysis and drafted the manuscript
Signature 	
Samantha Low Choy	Consulted on the development of the Bayesian model and assisted with preparing the manuscript, in particular with the description of the statistical model
Assaad Masri	Contributed knowledge about combustion and ignition
Richard Brown	Supervised the project, aided with the development of the paper and extensively revised the manuscript

**Principal Supervisor Confirmation**

I have sighted email or other correspondence from all co-authors confirming their certifying authorship.

<b>Name</b>	<b>Signature</b>	<b>Date</b>
Associate Professor Richard Brown		

**Abstract**

Introduced in this paper is a Bayesian model for isolating the resonant frequency from combustion chamber resonance. The model shown in this paper focused on characterising the initial rise in the resonant frequency to investigate the rise of in-cylinder bulk temperature associated with combustion. By resolving the model parameters, it is possible to determine: the start of pre-mixed combustion, the start of diffusion combustion, the initial resonant frequency, the resonant frequency as a function of crank angle, the in-cylinder bulk temperature as a function of crank angle and the trapped mass as a function of crank angle. The Bayesian method allows for individual cycles to be examined without cycle-averaging—allowing inter-cycle variability studies. Results are shown for a turbo-charged, common-rail compression ignition engine run at 2000 rpm and full load.

## 8.1 Introduction

Typically researchers interested in frequency content from engine signals (in-cylinder pressure, vibration and acoustic emission) have employed fast Fourier transforms (FFT) (Torregrosa et al., 2004; Payri et al., 2005). However, many authors have used more advanced techniques that are able to capture non-stationary frequencies, such as: finite element analysis (Hickling et al., 1983), Wigner-Ville methods (Stankovic and Bohme, 1999; Ren et al., 1999; Bhat et al., 2012), Hilbert transforms (Ren et al., 1999; Li and Zhang, 2010) and continuous wavelet transforms (Li et al., 2001; Jun and Bing, 2004). Fast Fourier transforms are common practice in basic spectral analysis mostly because of their ease of use and computational efficiency (Duhamel and Vetterli, 1990; Huang et al., 1998). However, many assumptions are made when using them—for example, the assumption of periodic stationary frequencies. Moreover, they can also have low resolution and are sensitive to noise and incomplete data (Bretthorst, 1988a; Jaynes, 1987)—low resolution may make it difficult to resolve close together frequencies (Dou and Hodgson, 1995). In his pioneering 1988 work, Bretthorst (Bretthorst, 1988a) explains that if there is complex phenomena, or evidence of more than a single stationary harmonic frequency, the Fourier method may yield incorrect or misleading results.

In order to avoid any misinterpretation of the data, the method of data analysis should be carefully selected. Under discussion here is the use of Bayesian modelling with the application of isolating features of the combustion resonance in a heavy-duty Cummins, multi-cylinder, turbo-charged, common-rail, direct-injection diesel engine. Of specific interest is the spectral content contained in the in-cylinder pressure signal; in particular the resonant frequency that occurs as a result of combustion. Isolation of this frequency is important as it is related to the speed of sound and hence in-cylinder bulk temperature (Hickling et al., 1983; Bohme and Konig, 1994; Ren et al., 1999; Torregrosa et al., 2004; Payri et al., 2005; Bodisco et al., 2012).

The challenge with isolating the resonant frequency information from the combustion resonance is that the frequency itself is an evolving frequency. In order for a FFT to produce meaningful results, multiple periods of data are required (Gregory and Loredó, 1992)—it is counter-intuitive in an application where a frequency is evolving to simultaneously analyse multiple periods of data. An immediate implication of this is that the FFT method will not be able to capture the transient nature of this signal, even if the data is analysed in *windows* such as those found in a spectrogram—the results would only be able to indicate a trend and likely not provide any definitive information. For a detailed study of combustion resonance, with the goal of isolating the initial resonant frequency (at the onset of combustion) and characterising its rise as the combustion chamber temperature increases, the FFT method will not be satisfactory.

Continuous wavelet transforms (CWT) have emerged in recent years as a solution to the

instantaneous frequency problem and have been used in a wide range of applications (Peng and Chu, 2004; Sen et al., 2008). In comparison to the spectrogram method (using short-time Fourier transforms), the time window is not held constant (Peng and Chu, 2004)—it is advantageous to not have constant time windows, automated or even manual selection of windows may cut useful information (Poggi et al., 2012). Rather, the time window of each wavelet is varied to fit the data; therefore, there is always a trade-off between the frequency and time resolutions. In relation to the application described in this paper, resolving a single evolving frequency with respect to crank-angle, the CWT method has a few key shortcomings. Namely: the results of the CWT are typically presented in scales which need to be estimated as frequencies (causing frequency resolution issues), difficulty with accurate automated feature detection (the results are normally analysed visually, other algorithms would need to be carefully generated to automate the feature extraction), wavelet selection effects the results and whilst the CWT method does isolate evolving frequencies well, there is no indication of uncertainty in the result and resolution issues can make detailed tracking of the frequency of interest difficult.

Other advanced techniques, which are capable of capturing the transient nature of engine signals, have issues of their own. These issues generally relate to undesirable assumptions inherent with the analysis technique, susceptibility to noise, resolution and cross-talk. Statistical modelling, within the Bayesian paradigm, is suggested to overcome these issues. As this is not a *one-size-fits-all* method, using this method is at the expense of simplicity (Bodisco et al., 2012). However, it can be argued that in data analysis more emphasis should be given to scientific interest and less to mathematical convenience (Box and Tiao, 1992). Here a solution is provided to this problem that does require access to computational support.

In the Bayesian paradigm all assumptions must be explicitly stated; this allows the analyst more control compared to other techniques (Bretthorst and Smith, 1989). Whilst this adds complexity, it also ensures that the analyst is completely aware of the problem they are solving and reduces the potential risk of obtaining a misleading result. Moreover, in this application it allows for the analysis to be conducted independently, on individual engine cycles; thereby, allowing for inter-cycle variability studies and effectively removing the need for *ad hoc* methods such as cycle averaging (Bodisco et al., 2012, 2013b).

Some work in this area has already been conducted by Bodisco et al. (2012; 2013b). Much like the current work detailed in this paper, previous work has resolved parameters in an empirical form of the in-cylinder pressure signal. In the original work (Bodisco et al., 2012) model development was shown for isolating the resonant frequency as a function of time in a four-cylinder DI naturally aspirated diesel engine—the model implementation was performed in pre-packaged software, WinBUGS (Spiegelhalter et al., 1999). However, the final model was kept simple and made some assumptions to reduce complexity. One such assumption was that the resonant frequency only decayed—i.e. there was no initial rise in

frequency with the corresponding increase in in-cylinder bulk temperature with combustion. In that work (Bodisco et al., 2012) the final conceptual model was:

$$\begin{aligned} y &= s(t) \sim N(\mu(t), \tau) \\ \mu(t) &= f_1(t) + H(t - \delta) \sum_{i=2}^3 f_i(t) \\ f_i(t) &= A_i e^{-\lambda_i t} \sin(W_i \omega_0 e^{-a_i t} t + \phi) \end{aligned}$$

where  $s(t)$  is the in-cylinder pressure signal with the motoring frequency information removed and is Normally distributed with time-varying mean,  $\mu(t)$ , and precision,  $\tau$ . The time-varying mean consists of the summation of three frequency ( $\omega_i(t) = W_i \omega_0 e^{-a_i t}$ ) and amplitude ( $A_i(t) = A_i e^{-\lambda_i t}$ ) decaying sinusoidal waves with the same phase shift,  $\phi$ , where  $i$  identifies the sinusoidal. In this model, sinusoidals  $i = \{2, 3\}$  are zero until  $t > \delta$  as controlled by the step function  $H(t - \delta)$ .

Extending the previous work (Bodisco et al., 2012), this paper will demonstrate the use of a more sophisticated model to estimate the rise of the resonant frequency in a heavy-duty Cummins, multi-cylinder, turbo-charged, common-rail, direct-injection diesel engine. Accurate isolation of the resonant frequency allows for an in-depth investigation into the combustion temperature. Moreover, as the Bayesian method allows for each cycle to be analysed independently, the inter-cycle variability of this important parameter can be investigated.

Experimental investigation into the combustion bulk temperature using an advanced technique, such as described in this paper, could significantly aid in the analysis of alternative fuels. In diesel engines, emission formation, especially  $\text{NO}_x$ , is temperature dependent (Ramadhas et al., 2005; Frassoldati et al., 2006). The strong dependency between emission and temperature indicates the need for more advanced methods of investigation into in-cylinder bulk temperature and temperature rate rise.

## 8.2 Experimental Configuration

Experiments were conducted at the QUT Biofuel Engine Research Facility (BERF) in August 2012. The engine under investigation is a 5.9  $\ell$  in-line six-cylinder, turbo-charged, common-rail Cummins diesel engine. This is a heavy-duty Euro 3 engine with advanced injection timing (around top dead centre) and variable injection pressure (250–1800 bar). Table 8.1 contains the technical specifications of the engine and data acquisition equipment.

Data was collected at 200 kHz use a Data Translation (DT9832) analogue-to-digital converter and National Instruments LabView. This engine was equipped with a high resolution crank angle sensors (operated at 0.5 crank angle degree resolution) and the data was col-

lected asynchronously. The location of the pressure transducer can be seen in Figure 8.1, an elevation is not shown because the cylinder head is flat. For the experimental results shown, the engine was run at 2000 rpm on neat automotive diesel at full load (760 Nm). A more detailed description of the engine setup can be found in Bodisco and Brown (2013a).

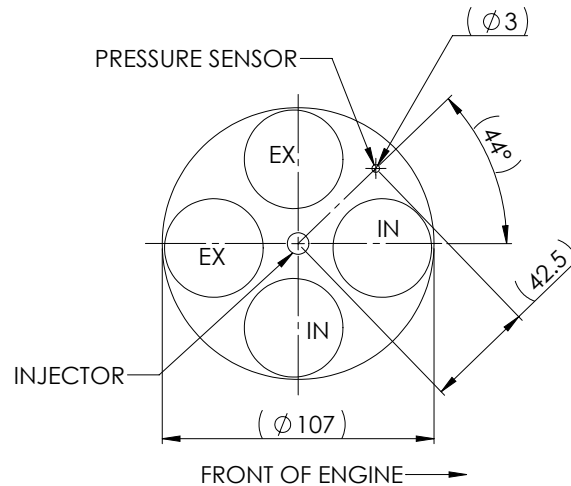


Figure 8.1: Location of in-cylinder pressure transducer

### 8.3 Experimental Data

Using a two channel analogue Krohn-Hite model 3202 filter, the in-cylinder pressure signal was band-pass filtered. The first channel was a high-pass filter with a threshold of 4 kHz and the second a low-pass filter with a threshold of 12 kHz. In contrast to the ignition delay study (Bodisco et al., 2013b), this frequency band was kept very close to the frequencies of interest. This was done to ensure that noise and vibration not directly related to the combustion resonance was minimised. A pilot study was performed with low-pass threshold frequencies ranging from 8-20 kHz. It was determined that this study could be performed at any of these filter settings; however, the band-pass range of 4-12 kHz was chosen because a low-pass threshold at 12 kHz produces a signal free from high frequency noise that qualitatively looks identical to those of lower thresholds.

Using the same acquisition system as described (Bodisco and Brown, 2013a; Bodisco et al., 2013b), the band-pass filtering took place whilst the signal was still in its analogue form; therefore, the dependent scale in Figure 8.2 is in Volts. Isolating the resonant frequency from in-cylinder pressure is scale independent; hence, there is no need to convert the input signal from a voltage signal into a pressure signal. Figure 8.2 shows an example of the band-pass filtered signal—it is taken from the same cycle as the in-cylinder pressure trace shown in Figure 8.3. The rise in signal ( $\sim 362$  degrees crank angle) immediately prior to the start

<b>Engine Specifications</b>	
Make	Cummins ISBe220 31
Capacity	5.9 ℓ
Maximum power	162 kW at 2000 rpm
Maximum torque	820 Nm at 1500 rpm
Number of cylinders	6
Number of valves per cylinder	4
Compression ratio	17.3:1
Bore	102 mm
Stroke length	120 mm
Dynamometer	Electronically controlled water brake dynamometer
Injection system	Common-rail
<b>Data acquisition</b>	
Pressure transducer	Kistler piezoelectric transducer (6053CC60)
Analogue-to-digital converter	Data Translation (DT9832)
Software	National Instruments LabView
Sample rate	200 kHz
Data collected	In-cylinder pressure Band-pass filtered in-cylinder pres- sure (allowing 4-12 kHz) Diesel injection timing Crank-angle rotation information

Table 8.1: Engine and data acquisition specifications

of the combustion resonance ( $\sim 364$  degrees crank angle) evident in Figure 8.2 is attributable to electronic noise from the injection signal and is not part of the combustion resonance.

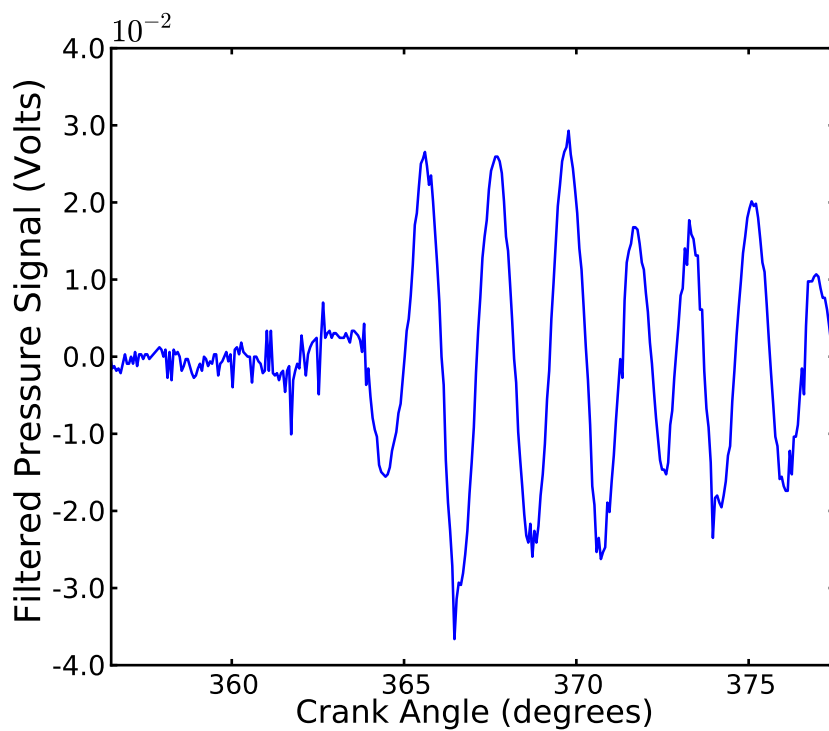


Figure 8.2: Band-pass (4-12 kHz) filtered pressure signal, full load, 2000 rpm

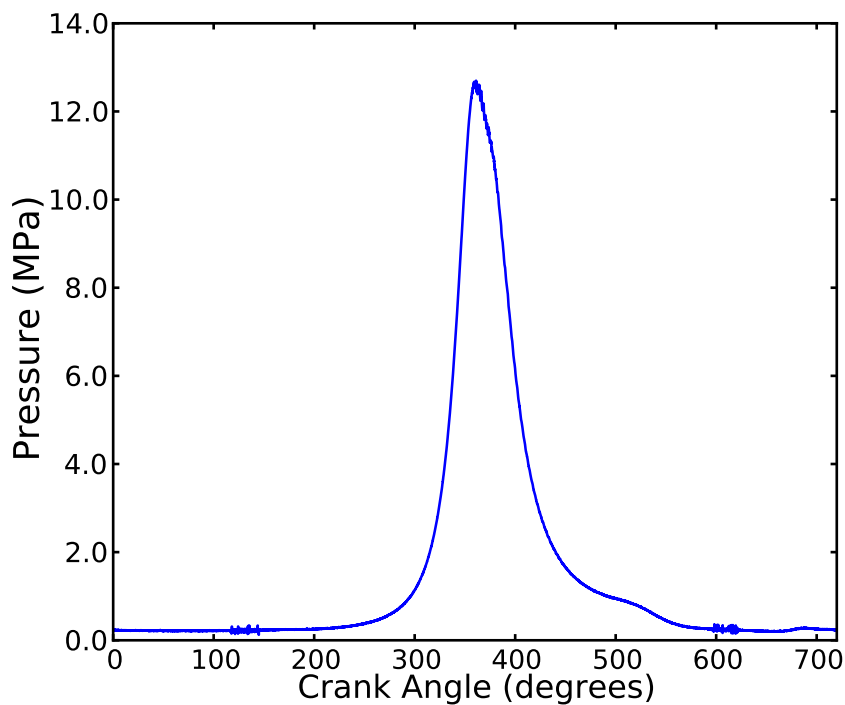


Figure 8.3: Pressure vs crank angle plot, full load, 2000 rpm



## 8.4 Conceptual Model

In Bodisco et al. (2013b), a statistical model was used to determine the start of combustion from in-cylinder pressure. The model employed was:

$$\begin{aligned} y &= s(t) \sim \text{N}(\mu(t), \sigma_y) \\ \mu(t) &= H(t - \delta)A \sin\left(\frac{2\pi}{\lambda}\omega t + \phi\right), \end{aligned} \quad (8.1)$$

where,  $s(t)$ , the band-pass in-cylinder pressure signal (such as the example in Figure 8.2), is assumed to be Normally distributed about some time varying mean,  $\mu(t)$ , with some standard deviation,  $\sigma_y$ —the independent variable  $t$  refers to the discrete time representation in the data related to the sampling rate (200,000 Hz). The change point factor,  $H(t - \delta)$ , switches the signal from Gaussian noise about 0 to a periodic sine wave of frequency  $\omega$ — $\lambda$  is the sample-rate in Hz and  $\phi$  is the phase-shift. Therefore, resolving the change point parameter,  $\delta$ , resolves the start of combustion.

As the work in Bodisco et al. (2013b) was primarily interested in resolving the start of combustion only, the window this analysis took place in was restricted to 200 data points. This allowed for the assumption that the resonance was from a stationary frequency. However, the present work is interested in characterising the rise in the resonant frequency and accurately resolving the initial resonant frequency.

This can be achieved with only slight modification to the model shown in Equation 8.1. In this implementation the amplitude,  $A$ , will be predetermined as a function of time and the resonant frequency,  $\omega$ , will be resolved as a function of time:

$$\begin{aligned} y &= s(t) \sim \text{N}(\mu(t), \sigma_y) \\ \mu(t) &= H(t - \delta_1)A(t) \sin\left(\frac{2\pi}{\lambda}\omega(t)t + \phi\right), \end{aligned} \quad (8.2)$$

The amplitude, henceforth termed the frequency envelope, is predetermined to ensure the frequency is correctly resolved—the other model parameters are conditional on the amplitude. This approach helped improve model fit, and is a generalisation of a common Bayesian computational practice to exploit hierarchical structure where possible. Hence, minimising issues with incorrect frequency envelope estimates artificially reducing the data likelihood estimates. Moreover, having the frequency envelope as a model input saves computation time, by not having to resolve it as part of the modelling process.

The method for resolving the frequency envelope used in this work has been kept simple, as it is not necessary for it to be precise. First, mean-average smoothing was applied to the band-pass filtered in-cylinder signal to reduce the effects of noise. This smoothed signal was then differentiated and the timing of all of the turning points was identified (when the

differentiated signal = 0). The absolute value of the original band-pass filtered in-cylinder signal (before smoothing) at each of the identified turning points was found and the frequency envelope was then determined by linearly interpolating between those points. This method is computationally efficient and consistently yielded a result that adequately fit the frequency envelope.

For modelling the rise of the resonant frequency, a multiplicative model was chosen as it can rise slowly or quickly and the rate only relies on one parameter—multiplicative models can be directly related to exponential models but are computationally easier to work with. Heat release has been modelled previously using an Arrhenius type exponential equation (Nishida and Hiroyasu, 1989; Jung and Assanis, 2001). In an auto-ignition process, such as that found in diesel engines, a pool of radicals needs to be developed as the fuel is gradually heating and mixing with the surrounding oxygen and combustion products. This may occur in a region just downstream of the exit plane of the penetrating spray jet where sufficient vaporisation has taken place. Ignition kernels will form and these would be convected with the flow until they encounter combustible mixtures, which are then ignited leading to extensive heat release. It is notable that in spray jets auto-igniting in a hot vitiated co-flow, the heat release is minimal in the region where the auto-igniting kernels are developed and increases significantly downstream in the jet where the main combustion is taking place (O’Loughlin and Masri, 2011, 2012). Such a scenario is also expected in the diesel engine considered here. Based on this, it is expected that the resonant frequency will rise slowly at the start of pre-mixed combustion (when the auto-igniting kernels are developing) and then more rapidly at the start of diffusion combustion (characterised by extensive heat release), eventually followed by a slow decline. The model used to empirically represent the resonant frequency in this study is:

$$\omega(t) = \begin{cases} \beta_0 & t < \delta_1 \\ \beta_1\omega(t-1) & \delta_1 \leq t < \delta_2 \\ \beta_2\omega(t-1) & \delta_2 \leq t < \delta_3 \\ \beta_3\omega(t-1) & t \geq \delta_3. \end{cases} \quad (8.3)$$

As the empirical relationship given in Equation 8.3 is a multiplicative model,  $\omega(t-1)$  refers to the value of  $\omega$  at the previous data point. The initial resonant frequency is given by  $\beta_0$ , the initial rise in resonant frequency (from pre-mixed combustion) is characterised by  $\beta_1$ , the rapid rise in resonant frequency (from diffusion combustion) by  $\beta_2$  and the decline in the resonant frequency by  $\beta_3$ . Similarly, the model parameter  $\delta_1$  (in both Equations 8.2 and 8.3) corresponds to the start of pre-mixed combustion,  $\delta_2$  corresponds to the start of diffusion combustion and  $\delta_3$  corresponds to the timing at which the resonant frequency begins to decline.

The Bayesian approach will provide marginal posterior plausibilities of each of the parameter values, based on the observed data. This allows the estimation of the model parameters. Bayes theorem states that the posterior distribution is proportional to the product of the likelihood of the data given the parameters and the *priori* distribution of the parameters (Gelman et al., 2003).

$$p(\theta|y) \propto p(y|\theta)p(\theta),$$

for this case,  $\theta = \{\delta_1, \delta_2, \delta_3, \beta_0, \beta_1, \beta_2, \beta_3, \phi, \sigma_y\}$  and  $y_i = s(t_i), t_i \in \mathcal{T}$ .

## 8.5 Priors

In a Bayesian approach, parameter values require specification of prior plausibility. In this analysis, what is known about each model parameter is independent of the other parameters; therefore:

$$p(\theta) = p(\delta_1)p(\delta_2)p(\delta_3)p(\beta_0)p(\beta_1)p(\beta_2)p(\beta_3)p(\phi)p(\sigma_y).$$

The prior distributions should encompass all plausible values a parameter can take (Gelman et al., 2003).

Using the same logic shown in Bodisco et al. (2013b),  $\phi \sim \text{Unif}(0, \pi)$  and  $\beta_0 \sim \text{Unif}(5000, 7000)$ . Combustion is assumed to occur approximately 4.5 degrees after the start of injection (approximately 100 data points after the nominal start of injection) (Bodisco et al., 2013b); therefore,  $\delta_1 \sim \text{N}(100, 25)$ . This prior assumes a 95% probability that combustion will occur in the time period,  $50 \leq t \leq 150$ .

The apparent rate of heat release diagram (generated from cycle-averaged data), shown in Figure 8.4, is constructed using the first law of thermodynamics as described by Heywood (1988) and does not account for heat losses. Examination of Figure 8.4 reveals an inflection at approximately 370 degrees (approx 250 data points after the nominal start of injection). This position corresponds to the timing at which the temperature begins to increase more rapidly. The same prior given to  $\delta_1$  is assigned to  $\delta_2$ ,  $\delta_2 \sim \text{N}(250, 25)$ . Experience and observation of the data, informs the last change point parameter,  $\delta_3$ . A slight decrease in the resonant frequency is typically observed shortly after the rapid rise; therefore,  $\delta_3 \sim \text{N}(300, 25)$ . Additionally,  $\delta_3$  has the restriction that it must be greater than  $\delta_2$ .

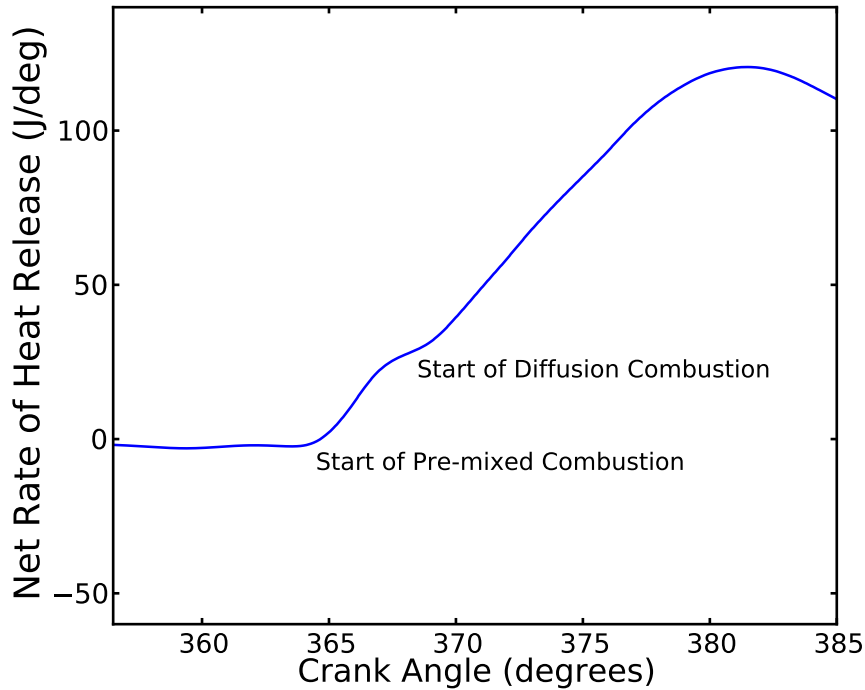


Figure 8.4: Apparent net rate of heat release, full load, 2000 rpm

Of interest in this study is the resonant frequency and how it evolves as a function of time. Because this is a multiplicative model, the parameter values of  $\beta_1$ ,  $\beta_2$  and  $\beta_3$  will be near 1. The model shown in Bodisco et al. (2013b) worked because the start of the combustion resonance can be assumed to be somewhat stationary. Therefore,  $\beta_1$  was assigned a prior that was very close to 1,  $\beta_1 \sim N(1.00005, 0.00005)$ . If a starting frequency of approximately 5700 Hz is assumed and a peak frequency of 6500 Hz, an approximation of  $\beta_2$  of 1.002 can be shown. Therefore,  $\beta_2 \sim N(1.002, 0.001)$ . Both  $\beta_1$  and  $\beta_2$  were restricted to be greater than 1.

Knowledge of  $\beta_3$  is more difficult to predict. Unlike  $\beta_1$  and  $\beta_2$ , where it can be assumed they are greater 1,  $\beta_3$  could potentially represent the beginning of the decline in the resonant frequency or it could represent the slowing down of the evolution. The prior selected has assumed a decline, but has not enforced it,  $\beta_3 \sim N(0.9999, 0.001)$ .

The model parameter  $\sigma_y$  is there to fit the Gaussian noise in the data. In Bayesian modelling it is common to consider the precision ( $\tau = \frac{1}{\sigma_y^2}$ ), rather than the standard deviation (Gelman et al., 2003). In a state of ignorance, this parameter is often assigned an uninformative Gamma prior,  $\tau \sim \text{Gamma}(0.01, 0.01)$ .

## 8.6 Model Implementation

Estimation of the posterior distributions of the model parameters is performed using a standard Bayesian computational approach based on simulation. The Metropolis-Hastings algorithm, a special case of the Markov-chain Monte Carlo (MCMC) algorithm (Gelman et al., 2003), has been used in this analysis as described in Bodisco et al. (2013b)—this section is a summary from the more detailed explanation in Bodisco et al. (2013b). In this implementation candidate parameters,  $\theta^*$ , are sampled from a proposal distribution dependent on the current parameter value,  $\theta^* \sim R(\theta)$ . For the parameters,  $\{\beta_0, \beta_1, \beta_2, \beta_3, \phi, \sigma_y\}$ :

$$\theta^* \sim N(\theta^{m-1}, \sigma_\theta)$$

and for the parameters,  $\{\delta_1, \delta_2, \delta_3\}$ :

$$\theta^* \sim \text{Unif}(\theta^{m-1} - n, \theta^{m-1} + n)$$

where,  $\sigma_\theta$  and  $n$  are tuning parameters which determine the potential range of the ‘walk’ at each iteration and  $m = 1, \dots, M$  denotes the  $m^{\text{th}}$  MCMC simulation from the chain. Therefore,

$$\theta^m = \begin{cases} \theta^* & \text{with probability } \alpha \\ \theta^{m-1} & \text{otherwise.} \end{cases}$$

where,

$$\alpha = \min \left\{ 1, \frac{R(\theta^*)}{R(\theta^{m-1})} \frac{p(\theta^*|\cdot)}{p(\theta^{m-1}|\cdot)} \right\}$$

and  $\cdot$  denotes the full set of parameters omitting the parameter of interest, here generically denoted as  $\theta$ .

The results from the model had a tendency to not correctly resolve the start of combustion,  $\delta_1$ . This issue occurred because of the predetermined frequency envelope causing issues with convergence. Potential solutions to this issue included: modelling the frequency envelope as part of the model instead of having it as an input parameter, developing a hierarchical model or predetermining the start of combustion and having it as an input parameter. Using the model described in Bodisco et al. (2013b) to determine the start of combustion,  $\delta_1$ , and then using  $\delta_1$  as an input parameter (non-updatable) was determined as the most computational efficient and reliable solution. Moreover, using the predetermined frequency envelope ensures that once the frequency has converged to the correct solution that the model will fit the data well and is therefore an important input parameter and removing it could result in convergence issues and greatly increased computation time.

## 8.7 Simulation Results

Figure 8.5 shows the model fit to the signal shown in Figure 8.2. It can be seen by observation, or by the residual plot shown in Figure 8.6, that the model has fit the data very well—indicating accurate isolation of the resonant frequency. This observation is made because the residual plot shows no distinctive features (i.e. it appears to be noise only without any repeating features). Table 8.2 shows the mean and standard deviation for each model parameters prior and posterior distributions.

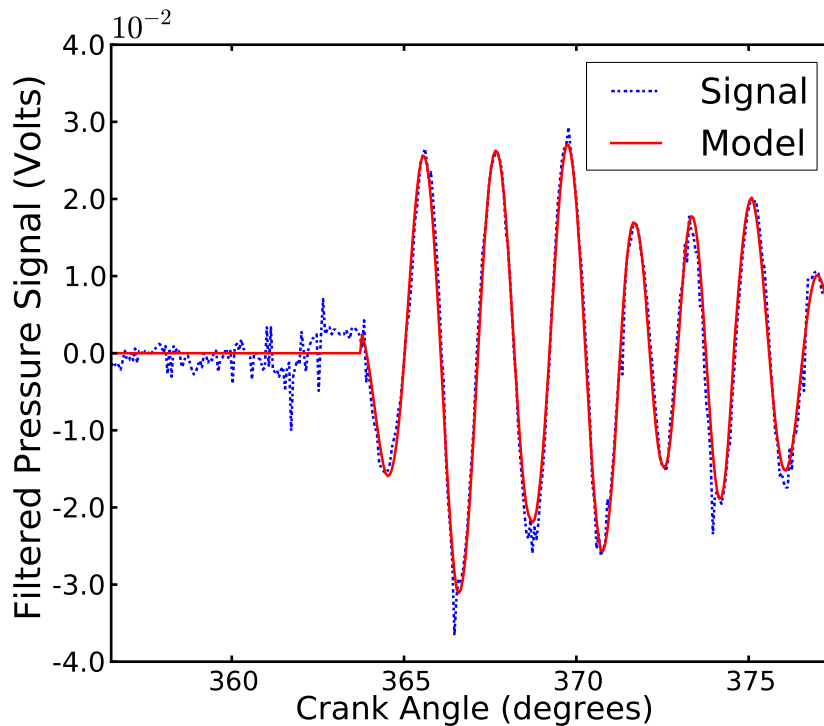


Figure 8.5: Model fit to signal shown in Figure 8.2

Parameter	Prior		Posterior	
	Mean	Standard Deviation	Mean	Standard Deviation
$\beta_1$	1.00005	0.00005	1.00023	$3.204 \times 10^{-5}$
$\beta_2$	1.002	0.001	1.00101	$2.869 \times 10^{-5}$
$\beta_3$	1.9999	0.001	1.00004	$3.381 \times 10^{-5}$
$\delta_1$	100 (362.3 degrees)	25 (1.5 degrees)	122 (363.7 degrees)	4 (0.3 degrees)
$\delta_2$	250 (371.5 degrees)	25 (1.5 degrees)	242 (371.0 degrees)	2 (0.2 degrees)
$\delta_3$	300 (374.6 degrees)	25 (1.5 degrees)	297 (374.5 degrees)	1 (0.1 degrees)
	Lower Bound	Upper Bound	Mean	Standard Deviation
$\beta_0$	5000	7000	5502	43
$\phi$	0	$\pi$	0.27	0.18

Table 8.2: Model parameter prior and posterior distributions

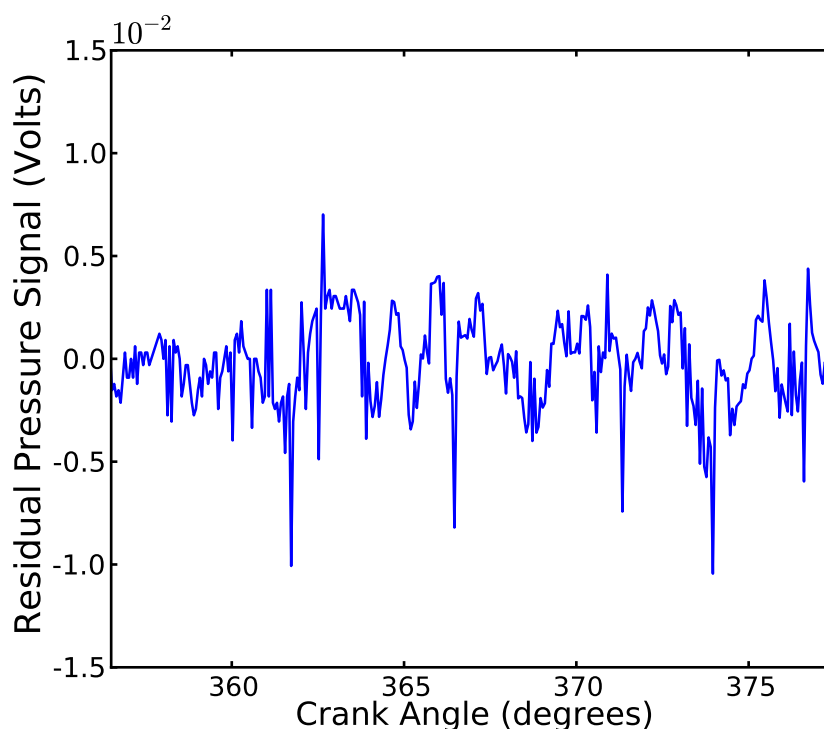


Figure 8.6: Residual plot showing that subtraction of the fitted model from the signal shown in Figures 8.2 and 8.5

Hence, as a function of crank angle, the resonant frequency of the signal shown in Figure 8.2, is modelled in Figure 8.7. For comparison to the continuous wavelet transform method, Figure 8.8 shows the corresponding result from a continuous wavelet analysis using 256

scales. It can be seen that both methods have isolated the frequency information well; however, owing to the resolution in the Bayesian method, results in Figure 8.7 allow for the determination of the start of pre-mixed and diffusion combustion and a greater ability to track the evolution of the frequency as a function of crank angle (or time). Some key features, however, can be noted in Figure 8.8 that correspond to Figure 8.7. Namely: the general range of the frequency is similar, the start of pre-mixed combustion can be seen at approximately 364 degrees and a sharper rise in frequency is also evident at approximately 371 degrees. From 500 consecutive engine cycles, Figure 8.9 shows the distribution of the initial resonant frequency,  $\beta_0$ .

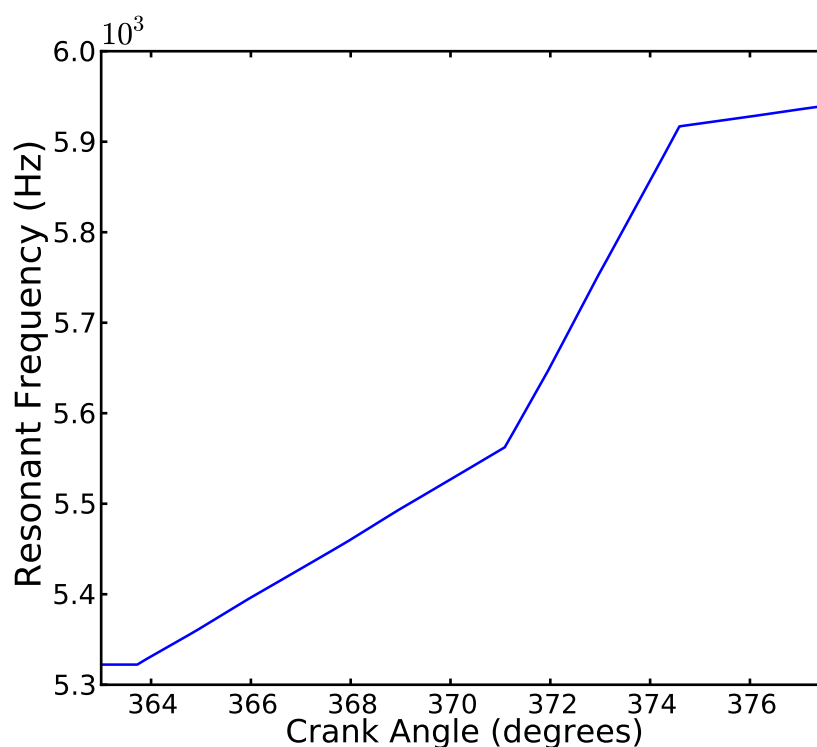


Figure 8.7: Example resonant frequency with respect to crank angle from model fit shown in Figure 8.5



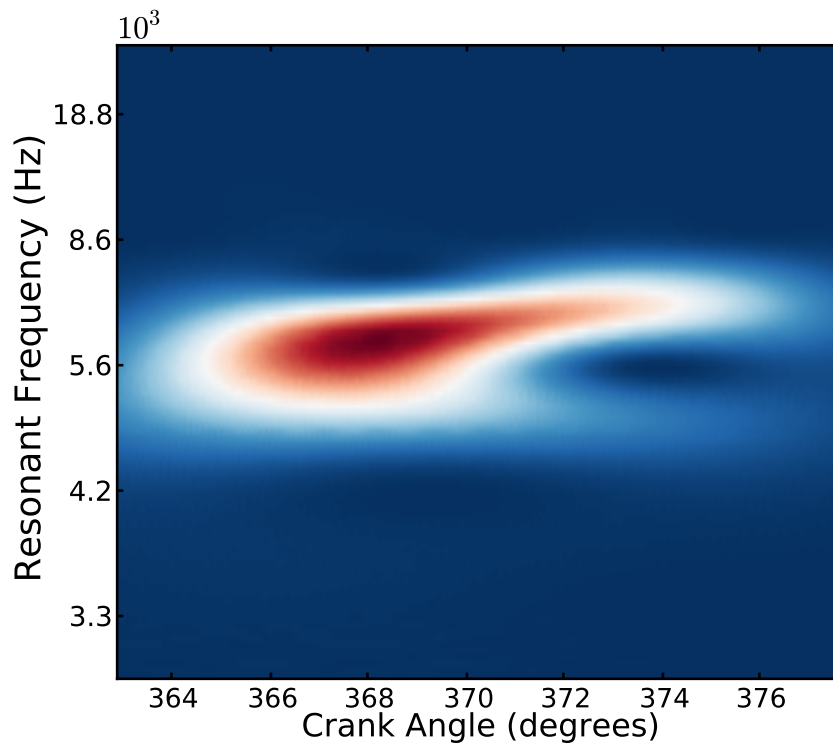


Figure 8.8: Resonant frequency of the signal shown in Figure 8.2 isolated using a continuous wavelet transform

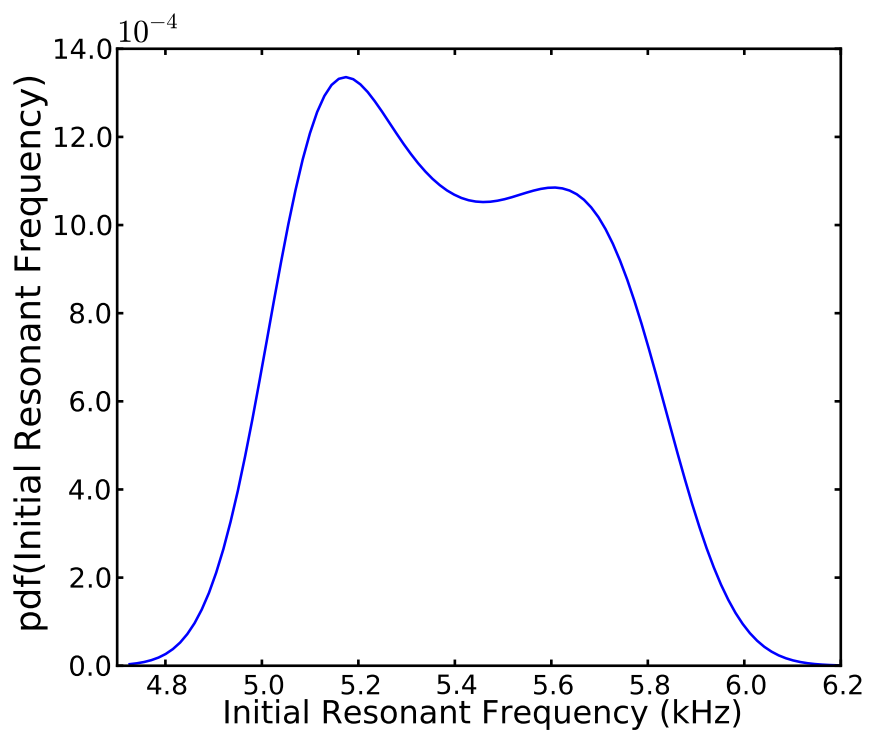


Figure 8.9: Distribution of the initial resonant frequency over 500 consecutive cycles

Although determined as an input parameter from the start of combustion model (Bodisco et al., 2013b), Figures 8.10 and 8.11 show the distribution of the start of combustion and the corresponding ignition delay. The model parameter  $\delta_2$  isolates the start of diffusion combustion—characterised by an increase in the rate of temperature rise. Figure 8.12 shows the distribution of the start of diffusion combustion. This timing matches well with an inflection seen in the net rate of heat release, shown in Figure 8.4. Corresponding to these change point parameters, Figure 8.13 shows the distribution of the multiplicative parameter  $\beta_1$  which corresponds to the initial rise in temperature during pre-mixed combustion and Figure 8.13 shows distribution of the multiplicative parameter  $\beta_2$  which corresponds to the more rapid rise in temperature from diffusion combustion. The results for the multiplicative parameter  $\beta_3$  were slightly different to expected. When the model was developed it was assumed that at the end of the diffusion combustion period the in-cylinder bulk temperature (and hence resonant frequency) would start decreasing. However, the results shown in Figure 8.15 indicated that this has only shown to be true on some cycles. On the majority of cycles, Figure 8.15 indicates that the rise in resonant frequency is slowed or perhaps stationary for a period before it decreases.

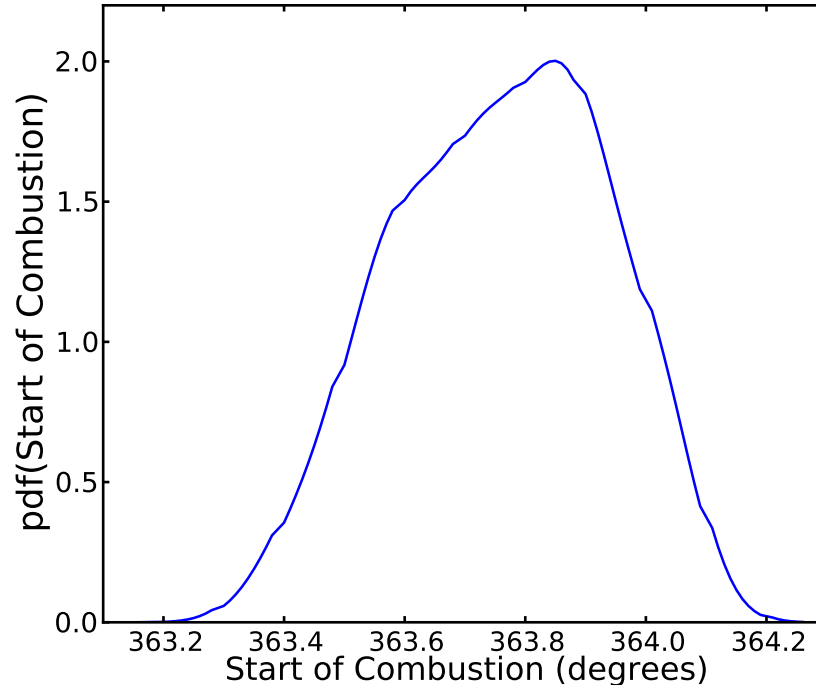


Figure 8.10: Distribution of the start of pre-mixed combustion over 500 consecutive cycles

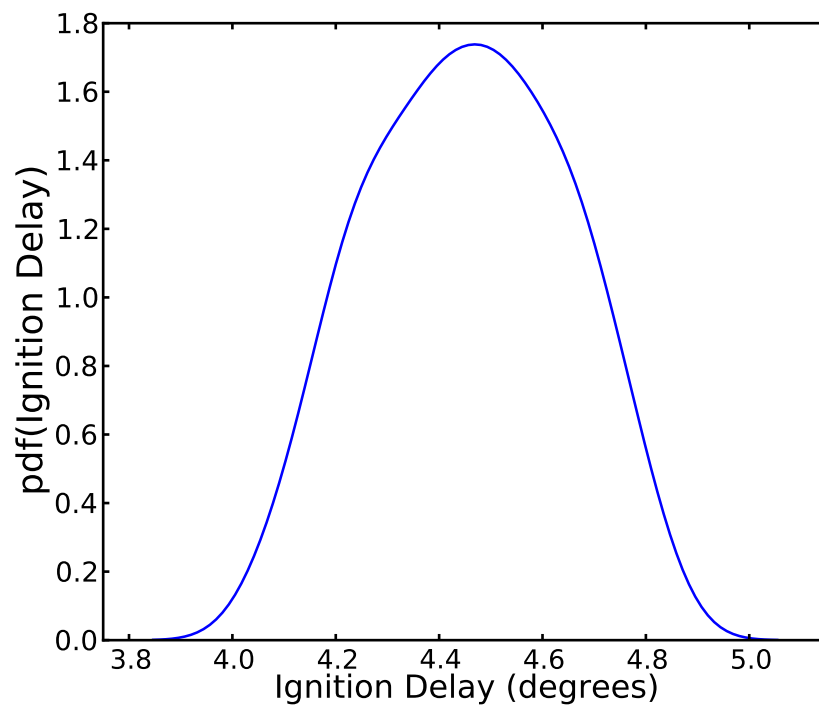


Figure 8.11: Distribution of the ignition delay over 500 consecutive cycles

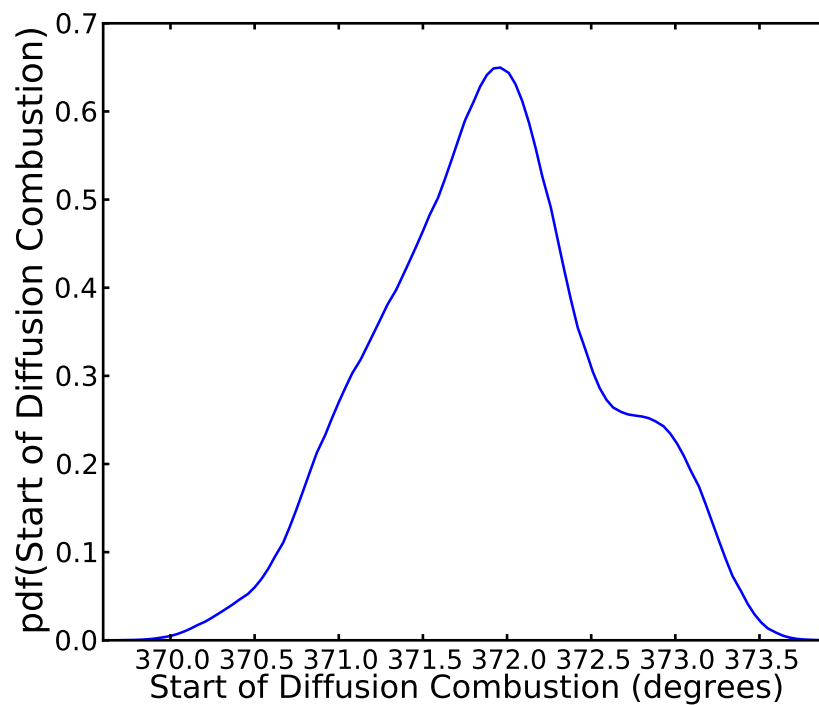


Figure 8.12: Distribution of the start of diffusion combustion over 500 consecutive cycles

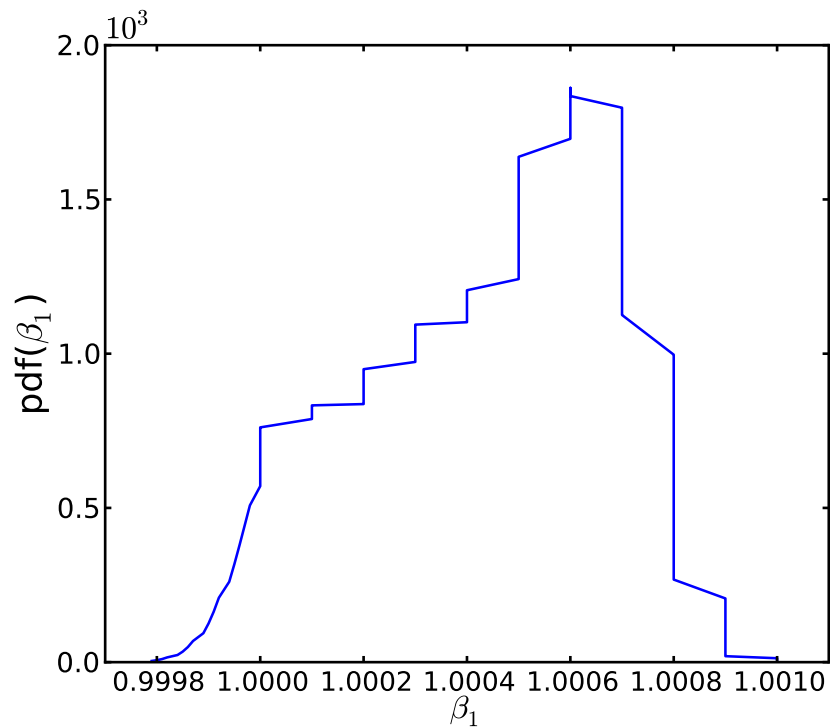


Figure 8.13: Distribution of the initial multiplicative parameter,  $\beta_1$ , over 500 consecutive cycles

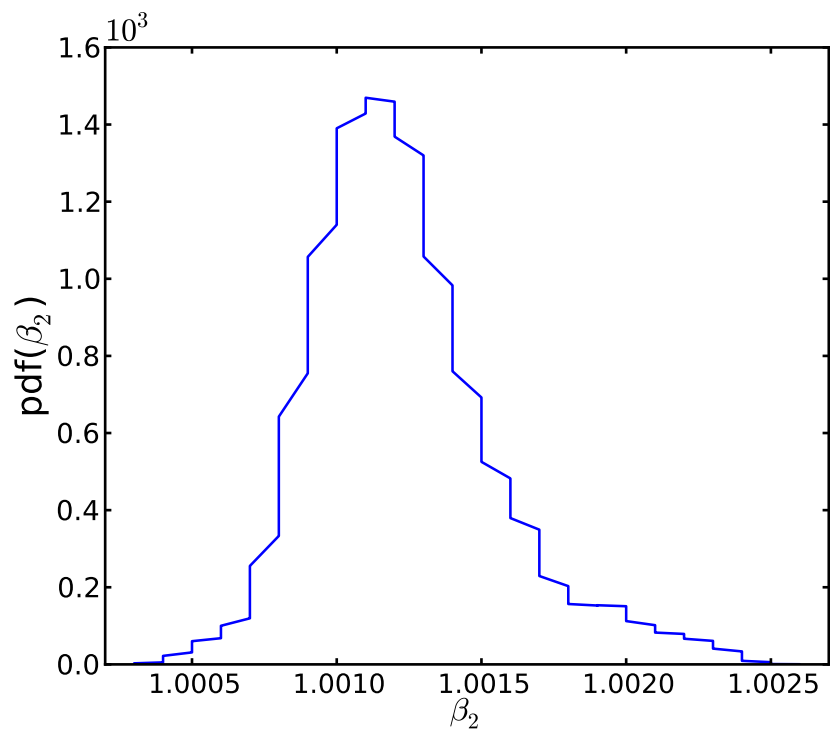


Figure 8.14: Distribution of the diffusion combustion multiplicative parameter,  $\beta_2$ , over 500 consecutive cycles

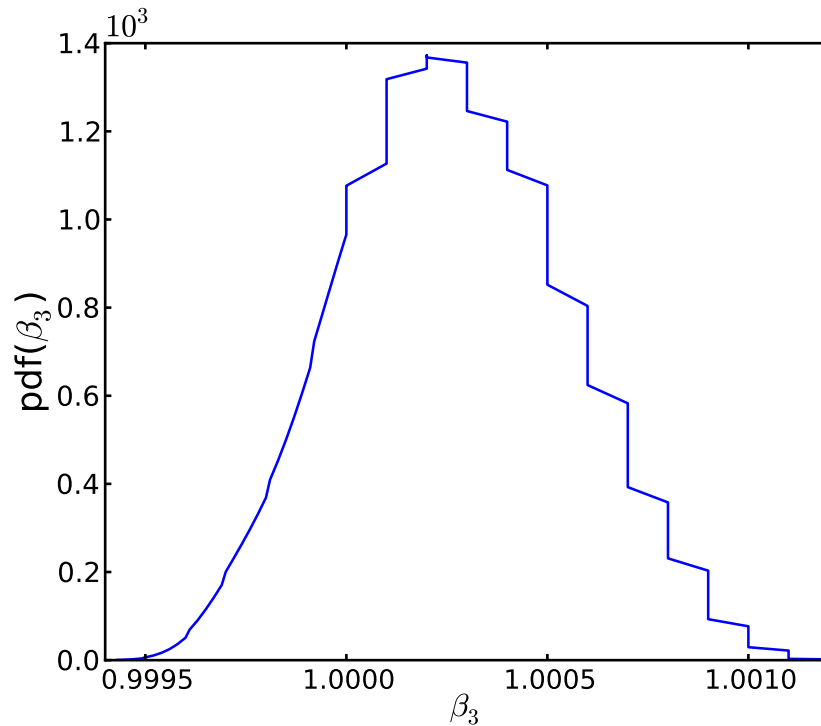


Figure 8.15: Distribution of the reduction in combustion intensity parameter,  $\beta_3$ , over 500 consecutive cycles

## 8.8 Application

A key feature of using a Bayesian modelling technique is being able to analyse individual cycles. Therefore, the analyst is able to investigate the inter-cycle variability of not only the model parameters, as shown in Section 8.7, but also the inter-cycle variability of the operating characteristics derived from the model results. Potential applications for these results are determining the in-cylinder bulk temperature and the trapped mass as a function of time (Hickling et al., 1983; Bodisco et al., 2012).

A nominal in-cylinder bulk temperature can be determined from the relationship to the speed of sound by assuming ideal behaviour and uniform gas composition in the combustion chamber—whilst these are not true assumptions, it does allow for an interesting investigation into the bulk temperature in the combustion chamber. The speed of sound,  $c$ , is related to the resonant frequency,  $f$ , by the following relationship (Hickling et al., 1983):

$$c = \frac{fB}{\alpha_{nm}} \quad (8.4)$$

where,  $B$  is the cylinder bore and  $\alpha_{nm}$  is a non-dimensional value associated with the frequency mode—in this study the resonant frequency represents the first circumferential frequency; therefore,  $\alpha_{nm} = 0.5861$  (Hickling et al., 1983; Bodisco et al., 2012). The speed of

sound is also related to temperature (Hickling et al., 1983):

$$c^2 = \gamma RT \quad (8.5)$$

where,  $\gamma$  is the ratio of specific heats,  $R$  is the characteristic gas constant and  $T$  is the in-cylinder bulk temperature. Combining Equations 8.4 and 8.5:

$$T = \frac{1}{\gamma R} \left( \frac{fB}{\alpha_{nm}} \right)^2 \quad (8.6)$$

and relating Equation 8.6 to the ideal gas law allows the determination of the trapped mass,  $m$ , as a function of time:

$$m(t) = \gamma P(t)V(t) \left( \frac{\alpha_{nm}}{f(t)B} \right)^2 \quad (8.7)$$

Owing to potential imperfections in the combustion chamber walls and design features that deviate from a perfectly round profile, the in-cylinder bulk temperature and therefore the trapped mass determined from Equations 8.6 and 8.7, respectively, will not be correct (Randall, 1987). However, a correction factor can be determined from knowledge of the trapped mass in the cylinder at the onset of combustion. In the engine setup utilised in this experiment in-take air and fuel flows are measured. The nominal distribution of trapped mass (at the onset of combustion), determined from Equation 8.7, is shown in Figure 8.16. Under the assumption that at the start of combustion there has been negligible blow-by, a correction factor can be found.

A rearrangement of the ideal gas law (with the correction factor ( $\zeta = 1.074$ ), shown in Equation 8.8) allows an in-cylinder bulk temperature profile to be created for each individual engine cycle, example in Figure 8.17, and investigation into the inter-cycle variability of the in-cylinder bulk temperature at the start of combustion, shown in Figure 8.18. This in-cylinder bulk temperature is associated with the spatial average temperature. In reality, it is expected that the changes between the different phases of combustion would be smoother; however, Figure 8.17 does give an accurate indication of the spatial average in-cylinder temperature with respect to crank angle.

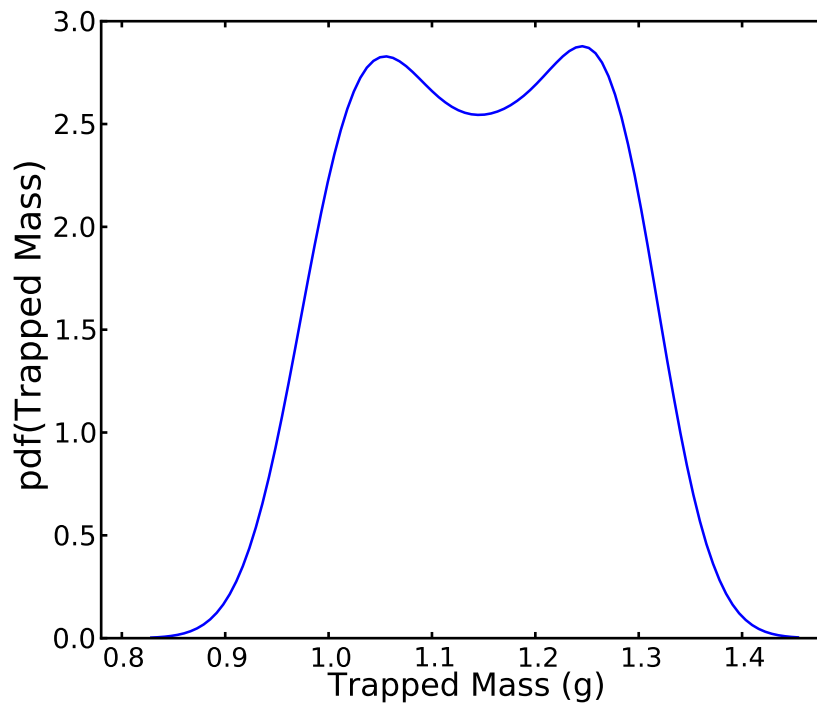


Figure 8.16: Distribution of the cycle resolved nominal trapped mass over 500 consecutive cycles

The bi-modal distribution of values shown in Figure 8.18 is interesting. It is showing that the predominate initial in-cylinder temperature is approximately 2000 K; but, it is also showing a significant second mode at approximately 2400 K. This bi-modal distribution is likely caused by instabilities in the control of the dynamometer. Data collected from this engine setup often shows a periodic time dependency, the spread of the distribution shown in Figure 8.18 is indicating that this variability has a significant impact on the in-cylinder temperature immediately prior to combustion. A bi-modal distribution, rather than a uni-modal distribution, is likely caused by bias in the sampling period—the dynamometer instability generally fluctuates with a period of approximately 50 seconds; therefore, a 60 second sample (as shown in this paper) will likely give bias to the repeated section of the sample period.

$$T = \frac{PV}{\zeta m R} \quad (8.8)$$

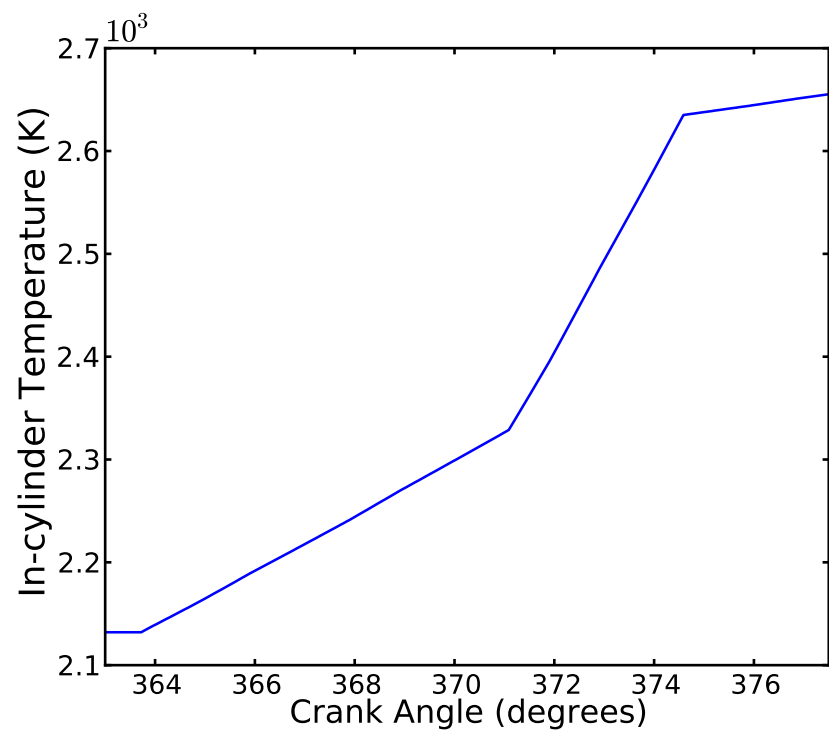


Figure 8.17: In-cylinder bulk temperature as a function of crank angle

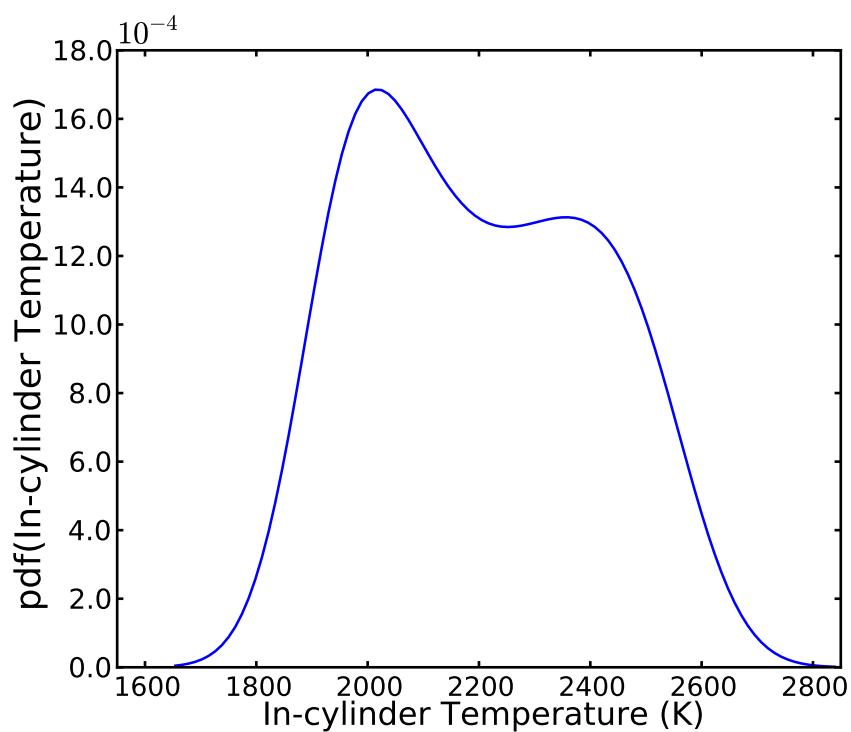


Figure 8.18: Distribution of the initial in-cylinder bulk temperature across 500 consecutive cycles



## 8.9 Conclusion

This paper has introduced a Bayesian model for analysing the combustion chamber resonant frequency. The model employed in this paper focused on capturing the rise in the resonant frequency associated with the increase in in-cylinder temperature from combustion. Applied to a band-pass filtered in-cylinder pressure signal, from a compression ignition engine, this model is capable of directly determining: the start of combustion, the start of diffusion combustion, the initial resonant frequency and the resonant frequency as a function of time. It has also been demonstrated that knowledge of the resonant frequency allows further investigation into the in-cylinder bulk temperature and trapped mass as a function of time. Results from the Bayesian model have been shown for 500 consecutive cycles of a turbo-charged, common-rail injection 5.9 l diesel engine run at full load and 2000 rpm.

The application of this technique to a modern compression ignition engine has shown that it is able to resolve a crank angle dependent (or time dependent) average spatial in-cylinder temperature profile and is useful for investigating the inter-cycle variability of the engine. A bi-modal distribution of in-cylinder temperature was shown and explained to be caused by engine operation instability. Moreover, this method for investigating the combustion chamber resonance also yields a new metric for describing the rate of increase in temperature during combustion, in terms of the model multiplicative parameters,  $\beta_i$ . Applications for this can include a more rigorous examination of the effect of alternative fuels and fuelling strategies, allowing the analyst a greater breadth of information to draw conclusions from.

## 8.10 Acknowledgements

The authors wish to thank Mr. Noel Hartnett for his work in maintaining the engine for research. Further thanks also to Technologist Mr. Ken McIvor for his assistance in setting up the data acquisition software and to Mr. Daniel Naylor for providing the technical drawing in Figure 8.1. For technical advice relating to thermoacoustics, the authors would also like to acknowledge Professor Wolfgang Polifke of Technische Universität München. This work was undertaken under an Australian Research Council Linkage Grant (LP0775178) in association with Peak3 P/L.

## 8.11 References

Bhat, C. S., Meckl, P. H., Bolton, J. S., and Abraham, J. Influence of fuel injection parameters on combustion-induced noise in a small diesel engine. *International Journal of Engine Research*, 13(2):130–146, 2012.

- Bodisco, T. and Brown, R. J. Inter-cycle variability of in-cylinder pressure parameters in an ethanol fumigated common rail diesel engine. *Energy*, 52(1):55–65, 2013a.
- Bodisco, T., Reeves, R., Situ, R., and Brown, R. J. Bayesian models for the determination of resonant frequencies in a DI diesel engine. *Mechanical Systems and Signal Processing*, 26:305–314, 2012.
- Bodisco, T., Low Choy, S., and Brown, R. J. A Bayesian approach to the determination of ignition delay. *Applied Thermal Engineering*, 60(1–2):79–87, 2013b.
- Bohme, J. F. and Konig, D. Statistical processing of car engine signals for combustion diagnosis. In *IEEE Seventh SP Workshop on Statistical Signal and Array Processing*, pages 369–374, 1994.
- Box, George and Tiao, George. *Bayesian Inference in Statistical Analysis*. John Wiley and Sons, 1992.
- Bretthorst, G. L. Excerpts from Bayesian spectrum analysis and parameter estimation. *Maximum Entropy and Bayesian Methods in Science and Engineering*, 1:75–145, 1988.
- Bretthorst, G. L. and Smith, C. R. Bayesian analysis of signals from closely-spaced objects. In *Infrared Systems and Components III, Proc. SPIE 1050*, 1989.
- Dou, L. and Hodgson, R. Bayesian inference and Gibbs sampling in spectral analysis and parameter estimation: I. *Inverse Problems*, 11(5):1069–1085, 1995.
- Duhamel, P. and Vetterli, M. Fast Fourier transforms: a tutorial review and a state of the art. *Signal Processing*, 19(4):259–299, 1990.
- Frassoldati, A., Faravelli, T., and Ranzi, E. A wide range modeling study of  $no_x$  formation and nitrogen chemistry in hydrogen combustion. *International Journal of Hydrogen Energy*, 31(15):2310–2328, 2006.
- Gelman, A., Carlin, J. B., Stern, H. S., and Rubin, D. B. *Bayesian Data Analysis: Second Edition*. Chapman & Hall/CRC, 2003.
- Gregory, P. C. and Loredo, T. J. A new method for the detection of a periodic signal of unknown shape and period. *Astrophysical Journal*, 398(1):146–168, 1992.
- Heywood, J. B. *Internal Combustion Engine Fundamentals*. McGraw-Hill, Inc., 1988.
- Hickling, R., Feldmaier, D. A., Chen, F. H. K., and Morel, J. S. Cavity resonances in engine combustion chambers and some applications. *Acoustical Society of America Journal*, 73: 1170–1178, 1983.

- Huang, N. E., Shen, Z., Long, S. R., Wu, M. C., Shih, H. H., Zheng, Q., Yen, N., Tung, C. C., and Liu, H. H. The empirical mode decomposition and the Hilbert spectrum for nonlinear and non-stationary time series analysis. *Proceedings: Mathematical, Physical and Engineering Sciences*, 454:903–995, 1998.
- Jaynes, E. T. Bayesian spectrum and chirp analysis. *Maximum-Entropy and Bayesian Spectral Analysis and Estimation Problems*, 1987.
- Jun, H. and Bing, H. Identification of diesel front sound source based on continuous wavelet transform. In *The 18th International Congress on Acoustics*, Kyoto, Japan, 2004.
- Jung, D. and Assanis, D. N. Multi-zone DI diesel spray combustion model for cycle simulation studies of engine performance and emissions. *Society of Automotive Engineers*, (SAE Paper 2001-01-1246), 2001.
- Li, H. and Zhang, Z. Diesel engine condition classification based on mechanical dynamics and time-frequency image processing. *Dynamical Systems*, pages 397–408, 2010.
- Li, W., Gu, F., Ball, A. D., Leung, A. Y. T., and Phipps, C. E. A study of the noise from diesel engines using the independent component analysis. *Mechanical Systems and Signal Processing*, 15(6):1165–1184, 2001.
- Nishida, K. and Hiroyasu, H. Simplified three-dimensional modeling of mixture formation and combustion in a D.I. diesel engine. *Society of Automotive Engineers*, (SAE Paper 890269), 1989.
- O’Loughlin, W. and Masri, A. A new burner for studying auto-ignition in turbulent dilute sprays. *Combustion and Flame*, 158:1577–1590, 2011.
- O’Loughlin, W. and Masri, A. The structure of the auto-ignition region of turbulent dilute methanol sprays issuing in a vitiated co-flow. *Flow Turbulence Combustion*, 89:13–35, 2012.
- Payri, F., Broatch, A., Tormos, B., and Marant, V. New methodology for in-cylinder pressure analysis in direct injection diesel engines: application to combustion noise. *Measurement Science and Technology*, 16(2):540–547, 2005.
- Peng, Z. and Chu, F. Application of the wavelet transform in machine condition monitoring and fault diagnostics: a review with bibliography. *Mechanical Systems and Signal Processing*, 18(2):199–221, 2004.
- Poggi, V., Faeh, D., and Giardini, D. Time-frequency-wavenumber analysis of surface waves using the continuous wavelet transform. *Pure and Applied Geophysics*, 170(3):319–335, 2012.

- Ramadhass, A. S., Muraleedharan, C., and Jayaraj, S. Performance and emission evaluation of a diesel engine fuelled with methyl esters of rubber seed oil. *Renewable Energy*, 30(12): 1789–1800, 2005.
- Randall, R. B. *Frequency Analysis*. Bruel & Kjaer, 1987.
- Ren, Y., Randall, R. B., and Milton, B. E. Influence of the resonant frequency on the control of knock in diesel engines. *Proceedings of the Institution of Mechanical Engineers: Part D: Journal of Automobile Engineering*. London, 213(2):127–133, 1999.
- Sen, A. K., Longwic, R., Litak, G., and Gorski, Z. Analysis of cycle-to-cycle pressure oscillations in a diesel engine. *Mechanical Systems and Signal Processing*, 22:362–373, 2008.
- Spiegelhalter, D. J., Thomas, A., and Best, N. G. *WinBUGS Version 1.2 User Manual*. MRC Biostatistics Unit, 1999.
- Stankovic, L. and Bohme, J. F. Time-frequency analysis of multiple resonances in combustion engine signals. *Signal Processing*, 79(1):15–28, 1999.
- Torregrosa, A. J., Broatch, A., and Margot, X. Combustion chamber resonances in direct injection automotive diesel engines: a numerical approach. *International Journal of Engine Research*, 5(1):83–91, 2004.

# Chapter 9

## Conclusions

This research program has filled a significant gap in the field of engine research by introducing novel techniques for analysing in-cylinder pressure signals. It has contributed to the alternative fuel debate by giving new evidence relating to the use of fumigated ethanol in a modern common-rail diesel engine. Moreover, the application of these techniques have highlighted the importance of being able to analyse individual consecutive engine cycles to gain an in-depth perspective of the effect an alternative fuelling strategy has on engine operation.

### 9.1 In-cylinder pressure techniques

The work contained in this dissertation has focused on in-cylinder pressure. In-cylinder pressure is an important parameter to investigate if knowledge of the combustion processes are to be understood. Therefore, a primary aim of this dissertation has been to improve the way in which engine researchers use in-cylinder pressure data.

Chapter 4 proposed the use of statistical modelling, in the Bayesian paradigm, to investigate combustion chamber resonance. Using pre-packaged software, WinBUGS, it was demonstrated that it is possible to isolate the resonant frequency as a function of time. Moreover, a high-level of cycle-to-cycle variation in this parameter was also shown and added a valuable perspective on the argument against cycle-averaging data.

Isolation of the resonant frequency is important as it is related to the speed of sound and hence temperature—knowledge of in-cylinder temperature is important because of its relationship to emission formation. Moreover, in-cylinder temperature can also be used to estimate the trapped mass in the combustion chamber, as a function of time; hence, this method can be extended to experimentally investigate piston blow-by.

A Bayesian technique is appropriate in engine research because of the variable nature in which an engine operates. Pre-fit data analysis solutions do not allow the analyst to include their own knowledge and assumptions into the analysis. This is a key feature of the Bayesian modelling techniques used in this dissertation, the analyst creates an empirical form of the data and can then resolve each parameter, with uncertainty. If the model has been setup well, the resolved parameters will inform the analyst about the operating characteristics of

the engine.

Chapters 5 and 6 introduced the concept of using a band-pass filtered in-cylinder pressure signal for the determination of the start of combustion. Initially in Chapter 5, this analysis was undertaken manually by observing the change in the band-pass in-cylinder pressure signal from high-frequency noise to an established periodic signal of approximately 6 kHz. However, the time-consuming nature of manual data analysis prohibited any true inter-cycle variability studies from being conducted.

In order to over-come the limitation of manual data analysis, an automated method was explored in Chapter 6. This method utilised a Bayesian approach, similar to Chapter 4. A simple model was used for this application to improve the computation time. The band-pass filtered in-cylinder pressure signal was modelled as a Normal distribution with a time varying mean,  $\mu(t)$ .

$$\mu(t) = H(t - \delta)A \sin(kwt + \phi)$$

This time varying mean is zero before the start of combustion and a stationary periodic wave after—resolving the change point parameter,  $\delta$ , resolves the start of combustion. Coupled with knowledge of the start of injection, the ignition delay can be determined with this method for consecutive individual cycles. Ignition delay results for an ethanol fumigation campaign are shown in Chapter 7.

Chapter 8 revisited the early work shown in Chapter 4. A key limitation of the final model shown in Chapter 4 was that it did not consider the rise in resonant frequency from the temperature rise during premixed combustion. Therefore, Chapter 8 examined the rise in resonant frequency at the onset of combustion. A new model was developed that focused on capturing this rise in resonant frequency and it was used to examine the inter-cycle variability of the initial in-cylinder temperature, the rate of in-cylinder temperature rise, the start of pre-mixed combustion and the start of diffusion combustion.

## 9.2 Inter-cycle variability

Inter-cycle variability featured throughout this entire work. However, it was most prominently investigated in Chapters 5 and 7. The extent of inter-cycle variability can be used as a parameter to investigate abnormal engine operation. Typically, this has been done by observing the coefficient of variation (COV) of the indicated mean effective pressure (IMEP). The COV is defined as the mean normalised standard deviation:

$$COV_x = \frac{\sigma_x}{\bar{x}}$$

Results from the ethanol fumigation campaign, shown in Chapter 5, have shown that the COV of IMEP is not necessarily a good measure of inter-cycle variability.

Results from a Bayesian analysis are typically viewed in kernel density estimates (probability density functions). This is done to check for skewness, evidence of multi-modal results and to estimate the uncertainty of the result. The shape of the kernel density estimate can also be used to indicate of non-convergence, limitations in the model or evidence of multiple possible results. Similarly, in-cylinder parameters from a large amount of consecutive engine parameter data can be viewed in this format.

Chapter 5 investigated the inter-cycle variability of key in-cylinder parameters: maximum rate of pressure rise, peak pressure, peak pressure timing and ignition delay—the ignition delay study in this chapter was preliminary work and was later covered in-depth in Chapters 6 and 7—for an engine operating on neat diesel fuel and fumigated ethanol with substitutions up to 40% by energy, see Table 5.1. For comparison to existing literature, this chapter also shows the COV of IMEP. These in-cylinder parameters were investigated by generating kernel density estimates from 4000 consecutive engine cycles.

Observing the results as kernel density estimates allowed for features such as multi-modal behaviour to be identified. A key limitation of singular values, COV or a standard deviation, for expressing inter-cycle variability is that it cannot inform the analyst of the nature of the variability. Non-unimodal or widely random behaviour is likely to have a greater effect on the engine (in terms of: noise, vibration and wear) than a large amount of variability, as indicated by the COV or a standard deviation, will.

A key outcome of Chapters 5 and 7 was a relationship between the absolute air to fuel ratio (on a mole basis) and inter-cycle variability. It was shown that for the heavy duty, common-rail Cummins diesel engine, under investigation in this work, that as long as it was operated with an air to fuel ratio greater than 110, the inter-cycle variability was not greatly effected. However, operation below an air to fuel ratio of 110 (particularly below 80) resulted in very significant inter-cycle variability.

### 9.3 Ethanol fumigation

Investigation into the ignition delay of the ethanol fumigated engine found results that were contradictory with the current published work. The current literature suggests that ethanol fumigation increases ignition delay because of the so-called “cooling effect” that ethanol has—the amount of energy required to heat ethanol is greater than air; therefore, the presence of ethanol in the charge air mixture causes a lower in-cylinder temperature at the time the diesel fuel is injected. However, Chapter 5 has highlighted that much of the ethanol fumigation work that has been done was performed on older engines operating with comparatively low IMEP and earlier injection timing. An engine operating with higher

fuel injection pressure at a far greater in-cylinder pressure (and consequently far greater in-cylinder temperatures before injection) will have very different combustion characteristics. This key difference manifests significantly with fumigated fuels.

It was shown in Sections 5.5.1, 5.5.2, 5.5.5 and Chapter 7 that ethanol fumigation can reduce the ignition delay. Further, ethanol was also shown to auto-ignite (without the presence of diesel) under high-loads and -substitutions. This was an important conclusion, as it shows that alternative fuel research needs to be conducted on engines that are representative of industry and transport if the results are to be directly transferable. It also demonstrates a gap in knowledge in alternative fuels research with modern heavy-duty engines.

## 9.4 Recommendations for the future

This dissertation offers a practical means for investigating the in-cylinder effects of alternative fuelling in diesel engines. As such, the most practical recommendation would be to apply these techniques to other alternative fuels—particularly, relevant biofuels. A key element to the success of alternative fuels (from a practical, non-economic and -political perspective) will be to have as complete as possible understanding of the implications involved with using them. The techniques available in this work will allow for more meaningful and comprehensive results.

The relationship between emission formation and in-cylinder temperature makes it likely that correlations will exist between exhaust emission and the parameters investigated in this dissertation—initial resonant frequency and rate of change of resonant frequency. Therefore, a practical study could be to characterise an engine (or multiple engines) and search for links between in-cylinder parameters and emission. This could be achieved by a combination of the techniques outlined in this dissertation and the use of principle component analysis—such as PROMETHEE-GAIA analysis.

The Bayesian modelling techniques developed in this dissertation are also applicable to vibration signals. These techniques would be ideal for inclusion in off-line condition monitoring of vibrating machinery and engines. Moreover, there would also be applications in civil engineering in building condition management.

The Bayesian techniques developed in this dissertation were primarily aimed at resolving frequency information; however, there are other applications outside of those from engines and vibrating machinery. Essentially, any complex signal with hard to resolve frequency components can be explored with a Bayesian modelling techniques. An application would be to investigate wake shedding in fluid flow under the influence of a geometry change.



---

[This page is intentionally left blank]

## Reference List

- Abu-Qudais, M., Haddad, O., and Qudaisat, M. The effect of alcohol fumigation on diesel engine performance and emissions. *Energy Conversion and Management*, 41(4):389–399, 2000.
- Ajav, E. A., Singh, B., and Bhattacharya, T. K. Thermal balance of a single cylinder diesel engine operating on alternative fuels. *Energy Conversion and Management*, 41(14):1533–1541, 2000.
- Alperstein, M., Swin, W. B., and Schweitzer, P. H. Fumigation kills smoke, improves diesel performance. *Society of Automotive Engineers*, (SAE Paper 580058), 1958.
- Amann, C. A. Cylinder-pressure measurement and its use in engine research. *Society of Automotive Engineers*, (SAE Paper 852067), 1986.
- Antoni, J. Cyclostationarity by examples. *Mechanical Systems and Signal Processing*, 23(4):987–1036, 2009.
- Antoni, J., Daniere, J., and Guillet, F. Effective vibration analysis of IC engines using cyclostationarity. Part I-A methodology for condition monitoring. *Journal of Sound and Vibration*, 257(5):815–837, 2002a.
- Antoni, J., Daniere, J., Guillet, F., and Randall, R. B. Effective vibration analysis of IC engines using cyclostationarity. Part II–new results on the reconstruction of the cylinder pressures. *Journal of Sound and Vibration*, 257(5):839–856, 2002b.
- Arnone, L., Manelli, S., Chiatti, G., and Chiavola, O. Engine block vibration measures for time detection of diesel combustion phases. *Society of Automotive Engineers*, (SAE Paper 2009-24-0035), 2009.
- Assanis, D. N., Filipi, Z. S., Fiveland, S. B., and Syrimis, M. A predictive ignition delay correlation under steady-state and transient operation of a direct injection diesel engine. *J. Eng. Gas Turbines Power*, 125(2):450–457, 2003.
- Australian National Greenhouse Accounts, . Quarterly Update of Australias National Greenhouse Gas Inventory. *March Quarter 2010*, 2010. URL <http://www.climatechange.gov.au/>.
- Badami, M., Nuccio, P., and Trucco, G. Influence of injection pressure on the performance of a DI diesel engine with a common rail fuel injection system. *Society of Automotive Engineers*, (SAE Paper 1999-01-0193), 1999.
- Beasley, M., Cornwell, R., Fussey, P., King, R., Noble, A., Salamon, T., and Truscott, A. Reducing diesel emissions dispersion by coordinated combustion feedback control. *Society of Automotive Engineers*, (SAE Paper 2006-01-0186), 2006.

- Berg, A., Meyer, R., and Yu, J. Deviance information criterion for comparing stochastic volatility models. *Journal of Business & Economic Statistics*, 22:107–120, 2002.
- Bhat, C. S., Meckl, P. H., Bolton, J. S., and Abraham, J. Influence of fuel injection parameters on combustion-induced noise in a small diesel engine. *International Journal of Engine Research*, 13(2):130–146, 2012.
- Bo, Z., Weibiao, F., and Jingsong, G. Study of fuel consumption when introducing DME or ethanol into diesel engine. *Fuel*, 85(5-6):778–782, 2006.
- Boashash, B. Note on the use of the Wigner distribution for time-frequency signal analysis. *IEEE Transactions on Acoustics, Speech and Signal Processing*, 36:1518–1521, 1988.
- Boashash, B. Estimating and interpreting the instantaneous frequency of a signal – Part 1: Fundamentals. In *IEEE, Proceedings.*, volume 80, pages 520–538, 1992.
- Bodisco, T. and Brown, R. J. Inter-cycle variability of in-cylinder pressure parameters in an ethanol fumigated common rail diesel engine. *Energy*, 52(1):55–65, 2013a.
- Bodisco, T., Reeves, R., Situ, R., and Brown, R. J. Bayesian models for the determination of resonant frequencies in a DI diesel engine. *Mechanical Systems and Signal Processing*, 26:305–314, 2012.
- Bodisco, T., Low Choy, S., and Brown, R. J. A Bayesian approach to the determination of ignition delay. *Applied Thermal Engineering*, 60(1–2):79–87, 2013b.
- Bohme, J. F. and Konig, D. Statistical processing of car engine signals for combustion diagnosis. In *IEEE Seventh SP Workshop on Statistical Signal and Array Processing*, pages 369–374, 1994.
- Boretti, A. Advantages of converting diesel engines to run as dual fuel ethanol/diesel. *Applied Thermal Engineering*, 47:1–9, 2012.
- Box, George and Tiao, George. *Bayesian Inference in Statistical Analysis*. John Wiley and Sons, 1992.
- Bretthorst, G. L. Excerpts from Bayesian spectrum analysis and parameter estimation. *Maximum Entropy and Bayesian Methods in Science and Engineering*, 1:75–145, 1988a.
- Bretthorst, G. L. Bayesian spectrum analysis and parameter estimation. *Lecture Notes in Statistics*, 48, 1988b.
- Bretthorst, G. L. and Smith, C. R. Bayesian analysis of signals from closely-spaced objects. In *Infrared Systems and Components III, Proc. SPIE 1050*, 1989.
- Broersen, P. M. T. Facts and fiction in spectral analysis. *Instrumentation and Measurement, IEEE Transactions on*, 49(4):766–772, 2000.
- Broukhiyan, E. M. H. and Lestz, S. S. Ethanol fumigation of a light duty automotive diesel engine. *Society of Automotive Engineers*, (SAE Paper 811209), 1981.
- Brown, E. R., Reuben, R. L., Neill, G. D., and Stell, J. A. Acoustic emission source discrimination using a piezopolymer based sensor. *Materials evaluation*, 57(5):515–520, 1999.

- Bruneaux, G. Liquid and vapor spray structure in high-pressure common rail diesel injection. *Atomization and Sprays*, 11(5):533–556, 2001.
- Brunt, M. and Platts, K. Calculation of heat release in direct injection diesel engines. *Society of Automotive Engineers*, (SAE Paper 1999-01-0187), 1999.
- Brunt, M. and Pond, C. Evaluation of techniques for absolute cylinder pressure correction. *Society of Automotive Engineers*, (SAE Paper 9700369), 1997.
- Brunt, M., Rai, H., and Emtage, A. The calculation of heat release energy from engine cylinder pressure data. *Society of Automotive Engineers*, (SAE Paper 981052), 1998.
- Burg, J. Maximum entropy spectral analysis. In Childers, D., editor, *Proceedings of the 37th Meeting of the Society of Exploration Geophysicists. Reprinted (1978) in Modern Spectrum Analysis*, 1967.
- Burg, J. The relationship between maximum entropy spectra and maximum likelihood spectra. *Geophysics*, 37(2):375–376, 1972.
- Burg, J. *Maximum entropy spectral analysis*. PhD thesis, Stanford University, 1975.
- Cancino, L., Fikri, M., Oliveira, A., and Schulz, S. Ignition delay times of ethanol containing multi-component gasoline surrogates: Shock-tube experiments and detailed modeling. *Fuel*, 90:1238–1244, 2011.
- Carlucci, A. P., Chiara, F. F., and Laforgia, D. Block vibration as a way of monitoring the combustion evolution in a direct injection diesel engine. *Society of Automotive Engineers*, (SAE Paper 2006-01-1532), 2006.
- Carlucci, A. P., de Risi, A., Laforgia, D., and Naccarato, F. Experimental investigation and combustion analysis of a direct injection dual-fuel diesel–natural gas engine. *Energy*, 33(2):256–263, 2008.
- Carolan, T. A., Kidd, S. R., Hand, D. P., Wilcox, S. J., Wilkinson, P., Barton, J. S., Jones, J. D. C., and Reuben, R. L. Acoustic emission monitoring of tool wear during the face milling of steels and aluminium alloys using a fibre optic sensor Part 2: frequency analysis. *Proceedings of the Institution of Mechanical Engineers, Part B: Journal of Engineering Manufacture*, 211(4):311–319, 1997.
- Carpenter, S. H. and Zhu, Z. Correlation of the acoustic emission and the fracture toughness of ductile nodular cast iron. *Journal of Materials Science*, 26(8):2057–2062, 1991.
- Chauhan, B. S., Kumar, N., Pal, S. S., and Du Jun, Y. Experimental studies on fumigation of ethanol in a small capacity diesel engine. *Energy*, 36(2):1030–1038, 2011.
- Chen, J., Gussert, D., Gao, X., Gupta, C., and Foster, D. Ethanol fumigation of a turbocharged diesel engine. *Society of Automotive Engineers*, (SAE Paper 810680), 1981.
- Cheng, C. H., Cheung, C. S., Chan, T. L., Lee, S. C., Yao, C. D., and Tsang, K. S. Comparison of emissions of a direct injection diesel engine operating on biodiesel with emulsified and fumigated methanol. *Fuel*, 87(10-11):1870–1879, 2008.

- Chiavola, O., Chiatti, G., Arnone, L., and Manelli, S. Combustion characterization in diesel engines via block vibration analysis. *Society of Automotive Engineers*, (SAE Paper 2010-01-0168), 2010.
- Choi, D., Miles, P., Yun, H., and Reitz, R. A parametric study of low-temperature late-injection combustion in a HSDI diesel engine. *JSME International Journal Series B*, 48(4):656–664, 2005.
- Cinar, C., Can, O., Sahin, F., and Yucesu, H. S. Effects of premixed diethyl ether (DEE) on combustion and exhaust emissions in a HCCI-DI diesel engine. *Applied Thermal Engineering*, 30(4):360–365, 2010.
- Cohn, D. R., Bromberg, L., and Heywood, J. B. Direct injection ethanol boosted gasoline engines: Biofuel leveraging for cost effective reduction of oil dependence and CO<sub>2</sub> emissions. *Massachusetts Institute of Technology*, 2005.
- Cooley, J. W. and Tukey, J. W. An algorithm for the machine calculation of complex Fourier series. *Mathematics of Computation*, 19(90):297–301, 1965.
- Cooley, J. W., Lewis, P. A. W., and Welch, P. D. The Fast Fourier transform and its applications. *Education, IEEE Transactions on*, 12(1):27–34, 1969.
- Curran, H., Gaffuri, P., Pitz, W., and Westbrook, C. A comprehensive modeling study of *n*-heptane oxidation. *Combustion and Flame*, 114:149–177, 1998.
- Curran, H., Gaffuri, P., Pitz, W., and Westbrook, C. A comprehensive modeling study of iso-octane oxidation. *Combustion and Flame*, 129(3):253–280, 2002.
- Dalai, A. K., Bakhshi, N. N., and Esmail, M. N. Conversion of syngas to hydrocarbons in a tube-wall reactor using Co—Fe plasma-sprayed catalyst: experimental and modeling studies. *Fuel Processing Technology*, 51(3):219–238, 1997.
- Demirbas, A. Progress and recent trends in biofuels. *Progress in Energy and Combustion Science*, 33(1):1–18, 2007.
- Demirbas, M. F. and Balat, M. Recent advances on the production and utilization trends of bio-fuels: A global perspective. *Energy Conversion and Management*, 47(15-16):2371–2381, 2006.
- Desantes, J. M., Galindo, J., Guardiola, C., and Dolz, V. Air mass flow estimation in turbocharged diesel engines from in-cylinder pressure measurement. *Experimental Thermal and Fluid Science*, 34:37–47, 2010.
- Diesel, R. German Patent 67207, 1892.
- Donkerbroek, A. J., Boot, M. D., Luijten, C. C. M., Dam, N. J., and ter Meulen, J. J. Flame lift-off length and soot production of oxygenated fuels in relation with ignition delay in a DI heavy-duty diesel engine. *Combustion and Flame*, 158(3):525–538, 2011.
- Dou, L. and Hodgson, R. Bayesian inference and Gibbs sampling in spectral analysis and parameter estimation: I. *Inverse Problems*, 11(5):1069–1085, 1995.

- Draper, C. S. Pressure waves accompanying detonation in the internal combustion engine. *Journal of Aeronautical Sciences*, 5(6):219–226, 1938.
- Duhamel, P. and Vetterli, M. Fast Fourier transforms: a tutorial review and a state of the art. *Signal Processing*, 19(4):259–299, 1990.
- EC, . EC, 2009. Regulation (EC) No 595/2009 of the European Parliament and the Council of 18 June 2009 on type-approval of motor vehicles and engines with respect to emissions from heavy duty vehicles (Euro VI), European Commission, Brussels, Belgium., 2009.
- El Ghamry, M., Reuben, R. L., and Steel, J. A. The development of automated pattern recognition and statistical feature isolation techniques for the diagnosis of reciprocating machinery faults using acoustic emission. *Mechanical Systems and Signal Processing*, 17: 805–823, 2003.
- El Ghamry, M. H., Brown, E. R., Ferguson, I., Gill, J. D., Reuben, R. L., Steel, J. A., Scaife, M., and Middleton, S. Gaseous airfuel quality identification for a spark ignition gas engine using acoustic emission analysis. In *Proceedings of the 11th International Conference on Condition Monitoring and Diagnostic Engineering Management (COMADEM 98)*, Launceston, Tasmania, Australia, pages 235–244, 1998.
- Ellison, A. Bayesian inference in ecology. *Ecology Letters*, 7(6):509–520, 2004.
- Everitt, B. S. *The Cambridge Dictionary of Statistics, Third Edition*. Cambridge University Press, 2006.
- Fang, Q., Fang, J., Zhuang, J., and Huang, Z. Influences of pilotinjection and exhaustgasrecirculation (EGR) on combustion and emissions in a HCCI-DI combustion engine. *Applied Thermal Engineering*, 48:97–104, 2012.
- Fitzgerald, W. J. Markov chain Monte Carlo methods with applications to signal processing. *Signal Processing*, 81(1):3–18, 2001.
- Fog, T. L. *Condition monitoring and fault diagnosis in marine diesel engines*. PhD thesis, Technical University of Denmark, 1998.
- Frassoldati, A., Faravelli, T., and Ranzi, E. A wide range modeling study of  $no_x$  formation and nitrogen chemistry in hydrogen combustion. *International Journal of Hydrogen Energy*, 31(15):2310–2328, 2006.
- Gelman, A., Carlin, J. B., Stern, H. S., and Rubin, D. B. *Bayesian Data Analysis: Second Edition*. Chapman & Hall/CRC, 2003.
- Genzale, C., Reitz, R., and Musculus, M. Effects of spray targeting on mixture development and emissions formation in late-injection low-temperature heavy-duty diesel combustion. *Proceedings of the Combustion Institute*, 32(2):2767–2774, 2009.
- Ghojel, J., Honnery, D., and Al-Khaleefi, K. Performance, emissions and heat release characteristics of direct injection diesel engine operating on diesel oil emulsion. *Applied Thermal Engineering*, 26(17-18):2132–2141, 2006.
- Greene, A. B. and Lucas, G. G. *The Testing of Internal Combustion Engines*. The English Universities Press Limited, 1969.

- Gregory, P. C. A Bayesian revolution in spectral analysis. In *AIP Conf. Proc.*, volume 568, pages 557–568, Gif-sur-Yvette (France), 2001. AIP.
- Gregory, P. C. and Loredo, T. J. A new method for the detection of a periodic signal of unknown shape and period. *Astrophysical Journal*, 398(1):146–168, 1992.
- Gupta, R. B. and Demirbas, A. *Gasoline, Diesel, and Ethanol Biofuels from Grasses and Plants*. Cambridge University Press, 2010.
- Hansen, A. C., Zhang, Q., and Lyne, P. W. L. Ethanol-diesel fuel blends – a review. *Bioresource Technology*, 96(3):277–285, 2005.
- Hardenberg, H. O. and Hase, F. W. An empirical formula for computing the pressure rise delay of a fuel from its cetane number and from the relevant parameters of direct-injection diesel engines. *Society of Automotive Engineers*, (SAE Paper 790493), 1979.
- Hasegawa, M., Shimasaki, Y., Yamaguchi, S., Kobayashi, M., Sakamoto, H., Kitayama, N., and Kanda, T. Study on ignition timing control for diesel engines using in-cylinder pressure sensor. *Society of Automotive Engineers*, (SAE Paper 2006-01-0180), 2006.
- Havemann, H. A., Rao, M. R. K., and Narasimhan, T. L. Alcohol in diesel engines. *Automotive Engineer*, pages 256–262, 1954.
- Hayes, T. K., Savage, L. D., and White, R. A. The effect of fumigation of different ethanol proofs on a turbocharge diesel engine. *Society of Automotive Engineers*, (SAE Paper 880497), 1988.
- Heisey, J. B. and Letsz, S. S. Aqueous alcohol fumigation of a single-cylinder direct injection diesel engine. *Society of Automotive Engineers*, (SAE Paper 811208), 1981.
- Henham, A. and Makkar, M. K. Combustion of simulated biogas in a dual-fuel diesel engine. *Energy Conversion and Management*, 39(16-18):2001–2009, 1998.
- Heywood, J. B. *Internal Combustion Engine Fundamentals*. McGraw-Hill, Inc., 1988.
- Hickling, R., Feldmaier, D. A., and Sung, S. H. Knock-induced cavity resonances in open chamber diesel engines. *Acoustical Society of America Journal*, 65(6):1474–1479, 1979.
- Hickling, R., Feldmaier, D. A., Chen, F. H. K., and Morel, J. S. Cavity resonances in engine combustion chambers and some applications. *Acoustical Society of America Journal*, 73: 1170–1178, 1983.
- Huang, G. H., Chen, F., Wei, D., Zhang, X., and Chen, G. Biodiesel production by microalgal biotechnology. *Applied Energy*, 87:38–46, 2010.
- Huang, N. E., Shen, Z., Long, S. R., Wu, M. C., Shih, H. H., Zheng, Q., Yen, N., Tung, C. C., and Liu, H. H. The empirical mode decomposition and the Hilbert spectrum for nonlinear and non-stationary time series analysis. *Proceedings: Mathematical, Physical and Engineering Sciences*, 454:903–995, 1998.
- ICF International, . Integrating climate change into the transportation planning process. Technical report, Federal Highway Administration, 2008.

- Jaye, J. R. Algorithm for determining the top dead center location in an internal combustion engine using cylinder pressure measurements. US Patent 6,367,317, 2002.
- Jaynes, E. T. Bayesian spectrum and chirp analysis. *Maximum-Entropy and Bayesian Spectral Analysis and Estimation Problems*, 1987.
- Jaynes, E. T. *Probability Theory: The Logic of Science*. Cambridge University Press, 2007.
- Johansson, B. Cycle to cycle variations in S.I. engines – the effects of fluid flow and gas composition in the vicinity of the spark plug on early combustion. *Society of Automotive Engineers*, (SAE Paper 962084), 1996.
- Jun, H. and Bing, H. Identification of diesel front sound source based on continuous wavelet transform. In *The 18th International Congress on Acoustics*, Kyoto, Japan, 2004.
- Jung, D. and Assanis, D. N. Multi-zone DI diesel spray combustion model for cycle simulation studies of engine performance and emissions. *Society of Automotive Engineers*, (SAE Paper 2001-01-1246), 2001.
- Kanda, T., Hakozaki, T., Uchimoto, T., Hatano, J., Kitayama, N., and Sono, H. PCCI operation with fuel injection timing set close to TDC. *Society of Automotive Engineers*, (SAE Paper 2006-01-0920), 2006.
- Kaplan, W. *Advanced Calculus*. Pearson Education, Inc., 5th edition, 2003.
- Karthikeyana, R. and Mahalakshmi, N. V. Performance and emission characteristics of a turpentine–diesel dual fuel engine. *Energy*, 32(7):1202–1209, 2007.
- Kim, S. and Dale, B. E. Global potential bioethanol production from wasted crops and crop residues. *Biomass and Bioenergy*, 26(4):361–375, 2004.
- Kim, S. and Min, K. Detection of combustion start in the controlled auto ignition engine by wavelet transform of the engine block vibration signal. *Measurement Science and Technology*, 19(8), 2008.
- Kistler, W. P. Swiss Patent 267431. 1950.
- Kouremenos, D. A., Rakopoulos, C. D., and Kotsiopoulos, P. Performance and emission characteristics of a diesel engine using supplementary diesel fuel fumigated to the intake air. *Heat Recovery Systems and CHP*, 9(5):457–465, 1989.
- Kouremenos, D. A., Rakopoulos, C. D., and Kotsiopoulos, P. Comparative performance and emission studies for vaporized diesel fuel and gasoline as supplements in swirl-chamber diesel engines. *Energy*, 15(12):1153–1160, 1990.
- Kouremenos, D. A., Rakopoulos, C. D., and Kotsos, K. G. A stochastic-experimental investigation of the cyclic pressure variation in a DI single-cylinder diesel engine. *International Journal of Energy Research*, 16(9):865–877, 1992.
- Lakshmanan, T. and Nagarajan, G. Experimental investigation of timed manifold injection of acetylene in direct injection diesel engine in dual fuel mode. *Energy*, 35(8):3172–3178, 2010.



- Lapuerta, M., Armas, O., and Hernandez, J. J. Diagnosis of DI Diesel combustion from in-cylinder pressure signal by estimation of mean thermodynamic properties of gas. *Applied Thermal Engineering*, 19:513–529, 1999.
- Lata, D. B. and Misra, A. Analysis of ignition delay period of a dual fuel diesel engine with hydrogen and LPG as secondary fuels. *International Journal of Hydrogen Energy*, 36(5): 3746–3756, 2011.
- Lavoie, G., Heywood, J., and Keck, J. Experimental and theoretical study of nitric oxide formation in internal combustion engines. *Combustion Science and Technology*, 1:313–326, 1970.
- Lee, J. W., Min, K. D., Kang, K. Y., Bae, C. S., Giannadakis, E., Gavaises, M., and Arcoumanis, C. Effect of piezo-driven and solenoid-driven needle opening of common-rail diesel injectors on internal nozzle flow and spray development. *International Journal of Engine Research*, 7:489–502, 2006.
- Lee, K., Yoon, M., and Sunwoo, M. A study on pegging methods for noisy cylinder pressure signal. *Control Engineering Practice*, 16:922–929, 2008.
- Li, H. and Zhang, Z. Diesel engine condition classification based on mechanical dynamics and time-frequency image processing. *Dynamical Systems*, pages 397–408, 2010.
- Li, W., Gu, F., Ball, A. D., Leung, A. Y. T., and Phipps, C. E. A study of the noise from diesel engines using the independent component analysis. *Mechanical Systems and Signal Processing*, 15(6):1165–1184, 2001.
- Lloyd, A. C. and Cackette, T. A. Diesel engines : Environmental impact and control. *Journal of the Air & Waste Management Association*, 51(6):809–847, 2001.
- Lucke, C. Kerosene versus gasoline in automobile engines. *Society of Automotive Engineers*, (SAE Paper 160022), 1916.
- Lujan, J. M., Bermudez, V., Guardiola, C., and Abbad, A. A methodology for combustion detection in diesel engines through in-cylinder pressure derivative signal. *Mechanical Systems and Signal Processing*, 24:2261–2275, 2010.
- Maas, U. and Warnatz, J. Ignition processes in hydrogen-oxygen mixtures. *Combustion and Flame*, 74:53–69, 1988.
- Machrafi, H., Cavadias, S., and Gilbert, P. An experimental and numerical analysis of the HCCI auto-ignition process of primary reference fuels, toluene reference fuels and diesel fuel in an engine, varying the engine parameters. *Fuel Processing Technology*, 89:1107–1016, 2008.
- Martin, W. and Flandrin, P. Wigner-Ville spectral analysis of nonstationary processes. *IEEE Transactions on Acoustics, Speech, and Signal Processing*, ASSP-33(6):1461–1470, 1985.
- McArdle, P., Lindstrom, P., and Calopedis, S. Emissions of greenhouse gases report. Technical Report DOE/EIA-0573(2006), Energy Information Administration, Office of Integrated Analysis and Forecasting, U.S. Department of Energy, Washington, DC, 2007. URL <http://www.eia.doe.gov/oiaf/1605/ggrpt/>.

- Merrion, D. F. Diesel engine design for the 1990s. *Society of Automotive Engineers*, (SAE Paper 940130), 1994.
- Midgley, T. and Boyd, T. A. Methods of measuring detonation in engines. *Society of Automotive Engineers*, (SAE Paper 220004), 1922.
- Miettinen, J. and Siekkinen, V. Acoustic emission in monitoring sliding contact behaviour. *Wear*, 181-183(Part 2):897–900, 1995.
- Monyem, A. and Van Gerpen, J. H. The effect of biodiesel oxidation on engine performance and emissions. *Biomass and Bioenergy*, 20(4):317–325, 2001.
- Morey, F. and Seers, P. Comparison of cycle-by-cycle variation of measured exhaust-gas temperature and in-cylinder pressure measurements. *Applied Thermal Engineering*, 30: 487–491, 2010.
- Morse, P. M. and Ingard, K. U. *Theoretical Acoustics*. McGraw-Hill Book Company, 1968.
- Needham, J. R., May, M. P., Doyle, D. M., Faulkner, S. A., and Ishiwata, H. Injection timing and rate control – a solution for low emissions. *Society of Automotive Engineers*, (SAE Paper 900854), 1990.
- Neill, G. D., Reuben, R. L., Sandford, P. M., Brown, E. R., and Steel, J. A. Detection of incipient cavitation in pumps using acoustic emission. *Proceedings of the Institution of Mechanical Engineers, Part E: Journal of Process Mechanical Engineering*, 311(4):267–277, 1997.
- Nilsson, Y and Eriksson, L. Determining TDC position using symmetry and other methods. *Society of Automotive Engineers*, (SAE Paper 2004-01-1458), 2004.
- Nishida, K. and Hiroyasu, H. Simplified three-dimensional modeling of mixture formation and combustion in a D.I. diesel engine. *Society of Automotive Engineers*, (SAE Paper 890269), 1989.
- Niven, R. K. Ethanol in gasoline: environmental impacts and sustainability review article. *Renewable and Sustainable Energy Reviews*, 9(6):535–555, 2005.
- O’Loughlin, W. and Masri, A. A new burner for studying auto-ignition in turbulent dilute sprays. *Combustion and Flame*, 158:1577–1590, 2011.
- O’Loughlin, W. and Masri, A. The structure of the auto-ignition region of turbulent dilute methanol sprays issuing in a vitiated co-flow. *Flow Turbulence Combustion*, 89:13–35, 2012.
- Oppenheim, A. V. and Schafer, R. W. *Digital Signal Processing*. Prentice-Hall, Inc., 1975.
- Papagiannakis, R.G and Hountalas, D.T. Experimental investigation concerning the effect of natural gas percentage on performance and emissions of a DI dual fuel diesel engine. *Applied Thermal Engineering*, 23(3):353–365, February 2003.
- Papandreou-Suppappola, A., editor. *Applications in Time-Frequency Signal Processing*. CRC Press, 2003.

- Parzen, E. On estimation of a probability density function and mode. *The Annals of Mathematical Statistics*, 33(3):1065–1076, 1962.
- Payri, F., Broatch, A., Tormos, B., and Marant, V. New methodology for in-cylinder pressure analysis in direct injection diesel engines: application to combustion noise. *Measurement Science and Technology*, 16(2):540–547, 2005.
- Payri, F., Lujan, J.M., Martin, J., and Abbad, A. Digital signal processing of in-cylinder pressure for combustion diagnosis of internal combustion engines. *Mechanical Systems and Signal Processing*, 24(6):1767–1784, 2010.
- Payri, R., Garcia-Oliver, J. M., Bardi, M., and Manin, J. Fuel temperature influence on diesel sprays in inert and reacting conditions. *Applied Thermal Engineering*, 35:185–195, 2012.
- Peng, Z. and Chu, F. Application of the wavelet transform in machine condition monitoring and fault diagnostics: a review with bibliography. *Mechanical Systems and Signal Processing*, 18(2):199–221, 2004.
- Pipitone, E. and Beccari, A. Determination of TDC in internal combustion engines by a newly developed thermodynamic approach. *Applied Thermal Engineering*, 30(14–15):1914–1926, 2007.
- Poggi, V., Faeh, D., and Giardini, D. Time-frequency-wavenumber analysis of surface waves using the continuous wavelet transform. *Pure and Applied Geophysics*, 170(3):319–335, 2012.
- Prabhakar, B. and Boehman, A. Effect of common rail pressure on the relationship between efficiency and particulate matter emissions at NOx parity. *Society of Automotive Engineers*, (SAE Paper 2012-01-0430), 2012.
- Prakash, G., Shaik, A. B., and Ramesh, A. An approach for estimation of ignition delay in a dual fuel engine. *Society of Automotive Engineers*, (SAE Paper 1999-01-0232), 1999.
- Rabiner, L. R. and Rader, C. M., editors. *Digital Signal Processing*. IEEE Press, New York, 1972.
- Ragauskas, A. J., Williams, C. K., Davison, B. H., Britovsek, G., Cairney, J., Eckert, C. A., Frederick, W. J., Hallett, J. P., Leak, D. J., Liotta, C. L., Mielenz, J. R., Murphy, R., Templer, R., and Tschaplinski, T. The path forward for biofuels and biomaterials. *Science*, 311(5760):484–489, 2006.
- Raje, A., Inga, J. R., and Davis, B. H. Fischer-Tropsch synthesis: Process considerations based on performance of iron-based catalysts. *Fuel*, 76(3):273–280, 1997.
- Rakopoulos, C. D. and Kyritsis, D. C. Comparative second-law analysis of internal combustion engine operation for methane, methanol, and dodecane fuels. *Energy*, 26(7):705–722, 2001.
- Rakopoulos, C. D., Antonopoulos, K. A., and Rakopoulos, D. C. Experimental heat release analysis and emissions of a HSDI diesel engine fueled with ethanol-diesel fuel blends. *Energy*, 32(10):1791–1808, 2007.

- Rakopoulos, C. D., Rakopoulos, D. C., Giakoumis, E. G., and Dimaratos, A. M. Investigation of the combustion of neat cottonseed oil or its neat bio-diesel in a hsd diesel engine by experimental heat release and statistical analysis. *Fuel*, 89:3814–3826, 2010.
- Rakopoulos, C.D., Antonopoulos, K.A., and Rakopoulos, D.C. Multi-zone modeling of diesel engine fuel spray development with vegetable oil, bio-diesel or diesel fuels. *Energy Conversion and Management*, 47(11-12):1550–1573, 2006.
- Rakopoulos, D. C. Combustion and emissions of cottonseed oil and its bio-diesel in blends with either *n*-butanol or diethyl ether in HSDI diesel engine. *Fuel*, 2012.
- Rakopoulos, D. C., Rakopoulos, C. D., Giakoumis, E. G., Papagiannakis, R. G., and Kyritsis, D. C. Experimental-stochastic investigation of the combustion cyclic variability in HSDI diesel engine using ethanol-diesel fuel blends. *Fuel*, 87(8-9):1478–1491, 2008.
- Rakopoulos, D. C., Rakopoulos, C. D., Papagiannakis, R. G., and Kyritsis, D. C. Combustion heat release analysis of ethanol or *n*-butanol diesel fuel blends in heavy-duty DI diesel engine. *Fuel*, 90:1855–1867, 2011.
- Ramadhas, A. S., Muraleedharan, C., and Jayaraj, S. Performance and emission evaluation of a diesel engine fuelled with methyl esters of rubber seed oil. *Renewable Energy*, 30(12): 1789–1800, 2005.
- Randall, R. B. *Frequency Analysis*. Bruel & Kjaer, 1987.
- Randolph, A. L. Methods of processing cylinder-pressure transducer signals to maximize data accuracy. *Society of Automotive Engineers*, (SAE Paper 900170), 1990.
- Ren, Y., Randall, R. B., and Milton, B. E. Influence of the resonant frequency on the control of knock in diesel engines. *Proceedings of the Institution of Mechanical Engineers: Part D: Journal of Automobile Engineering*. London, 213(2):127–133, 1999.
- Ren, Y., Huang, Z., Jiang, D., Liu, L., Zeng, K., Liu, B., and Wang, X. Combustion characteristics of a compression-ignition engine fuelled with diesel-dimethoxy methane blends under various fuel injection advance angles. *Applied Thermal Engineering*, 26(4): 327–337, 2006.
- Reyes, M., Tinaut, F. V., Andres, C., and Perez, A. A method to determine ignition delay times for Diesel surrogate fuels from combustion in a constant volume bomb: Inverse Livengood-Wu method. *Fuel*, 102:289–298, 2012.
- RIRDC, . Biofuels in Australia—issues and prospects. *Australian Government: Rural Industries Research and Development Corporation Publication Number 07/071*, 2007.
- Rodriguez, R., Sierens, R., and Verhelst, S. Ignition delay in a palm oil and rapeseed oil biodiesel fuelled engine and predictive correlations for the ignition delay period. *Fuel*, 90: 766–772, 2011.
- Rogers, L. M., Cullen, J., Phillips, P., and Carlton, J. S. Use of acoustic emission methods for crack growth detection in offshore and other structures. discussion. *Transactions - Institute of Marine Engineers*, 110(3):171–180, 1998.

- Rosenblatt, M. Remarks on some nonparametric estimates of a density function. *The Annals of Mathematical Statistics*, 27(3):832–837, 1956.
- Rosillo-Calle, F. and Walter, A. Global market for bioethanol: historical trends and future prospects. *Energy for Sustainable Development*, 10(1):20–32, 2006.
- Rothamer, D. and Murphy, L. Systematic study of ignition delay for jet fuels and diesel fuel in a heavy-duty diesel engine. *Proceedings of the Combustion Institute*, 2012.
- Saeed, M. N. and Henein, N. A. Combustion phenomena of alcohols in C.I. engines. *Journal of Engineering for Gas Turbines and Power*, 111(3):439–444, 1989.
- Sahin, Z. and Durgun, O. High speed direct injection (DI) light-fuel (gasoline) fumigated vehicle diesel engine. *Fuel*, 86(3):388–399, 2007.
- Sahin, Z., Durgun, O., and Bayram, C. Experimental investigation of gasoline fumigation in a single cylinder direct injection (DI) diesel engine. *Energy*, 33(8):1298–1310, 2008.
- Sahoo, B. B., Sahoo, N., and Saha, U. K. Effect of engine parameters and type of gaseous fuel on the performance of dual-fuel gas diesel engines—a critical review. *Renewable and Sustainable Energy Reviews*, 13(6-7):1151–1184, 2009.
- Sahoo, P. K. and Das, L. M. Combustion analysis of Jatropha, Karanja and Polanga based biodiesel as fuel in a diesel engine. *Fuel*, 88(6):994–999, 2009.
- Saisirirat, P., Foucher, F., Chanchaona, S., and Mounaim-Rouselle, C. A study of *n*-heptane/ethanol HCCI combustion characteristics by experiment and detailed chemical kinetics simulation. *Proceedings of the European Combustion Meeting*, 2009.
- Saisirirat, P., Togbe, C., Chanchaona, S., Foucher, F., Mounaim-Rouselle, C., and Dagaut, P. Auto-ignition and combustion characteristics in HCCI and JSR using 1-butanol/*n*-heptane and ethanol/*n*-heptane blends. *Proceedings of the Combustion Institute*, 33:3007–3014, 2011.
- Saleh, H. E. The preparaton and shock tube investigation of comparative ignition delays using blends of diesel fuel with bio-diesel of cottonseed oil. *Fuel*, 90(1):421–429, 2011.
- Samimy, B. and Rizzoni, G. Mechanical signature analysis using time-frequency signal processing: application to internal combustion engine knock detection. *Proceedings of the IEEE*, 84(9):1330–1343, 1996.
- Schaberg, P. W., Priede, T., and Dutkiewicz, R. K. Effects of a rapid pressure rise on engine vibration and noise. *Society of Automotive Engineers*, (SAE Paper 900013), 1990.
- Schmillen, K. and Wolschendorf, J. Cycke-to-cycle variations of combustion noise in diesel engines. *Society of Automotive Engineers*, (SAE Paper 890129), 1989.
- Schubert, A., Maiwald, O., Koenig, K., Schiessl, R., and Maas, U. An approach to the efficient modeling of lean premixed HCCI-operation. *Proceedings of the European Combustion Meeting*, 2005.
- Secor, J. A. Kerosene engines. *Society of Automotive Engineers*, (SAE Paper 130019), 1913.

- Selim, M. Y.E. Effect of engine parameters and gaseous fuel type on the cyclic variability of dual fuel engines. *Fuel*, 84(7-8):961–971, 2005.
- Selim, M. Y.E., Radwan, M. S., and Saleh, H. E. Improving the performance of dual fuel engines running on natural gas/LPG by using pilot fuel derived from jojoba seeds. *Renewable Energy*, 33(6):1173–1185, 2008.
- Sellnau, M. C., Matekunas, F. A., Battiston, P. A., Chang, C., and Lancaster, D. Cylinder-pressure-based engine control using pressure-ratio management and low-coast non-intrusive cylinder pressure sensors. *Society of Automotive Engineers*, (SAE Paper 2000-01-0932), 2000.
- Sen, A. K., Longwic, R., Litak, G., and Gorski, Z. Analysis of cycle-to-cycle pressure oscillations in a diesel engine. *Mechanical Systems and Signal Processing*, 22:362–373, 2008.
- Shafiee, S. and Topal, E. When will fossil fuel reserves be diminished. *Energy Policy*, 37: 181–189, 2009.
- Shehata, M. S. Cylinder pressure, performance parameters, heat release, specific heats ratio and duration of combustion for spark ignition engine. *Energy*, 35(12):4710–4725, 2010.
- Shimasaki, Y., Kobayashi, M., Sakomoto, H., Ueno, M., Hasegawa, M., Yamaguchi, S., and Suzuki, T. Study on engine management system using chamber pressure sensor integrated with spark plug. *Society of Automotive Engineers*, (SAE Paper 2004-01-0519), 2004.
- Shindell, D., Faluvegi, G., Walsh, M., Anenberg, S. C., van Dingenen, R., Muller, N. Z., Austin, J., Koch, D., and Milly, G. Climate, health, agricultural and economic impacts of tighter vehicle-emission standards. *Nature Climate Change*, 1:59–66, 2011.
- Shropshire, G. J. and Goering, C. E. Ethanol injection into a diesel engine. *Transactions of the ASAE*, 25(3):570–575, 1982.
- Sion, R. and Atkinson, J. A novel low-cost sensor for measuring cylinder pressure and improving performance of an internal combustion engine. *Sensor Review*, 22(2):139–148, 2002.
- Skelton, B. Special issue: Bio-fuels. *Process Safety and Environmental Protection*, 85(5): 347–347, 2007.
- Song, C., Gong, G., Song, J., Lv, G., Cao, X., Liu, L., and Pei, Y. Potential for reduction of exhaust emissions in a common-rail direct-injection diesel engine by fueling with FischerTropsch diesel fuel synthesized from coal. *Energy Fuels*, 26(1):530–535, 2012.
- Sorda, G., Banse, M., and Kemfert, C. An overview of biofuel policies across the world. *Energy Policy*, 38(11):6977–6988, 2010.
- Spiegelhalter, D. J., Thomas, A., and Best, N. G. *WinBUGS Version 1.2 User Manual*. MRC Biostatistics Unit, 1999.
- Spiegelhalter, David J., Best, Nicola G., Carlin, Bradley P., and Linde, Angelika van der. Bayesian measures of model complexity and fit. *Journal of the Royal Statistical Society. Series B (Statistical Methodology)*, 64(4):583–639, 2002.

- Stankovic, L. A multitime definition of the Wigner higher order distribution: L-Wigner distribution. *Signal Processing Letters, IEEE*, 1(7):106–109, 1994a.
- Stankovic, L. A method for time-frequency analysis. *Signal Processing, IEEE Transactions on*, 42(1):225–229, 1994b.
- Stankovic, L. and Bohme, J. F. Time-frequency analysis of multiple resonances in combustion engine signals. *Signal Processing*, 79(1):15–28, 1999.
- Stas, M. J. A universally applicable thermodynamic method for TDC determination. *Society of Automotive Engineers*, (SAE Paper 2000-01-0561), 2000.
- Steel, J. A. and Reuben, R. L. Recent developments in monitoring of engines using acoustic emission. *The Journal of Strain Analysis for Engineering Design*, 40(1):45–57, 2005.
- Stone, R. *Introduction to Internal Combustion Engines*. Macmillan Press Ltd, London, 1999.
- Suh, H. K. and Lee, C. S. Experimental and analytical study on the spray characteristics of dimethyl ether (DME) and diesel fuels within a common-rail injection system in a diesel engine. *Fuel*, 87(6):925–932, 2008.
- Surawski, N. C., Miljevic, B., Roberts, B. A., Modini, R. L., Situ, R., Brown, R. J., Bottle, S. E., and Ristovski, Z. D. Particle emissions, volatility, and toxicity from an ethanol fumigated compression ignition engine. *Environmental Science & Technology*, 44(1):229–235, 2010.
- Surawski, N. C., Ristovski, Z. D., Brown, R. J., and Situ, R. Gaseous and particle emissions from an ethanol fumigated compression ignition engine. *Energy Conversion and Management*, 54(1):145–151, 2012.
- Tauzia, X., Maiboom, A., and Shah, S. R. Experimental study of inlet manifold water injection on combustion and emissions of an automotive direct injection diesel engine. *Energy*, 35(9):3628–3639, 2010.
- Taylor, C. F. and Taylor, E. D. *The Internal-Combustion Engine*. International Textbook Company, 1966.
- Tierney, L. Markov chains for exploring posterior distributions. *The Annals of Statistics*, 22(4):1701–1728, 1994.
- Torregrosa, A. J., Broatch, A., and Margot, X. Combustion chamber resonances in direct injection automotive diesel engines: a numerical approach. *International Journal of Engine Research*, 5(1):83–91, 2004.
- Torregrosa, A. J., Broatch, A., Novella, R., and Monico, L. F. Suitability analysis of advanced diesel combustion concepts for emissions and noise control. *Energy*, 36(2):825–838, 2011.
- Tsang, K. S., Zhang, Z. H., Cheung, C. S., and Chan, T. L. Reducing emissions of a diesel engine using fumigation ethanol and a diesel oxidation catalyst. *Energy & Fuels*, 24:6156–6165, 2010.

- Uchida, N., Shimokawa, K., Kudo, Y., and Shimoda, M. Combustion optimization by means of common rail injection system for heavy-duty diesel engines. *Society of Automotive Engineers*, (SAE Paper 982679), 1998.
- US Department of Transportation, . Transportation and global climate change: a review and analysis of the literature. Technical Report DOT-T-97-03, Federal Highway Administration, Office of Environment and Planning, Washington, DC, 1998. URL <http://www.fhwa.dot.gov/environment/lit.htm>.
- Valentino, G., Corcione, F., Iannuzzi, E., and Serra, S. Experimental study on performance and emissions of a high speed diesel engine fuelled with n-butanol diesel blends under premixed low temperature combustion. *Fuel*, 92:295–307, 2012.
- Van Gerpen, J. H., Hammond, E. G., Johnson, L. A., Marley, S. J., Yu, L., Lee, I., and Monyem, A. Determining the influence of contaminants on biodiesel properties. *Society of Automotive Engineers*, (SAE Paper 971685), 1997.
- Van Overbeke, C. W. Manifold introduction of hydrocarbons as an aid for starting. Master's thesis, The Pennsylvania State University, 1942.
- Velders, G., Geilenkirchen, G., and de Lange, R. Higher than expected  $NO_x$  emission from trucks may affect attainability of  $NO_2$  limit values in the netherlands. *Atmospheric Environment*, 45(16):3025–3033, 2011.
- Ville, J. Theory and applications of the notion of a complex signal. *Cables et Transmissions*, 2A:61–74, 1948.
- Wang, C., Zhang, Y., and Zhong, Z. Fault diagnosis for diesel valve trains based on time-frequency images. *Mechanical Systems and Signal Processing*, 22(8):1981–1993, 2008.
- Warnatz, J., Maas, U., and Dibble, R. *Combustion: Third Edition*. Springer Verlag, 2001.
- Warnatz, J., Dibble, R., and Maas, U. *Combustion – Physical and Chemical Fundamentals, Modeling and Simulation, Experiments, Pollutant Formation: Fourth Edition*. Springer Verlag, 2006.
- Worm, J. An evaluation of several methods for calculating transient trapped mass with emphasis on the Delta P approach. *Society of Automotive Engineers*, (SAE Paper 2005-01-0990), 2005.
- Xu-Guang, T., Hai-Lang, S., Tao, Q., Zhi-Qiang, F., and Wen-Hui, Y. The impact of common rail systems control parameters on the performance of high-power diesel. *Energy Procedia*, 16:2067–2072, 2012.
- Yusuf, N. N. A. N., Kamarudin, S. K., and Yaakub, Z. Overview on the current trends in biodiesel production. *Energy Conversion and Management*, 52(7):2741–2751, 2011.
- Zamboni, G. and Capobianco, M. Experimental study on the effects of HP and LP EGR in an automotive turbocharged diesel engine. *Applied Energy*, 94:117–128, 2012.



# Appendix

---

[This page is intentionally left blank]

## A.1 Comment on Error

### A.1.1 Experimental Error

Possible sources of experimental error are from the in-cylinder pressure transducer and the crank angle sensor. It can be reasonably assumed that the in-cylinder pressure transducer was operating within 2% (from manufacturers (Kistler) specification) throughout these experiments. However, it was shown in Chapter 3 that the PCB transducer in the Ford engine (under investigation in Chapter 4) was operating with approximately 1% error. It is likely that the Kistler in-cylinder pressure transducer in the Cummins engine was also performing within a percent error.

Any slight deviation between the measured in-cylinder pressure and the true in-cylinder pressure will only have an impact on the calculation of the: indicated work, indicated power, indicated mean effective pressure, peak pressure and the maximum rate of pressure rise. However, these parameters potentially influenced by the calibration of the pressure transducer were primarily discussed in terms of their inter-cycle variability. As such, if it is assumed that any error in the measurement of the in-cylinder pressure was consistent across an experiment, then the inter-cycle variability results, and hence the conclusions, should be reasonably unaffected. Therefore, any potential in-cylinder pressure measurement error would have had a negligible effect on the results shown in this dissertation.

The crank angle sensor (Kistler) used in this work has a resolution of half a crank angle degree and has been calibrated at top dead centre. This calibration has been performed using multiple methods (Jaye, 2002; Stas, 2000; Nilsson and Eriksson, 2004; Pipitone and Beccari, 2007) and it can be assumed that the measured crank angle is within 0.1 of a crank angle degree of the true position. Any deviation from the true crank angle position can, therefore, be assumed negligible.

The introduced Bayesian modelling techniques in this dissertation are not sensitive to slight deviations between the measured and the true in-cylinder pressure—empirical models were developed to fit the band-pass filtered in-cylinder pressure signal, as opposed to modelling the absolute in-cylinder pressure signal. An approach not reliant on absolute measured values is advantageous, especially with the determination of ignition delay (Chapters 6, 7 and 8), because other current methods typically involve the calculation of heat release and are therefore sensitive to the accurate measurement of both in-cylinder pressure and crank angle.

Determination of the in-cylinder temperature from the resonant frequency (Chapters 4 and 8) does rely on accurately measured in-cylinder pressure and crank angle data. However, it can be assumed that any deviation from the true value to the measured value will be contained in the correction factor (Chapter 8) determined from the mean engine in-take. Moreover, any potential error in the measurement of the in-cylinder pressure and crank angle is likely to be minimal with this calculation compared to the accurate measurement of the engine in-take and the assumptions that each cylinder receives an equal quantity of charge-air and that the bulk temperature is uniformly distributed throughout the combustion chamber. Therefore, the determined in-cylinder temperature with the Bayesian modelling technique can be considered a representative value only. However, this does not detract from its utility, especially for inter-cycle variability studies.

---

### A.1.2 Modelling Error

In Bayesian analysis, the model parameters are resolved into posterior distributions rather than single values—these distributions represent the probability density estimate of the true value of the model parameter. This feature is a result of the iterative nature of a Monte Carlo technique and is important—if a model parameter does not explore the parameter space (and converge about a solution) then there would be no evidence that the posterior distribution of the model parameter is representative of a possible solution. The posterior distribution of a model parameter is generated by creating a kernel density estimate from a suitably large number of parameter updates, after enough iterations have occurred for the model to have converged on a solution (this time is known as the ‘burn-in’).

If a single value is required for further analysis, typically the modal value of the model parameter is used (indicated by the peak of the kernel density estimate). The uncertainty of this value would normally be discussed in one of two ways: 95% credibility intervals or examination of the standard deviation. Representative results in Chapters 6 and 8 are shown in tables with the prior and posterior means and standard deviations. This approach was taken to show what was learned about the model parameters as a result of the analysis. Specifics of the uncertainties are discussed in the relevant chapters.

### A.1.3 References

- Jaye, J. R. Algorithm for determining the top dead center location in an internal combustion engine using cylinder pressure measurements. US Patent 6,367,317, 2002.
- Nilsson, Y and Eriksson, L. Determining TDC position using symmetry and other methods. *Society of Automotive Engineers*, (SAE Paper 2004-01-1458), 2004.
- Pipitone, E. and Beccari, A. Determination of TDC in internal combustion engines by a newly developed thermodynamic approach. *Applied Thermal Engineering*, 30(14–15): 1914–1926, 2007.
- Stas, M. J. A universally applicable thermodynamic method for TDC determination. *Society of Automotive Engineers*, (SAE Paper 2000-01-0561), 2000.

---

## A.2 Fuel Certificates

The diesel fuel used in the campaign that this thesis is based on was a blend of the following two batches of fuel. This blend was used for all of the results shown in this thesis, with the exception of Chapter 4.

P.O. Box 40  
Wynnum QLD 4178  
Telephone: +61 7 3362 7291  
Facsimile: +61 7 3362 7295

## Automotive Diesel -Xtra Low Sulfur



Date : 16-06-2011 Tank : 68  
Batch No: DX523 Product Code: DXLQS

**CALTEX**

METHOD	TEST	SPECIFICATION		RESULT	UNITS
ASTM D4176	Appearance @ 25°C	1	max	1	
ASTM D4737A	Cetane Index (Calculated)	46	min	51.2	
ASTM D5773	Cloud Point (D2500 equivalent)	-1.0	max	-1	deg C
ASTM D1500	Colour (ASTM)	2.0	max	1.0	
ASTM D2624	Conductivity	80	min	265	pS/m
ASTM D2624	Temperature at time of measurement	Report		20.7	deg C
ASTM D130	Copper Corrosion (3 Hrs @ 50 deg C)	1	max	1a	
ASTM D4052	Density @ 15 deg C	0.820-0.850		0.8363	kg/L
ASTM D86	10% Recovered	Report		211.8	deg C
ASTM D86	50% Recovered	Report		264.5	deg C
ASTM D86	90% Recovered	Report		323.7	deg C
ASTM D86	95% Recovered	360	max	338.3	deg C
ASTM D86	FBP	Report		350.3	deg C
IP 387	Filter Blocking Tendency	1.41	max	1.01	
ASTM D93	Flash Point	64.0	min	69.0	deg C
IP 450	Lubricity (wsd 1.4) @ 60°C	0.460	max	0.412	mm
Declaration	Lubricity Additive - Total 9121	200	max	120	mg/kg
Calculated	Static dissipator content - statis 450	7	max	3	mg/L
ASTM D7039	Sulfur (Total)	10	max	7.3	mg/kg
ASTM D2709	Water and Sediment	0.05	max	0.000	vol%
Declaration	Additives (other)	Report		0.0	mg/L
ASTM D974	Acid Number (Strong)	nil		* 0.00	mg KOH/g
ASTM D974	Acid Number (Total)	0.30	max	* 0.03	mg KOH/g
ASTM D482	Ash	100	max	* 1	mg/kg
ASTM D4530	Carbon Residue (10 % Bottoms)	0.20	max	* 0.03	mass%
ASTM D2274	Oxidation Stability	25	max	* 3	mg/L
ASTM D445	Viscosity @ 40 deg C	2.0-4.5		* 2.651	sq.mm/sec
ASTM D6591	Polycyclic Aromatic hydrocarbons	11	max	4.4	mass%
ASTM D6591	Total Aromatic hydrocarbons	15	min	30.8	mass%

\* Based on frequency testing

# Denotes result off specification

Notes: Nil Bio-Diesel (FAME) has been added to this product.

This fuel conforms to Australian National Fuel Standards for 2001.

All tests have been performed with the latest revision of the tests indicated. The accuracy of the test results is within the limits of precision shown in the methods.

This certificate relates specifically to the sample tested, but relates also to the entire batch in so far as the sample is drawn according to ASTM D4057.

Date testing completed: 16-06-2011

Approved Signatory

Name:

G. Kenyon.

ID : 482734

Date : 16-06-2011

P.O. Box 40  
Wynnum QLD 4178  
Telephone: +61 7 3362 7291  
Facsimile: +61 7 3362 7295

## Automotive Diesel -Xtra Low Sulfur



Date : 19-06-2011 Tank : 85  
Batch No: DX524 Product Code: DXLQS

METHOD	TEST	SPECIFICATION	RESULT	UNITS
ASTM D4176	Appearance @ 25°C	1 max	1	
ASTM D4737A	Cetane Index (Calculated)	46 min	51.0	
ASTM D5773	Cloud Point (D2500 equivalent)	-1.0 max	-1	deg C
ASTM D1500	Colour (ASTM)	2.0 max	L0.5	
ASTM D2624	Conductivity	80 min	395	pS/m
ASTM D2624	Temperature at time of measurement	Report	18.2	deg C
ASTM D130	Copper Corrosion (3 Hrs @ 50 deg C)	1 max	1a	
ASTM D4052	Density @ 15 deg C	0.820-0.850	0.8387	kg/L
ASTM D86	10% Recovered	Report	214.6	deg C
ASTM D86	50% Recovered	Report	266.2	deg C
ASTM D86	90% Recovered	Report	327.1	deg C
ASTM D86	95% Recovered	360 max	343.8	deg C
ASTM D86	FBP	Report	351.3	deg C
IP 387	Filter Blocking Tendency	1.41 max	1.01	
ASTM D93	Flash Point	64.0 min	71.0	deg C
IP 450	Lubricity (wsd 1.4) @ 60°C	0.460 max	0.430	mm
Declaration	Lubricity Additive - Infineum R655	200 max	2	mg/kg
Declaration	Lubricity Additive - Tolad 9121	200 max	116	mg/kg
Calculated	Static dissipator content - stadis 450	7 max	3	mg/L
ASTM D7039	Sulfur (Total)	10 max	9.0	mg/kg
ASTM D2709	Water and Sediment	0.05 max	0.000	vol%
Declaration	Additives (other)	Report	0.0	mg/L
ASTM D974	Acid Number (Strong)	nil	* 0.00	mg KOH/g
ASTM D974	Acid Number (Total)	0.30 max	* 0.03	mg KOH/g
ASTM D482	Ash	100 max	* 1	mg/kg
ASTM D4530	Carbon Residue (10 % Bottoms)	0.20 max	* 0.03	mass%
ASTM D2274	Oxidation Stability	25 max	* 3	mg/L
ASTM D445	Viscosity @ 40 deg C	2.0-4.5	* 2.651	sq.mm/sec
ASTM D6591	Polycyclic Aromatic hydrocarbons	11 max	4.0	mass%
ASTM D6591	Total Aromatic hydrocarbons	15 min	29.6	mass%

\* Based on frequency testing

# Denotes result off specification

Notes: Nil Bio-Diesel (FAME) has been added to this product.

This fuel conforms to Australian National Fuel Standards for 2001.

All tests have been performed with the latest revision of the tests indicated. The accuracy of the test results is within the limits of precision shown in the methods.

This certificate relates specifically to the sample tested, but relates also to the entire batch in so far as the sample is drawn according to ASTM D4057.

Date testing completed: 19-06-2011

Approved Signatory

Name:

ZINA FILIPACCO

ID : 482972

Date : 19-06-2011